

STUDY OF EMISSION LINE STARS IN YOUNG OPEN CLUSTERS

A thesis

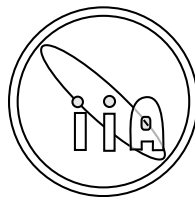
submitted for the degree of
DOCTOR OF PHILOSOPHY

in

The Faculty of Science
UNIVERSITY OF CALICUT, CALICUT

by

BLESSON MATHEW



INDIAN INSTITUTE OF ASTROPHYSICS

Bangalore 560 034, India

January 2010

To my family and friends

DECLARATION

I hereby declare that the matter contained in this thesis is the result of the investigations carried out by me at the Indian Institute of Astrophysics, Bangalore, under the supervision of Dr. Annapurni Subramaniam. This thesis has not been submitted for the award of any degree, diploma, associateship, fellowship etc. of any university or institute.

Dr. Annapurni Subramaniam

(Thesis Supervisor)

Blesson Mathew

(Ph.D. Candidate)

Indian Institute of Astrophysics

Bangalore 560 034, INDIA

January, 2010

CERTIFICATE

This is to certify that the thesis entitled “**Study of emission line stars in young open clusters**” submitted to the University of Calicut by **Mr. Blesson Mathew** for the award of the degree of *Doctor of Philosophy* in the faculty of Science, is based on the results of the investigations carried out by him under my supervision and guidance, at the Indian Institute of Astrophysics, Bangalore. This thesis has not been submitted for the award of any degree, diploma, associateship, fellowship etc. of any university or institute.

Dr. Annapurni Subramaniam
(Thesis Supervisor)

Indian Institute of Astrophysics
II Block, Koramangala
Karnataka
January, 2010

ACKNOWLEDGMENTS

I would like to express my sincere thanks to my supervisor Dr. Annapurni Subramaniam for introducing me to the field of Be stars and providing all the support and guidance. I would like to take this opportunity to thank the Director of Indian Institute of Astrophysics, Prof. Siraj Hassan for giving me the opportunity to work in this institute and providing all the facilities required for research work. I also thank Prof. Harish Bhatt, Prof. Vinod, Prof. Saha, Dr. G. Pandey, Dr. E. Reddy, Dr. M. Mekkaden, Dr. Ravindran, Dr. Ramesh and all members of Board of Graduate Studies for the help and support provided throughout the course of my work. I thank Dr. Anupama for the encouragement I got during project work. I thank IIA library staff, and the Librarian Ms. Christina Birdie for providing all the assistance required in making the books and journals available for reference. I thank all the faculty of IIA for the fruitful discussions I had with them and providing a research environment. I thank all the instructors who ignited the passion for astronomy during course work.

I would like to thank Prof. B. R. S. Babu, Dr. Ravikumar and all the faculty of Department of Physics, Calicut university for their valuable advice and suggestions. I sincerely thank administrative staff of the department and CDC for helping me during registration. I remember the encouragement and guidance I got during M.Sc period from the faculty and staff of CUSAT, especially, Dr. Mr. R. Anantharaman, Dr. Jayalakshmi, Dr. V. C. Kuriakose and Dr. Ramesh Babu. My heartfelt thanks to all my teachers during school and college days, especially Mr. Lakshmanan Pillai, Mr. Haneefa, Mr. Joseph Sebastian, Mr. T. G. Gopinathan, Mr. Sebastian Mathew, Mr. Raghupathy and all the teachers is K. E. College, who provided me a platform to write this thesis.

I would like to thank the faculty and present/former staff of CREST, Dr. B. C. Bhatt (our collaborator), Dr. P. Parihar, Dr. D. K. Sahu, Dr. Muneer, Dr. Shantikumar, Ms. Bama, Nandkumar, Vanni, Srividya, Ravi, Sasikumar, Aman, Ritu and Manjunath for the help and guidance they provided for observations throughout the research period. I like to thank all the staff of VBO Kavalur, Dr. Muthumariappan, Mr. Anbazhagan, Mr. Murthy, Mr. Appakutty, Mr. Jayakumar, Mr. Velu, Mr. Kuppusamy, Mr. Selvakumar, Mr. Sivakumar, Mr. Dinakaran, Mr. Ramachandran and Mr. Ramesh for parting their rich experience as observers. I also thank all the office staff of IIA including Administrative Officer, Mr. Narasimha Raju, Mr. Mohan Kumar, Mr. Murali, Mr. Sankar, Mr. Valsalan, Mr. Ramesh and Mr. Monappa for all the help they have provided. I thank all the technical staff including Dr. Baba, Mr. Fayaz and Mr. Ashok for helping with computer related issues.

I extend my heartfelt thanks to my friends Vigeesh, Nagaraj, Bharat, Uday, Nataraj, Malay, Rumpa, Smitha, Reks, Tapan, Girijesh, Veeru, Chandru, Krishna, Amit, Pradeep, Abhay, Drisya, Anant, Madhu, Indu, Ramya, Ratnakumar, Prasanth, Dinesh, Arya, Sinduja, Hema, Sudhakar, Veena, Preeja, Mr. Paul, Ms. Lovely, Sasi, Ann, Int.PhD & Int.M-Tech buddies and summer project students for the support and encouragement throughout my stay in IIA. I thank all my seniors, especially Maheswar, Manoj, Shalima, Ravi, Kathir, Reji, Baliga, from whom I learned lots of things. I thank Ramya and Jessy for giving me the fundas of data reduction. I thank Saju, Swapnechi, Umamaya, Ambadan, Koshy, Sajeevettan, Saravanan, Sridharan, Bhavya, Ginu, Vineeth, Bijoy, Chitra, Radha, Kishore, Jisha, Sne, Ranjith, Manu, Simil, Ajith, Norin, Jissa, Rejini, Sini, Vinay, Vivek, Shahi & family, Paulraj & family, Rakesh, Nimesh & co. and all friends in CUSAT for their support and affection.

Finally I thank my parents, my brother Jeeson and my love Sree for the belief and trust they had in me.

LIST OF PUBLICATIONS

Papers published / accepted in refereed journals:

1. Be phenomenon in open clusters: results from a survey of emission-line stars in young open clusters, **Mathew, Blesson.**, Subramaniam, A., Bhatt, B. C., 2008, MNRAS, 388, 1879.
2. Optical and near-IR photometric study of the open cluster NGC 637 and NGC 957, R. K. S. Yadav., B. Kumar., A. Subramaniam., R. Sagar., **Mathew, Blesson.**, 2008, MNRAS, 390, 985
3. Pre-main sequence stars, emission stars and recent star formation in the Cygnus region, Bhavya, B., **Mathew, Blesson.**, Subramaniam, A., 2007, BASI, 35, 383.
4. Star formation in the region of young open cluster - NGC 225, Subramaniam, A., **Mathew, Blesson.**, Kartha, S. S., 2006, BASI, 34, 315.
5. NGC 7419: a young open cluster with a number of very young intermediate mass pre-MS stars, Subramaniam, A., **Mathew, Blesson.**, Bhatt, B. C., Ramya, S., 2006, MNRAS, 370, 743.

Papers submitted in refereed journals / under preparation:

1. Spectroscopic study of a few Herbig Ae/Be stars in Young Open Clusters, **Mathew, Blesson.**, Subramaniam, A., B.Bhavya (submitted to BASI)
2. Spectroscopic characteristics of Classical Be stars in open clusters: Evidence

for bimodal origin, **Mathew, Blesson.**, Subramaniam, A.(in preparation)

3. CCD photometry of young open clusters with Be stars: NGC 2345, NGC 6756, King 21, Subramaniam, A., **Mathew, Blesson.**, Bhatt, B. C.(in preparation)

4. On the binarity of HR 2142, Th.Rivinius, **Mathew, Blesson.**, S.Stefl.(in preparation)

Papers presented in meetings

1. **Mathew, Blesson.**, Subramaniam, A., *Spectroscopy of Be stars in young open clusters*, 'Interstellar Matter and Star Formation - A Multi-Wavelength Perspective' held at TIFR National Balloon Facility, Hyderabad, October 5 - 7, 2009.

2. **Mathew, Blesson.**, Subramaniam, A., Bhatt, B. C., Be phenomenon in open clusters: Results from a survey of emission-line stars in young open clusters, 'The Interferometric View on Hot Stars', March 3 - 6, 2009, ESO, Chile.

3. **Mathew, Blesson.**, Subramaniam, A., *Spectroscopy of field CBe stars- A probe to understand Be phenomenon*, 27th meeting of Astronomical Society of India, Bangalore, February 18 - 20, 2009.

4. **Mathew, Blesson.**, Subramaniam, A., *Spectroscopic study of Be stars in young open clusters*, 27th meeting of Astronomical Society of India, Bangalore, February 18 - 20, 2009.

5. Paul. K.T., Subramaniam, A., **Mathew, Blesson.**, R. E. Mennickent., *How Different are the Be stars in Magellanic Clouds*, 27th meeting of Astronomical Society of India, Bangalore, February 18 - 20, 2009.

6. Bhavya. B., Subramaniam, A., Subramaniam, S., **Mathew, Blesson.**, V. C. Kuriakose., *Duration of star formation in the double cluster h & chi Persei*, 27th meeting of Astronomical Society of India, Bangalore, February 18 - 20, 2009.
7. Subramaniam, A., **Mathew, Blesson.**, B. C. Bhatt., *CCD Photometric study of three young open clusters with Be stars*, 27th meeting of Astronomical Society of India, Bangalore, February 18 - 20, 2009.
8. Subramaniam, A., **Mathew, Blesson.**, *Spectroscopic survey of emission line stars in open clusters*, Recent Advances in Spectroscopy; Astrophysical, Theoretical and Experimental Perspective, Kodaikanal, January 28-31, 2009.
9. **Mathew, Blesson.**, Subramaniam, A., *Survey of emission line stars in open clusters*, 25th meeting of Astronomical Society of India, Hyderabad, February, 2007.
10. **Mathew, Blesson.**, Subramaniam, A., *Characteristics of emission line stars in open clusters*, 25th meeting of Astronomical Society of India, Hyderabad, February, 2007.
11. Subramaniam, A., **Mathew, Blesson.**, Varricatt, W., Bhatt, B. C., Ashok, N. M., Banerjee, D., *NGC 6834 - 80 Myr old cluster with 4 emission line stars*, 25th meeting of Astronomical Society of India, Hyderabad, February, 2007.

Table of Contents

List of Tables	xiv
List of Figures	xxvii
Abstract	xxviii
1 Classical Be stars	2
1.1 Introduction	2
1.2 Be phenomenon	4
1.2.1 Rapid rotation	6
1.2.2 Stellar winds	7
1.2.3 Non-radial pulsations	8
1.2.4 Magnetic field	9
1.2.5 Binarity	10
1.2.6 Role of stellar evolution in Be phenomenon	11
1.2.7 Role of metallicity in Be phenomenon	12
1.3 Multiwavelength studies of Be stars	13
1.3.1 Optical Photometry & Spectroscopy	14
1.3.1.1 Methods to detect Be stars in clusters	17
1.3.2 Infra-red	18
1.3.3 Ultra-violet	19
1.3.4 X-ray & γ -ray	20

1.4	Outline of the Thesis	21
1.4.1	Chapter 1	21
1.4.2	Chapter 2	22
1.4.3	Chapter 3	22
1.4.4	Chapter 4	23
1.4.5	Chapter 5	24
1.4.6	Chapter 6	25
2	Survey of emission-line stars in young open clusters	26
2.1	Introduction	26
2.2	Observation & Analysis	28
2.2.1	Slitless Spectroscopy	28
2.2.2	Slit Spectroscopy	29
2.2.3	Photometry	50
2.3	Analysis of clusters with e-stars	50
2.3.1	Berkeley 62	53
2.3.2	Berkeley 63	55
2.3.3	Berkeley 86	56
2.3.4	Berkeley 87	58
2.3.5	Berkeley 90	60
2.3.6	Bochum 2	61
2.3.7	Collinder 96	62
2.3.8	IC 4996	64
2.3.9	King 10	66
2.3.10	King 21	68
2.3.11	NGC 146	69
2.3.12	NGC 436	71
2.3.13	NGC 457	73
2.3.14	NGC 581	74

2.3.15	NGC 637	76
2.3.16	NGC 654	77
2.3.17	NGC 659	79
2.3.18	NGC 663	81
2.3.19	NGC 869	84
2.3.20	NGC 884	86
2.3.21	NGC 957	88
2.3.22	NGC 1220	89
2.3.23	NGC 1624	91
2.3.24	NGC 1893	93
2.3.25	NGC 2345	95
2.3.26	NGC 2414	97
2.3.27	NGC 2421	98
2.3.28	NGC 6649	101
2.3.29	NGC 6756	103
2.3.30	NGC 6834	105
2.3.31	NGC 6910	106
2.3.32	NGC 7039	109
2.3.33	NGC 7128	111
2.3.34	NGC 7235	112
2.3.35	NGC 7261	114
2.3.36	NGC 7419	115
2.3.37	NGC 7510	119
2.3.38	Roslund 4	120
2.4	Conclusion	122

3 Be phenomenon in open clusters: results from a survey of emission-line stars in young open clusters **124**

3.1	Introduction	124
-----	--------------	-----

3.2	Results and Discussion	125
3.2.1	Colour-Magnitude Diagram of the e-stars	125
3.2.2	M_v versus age of the e-stars	128
3.2.3	Distribution of e-stars versus cluster Age	129
3.2.4	Distribution of e-stars as a function of spectral type	132
3.2.5	Be star fraction	134
3.2.6	Distribution of e-stars in near-IR CCDm	135
3.2.7	Location of clusters with e-stars in the Galaxy	137
3.3	Conclusion	138

4 Spectroscopic characteristics of Classical Be stars in open clusters:

	Evidence for bimodal origin	144
4.1	Introduction	144
4.2	Results: Spectral line analysis	146
4.2.1	Distribution of H_α equivalent width	146
4.2.2	Correlation between OI lines	147
4.2.3	Iron and metallic lines	149
4.2.4	CaII and P14 lines	149
4.2.5	Spectral type estimation	150
4.2.6	The distribution of Balmer decrement (D_{34})	151
4.2.7	Relationship between OI(8446) and Balmer line profiles	155
4.2.8	The variation of H_α EW as a function of age	158
4.2.9	Estimation of H_α emission radius	159
4.2.10	Rotation velocity estimation	161
4.2.11	The evolution of rotation velocity as a function of age	164
4.2.12	Variability of H_α profile	167
4.3	Discussion	170
4.4	Conclusion	172

5	Spectroscopic study of a few Herbig Ae/Be stars in Young Open Clusters	177
5.1	Introduction	177
5.2	Observations	178
5.3	Results and Discussion	180
5.3.1	Correlation of H_{α} EW with Near-IR Colour excess	180
5.3.2	Correlation of OI, P14 and CaII triplet EW with $(H-K_s)_0$ colour	183
5.4	H AeBe stars as members of parent clusters	185
5.4.1	Bochum 6	186
5.4.2	IC 1590	190
5.4.3	NGC 6823	193
5.4.4	NGC 7380	196
5.5	Conclusion	198
6	Summary & Future Plans	201
6.1	Summary	201
6.2	Impact of this work	204
6.3	Future Plans	205

List of Tables

1.1	The mean rotation velocities of Be stars in the SMC, LMC and Milky Way in various mass bins. For each sample, the mean age, mass, rotation velocity and the number of stars are given.	14
2.1	List of surveyed clusters.	31
2.2	List of e-stars from the slitless survey	35
2.3	Spectral lines identified in e-stars	41
3.1	Details of e-stars in surveyed clusters. Clusters with ‘*’ in the last column are those with Be stars identified for the first time from this survey.	141
3.2	The list of clusters with and without e-stars in various age bins. For comparison, values obtained by McSwain & Gies (2005) are given in parenthesis.	143
4.1	Spectral lines identified in the surveyed e-stars, with the number of emission and absorption profiles in brackets.	175
4.2	The estimated H_{α} emission region, in terms of stellar radius, for e-stars which showed double-peak profile.	176
5.1	Photometric parameters of identified HAeBe stars	185
5.2	Spectral lines identified in HAeBe stars	187

List of Figures

1.1	Schematic structure of the envelope of a Be star.	4
1.2	Schematic profiles of Balmer lines in B and Be stars.	5
1.3	Relation between the number ratio Be/(B+Be) and the local metallicity for groups of clusters. The number counts were made in different magnitude intervals, the dots refer to counts made in the magnitude interval $M_v = -5, -1.4$, the crosses to the interval $-5, -2$ and the triangles to the interval $-4, -2$	13
1.4	Schematic view of α Ara circumstellar environment	19
2.1	The slitless spectral image of NGC 7419. 25 e-stars are identified from this image.	29
2.2	(a) Optical CMD of the cluster Berkeley 62 is shown with the e-stars shown as solid circles. The ZAMS is shown in solid line while isochrone as dashed line. (b) The near-IR CCDm is shown with e-stars shown as filled triangles. (c) The spectra of the e-star Berkeley 62(1) are shown in the wavelength range $3800 - 9000 \text{ \AA}$	54
2.3	(a) The near-IR CCDm of the cluster Berkeley 63 is shown with e-stars shown as filled triangles. (b) The spectra of the e-star in the cluster are shown in the wavelength range $3800 - 9000 \text{ \AA}$	56

2.4	(a) Optical CMD of the cluster Berkeley 86 is shown with the e-stars shown as solid circles. (b) The near-IR CCDm is shown with e-stars shown as filled triangles. (c) The spectra of the e-stars Berkeley 86(9) and Berkeley 86(26), in the wavelength range 3800 – 9000 Å, are shown from bottom to top	57
2.5	(a) Optical CMD of the cluster Berkeley 87 is shown with the e-stars shown as solid circles. (b) The near-IR CCDm is shown with e-stars shown as filled triangles. (c) The spectra of the e-stars Berkeley 87(1), Berkeley 87(2), Berkeley 87(3) and Berkeley 87(4) are shown in order from bottom to top.	59
2.6	(a) The near-IR CCDm of the cluster Berkeley 90 is shown with e-stars shown as filled triangles. (b) The spectra of the e-star are shown in the wavelength range 3800 – 9000 Å.	61
2.7	(a) The near-IR of the cluster Bochum 2 is shown with e-stars shown as filled triangles. (b) The spectra of the e-star are shown in the wavelength range 3800 – 9000 Å.	62
2.8	(a) Optical CMD of the cluster Collinder 96 is shown with the e-stars shown as solid circles. (b) The near-IR CCDm is shown with e-stars shown as filled triangles.	63
2.9	The spectra of the e-stars Collinder 96(1) and Collinder 96(2), in the wavelength range 3800 – 9000 Å, are shown from bottom to top.	64
2.10	(a) Optical CMD of the cluster IC 4996 is shown with the e-stars shown as solid circles. (b) The near-IR CCDm is shown with e-stars shown as filled triangles. (c) The spectra of the e-star are shown in the wavelength range 3800 – 9000 Å.	65

2.11	(a) Optical CMD of the cluster King 10 is shown with the e-stars shown as solid circles. (b) The near-IR CCDm is shown with e-stars shown as filled triangles. (c) The spectra of the e-stars King 10(A), King 10(B), King 10(C), King 10(E), in the wavelength range 3800 – 9000 Å, are shown from bottom to top.	67
2.12	(a) Optical CMD of the cluster King 21 is shown with the e-stars shown as solid circles. (b) The near-IR CCDm is shown with e-stars shown as filled triangles. (c) The spectra of the e-stars King 21(B), King 21(C), King 21(D), in the wavelength range 3800 – 9000 Å, are shown from bottom to top.	68
2.13	(a) Optical CMD of the cluster NGC 146 is shown with the e-stars shown as solid circles. (b) The near-IR CCDm is shown with e-stars shown as filled triangles.	70
2.14	The spectra of the e-stars NGC 146(S1) and NGC 146(S2), in the wavelength range 3800 – 9000 Å, are shown from bottom to top. . .	71
2.15	(a) Optical CMD of the cluster NGC 436 is shown with the e-stars shown as solid circles. (b) The near-IR CCDm is shown with e-stars shown as filled triangles. (c) The spectra of the e-stars NGC 436(1), NGC 436(2), NGC 436(3), NGC 436(4), NGC 436(5) in the wavelength range 3800 – 9000 Å, are shown from bottom to top. . .	72
2.16	(a) Optical CMD of the cluster NGC 457 is shown with the e-stars shown as solid circles. (b) The near-IR CCDm is shown with e-stars shown as filled triangles.	73
2.17	The spectra of the e-stars NGC 457(1) and NGC 457(2), in the wavelength range 3800 – 9000 Å, are shown from bottom to top. . .	74

2.18	(a) Optical CMD of the cluster NGC 581 is shown with the e-stars shown as solid circles. (b) The near-IR CCDm is shown with e-stars shown as filled triangles. (c) The spectra of the e-stars NGC 581(1), NGC 581(2), NGC 581(3), NGC 581(4), in the wavelength range 3800 – 9000 Å, are shown from bottom to top.	75
2.19	(a) Optical CMD of the cluster NGC 637 is shown with the e-stars shown as solid circles. (b) The near-IR CCDm is shown with e-star shown as filled triangle.	76
2.20	The spectra of the e-star in the cluster NGC 637 are shown in the wavelength range 3800 – 9000 Å.	77
2.21	(a) Optical CMD of the cluster NGC 654 is shown with the e-star shown as solid circle. (b) The near-IR CCDm is shown with e-star shown as filled triangle. (c) The spectra of the e-star in the cluster NGC 654 are shown in the wavelength range 3800 – 9000 Å.	78
2.22	(a) Optical CMD of the cluster NGC 659 is shown with the e-stars shown as solid circles. (b) The near-IR CCDm is shown with e-stars shown as filled triangles. (c) The spectra of the e-stars NGC 659(1), NGC 659(2), NGC 659(3), in the wavelength range 3800 – 9000 Å, are shown from bottom to top.	80
2.23	(a) Optical CMD of the cluster NGC 663 is shown with the e-stars shown as solid circles. (b) The near-IR CCDm is shown with e-stars shown as filled triangles.	81
2.24	The spectra of the e-stars NGC 663(1), NGC 663(2), NGC 663(3), NGC 663(4), NGC 663(5), NGC 663(6), NGC 663(7), NGC 663(9), NGC 663(11) and NGC 663(12), in the wavelength range 3800 – 9000 Å, are shown from bottom to top.	83

2.25	The spectra of the e-stars NGC 663(12V), NGC 663(13), NGC 663(14), NGC 663(15), NGC 663(16), NGC 663(24), NGC 663(P5), NGC 663(P6), NGC 663(P8), NGC 663(P23), NGC 663(P25) and NGC 663(P151) in the wavelength range 3800 – 9000 Å, are shown from bottom to top.	84
2.26	(a) Optical CMD of the cluster NGC 869 is shown with the e-stars shown as solid circles. (b) The near-IR CCDm is shown with e-stars shown as filled triangles. (c) & (d) The spectra of the e-stars NGC 869(1), NGC 869(2), NGC 869(3), NGC 869(4), NGC 869(5) and NGC 869(6), in the wavelength range 3800 – 9000 Å, are shown from bottom to top.	85
2.27	(a) Optical CMD of the cluster NGC 884 is shown with the e-stars shown as solid circles. (b) The near-IR CCDm is shown with e-stars shown as filled triangles. (c) & (d) The spectra of the e-stars NGC 884(1), NGC 884(2), NGC 884(3), NGC 884(4), NGC 884(5) and NGC 884(6), in the wavelength range 3800 – 9000 Å, are shown from bottom to top.	87
2.28	(a) Optical CMD of the cluster NGC 957 is shown with the e-stars shown as solid circles. (b) The near-IR CCDm is shown with e-stars shown as filled triangles. (c) The spectra of the e-stars NGC 957(1) and NGC 957(2), in the wavelength range 3800 – 9000 Å, are shown from bottom to top.	89
2.29	(a) Optical CMD of the cluster NGC 1220 is shown with the e-star shown as solid circles. (b) The near-IR CCDm is shown with e-star shown as filled triangle.	90
2.30	The spectra of the e-star in NGC 1220 are shown in the wavelength range 3800 – 9000 Å.	91

2.31	(a) Optical CMD of the cluster NGC 1624 is shown with the e-star shown as solid circle. (b) The near-IR CCDm is shown with e-star shown as filled triangle. (c) The spectra of the e-stars in the cluster are shown in the wavelength range 3800 – 9000 Å.	92
2.32	(a) Optical CMD of the cluster NGC 1893 is shown with the e-star shown as solid circle. (b) The near-IR CCDm is shown with e-star shown as filled triangle.	94
2.33	The spectra of the e-star in the cluster NGC 1893 are shown in the wavelength range 3800 – 9000 Å.	95
2.34	(a) Optical CMD of the cluster NGC 2345 is shown with the e-stars shown as solid circles. (b) The near-IR CCDm is shown with e-stars shown as filled triangles.	96
2.35	(a) & (b) The spectra of the e-stars NGC 2345(2), NGC 2345(5), NGC 2345(20), NGC 2345(24), NGC 2345(27), NGC 2345(32), NGC 2345(35), NGC 2345(44), NGC 2345(59), NGC 2345(61), NGC 2345(X1) and NGC 2345(X2), in the wavelength range 3800 – 9000 Å, are shown from bottom to top.	97
2.36	(a) The near-IR CCDm of the cluster NGC 2414 is shown with e-stars shown as filled triangles. (b) The spectra of the e-stars NGC 2414(1) and NGC 2414(2), in the wavelength range 3800 – 9000 Å, are shown from bottom to top.	98
2.37	(a) Optical CMD of the cluster NGC 2421 is shown with the e-stars shown as solid circles. (b) The near-IR CCDm is shown with e-stars shown as filled triangles.	99
2.38	The spectra of the e-stars NGC 2421(1), NGC 2421(2), NGC 2421(3) and NGC 2421(4), in the wavelength range 3800 – 9000 Å, are shown from bottom to top.	100

2.39	(a) Optical CMD of the cluster NGC 6649 is shown with the e-stars shown as solid circles. (b) The near-IR CCDm is shown with e-stars shown as filled triangles.	101
2.40	(a) & (b) The spectra of the e-stars NGC 6649(1), NGC 6649(2), NGC 6649(3), NGC 6649(4), NGC 6649(5), NGC 6649(6) and NGC 6649(7), in the wavelength range 3800 – 9000 Å, are shown from bottom to top.	102
2.41	(a) Optical CMD of the cluster NGC 6756 is shown with the e-stars shown as solid circles. (b) The near-IR CCDm is shown with e-stars shown as filled triangles. (c) The spectra of the e-stars NGC 6756(2) and NGC 6756(3), in the wavelength range 3800 – 9000 Å, are shown from bottom to top.	104
2.42	(a) Optical CMD of the cluster NGC 6834 is shown with the e-stars shown as solid circles. (b) The near-IR CCDm is shown with e-stars shown as filled triangles. (c) The spectra of the e-stars NGC 6834(1), NGC 6834(2), NGC 6834(3) and NGC 6834(4), in the wavelength range 3800 – 9000 Å, are shown from bottom to top.	106
2.43	(a) Optical CMD of the cluster NGC 6910 is shown with the e-stars shown as solid circles. (b) The near-IR CCDm is shown with e-stars shown as filled triangles.	107
2.44	The spectra of the e-stars NGC 6910(A) and NGC 6910(B), in the wavelength range 3800 – 9000 Å, are shown from bottom to top. . .	108
2.45	(a) Optical CMD of the cluster NGC 7039 is shown with the e-stars shown as solid circles. (b) The near-IR CCDm is shown with e-stars shown as filled triangles. (c) The spectra of the e-star in the cluster are shown in the wavelength range 3800 – 9000 Å.	110
2.46	(a) Optical CMD of the cluster NGC 7128 is shown with the e-stars shown as solid circles. (b) The near-IR CCDm is shown with e-stars shown as filled triangles.	111

2.47	The spectra of the e-stars NGC 7128(1), NGC 7128(2) and NGC 7128(3), in the wavelength range 3800 – 9000 Å, are shown from bottom to top.	112
2.48	(a) Optical CMD of the cluster NGC 7235 is shown with the e-star shown as solid circle. (b) The near-IR CCDm is shown with e-star shown as filled triangle. (c) The spectra of the e-star in the cluster are shown in the wavelength range 3800 – 9000 Å.	113
2.49	(a) The near-IR CCDm of the cluster NGC 7261 is shown with e-stars shown as filled triangles. (b) The spectra of the e-stars NGC 7261(1), NGC 7261(2) and NGC 7261(3), in the wavelength range 3800 – 9000 Å, are shown from bottom to top.	115
2.50	(a) Optical CMD of the cluster NGC 7419 is shown with the e-stars shown as solid circles. (b) The near-IR CCDm is shown with e-stars shown as filled triangles. (c) & (d) The spectra of the e-stars NGC 7419(A), NGC 7419(B), NGC 7419(C), NGC 7419(D), NGC 7419(E), NGC 7419(F), NGC 7419(G), NGC 7419(H), NGC 7419(I) and NGC 7419(I1), in the wavelength range 3800 – 9000 Å, are shown from bottom to top.	116
2.51	(a) & (b) The spectra of the e-stars NGC 7419(J), NGC 7419(K), NGC 7419(L), NGC 7419(M), NGC 7419(N), NGC 7419(O), NGC 7419(P), NGC 7419(Q), NGC 7419(R) and NGC 7419(1), in the wavelength range 3800 – 9000 Å, are shown from bottom to top. . .	117
2.52	(a) & (b) The spectra of the e-stars NGC 7419(2), NGC 7419(3), NGC 7419(4), NGC 7419(5) and NGC 7419(6), in the wavelength range 3800 – 9000 Å, are shown from bottom to top.	118
2.53	(a) Optical CMD of the cluster NGC 7510 is shown with the e-stars shown as solid circles. (b) The near-IR CCDm is shown with e-stars shown as filled triangles.	119

2.54	The spectra of the e-stars NGC 7510(1A), NGC 7510(1B) and NGC 7510(1C), in the wavelength range 3800 – 9000 Å, are shown from bottom to top.	120
2.55	(a) Optical CMD of the cluster Roslund 4 is shown with the e-stars shown as solid circles. (b) The near-IR CCDm is shown with e-stars shown as filled triangles. (c) The spectra of the e-stars Roslund 4(1) and Roslund 4(2), in the wavelength range 3800 – 9000 Å, are shown from bottom to top.	121
3.1	The CMD of the e-stars is shown in figure with Y-axis being the absolute magnitude and X-axis being the reddening corrected colour.	126
3.2	A plot of M_v versus the age in Myr of the e-stars is shown. The e-star belonging to cluster NGC 7039 is not plotted due to uncertainty in age estimation.	128
3.3	Fraction of clusters which have e-stars with respect to the total number of clusters surveyed is shown in the figure.	130
3.4	The distribution of the surveyed e-stars with respect to the spectral type is given in figure. The solid squares show the total candidates while the open circles show the number of candidates after removing the contribution from 5 rich clusters.	133
3.5	The figure shows the ratio of Be stars with respect to all B type stars in the surveyed clusters.	134
3.6	Extinction corrected near-IR CCDm of e-stars (open triangles) in open clusters with MS (bold curve) and reddening vectors (dashed lines). The field CBe stars (filled squares) and HBe stars (filled circles) from the catalogue are also shown in figure.	136

3.7	(a) Distribution of clusters with e-stars (filled triangles) and clusters without e-stars (open triangles) is shown in the figure. (b) The figure shows the distribution of clusters with e-stars (filled triangles) and without e-stars (open triangles). The axes are given in units of kilo parsecs.	138
4.1	(a) H_α EW distribution of surveyed stars. (b) The correlation between H_α and H_β EWs.	147
4.2	Distribution of emission stars with respect to Spectral type.	150
4.3	(1) The Balmer decrement distribution of surveyed stars. (2) The H_α and H_β line profiles of Berkeley 87(4) are given in (a) and (b) while those of NGC 663(P25) are given in (c) and (d).	152
4.4	(a) The variation of Balmer Decrement with respect to the near-IR colour $(H-K)_0$. (b) The variation of H_α EW with respect to spectral type.	153
4.5	(a) The variation of D_{34} with respect to spectral type is shown in left panel while the variation of D_{34} with age is shown in right panel. (b) A plot of D_{34} with respect to H_α EW of CBe stars.	154
4.6	(a) The OI(8446) emission strength is plotted with respect to H_α emission strength. (b) A plot of EW of OI(8446) against H_α EW. (c) A plot of EW of OI(8446) against H_β EW.	156
4.7	(a) The H_α EW of the surveyed e-stars are plotted with respect to the age of the cluster to which they are associated. (b) The H_α EW of e-stars is shown with respect to age for various spectral bins. . .	158
4.8	Presently estimated $v \sin i$ values of field CBe stars is shown against those estimated by Slettebak. The linear fit which gives the best correlation is also shown.	160

4.9	(a) The histograms show the $v \sin i$ distribution of our candidates (oblique shaded histograms) and field CBe stars (open histograms), estimated from HeI 4471 Å line profile. (b) The $v \sin i$ distribution estimated from H_α line profile is shown with candidate stars as oblique shaded histograms, field CBe stars as unshaded ones and HAeBe stars as horizontally shaded histograms.	162
4.10	The disk rotation velocity is shown with respect to age for different spectral bins.	165
4.11	The stellar rotation velocity is shown with respect to age for different spectral bins.	166
4.12	The variation in H_α profile for e-stars (1) Berkeley 87(3), (2) NGC 659(2), (3) NGC 663(3), (4) NGC 663(13), (5) NGC 869(4), (6) NGC 884(1), (7) NGC 7419(H), (8) NGC 7419(K), (9) NGC 7419(P) are shown. Initial observation is shown as solid line followed by repeated observations in dashed and dotted lines respectively. . . .	168
5.1	(a) Correlation between H_α EW and $E(V-K_s)$ for all e-stars. The candidate CBe stars are shown as open circles while the suspected HAeBe stars are shown as filled circles. (b) Correlation between H_α EW and $(H-K_s)_0$ for all e-stars. Our candidate e-stars are shown as open triangles while the Herbig Be stars from The et al. (1994) is shown as filled circles and CBe stars from Jaschek and Egret (1982) as filled squares.	181
5.2	A plot of $(H-K_s)_0$ vs EW of CaII (a), P14 (b) and OI (c) are shown. The e-stars which were found to belong to HAeBe category are shown as solid circles while all the other e-stars are shown as open circles.	184

5.3	The Spectral Energy Distribution for e-stars IC 1590(3) (bold-line + triangle), IC 1590(1) (dot line + triangle), IC 1590(2) (short-dash + triangle), Bochum 6(1) (long-dash + triangle), NGC 6823(1) (dot-line + circle) and NGC 7380(4) (short-dash + circle) are shown. The CBe star IC 1590(3) is shown as reference.	186
5.4	(a) Near-IR CCDm of Bochum 6. The normal stars in cluster are shown as small circles. Encircled ones are candidate PMS stars and filled circle represents e-star. (b) Optical CMD of Bochum 6. PMS isochrones of ages 0.5–10 Myr are plotted. The e-star is found to occupy 0.5 Myr isochrone.	188
5.5	(a) Location of PMS stars and e-stars are shown in the field of Bochum 6. (b) The spectra of the e-star Bochum 6(1) in the wavelength range 3800 – 9000 Å.	189
5.6	(a) The near-IR CCDm of the cluster IC 1590 is shown with PMS candidates as encircled symbols and e-stars as filled circles. (b) Optical CMD of IC 1590. PMS isochrones of ages 2–10 Myr are plotted. IC 1590-1 and IC 1590-2 occupy 2 Myr and 3 Myr PMS isochrones respectively.	191
5.7	(a) Location of PMS stars and e-stars are shown in the field of IC 1590. (b) The spectra of e-stars IC 1590(1), IC 1590(2) and IC 1590(3), in the wavelength range 3800 – 9000 Å, is given from bottom to top.	192
5.8	(a) The near-IR CCDm of the cluster NGC 6823 is shown in figure with e-stars shown as filled triangles. (b) Optical CMD of NGC 6823. PMS isochrones of ages 0.25–7.5 Myr are plotted. The e-star is found to lie between 0.5 and 1 Myr isochrone.	194
5.9	(a) Location of PMS stars and e-stars are shown in the field of NGC 6823. (b) The spectra of the e-star NGC 6823(1) in the wavelength range 3800 – 9000 Å.	195

5.10	(a) The near-IR CCDm of the cluster NGC 7380 is shown with e-stars as filled circles and PMS as encircled symbols. (b) Optical CMD of NGC 7380. PMS isochrones of ages 0.25–7.5 Myr are plotted. The star NGC 7380(4) seems to be young than 0.25 Myr since it is found to lie beyond 0.25 Myr isochrone.	196
5.11	(a) Location of PMS stars and e-stars are shown in the field of NGC 7380. (b) The spectra of the e-stars NGC 7380(1), NGC 7380(2), NGC 7380(3) and NGC 7380(4), in the wavelength range 3800 – 9000 Å, is given from bottom to top.	197

ABSTRACT

Emission-line stars in young open clusters are identified to study their properties, as a function of age, spectral type and evolutionary state. 207 open star clusters were observed using the slitless spectroscopy method and 157 emission stars were identified in 42 clusters. We have found 54 new emission-line stars in 24 open clusters, out of which 19 clusters are found to house emission stars for the first time. From optical/near-IR photometry and spectroscopy, we suggest that Bochum 6(1), IC 1590(1) and NGC 6823(1) are Herbig Be while IC 1590(2) and NGC 7380(4) are Herbig Ae candidates. The Classical Be stars are located all along the main sequence (MS) in the optical colour magnitude diagram (CMD) of clusters of all ages, which indicates that the Be phenomenon is unlikely only due to core contraction near the turn-off. A spectroscopic study of 152 Classical Be stars in 42 young open clusters was performed using medium resolution spectra in 3700–9000 Å range, to understand the Be phenomenon. We found Lyman β fluorescence as the mechanism for the production of OI 8446 Å line in 24% of the surveyed stars, while collisional excitation is the likely excitation mechanism for OI 8446 Å and 7772 Å lines found in 47% of the stars, suggesting a denser disk. The Balmer decrement ($(I(H_\alpha)/I(H_\beta))$) is found to have a bimodal distribution which is correlated with the nature of H_β profile. Candidates with higher Balmer decrement (76%) were found to have more number of spectral lines, higher H_α equivalent width and $(H-K)_0$ values, suggesting an optically and geometrically thick disk. Massive Be stars of spectral type B0–B4 are found to have enhanced H_α emission at the end of their main sequence lifetime, as inferred from the enhancements observed at 12.5 and 25 Myr. The angular momentum evolution of stars as a function of age and spectral type also suggest a bimodal origin of Be stars. Stars in the B0–B2 spectral bin are found to be spun up towards the end of their MS life time, suggesting that early type stars evolve to become Be stars. Similar variation in properties

were not found for stars in the later spectral types (B4–A0), suggesting that the Be phenomenon differs in early type and late type stars. Spectroscopic studies were done for the identified Herbig Ae/Be (HAeBe) stars. The star formation history of the hosting cluster was estimated by identifying pre-MS stars. The ages of HAeBe stars were estimated. The duration of star formation in the hosting cluster were found to be about 10 Myr.

STUDY OF EMISSION LINE STARS IN YOUNG
OPEN CLUSTERS

Chapter 1

Classical Be stars

1.1 Introduction

A Classical Be star (CBe) is a rapidly rotating B-type star with an equatorial circumstellar decretion disk, which is not related to the natal disk the star had during its accretion phase (Porter and Rivinius, 2003). Struve (1931) suggested that rapidly rotating single stars of spectral class B are unstable, which eject matter at the equator, thus forming a nebulous ring which revolves around the star and gives rise to emission lines. The present working definition of a Be star is given as a non-supergiant B star whose spectrum has, or had at sometime, one or more Balmer lines in emission (Collins, 1987). The term classical has been used to distinguish them from Herbig Ae/Be (HAeBe) stars, which are intermediate mass ($2-10 M_{\odot}$) pre-main sequence (PMS) candidates with circumstellar accretion disk. From here onwards CBe/Be is used to represent classical Be stars. Recent studies point out that Be stars are not rotating at critical velocity and the circumstellar disk is formed by episodic mass loss from the central star. CBe stars rotate at 70–80% of their critical velocity and hence the reason for the formation of disk may not be equatorial mass loss mechanism. Jaschek and Jaschek (1983) identified 12% of the stars in the Bright Star Catalogue as Be stars. The consensus is that the highest fraction of Be stars appears around early spectral type.

The schematic diagram of a Be star is shown in figure 1.1 (Kogure and Hirata,

1982). CBe stars falls into 3 categories based on the viewing angle. They are normal Be stars (non-supergiants), B-type shell stars and Pole-on stars (Kogure and Hirata, 1982; Jaschek et al., 1981). Normal Be stars (non-supergiants) show double-peaked emission lines whose central reversals are not deeper than the continuum. B-type shell stars are characterized by shell lines in Balmer lines and metallic lines from ground states or metastable levels. The properties of shell lines are that they are usually sharp and their central depths are usually deeper than the continuum. Pole-on stars are characterized by single-peaked emission lines on broader photospheric absorption lines. They also show narrow HeI absorption lines. Pole-on stars are seen in the direction of rotation axis while shell stars are seen at an inclination angle of 90° , along the equator (Hirata and Kogure, 1984; Porter, 1996). The schematic diagram showing the Balmer line profiles of above mentioned categories of Be stars is given in figure 1.2 (Kogure and Hirata, 1982).

Conventionally the mass and radius were determined for Be stars which were part of eclipsing binary systems. But the problem here is that these systems are semi-detached/interacting binaries, which result in unreliable estimations. However, Popper (1980) estimated the masses and radii of Be stars in the spectral range B0–B8 as $16\text{--}3.5 M_\odot$ and $7\text{--}2.7 R_\odot$ respectively.

The properties of Be stars can be summarized as

1. Be stars are one of the fastest rotators in the Galaxy ($v \sin i > 100 \text{ km/s}$) which rotate close to the critical limit, where the centrifugal force balances gravity, as first stated by Struve (1931).
2. Emission lines are present in optical and infrared spectra indicating the presence of a circumstellar envelope (Struve, 1931). The circumstellar regions are cooler (electron temperature $\leq 10^4 \text{ K}$) than photosphere and the electron densities are of the order of 10^{11} to 10^{12} electrons per cm^3 . The mass loss rate derived from Infra-red (IR) measurements is about $10^{-8} M_\odot/\text{year}$ (Hartmann, 1978; Waters, 1986).

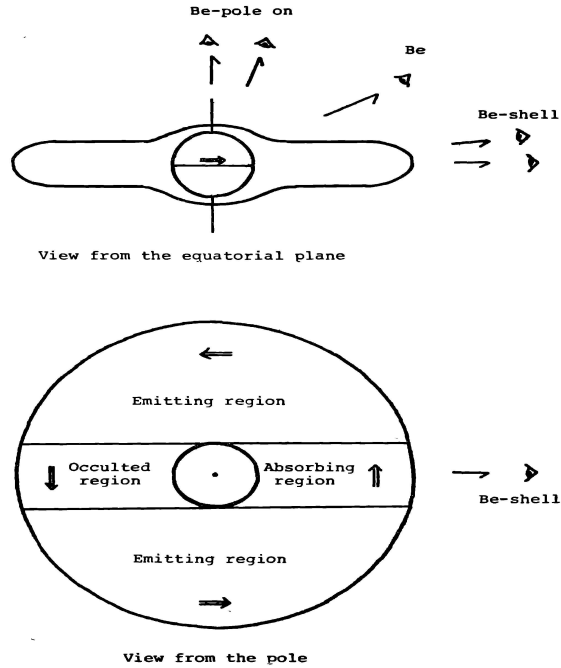


Figure 1.1: Schematic structure of the envelope of a Be star.

3. The study of resonance lines in ultraviolet spectra of early Be stars indicates high velocity (500–1000 km/s), rarefied (10^9cm^{-3}) polar winds with a mass loss rate $10^{-10} M_{\odot}/\text{year}$ (Snow and Marlborough, 1976; Snow, 1981). The mass loss rates and density in polar region are about 100 times less than equatorial value. This suggests that the winds of Be stars are asymmetric (Waters et al., 1987).
4. Be stars show photometric and spectroscopic long and short term variability (Doazan and Thomas, 1982).

1.2 Be phenomenon

Although it has been 143 years since Father Angelo Secchi discovered first Be star (γ Cassiopeia), the Be phenomenon still eludes explanation. Be stars are normal B-type stars with an optically and geometrically thin circumstellar disk, which is inferred from emission lines, IR excess and intrinsic polarization. The ‘Be phe-

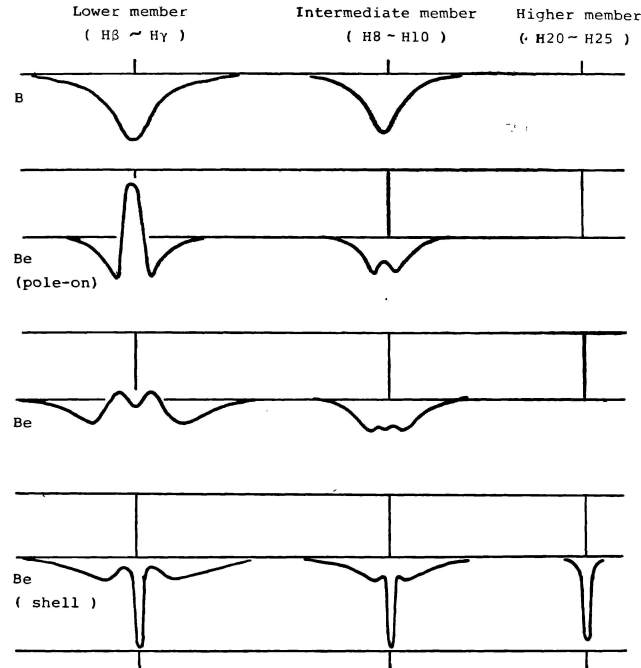


Figure 1.2: Schematic profiles of Balmer lines in B and Be stars.

phenomenon' is the episodic occurrence of mass loss in these stars, resulting in Balmer emission. While the Be phenomenon can be observed in some late O and early A stars, it is mainly confined to stars of B spectral type. The production of disk in CBe stars is still a mystery and majority of the studies point towards an optically thin equatorial disk formed by channeling of matter from the star through wind, rotation and magnetic field (Porter and Rivinius, 2003).

Rapid rotation, stellar wind, non-radial pulsation, magnetic field and binary interaction are the proposed mechanisms to explain Be phenomenon in Be stars. In the following subsections each of these mechanisms are discussed.

1.2.1 Rapid rotation

Be stars rotate faster than normal B stars, although they do not rotate at break-up velocity (Slettebak, 1979). The effect of rotation in the evolution of massive stars is not fully understood. The outer layers of rotating massive stars may spin up due to the evolution of the angular momentum distribution (Langer and Heger, 1998; Heger and Langer, 2000). When the star rotates at critical speed, it reaches ω limit, and the effective gravity becomes zero (Maeder, 1999). It has been found that Be stars rotate only at 70% of critical velocity (V_{crit}) (Chen and Huang, 1987; Porter, 1996). By taking the effects of equatorial gravity darkening, Townsend et al. (2004) argued that Be stars may be rotating close to critical velocity. Gravity darkening is the phenomenon in which fast rotation produces equatorial stretching of stars, which in turn induces non-uniform surface gravity and temperature distributions (von Zeipel, 1924). Using Monte Carlo modeling Cranmer (2005) found that late type Be stars (B3 and later) can rotate close to V_{crit} while early type rotate at 40–60% of the critical value.

From an analysis of 183 stars brighter than $V = 6$ mag, Slettebak (1982) found the distribution of Be stars to peak in B2 spectral type. The mean $v \sin i$ values for both main sequence (MS) and luminosity class III and IV Be stars were found to be in the range 200–250 km/s (Slettebak, 1982). The full width at half maximum (FWHM) values of the line profiles are used to estimate rotation velocity, which is the azimuthal component of velocity. The rotation velocity can be calculated by treating the circumstellar disk to be Keplerian or non-Keplerian. Hummel and Vrancken (2000) found that the line profiles produced using a Keplerian disk is indistinguishable from angular momentum conserving disk by changing the density structure of the disk. They found the value of rotational parameter 'j' to be less than 0.65 in the relation for rotation velocity, $V_{\phi} \propto R^{-j}$, where ϕ is the azimuthal angle. This value is quite near to the Keplerian value, which is $j = 0.5$. Apart

from azimuthal velocities, radial velocity component is used to understand the disk formation and dissipation process. The line profiles from shell stars have been used as diagnostics of radial outflow.

1.2.2 Stellar winds

A stellar wind is the continuous, supersonic outflow of matter from a star. In massive stars, the winds (driven by radiation pressure) influence the star's evolution as well as the interstellar medium. The circumstellar material in Be stars is concentrated in a disk with a high density and relatively low temperature. In the polar regions of the star the mass flux is lower which produces a low density wind with large velocities (typically 1000 to 2000 km/s). The super-ionization occurs in this low density wind (Poeckert, 1982). This model does not explain why the Be phenomenon can vanish and re-appear on timescales of the order of years. An alternative model was proposed by Doazan and Thomas (1982). They assume that the Be star is surrounded by a spherically symmetric corona, in which the material can be accelerated to large velocities of the order of 1000 km/s. Outside this corona the wind is decelerated by interaction with the circumstellar material. This produces a very extended region of moderately high density, which produces the H_α emission. In this model the long time scale variations of the emission line phenomena are explained by the presence or absence of the material which is collected in the decelerating region. The wind compressed disk (WCD) model of Bjorkman and Cassinelli (1993) proposes the formation of dense equatorial disk by radiation-driven wind, in which the ram pressure of the polar wind compresses and confines the disk. However it has been estimated from numerical hydrodynamic simulation that the disk generated by WCD model is not dense enough to produce enough IR/radio continuum emission (Owocki et al., 1994).

1.2.3 Non-radial pulsations

Be stars are found to occupy the same region in the HR diagram as β Cephei and Slowly Pulsating B-type (SPB) stars. Hence it is assumed that the pulsation belongs to p and/or g-mode driven by the κ (kappa) mechanism associated with the Iron bump. The rapid photometric and spectroscopic variability in Be stars has been attributed to non-radial pulsations (NRP) phenomenon (Baade, 1982; Rivinius et al., 2003; Rivinius, 2007). The wave-rotation interaction in rotating systems was examined by Ando (1982) and he showed that differential rotation can be amplified by a redistribution of angular momentum, through the transfer of energy from wave (NRP) to rotation. Cranmer (2009) developed this idea and proposed the formation of dense Keplerian disks in Be stars even if the underlying photosphere is rotating at 60% of critical velocity. The possible connection between pulsation and episodic mass loss in Be stars has been explored by various authors (Baade, 1985; Ando, 1986; Osaki, 1986; Townsend, 2007). Another proposed mechanism for the formation of disk is by episodic ejections of material from some specific region on the star (Kroll and Hanuschik, 1997; Owocki and Cranmer, 2002).

The early type Be stars exhibit line profile variability (lpv) in absorption over a period of 0.5 to 2 days. Rivinius et al. (2003) analysed 3000 high resolution spectra of 27 early-type stars and assigned short term variability to NRP, with most of them favoring $l = m = +2$ pulsation mode. They have demonstrated that the appearance of lpv depends mostly on the projected rotational velocity, $v \sin i$. The Be star μ Cen has been used to study the correlation between stellar pulsation and disk formation (Rivinius et al. 1998a; Rivinius et al. 1998b). The input of mass and angular momentum by the star onto the disk was demonstrated by the beating in phase of multiple NRP periods with outbursts of circumstellar material. Štefl et al. (2003) demonstrated that similar kind of outbursts can be seen for Be

stars with single pulsation period, like in the case of ω CMa. Hubert and Floquet (1998) showed that pulsations in B6-B9 type stars are much less common than in their early-type counterparts. Baade (1989) did not detect lpv in the spectra of B8–B9.5 Be stars while Saio et al. (2007) found low amplitude g-modes in β CMi, which is a B8Ve star. Diago et al. (2009a) detected g-mode pulsations in B8IVe star HD 50209 from time series analysis of photometric data observed by CoRoT (Convection, Rotation and planetary Transits) space mission. It can be inferred from these observations that some Be stars might exhibit NRP which plays a critical role in the mass ejection mechanism.

1.2.4 Magnetic field

Intermediate and high-mass stars are mostly non-magnetic with a few percent (depending on the spectral type) showing detectable magnetic fields (Landstreet, 1992). Cassinelli et al. (2002) proposed a magnetically torqued disk model for Be stars, in which a strong magnetic field of $\sim 300\text{G}$ channels the flow of wind material to form an equatorial circumstellar disk (Poe and Friend, 1986; Ud-Doula et al., 2008). The magnetic rotator wind disk model proposes the formation of Keplerian disks around Be stars by magnetic fields of the order of a few tens of Gauss (Maheswaran, 2003, 2005). Maheswaran and Cassinelli (2009) proposed that magneto-rotational instability can assist the formation of quasi-steady disk, for a magnetic field of a few tens of Gauss.

The magnetic field in Be stars are detected through spectropolarimetry, from Zeeman splitting of spectral lines. The result of the measurement of circular polarization is usually described by deducing the mean longitudinal field, $\langle B_z \rangle$. Recent development in observations is the detection of magnetic field in the range 40–150 G for eight CBe stars using FORS1 instrument installed at VLT . Among

these stars, λ Eri shows a cyclic variability in magnetic field and the period was found to be 21.1 minutes (Yudin et al., 2009). Hubrig et al. (2009) detected weak magnetic fields in four Be stars, HD 62367, μ Cen, \omicron Aqr and ϵ Tuc with HD 62367 having a strong longitudinal field, $\langle B_z \rangle = 117 \pm 38$ G.

1.2.5 Binarity

Kriz and Harmanec (1975) presented a general hypothesis that a large portion of Be stars are interacting binaries undergoing mass transfer from the secondary component filling its Roche lobe. Harmanec (1985) proposed that the unstable secondary contracts towards the helium MS, since most of the Be stars lack detectable secondaries. Gies (2001) categorized Be binaries in four groups (1) hot Algols (i.e. interacting binaries which were the essence of the hypothesis by Kriz and Harmanec (1975)), (2) Be + He stars (binary model modification by Harmanec (1985)), (3) Be X-ray binaries and (4) Be + white dwarf (WD) combinations (Koubský, 2005). About 70% of the evolved Be binary systems should have a white dwarf companion, 20% a helium star (sdO) and 10% a neutron star (NS) (van Bever and Vanbeveren, 1997; Raguzova, 2001). About 30 Be/X-ray binaries with a NS companion has been detected (van den Heuvel and Rappaport, 1987). The Be + WD binaries can be identified as low luminosity X-ray sources and despite the large predicted number none has been discovered yet. The only confirmed candidate belonging to Be + sdO class is ϕ Per (Gies et al., 1998) while more evidence is pouring in to include 59 Cyg (Maintz et al., 2005; Rivinius and Štefl, 2000) and HR 2142 (Peters, 1983; Peters and Gies, 2002). Plavec and Polidan (1976) pointed out the close relationship between Be stars and Algol eclipsing binaries and concluded that mass transfer in Algols of longer periods may probably produce a Be star. Since binarity is not confirmed in many Be stars, it is now generally accepted that Be stars can be formed as single stars and in binaries.

1.2.6 Role of stellar evolution in Be phenomenon

Schmidt-Kaler (1964) claimed that Be phenomenon occurs during the overall contraction phase following the exhaustion of hydrogen in the core. Hardorp and Strittmatter (1970) cast some doubts on this claim and showed that one observes a larger percentage of Be stars than allowed by the small fraction of the MS lifetime spent in this particular phase. Schild and Romanishin (1976) concluded that the fraction of Be stars remains constant during 80% of the MS phase, but undergoes a four-fold increase at the onset of the core contraction phase. Stars in this phase were identified with the extreme Be stars (Bex) by Schild (1966), who identified the spectroscopic features that characterize them. Slettebak (1985) stated that Be stars may be found above the zero-age main sequence (ZAMS) because of evolutionary effects, envelope reddening or rotationally induced gravity darkening of the underlying star, or some combination of the three. Keller et al. (2000, 2001) found most of the Be stars close to the turn-off of the star clusters they observed. Fabregat and Torrejón (2000) suggested the Be phenomenon will start to develop only in the second half of a B star's MS lifetime, because of structural changes in the star. They noted that Be star-disk systems should start to appear in clusters 10 Myr old, corresponding to the midpoint MS lifetime of B0 stars, and their frequency should peak in clusters 13–25 Myr, corresponding to the midpoint MS lifetime of B1-B2 stars. The theoretical models of Meynet and Maeder (2000) and Maeder and Meynet (2001) indicate that the ratio of angular velocity to critical angular velocity steadily increases throughout the MS lifetime of early-type B stars. This might explain why the Be phenomenon is prevalent in the later part of a B star's MS lifetime.

1.2.7 Role of metallicity in Be phenomenon

Feast (1972) found that about 50% of B stars in the Small Magellanic Cloud (SMC) cluster NGC 330 show Be phenomenon. This is quite a high fraction compared to 10–20% in Milky Way (Grebel et al., 1992). Maeder et al. (1999) suggested the influence of metallicity in Be star formation by indicating a higher fraction of Be stars in low-metallicity clusters (figure 1.3). In the magnitude interval $M_v = -5$ to -1.4 (O9–B3) they obtained a ratio $\text{Be}/(\text{B}+\text{Be}) = 0.11, 0.19, 0.23$ and 0.39 for 21 clusters located in the interior of the Galaxy, the exterior of the Galaxy, the Large Magellanic Cloud (LMC) and SMC respectively. They have taken a mean metallicity value of $Z = 0.014$ for clusters towards center of Galaxy, 0.020 in anti-center direction, 0.007 in LMC and 0.002 in SMC. Keller (2004) explored the role of metallicity in the $v \sin i$ value of B stars in field and young clusters of the LMC and Galaxy. He found that B-type stars in clusters rotate rapidly compared to the field counterparts. Moreover the average $v \sin i$ of B stars in the LMC clusters is found to be 146 km/s while in the Galaxy, it is 116 km/s. In low metallicity environments radiative winds are less efficient in B-type stars which result in the increment of rotation velocity rates, in order to conserve angular momentum. This suggests the possibility of producing more Be stars in the Magellanic clouds since rapid rotation enhances the production of circumstellar disk in B-type stars.

Pamyatnykh (1999) showed that the β Cephei and SPB instability strips vanish at $Z \leq 0.01$ and $Z \leq 0.006$ respectively. Hence it is expected to find less number of pulsators in LMC and no B-type pulsators in SMC. However Maeder and Meynet (2001) proposed the trigger of pulsation mechanism in rapid rotators through surface metal enrichment. Diago et al. (2009b) detected β Cephei and SPB-type pulsators in low metallicity environments in contrast with the predictions of the current theoretical models. For Be stars, an increase in rotation at low metallicity can enhance non-radial pulsations or amplify the existing modes.

Martayan et al. (2006, 2007b) performed spectroscopic observations of B and Be stars in the LMC cluster NGC 2004 and the SMC cluster NGC 330 using VLT-GIRAFFE facility in MEDUSA mode. They found Be stars of similar age and mass rotate faster in the SMC than in the LMC, and are large compared to the Milky Way values (see Table 1.1). They postulated that Be stars begin their MS life with a high initial rotation velocity than B stars.

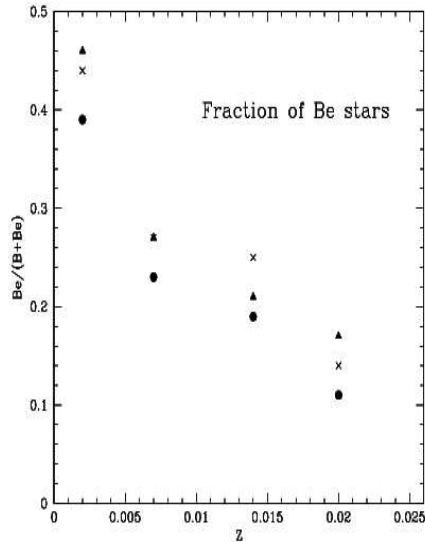


Figure 1.3: Relation between the number ratio $\text{Be}/(\text{B}+\text{Be})$ and the local metallicity for groups of clusters. The number counts were made in different magnitude intervals, the dots refer to counts made in the magnitude interval $M_v = -5, -1.4$, the crosses to the interval $-5, -2$ and the triangles to the interval $-4, -2$.

1.3 Multiwavelength studies of Be stars

Be stars are studied across the electromagnetic spectrum to understand Be phenomenon. The major studies in various bands are given below.

Table 1.1: The mean rotation velocities of Be stars in the SMC, LMC and Milky Way in various mass bins. For each sample, the mean age, mass, rotation velocity and the number of stars are given.

			2–5 M_{\odot}			5–10 M_{\odot}		
	age	M/M_{\odot}	$v \sin i$	N*	age	M/M_{\odot}	$v \sin i$	N*
SMC Be	8.0	3.7	277	14	7.6	7.6	297	81
LMC Be				0	7.5	7.7	285	21
MW Be	8.1	4.4	241	18	7.6	7.3	234	52
			10–12 M_{\odot}			12–18 M_{\odot}		
	age	M/M_{\odot}	$v \sin i$	N*	age	M/M_{\odot}	$v \sin i$	N*
SMC Be	7.4	10.8	335	13	7.2	13.5	336	14
LMC Be	7.3	11	259	13	7.2	14.6	224	10
MW Be	7.2	10.6	231	9	6.8	14.9	278	17

1.3.1 Optical Photometry & Spectroscopy

The first comprehensive catalogue of Be stars is the Mount Wilson Catalogue (MWC) by Merrill and Burwell (1933, 1943, 1949, 1950) which contains 1600 Be, Ae stars and related objects. Photographic spectral atlas by Hubert-Delplace and Hubert (1979) contains spectra of 148 Be stars in the wavelength region 3800–6600 Å. A collection of high dispersion H α and FeII line profiles of 77 Be stars were obtained by Hanuschik et al. (1996). An atlas of far ultra-violet (1200–3000 Å) and optical high resolution spectra of 166 Be stars have been given by Doazan et al. (1991). Andrillat et al. (1988, 1994) have done a spectral survey of 97 Be stars in the wavelength range 7500–8800 Å and 74 Be stars in the spectral range 9840–10200 Å. Bidelman (1976) had included Be supergiants and quasi-planetary nebulae into the class of Be stars. Later Jaschek et al. (1981) limited the discussion of Be stars as those which belong to the luminosity class III-V. Jaschek and Egret

(1982) compiled a comprehensive catalogue of 1100 Be stars from the emission line star (e-star) catalogues of Wackerling (1970) and Bidelman and MacConnell (1973).

Early work on emission line and shell spectra started as early as the 1920s and 30s by M. Wolf, O. Struve, A. H. Joy, L. B. Andrews, P. Swings and others. It was the pioneering work by Merrill (1949) who compiled several lists of stars with shell spectra that attracted the attention of observers. The field opened up by a comprehensive paper by Herbig in 1954 on NGC 2264 on the basis of spectroscopic data of e-stars. A systematic study of open clusters undertaken by Walker (1956, 1957, 1961) was the basis of subsequent research in this field; he included clusters such as NGC 2264, NGC 6530, NGC 6583, NGC 6611. The number of Be stars in open clusters has greatly increased in past years because of the search conducted by Schild and Romanishin (1976) in 29 northern clusters and by Lloyd Evans (1980) in NGC 3766 and IC 2581. Large surveys in the southern Milky way by Stephenson and Sanduleak (1977) and MacConnell (1981), and in the northern Milky way by the Vatican observers (Coyne et al., 1978) yielded an appreciable number of new Be stars in open clusters. Recently, McSwain and Gies (2005b) conducted a photometric survey of 55 southern open clusters and identified 52 definite Be stars and 129 probable candidates.

The photospheric absorption spectra of Be stars typically show broad absorption lines due to rotation, but are normal in terms of equivalent width (EW), ie. gravity, temperature and abundance (Slettebak, 1982). From an atlas of high-resolution ($R = 50000$), high signal to noise ratio H_α profiles of 24 bright southern Be stars, Hanuschik (1986) explained the inflections in the flanks of the profiles due to two-component structure. The inner broadened component is emitted at a radial distance of around 4 stellar radius while the outer component has an envelope boundary of 20 stellar radius. The inner component of H_α profile is broadened by Thomson scattering in addition to rotational and thermal broadening.

McLaughlin described three types of variability in the spectra of Be and shell stars: (a) E/C variation, which is the change in the ratio of intensity of the emission lines with respect to continuum.

(b) V/R variation, which is the change in the ratio of the intensity of the violet to red component of double-peaked emission lines.

(c) appearance and disappearance of a shell-absorption spectrum, as seen in the case of Pleione (Gulliver, 1977).

The V/R variations on the timescale of years arise from velocity fields and non-axisymmetric density distributions in the circumstellar disk. The periodic component of this slow V/R variability can be understood by global one-armed oscillations (Okazaki, 1991; Hummel and Hanuschik, 1997).

Polarization in Be stars arises predominantly from Thomson scattering in the ionized, circumstellar material. From polarization measurements it is found that the optical radiation from Be stars is intrinsically polarized, which can be as high as 2%. This provides evidence for the disk like geometry of circumstellar envelope in Be stars (Coyne and McLean, 1982). Polarization strength may vary with emission strength and V/R ratio while the polarization angles are constant (Wood et al., 1997).

The disk geometry of the circumstellar envelope in Be stars is revealed through interferometric observations (Thom et al., 1986; Mourard et al., 1989; Stee et al., 1995; Quirrenbach et al., 1994). From the interferometric measurements of seven Be stars in H_α , Quirrenbach et al. (1997) found that the H_α emission region extends up to 12 stellar radii, with a possible dependence on spectral type. From a correlated analysis of interferometric and spectropolarimetric observations, they derived a disk opening angle of around 20° . Wood et al. (1997) estimated a disk opening angle of 2.5° for ζ Tau from Be star models and on comparison with the observations of Quirrenbach et al. (1997). Tycner et al. (2005) found a relationship between the physical extent of H_α emitting region and net H_α luminosity from the

analysis of H_α line profiles and interferometric observations. Interferometric studies have confirmed that the geometry of the circumstellar gas is disk-like and the estimates of opening angles point to a relatively thin disk.

1.3.1.1 Methods to detect Be stars in clusters

Objective-prism spectroscopy is the conventional technique used for detecting e-stars, in which a low dispersion prism (or a grating) is placed in front of the telescope objective and produces low resolution spectra in the focal surface, of all the objects in the field of view. The technique has been used for many years, mostly in conjunction with Schmidt telescopes. Grebel et al. (1992) surveyed clusters using Strömgren filters y , b and an H_α filter of intermediate width. They used two-colour diagram ($b-y$) and ($H_\alpha - y$) to distinguish Be stars from B stars and bright supergiants. For the detection of Be stars in Magellanic cloud clusters like NGC 330, NGC 346, NGC 1818, NGC 1948, NGC 2004 and NGC 2100, Keller et al. (1999) used the difference between R band and narrow-band H_α CCD images. McSwain and Gies (2005a) identified Be stars in open clusters using Strömgren b , y and narrowband H_α photometry. They identified the B-type stars in the cluster using a theoretical isochrone fit to the ($b-y$, y) colour-magnitude diagram. This has been combined with ($b-y$, $y-H_\alpha$) colour-colour diagram to identify Be stars. Detection techniques used by various authors for individual clusters are discussed in next chapter.

We have used slitless spectroscopy to detect Be stars in young open clusters. The cluster region was observed with R band / Grism combination, which gives the dispersed image of stars in the field of view. By comparing with R band image, stars which show H_α in emission are identified. The details of the setup and the techniques used will be explained in the next chapter.

1.3.2 Infra-red

The IR excess of Be stars is due to the presence of a large amount of circumstellar material with a relatively high density, since the emissivity for free-free radiation depends on the square of electron density (ρ^2). Gehrz et al. (1974) found a considerable excess with an energy distribution typical for free-free emission, i.e. an excess which increases with wavelength. Their data showed some evidence for a deviation in the energy distribution near $10\mu\text{m}$ (turnover point). Gehrz et al. (1974) interpreted the excess in terms of free-free emission from a circumstellar shell and derived a typical density for these shells as 10^{11} to 10^{12} cm^{-3} for a representative set of Be stars and shell stars. For the physical conditions of Be envelope mentioned in Gehrz et al. (1974), the contributions from free-free and free-bound to the total nebular emission at $2.2\mu\text{m}$ were found to be 63% and 37% respectively (Ashok et al., 1984). The flux from the central star in the wavelength region $15\text{--}20\mu\text{m}$ is about 10–50 times fainter compared to the flux at $2\mu\text{m}$. The disk extension is a function of wavelength in IR region with 16 stellar radius (R_s) from 12, 25, $60\mu\text{m}$ measurements (Waters, 1986), $8R_s$ from 2.3, $19.5\mu\text{m}$ (Gehrz et al., 1974), $20R_s$ in near-IR (Dougherty et al., 1994) and $40R_s$ using $\text{Br}\gamma$ line (Stee and Bittar, 2001). The envelope size of α Ara (B3Ve) in N band has been estimated to be $14R_s$ from VLTI/MIDI observations (Chesneau et al., 2005). The schematic view of α Ara circumstellar environment used by the authors is given in figure 1.4.

Ashok et al. (1984) performed IR photometric studies of 55 northern Be stars in JHK broadbands and 15 in L band. The observed infrared continuum luminosity (L_{IR}) of the circumstellar envelope was found to exceed the energy input from the Lyman continuum luminosity (L_L). They also found a correlation between L_{IR} and bolometric luminosity of the central star. Dachs and Wamsteker (1982)

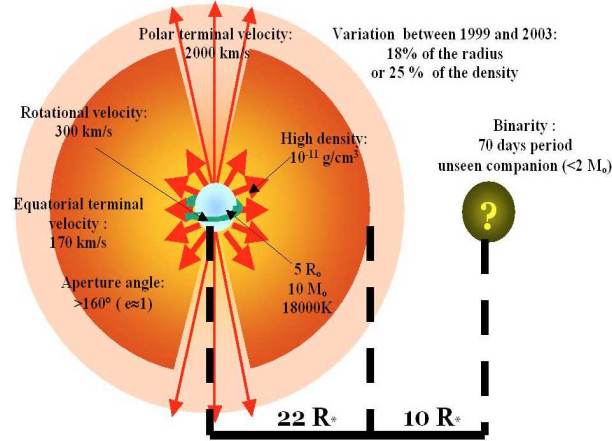


Figure 1.4: Schematic view of α Ara circumstellar environment

performed broadband IR photometry in the JHKLM bands for 46 bright southern e-stars and N-band photometry for 8 of them. They found (J–M) colour index strongly correlated with H_{α} EW for Be stars earlier than B6. In the far IR, the observed spectral energy distribution index α , in the relation $S_{\nu} \propto \nu^{\alpha}$, changes from $\alpha = 0.6$ to $\alpha > 1$ in the radio regime. This indicates some structural changes far away from the central star (Waters and Marlborough, 1994). Here ν represents the frequency of the electromagnetic radiation.

1.3.3 Ultra-violet

Snow (1987) and Snow and Stalio (1987) used ultraviolet observations to discuss the phenomenon of super-ionization in Be stars. This refers to the presence of ionization stages higher than normally found in equilibrium at photospheric temperature. Be stars are found to be much more superionized than normal B-type stars since C IV and Si IV are observed in Be stars as late as B9 while they are only seen upto B2 and B5 respectively in normal B-type MS stars (Grady et al.,

1987). The detection of NV and OVI spectral lines indicate that the winds are superionized (Marlborough, 1977).

1.3.4 X-ray & γ -ray

Quite a number of X-ray bright objects ($L_X \sim 10^{35}$ – 10^{38} ergs/s) belong to the class of X-ray binaries in which a neutron star or a black hole forms a binary system with a companion star. In High Mass X-ray binaries (HMXB), mass is accreted (10^{-11} – $10^{-8} M_\odot/\text{yr}$) from the donor star (OB supergiant or Be star) onto the compact object. X-ray binary pulsars are neutron star HMXBs which emit pulsed X-rays (Sasaki et al., 2003). The mechanism of X-ray outburst occur when a neutron star, which is in wide and eccentric orbit, passes close to the circumstellar disk of a Be star (Apparao, 1985; Okazaki and Negueruela, 2001). This binary system is of astrophysical interest since it is possible to determine the mass and radius of the Be star, the mass of the neutron star, an estimate of stellar wind intensity, mass transfer mechanisms and evolutionary history from optical and X-ray observations (Rappaport and van den Heuvel, 1982). The Be/X-ray binary system constitutes 60–70% of the population of HMXBs in Milky Way and the LMC while it is more than 90% in the SMC (Haberl and Sasaki, 2000).

Gamma-ray (γ -ray) binaries are HMXBs that exhibit very high energy emission in the MeV-TeV range. The following candidates are identified as part of VHE observations, whose companion is reported to be a Be star. PSR B1259-63/SS 2883 is a binary system of a 48 ms pulsar in orbit around a B2e companion star (Johnston et al., 1992). Aharonian et al. (2005) reported the discovery of very-high energy γ -ray emission (\sim TeV) from this system. The Be/X-ray binary LS I +61 303 is one of the brightest known γ -ray sources, detected by COS B (Hermsen et al., 1977; Albert et al., 2008). The Be companion is of B0Ve spectral type and

is in a highly eccentric orbit with a period of 26.5 days (Grundstrom et al., 2007). HESS J0632+057 is a γ -ray binary identified in HESS survey and the follow-up observation with XMM-Newton identified it as a massive star MWC 148 of spectral type B0pe (Hinton et al., 2009).

1.4 Outline of the Thesis

We have done a survey to search for e-stars in northern open clusters, belonging to different parts of the Galactic disk. Compared to field CBe stars, cluster candidates offer precise values of distance, reddening and chemical composition, which helps to understand their evolutionary state better. We used slitless spectroscopy to find e-stars in clusters, which is an innovative concept for a survey of this magnitude. The medium resolution spectra of identified e-stars are taken and the spectral parameters like EW and rotation velocity have been used to understand the properties of disk and angular momentum evolution. The sample of 157 stars in 42 clusters has been used to derive conclusion about the role of environment and mechanisms for the formation of Be stars. From photometric and spectroscopic studies, we propose a bimodal distribution in Be star population. The early subtype (B0–B2) evolve to become Be stars while others (B2–A0) are born in Be phase. The detailed description of the studies summarized in each chapter is given below.

1.4.1 Chapter 1

In Chapter 1, we have given an introduction to Be stars. We have explained Be phenomenon in CBe stars and the efforts underway to resolve the puzzle. Rapid rotation, stellar wind, non-radial pulsation, magnetic field and binary interaction

are the proposed mechanisms to resolve Be phenomenon in Be stars. We have explored the theoretical aspects of each of these mechanisms with the observational developments in each front. Be stars are studied in various bands in the electromagnetic spectrum, to understand the nature of the star with the formation and evolution of circumstellar disk. A quick glance on prominent studies in optical, IR, UV, X-ray and γ -ray are presented.

1.4.2 Chapter 2

The details of the survey to search for e-stars in 207 young open clusters using slitless spectroscopy are explained in this chapter. We found 157 e-stars in 42 open clusters, most of which are aged less than 100 Myr. The properties of these e-stars are discussed in the context of the clusters which harbour them. The youngest clusters to have CBe stars are IC 1590, NGC 637 and NGC 1624 (all 4 Myr old) while NGC 6756 (125 – 150 Myr) is the oldest cluster to have CBe stars. A detailed description of the studies conducted in each of these 42 clusters is given in this chapter. The optical V vs (B–V) colour magnitude diagram (CMD) with near infra-red (J–H) vs (H–K_s) colour-colour diagram (near-IR CCDm) are used to classify CBe stars from HAeBe stars in terms of near-IR excess. The spectra of the e-stars along with the line details are given.

1.4.3 Chapter 3

The statistical analysis of the collective sample of 157 e-stars are presented in this chapter. The optical photometric data are taken from the references listed in WEBDA (<http://www.univie.ac.at/webda/navigation.html>) while near-IR data are taken from 2MASS (<http://vizier.u-strasbg.fr/cgi-bin/VizieR?-source=II/246>). We have explored the role of evolution in Be phenomenon by locating the position

of Be stars in optical CMD, which was explained in previous chapter. The CBe stars are located all along the MS in the optical CMDs of clusters of all ages, which indicates that the Be phenomenon is unlikely only due to core contraction near the turn-off. The spectral type shows a bimodal distribution, peaking in B1–B2 and B6–B7 spectral bins. Rich clusters like NGC 7419, NGC 2345, NGC 663 and η & χ Persei are found to favour the formation of early-type Be stars. Most of the identified e-stars are CBe candidates (145 stars, 92%), while some are Herbig Be (HBe; 10, 6%) and Herbig Ae (HAe; 2, 2%) candidates. Our survey is more or less complete in the northern sky and it covers various star forming regions in the Galaxy like Perseus, Monoceros and Cygnus. Most of the surveyed clusters were found to have Be star fraction ($N(\text{Be})/N(\text{B}+\text{Be})$) to be less than 10%, which agrees with previous studies. We propose two mechanisms responsible for CBe phenomenon. The first mechanism is where some stars are born CBe stars, which may happen for spectral types later than B1. The second mechanism is where the B stars evolve to CBe stars, likely due to evolution, enhancement of rotation or structural changes at the end of the MS. This is likely to happen in early B spectral types.

1.4.4 Chapter 4

From the spectroscopic survey of 152 CBe stars, various spectral and evolutionary properties of stars and their disk are studied. Apart from the Balmer lines in emission, spectra of most of the stars show FeII, Paschen and OI lines in emission while HeI is seen in absorption. The Balmer decrement (D_{34}) of Be stars is found to show bimodal distribution with peak values of 2.5 and 3.9, unlike the typical nebular value of 2.7. Majority of surveyed stars (76%) may have optically thick disks, identified by the presence of large D_{34} , high H_α EW, metallic lines and high $(H-K_s)_0$ values. We found Lyman β fluorescence as the mechanism for the pro-

duction of 8446 Å line in 24% of the surveyed stars and 47% show line formation (OI 8446 Å & 7772 Å lines) due to collisional excitation. The rotation velocity of candidate stars is found to be in the range 150–300 km/s, which matches with the values of field CBe stars. The rotation velocity of the disks were found to range between 50–250 km/s, thus the circumstellar disk is found to lag behind the star by 50–100 km/s. The angular momentum evolution of stars and disk as a function of age and spectral type suggest bimodal origin of Be stars. Our results suggest that stars in the B0–B2 spectral bin are found to spin up towards the end of their MS life time, which is 10–20 Myr. Stars in the B0–B4 bin show enhanced H_{α} emission at the end of their MS lifetime, as inferred from the enhancements observed at 12.5 and 25 Myr. All the above results indicate that the activity in early type Be stars gets accelerated towards the end of the MS evolution. Thus early type stars evolve to become Be stars. Similar variation in properties were not found for stars in the later spectral types (B4–A0), suggesting that the Be phenomenon differs in early and late type stars.

1.4.5 Chapter 5

H AeBe and CBe stars are e-stars in different evolutionary phases. The nature and formation of circumstellar disk in these stars are different. As explained in Chapter 3, we found that 8 percent of the surveyed e-stars belongs to HAeBe category. In this chapter we have identified sure candidates from optical and near-IR photometry, Spectral Energy Distribution (SED) and spectroscopy. We found 3 HBe and 2 HAe candidates from a sample of 157 e-stars. The age of these HAeBe stars, estimated using PMS isochrones, were found to range between 0.25 - 3 Myr. We combined the optical and near-IR photometry to estimate the duration of star formation in the clusters, Bochum 6, IC 1590, NGC 6823 and NGC 7380. We found ongoing star formation in all these clusters, with an appreciable number of

PMS stars. All the four clusters were found to be forming stars for the last 10 Myr.

1.4.6 Chapter 6

Summary of this thesis study is presented here along with the future plans.

Chapter 2

Survey of emission-line stars in young open clusters

2.1 Introduction

Open clusters are dynamically associated system of stars which are found to be formed from giant molecular clouds through bursts of star formation. Apart from the coeval nature of the stars, they are assumed to be at the same distance and have the same chemical composition. Hence it is a perfect place to study e-stars since we do not have a hold on these parameters in the field. Young open clusters are found to contain CBe stars of all spectral types.

In order to study the Be phenomenon, Schild and Romanishin (1976) identified 41 Be stars in 29 clusters. Abt (1979) found that the Be stars in clusters exhibit a relatively constant frequency, roughly equal to that of Be field stars. Lloyd Evans (1980) identified and studied Be stars in NGC 3766 and IC 2581. Mermilliod (1982) studied 94 Be stars in 34 open clusters. He found that the distribution of Be stars peaked at spectral type B1–B2 and B7–B8, confirming earlier results. He also found that the Be stars occupy the whole MS band and are not confined to the region of termination of the MS. Recently, McSwain and Gies (2005b) conducted a photometric survey of 55 southern open clusters and identified 52 definite Be stars and 129 probable candidates. They also reported that the spin-up effect

at the end of the MS phase cannot explain the observed distribution of Be stars while 73% of the candidates were spun-up by binary mass transfer. Keller et al. (2000, 2001) found most of the Be stars to be located close to the turn-off of the clusters they observed. Wisniewski and Bjorkman (2006) identified numerous candidate Be stars of spectral types B0–B5 in clusters of age 5–8 Myr, challenging the suggestion of Fabregat & Torrejon (2000) that CBe stars should only be found in clusters at least 10 Myr old. These results suggest that a significant number of B-type stars must emerge onto the ZAMS as rapid rotators. They detected an enhancement in the fractional content of early-type candidate Be stars in clusters of age 10–25 Myr, suggesting that the Be phenomenon does become more prevalent with evolutionary age. Wisniewski et al. (2007) performed detailed imaging polarization observations of six SMC and six LMC clusters, known to have large populations of B-type stars. Their results support the suggestion of Wisniewski and Bjorkman (2006) that CBe stars are present in clusters of age 5–8 Myr.

In this study, we have performed a systematic survey of young open clusters in the northern sky, in order to increase the sample of e-stars in clusters and to study their properties and resolve the above inconsistencies. We performed this survey during the period 2003–2006, using the method of slitless spectroscopy. Due to the location of this telescope, the survey mainly concentrated on clusters in the northern declinations and those north of the declination of -30° . Hence the objects in the RA range of 8 to 18 hours were not observed.

2.2 Observation & Analysis

2.2.1 Slitless Spectroscopy

The spectroscopic and the R band imaging observations of the clusters were obtained using the HFOSC instrument, available with the 2.0m Himalayan Chandra Telescope (HCT), located at HANLE and operated by the Indian Institute of Astrophysics. Details of the telescope and the instrument are available at the institute's homepage (<http://www.iiap.res.in/>). The CCD used for imaging is a $2\text{ K} \times 4\text{ K}$ CCD, where the central $2\text{ K} \times 2\text{ K}$ pixels were used for imaging. The pixel size is $15\ \mu$ with an image scale of $0.297\text{ arcsec/pixel}$. The total area observed is approximately $10 \times 10\text{ arcmin}^2$. The cluster region was observed in the slit-less spectral mode with grism as the dispersing element using the HFOSC in order to identify stars which show H_α in emission. This mode of observation using the HFOSC yields an image where the stars are replaced by their spectra. The cluster region was initially observed in R band to obtain the positions of stars. Then the grism was introduced to obtain the spectra. These two frames are blinked/combined in order to identify stars which show emission in slitless (dispersed) image. The broad band R filter ($7100\ \text{\AA}$, $\text{BW}=2200\ \text{\AA}$) and Grism 5 ($5200\text{--}10300\ \text{\AA}$, low resolution) of HFOSC CCD system were used in combination without any slit. This combination provides spectra in the H_α region. A sample spectral image of the cluster NGC 7419 is shown in figure 2.1. The integration time used to obtain this image is 10 minutes. The bead like enhancements over the continuum correspond to emission in H_α . The clusters were observed more than once to confirm detections and to detect variable e-stars. We have used graded exposures for regions where bright stars are present. The crowded clusters were rotated to account for the overlap of dispersed image. Certain clusters were imaged with H_α filters to check for nebulosity. We performed the observations during the period 2003–2006 and the log of the observations is given in <http://arxiv.org/pdf/0804.1498>.

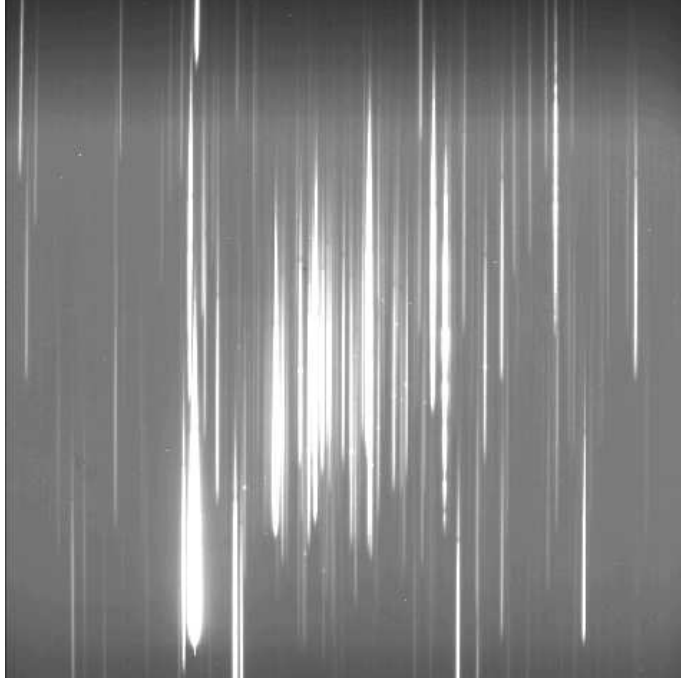


Figure 2.1: The slitless spectral image of NGC 7419. 25 e-stars are identified from this image.

The above mentioned technique identifies only stars with emission in H_α above the continuum. Stars with emission just enough to fill the H_α line, or those with partial filling cannot be identified. Thus this survey identifies stars with definite emission. Thus, the identifications, numbers and statistics presented can be taken as a lower limit.

2.2.2 Slit Spectroscopy

Slit spectra of 157 e-stars were obtained using Grism 7 ($3800 \text{ \AA} - 6800 \text{ \AA}$) and 167μ slit combination in the blue region which gives an effective resolution of 10 \AA around H_β line (dispersion relation = $1.47 \text{ \AA} / \text{pixel}$). The spectra in the red region were obtained using Grism 8 ($5800 \text{ \AA} - 9000 \text{ \AA}$) / 167μ slit setup, which gives an effective resolution of 7 \AA around H_α line profile ($1.25 \text{ \AA} / \text{pixel}$). The spectra

were found to have signal to noise ratio greater than 100. Spectrophotometric standards such as Fiege 34, Wolf 1346, BD 284211 and Hiltner 600, observed on corresponding nights were used for flux calibration. All the observed spectra were wavelength calibrated and corrected for instrument sensitivity using IRAF tasks. The resulting flux calibrated spectra were normalized and continuum fitted using IRAF tasks. We performed repeated observations for the candidate stars to check the consistency of line features and to study line profile variability. The slit spectra of the identified e-stars were taken during 2005–2008.

Table 2.1: List of surveyed clusters.

Cluster name	RA	Dec	Cluster name	RA	Dec
Basel 1	18:48:12	-05:51:00	Bochum 3	07:03:24	-05:03:00
Basel 4	05:48:30	+30:13:00	Bochum 4	07:31:37	-17:11:36
Basel 6	20:06:48	+38:21:00	Bochum 5	07:31:00	-16:56:00
Basel 7	06:36:36	+08:21:00	Bochum 6	07:32:00	-19:25:00
Basel 11b	05:58:12	+21:58:00	Bochum 14	18:02:00	-23:41:00
Basel 10	02:18:48	+58:19:00	BH245	17:46:16	-29:42:00
Berkeley 6	01:51:12	+61:05:00	Biurakan 2	20:09:12	+35:29:00
Berkeley 7	01:54:12	+62:22:00	Collinder 96	06:30:18	+02:52:00
Berkeley 11	04:20:36	+44:55:00	Collinder 110	06:38:24	+02:01:00
Berkeley 28	06:52:12	+02:56:00	Collinder 469	18:16:15	-18:16:00
Berkeley 43	19:15:36	+11:13:00	Czernik 8	02:33:00	+58:44:00
Berkeley 45	19:19:12	+15:43:00	Czernik 13	02:44:42	+62:21:00
Berkeley 62	01:01:00	+63:57:00	Czernik 20	05:20:06	+39:28:00
Berkeley 63	02:19:36	+63:43:00	Dolidze 25	06:45:06	+00:18:00
Berkeley 65	02:39:00	+60:25:00	Dolidze 42	20:19:42	+38:08:00
Berkeley 79	18:45:12	-01:13:00	Haffner 7	07:22:55	-29:30:00
Berkeley 82	19:11:24	+13:04:00	Haffner 16	07:50:20	-25:28:00
Berkeley 84	20:04:43	+33:54:18	Haffner 18	07:52:39	-26:23:00
Berkeley 86	20:20:24	+38:42:00	Haffner 19	07:52:47	-26:17:00
Berkeley 87	20:21:42	+37:22:00	Haffner 21	08:01:09	-27:13:00
Berkeley 90	20:35:18	+46:50:00	IC 348	03:44:30	+32:17:00
Berkeley 93	21:56:12	+63:56:00	IC 361	04:19:00	+58:18:00
Berkeley 94	22:22:42	+55:51:00	IC 1369	21:12:06	+47:44:00
Berkeley 96	22:29:24	+55:24:00	IC 1442	22:16:30	+54:03:00
Bochum 1	06:25:30	+19:46:00	IC 1590	00:52:48	+56:37:00
Bochum 2	06:48:54	+00:23:00	IC 1805	02:32:42	+61:27:00

Cluster name	RA	Dec	Cluster name	RA	Dec
IC 1848	02:51:12	+60:26:00	NGC 581	01:33:23	+60:39:00
IC 2157	06:05:00	+24:00:00	NGC 637	01:43:04	+64:02:24
IC 4996	20:16:30	+37:38:00	NGC 654	01:44:00	+61:53:06
IC 5146	21:53:24	+47:16:00	NGC 659	01:44:24	+60:40:24
King 1	00:22:00	+64:23:00	NGC 663	01:46:09	+61:14:06
King 4	02:35:42	+59:00:00	NGC 744	01:58:33	+55:28:24
King 6	03:28:06	+56:27:00	NGC 869	02:19:00	+57:07:42
King 10	22:54:54	+59:10:00	NGC 884	02:22:18	+57:08:12
King 12	23:53:00	+61:58:00	NGC 957	02:33:21	+57:33:36
King 13	00:10:06	+61:10:00	NGC 1220	03:11:40	+53:20:42
King 14	00:31:54	+63:10:00	NGC 1348	03:34:06	+51:24:30
King 21	23:49:54	+62:43:00	NGC 1444	03:49:25	+52:39:30
Kharchenko 1	06:08:48	+24:19:54	NGC 1502	04:07:50	+62:19:54
Markarian 38	18:15:17	-19:00:00	NGC 1513	04:09:57	+49:30:54
Markarian 50	23:15:18	+60:28:00	NGC 1605	04:34:53	+45:16:12
Mayer 2	04:19:45	+53:10:00	NGC 1624	04:40:36	+50:27:42
NGC 103	00:25:16	+61:19:24	NGC 1758	05:04:35	+23:47:54
NGC 133	00:31:19	+63:21:00	NGC 1778	05:08:04	+37:01:24
NGC 136	00:31:31	+61:30:36	NGC 1893	05:22:44	+33:24:42
NGC 146	00:33:03	+63:18:06	NGC 1912	05:28:40	+35:50:54
NGC 189	00:39:35	+61:05:06	NGC 1931	05:31:25	+34:14:42
NGC 225	00:43:39	+61:46:30	NGC 1960	05:36:18	+34:08:24
NGC 366	01:06:26	+62:13:48	NGC 2129	06:00:41	+23:19:06
NGC 433	01:15:11	+60:07:36	NGC 2168	06:09:00	+24:21:00
NGC 436	01:15:58	+58:48:42	NGC 2169	06:08:24	+13:57:54
NGC 457	01:19:35	+58:17:12	NGC 2175	06:09:39	+20:29:12

Cluster name	RA	Dec	Cluster name	RA	Dec
NGC 2186	06:12:07	+05:27:30	NGC 2467	07:52:26	-26:26:12
NGC 2264	06:40:58	+09:53:42	NGC 2483	07:55:39	-27:53:42
NGC 2270	06:43:58	+03:28:48	NGC 2539	08:10:37	-12:49:06
NGC 2302	06:51:55	-07:05:00	NGC 2571	08:18:56	-29:45:00
NGC 2309	06:56:03	-07:10:30	NGC 2678	08:50:02	+11:20:18
NGC 2311	06:57:46	-04:36:36	NGC 3231	10:27:29	+66:47:54
NGC 2319	07:00:43	+03:02:23	NGC 6520	18:03:24	-27:53:18
NGC 2323	07:02:42	-08:23:00	NGC 6525	18:02:06	+11:01:24
NGC 2324	07:04:07	+01:02:42	NGC 6531	18:04:13	-22:29:24
NGC 2343	07:08:06	-10:37:00	NGC 6604	18:18:03	-12:14:30
NGC 2345	07:08:18	-13:11:36	NGC 6611	18:18:48	-13:48:24
NGC 2353	07:14:30	-10:16:00	NGC 6613	18:19:58	-17:06:06
NGC 2355	07:16:59	+13:45:00	NGC 6618	18:20:47	-16:10:18
NGC 2362	07:18:41	-24:57:18	NGC 6649	18:33:27	-10:24:12
NGC 2364	07:20:46	-07:33:00	NGC 6664	18:36:42	-08:13:00
NGC 2367	07:20:06	-21:52:54	NGC 6683	18:42:13	-06:12:42
NGC 2368	07:21:06	-10:22:18	NGC 6694	18:45:18	-09:23:00
NGC 2374	07:23:56	-13:15:48	NGC 6704	18:50:45	-05:12:18
NGC 2383	07:24:40	-20:56:54	NGC 6709	18:51:18	+10:19:06
NGC 2384	07:25:10	-21:01:18	NGC 6756	19:08:42	+04:42:18
NGC 2396	07:28:01	-11:43:12	NGC 6832	19:48:15	+59:25:18
NGC 2401	07:29:24	-13:58:00	NGC 6823	19:43:09	+23:18:00
NGC 2414	07:33:12	-15:27:12	NGC 6830	19:50:59	+23:06:00
NGC 2421	07:36:13	-20:36:42	NGC 6834	19:52:12	+29:24:30
NGC 2428	07:39:25	-16:31:48	NGC 6871	20:05:59	+35:46:36
NGC 2439	07:40:45	-31:41:36	NGC 6882	20:11:47	+26:48:42
NGC 2453	07:47:35	-27:11:42	NGC 6910	20:23:12	+40:46:42

Cluster name	RA	Dec	Cluster name	RA	Dec
NGC 6913	20:23:57	+38:30:30	Ruprecht 44	07:58:51	-28:35:00
NGC 6991	20:54:32	+47:27:00	Ruprecht 49	08:03:15	-26:46:00
NGC 6996	20:56:30	+45:38:24	Ruprecht 135	17:58:12	-11:39:00
NGC 7024	21:06:09	+41:29:18	Ruprecht 141	18:31:19	-12:19:11
NGC 7039	21:10:48	+45:37:00	Ruprecht 144	18:33:34	-11:25:00
NGC 7063	21:24:21	+36:29:12	Ruprecht 148	04:46:30	+44:44:00
NGC 7067	21:24:23	+48:00:36	Stock 7	02:29:36	+60:39:00
NGC 7128	21:43:57	+53:42:54	Stock 8	05:27:36	+34:25:00
NGC 7160	21:53:40	+62:36:12	Stock 17	23:46:00	+62:11:00
NGC 7235	22:12:25	+57:16:12	Stock 24	00:39:42	+61:57:00
NGC 7245	22:15:11	+54:20:36	Teutsch 7	08:31:47	-39:04:48
NGC 7261	22:20:11	+58:07:18	Turner 1	19:48:25	+27:17:35
NGC 7296	22:28:02	+52:19:00	Turner 3	18:17:34	-18:51:50
NGC 7380	22:27:21	+58:07:54	Turner 4	18:17:08	-18:42:00
NGC 7419	22:54:20	+60:48:54	Turner 8	19:45:16	+27:50:30
NGC 7423	22:55:08	+57:05:54	Trumpler 1	01:35:42	+61:17:00
NGC 7510	23:11:03	+60:34:12	Trumpler 7	07:27:22	-23:57:00
NGC 7654	23:24:48	+61:35:36	Trumpler 9	07:55:40	-25:53:00
NGC 7788	23:56:45	+61:23:54	Trumpler 33	18:24:42	-19:43:00
NGC 7790	23:58:24	+61:12:30	Trumpler 35	18:42:54	-04:08:00
Roslund 3	19:58:42	+20:29:00	Tombaugh 4	02:28:54	+61:47:00
Roslund 4	20:04:54	+29:13:00	vdB 85	06:46:54	+01:20:00
Ruprecht 18	07:24:39	-26:13:00	vdB-Hagen 1	07:22:55	-29:30:00
Ruprecht 32	07:45:10	-25:32:00	vdB-Hagen 80	06:30:48	-09:40:00
Ruprecht 36	07:48:23	-26:18:00			

Table 2.2: List of e-stars from the slitless survey

Emission star	V mag	(B–V)	Spectral Type	RA	Dec
Berekeley 62(1)	14.445	0.496	B8	01:01:25.77	+63:58:24.0
Berekeley 63(1)	*	*	*	02:19:32.26	+63:43:46.4
Berekeley 86(9)	11.880	1.090	B5	20:20:10.75	+38:37:30.9
Berekeley 86(26)	12.620	1.130	B7	20:20:20.43	+38:37:36.7
Berekeley 87(1)	12.440	1.580	B1V	20:21:59.99	+37:26:24.1
Berekeley 87(2)	12.090	1.330	B1.5V	20:21:24.81	+37:22:48.3
Berekeley 87(3)	14.240	1.690	B4V	20:21:28.36	+37:26:18.9
Berekeley 87(4)	11.840	1.540	B1.5	20:21:33.55	+37:24:52.2
Berekeley 90(1)	*	*	*	20:35:41.56	+46:46:48.9
Bochum 2(1)	*	*	*	06:49:07.43	+00:21:56.3
Bochum 6(1)	13.300	0.590	B6	07:31:48.84	-19:27:37.2
Collinder 96(1)	8.750	0.330	B1	06:30:17.69	+02:50:52.8
Collinder 96(2)	10.630	0.320	B5.5V	06:30:30.02	+02:53:22.0
IC 1590(1)	13.430	0.390	B8.5	00:52:51.22	+56:36:56.0
IC 1590(2)	13.950	0.300	A0V	00:52:45.67	+56:37:53.8
IC 1590(3)	11.230	0.150	B2	00:52:44.38	+56:37:03.3
IC 4996(1)	11.890	0.540	B2	20:16:29.03	+37:38:52.3
King 10(A)	12.990	1.250	B1	22:54:53.19	+59:09:33.3
King 10(B)	13.000	1.110	B1	22:55:12.43	+59:07:46.5
King 10(C)	14.420	1.000	B2.5	22:55:06.47	+59:13:10.6
King 10(E)	13.750	1.010	B2	22:54:56.64	+59:10:22.7
King 21(B)	13.727	0.766	B3.5	23:49:46.84	+62:42:35.3
King 21(C)	11.436	0.628	B0.5	23:49:57.83	+62:42:07.4
King 21(D)	12.926	0.763	B2.5	23:49:59.04	+62:46:21.9
NGC 146(S1)	11.980	0.330	B2V	00:32:44.72	+63:18:15.6
NGC 146(S2)	13.650	0.380	B6.5V	00:33:18.17	+63:18:37.8

Emission star	V mag	(B-V)	Spectral Type	RA	Dec
NGC 436(1)	13.652	0.390	B7V	01:15:56.29	+58:48:12.4
NGC 436(2)	13.270	0.390	B6	01:15:20.26	+58:50:02.3
NGC 436(3)	*	*	*	01:16:13.12	+58:52:55.0
NGC 436(4)	13.041	0.359	B5.5V	01:15:40.89	+58:49:02.2
NGC 436(5)	12.440	0.821	B3	01:15:58.39	+58:49:15.1
NGC 457(1)	13.033	0.297	B6	01:19:02.36	+58:19:20.2
NGC 457(2)	13.471	0.350	B7V	01:19:32.98	+58:17:25.5
NGC 581(1)	11.355	0.294	B2	01:33:41.87	+60:42:19.4
NGC 581(2)	10.590	0.170	B1V	01:33:24.25	+60:39:44.9
NGC 581(3)	11.889	0.185	B3V	01:33:15.16	+60:41:01.7
NGC 581(4)	11.755	0.249	B2.5	01:33:10.96	+60:39:30.8
NGC 637(1)	13.645	0.495	B6.5V	01:43:22.10	+64:01:18.3
NGC 654(2)	12.292	0.816	B2	01:44:02.95	+61:53:20.3
NGC 659(1)	12.862	0.445	B2.5	01:44:33.09	+60:40:56.2
NGC 659(2)	10.691	0.496	B0	01:44:28.22	+60:40:03.4
NGC 659(3)	12.385	0.329	B2	01:44:22.80	+60:40:43.8
NGC 663(1)	13.993	0.633	B7V	01:46:02.06	+61:15:04.2
NGC 663(2)	11.470	0.660	B1	01 46 06.09	+61 13 39.1
NGC 663(3)	13.249	0.677	B5	01:46:14.01	+61:13:43.9
NGC 663(4)	12.261	0.559	B2V	01:46:30.63	+61:14:29.2
NGC 663(5)	11.891	0.450	B2	01:45:46.39	+61:09:20.9
NGC 663(6)	13.580	0.600	B6	01:46:24.41	+61:10:37.3
NGC 663(7)	10.203	0.658	B0	01 46 35.53	+61 15 47.88
NGC 663(9)	12.334	0.579	B2.5V	01:46:35.60	+61:13:39.1
NGC 663(11)	11.924	0.539	B2V	01 46 20.21	+61 14 21.57
NGC 663(12)	12.490	0.521	B2.5	01:45:37.81	+61:07:59.1
NGC 663(12V)	10.620	0.570	B0.5	01:46:26.84	+61:07:41.7

Emission star	V mag	(B-V)	Spectral Type	RA	Dec
NGC 663(13)	13.535	0.598	B6	01 46 34.85	+61 06 27.75
NGC 663(14)	13.455	0.635	B5.5V	01 46 59.55	+61 12 29.8
NGC 663(15)	12.620	0.720	B2.5	01 47 39.34	+61 18 20.7
NGC 663(16)	10.090	0.420	B0/O9	01 45 18.02	+61 06 56.48
NGC 663(24)	12.678	0.562	B2.5V	01 46 28.61	+61 13 50.42
NGC 663(P5)	11.900	0.650	B2	01 45 56.11	+61 12 45.41
NGC 663(P6)	10.560	0.650	B0.5	01 45 59.30	+61 12 45.67
NGC 663(P8)	12.573	0.596	B2.5V	01 45 39.63	+61 12 59.6
NGC 663(P23)	12.362	-0.282	B2.5	01:47:03.74	+61:17:32.0
NGC 663(P25)	11.881	0.423	B2	01:47:26.76	+61:08:44.2
NGC 663(P151)	14.200	*	B8	01 47 17.46	+61 13 18.2
NGC 869(1)	9.559	0.493	B0	02:19:26.65	+57:04:42.1
NGC 869(2)	11.645	0.437	B2.5	02:19:28.95	+57:11:25.1
NGC 869(3)	11.003	0.530	B2	02:19:28.98	+57:07:05.3
NGC 869(4)	9.127	0.385	B0/O9	02:18:47.98	+57:04:03.0
NGC 869(5)	10.229	0.420	B1	02:19:13.77	+57:07:45.0
NGC 869(6)	12.370	0.395	B5V	02:19:08.73	+57:03:50.0
NGC 884(1)	10.671	0.417	B1	02:22:48.07	+57:12:03.6
NGC 884(2)	9.700	0.386	B0.5	02:22:06.59	+57:05:24.6
NGC 884(3)	10.162	0.325	B0.5V	02:21:52.95	+57:09:59.3
NGC 884(4)	11.706	0.412	B2.5	02:21:44.56	+57:10:53.9
NGC 884(5)	9.306	0.341	B0	02:21:43.39	+57:07:31.7
NGC 884(6)	10.938	0.362	B2	02:22:02.51	+57:09:21.1
NGC 957(1)	11.130	0.660	B2	02:33:10.45	+57:32:52.8
NGC 957(2)	11.990	0.540	B2.5	02:33:39.44	+57:33:51.7
NGC 1220(1)	13.798	0.693	B9.5	03:11:40.86	+53:21:03.8
NGC 1624(1)	13.393	0.623	B1	04:40:37.25	+50:27:40.4
NGC 1893(1)	13.500	0.740	B6	05:22:42.95	+33:25:05.3

Emission star	V mag	(B-V)	Spectral Type	RA	Dec
NGC 2345(2)	11.860	0.390	B5.5V	07:08:10.47	-13:15:36.7
NGC 2345(5)	13.420	0.540	B9	07:08:07.53	-13:13:20.7
NGC 2345(20)	13.900	0.690	B9	07:08:12.49	-13:10:35.8
NGC 2345(24)	13.980	1.000	B6V	07:08:11.59	-13:09:27.8
NGC 2345(27)	13.660	0.630	B8.5	07:08:16.09	-13:10:03.6
NGC 2345(32)	13.860	0.610	A5	07:08:19.58	-13:09:41.0
NGC 2345(35)	10.930	0.510	B2	07:08:22.84	-13:10:16.5
NGC 2345(44)	13.320	0.400	A0/B9	07:08:25.55	-13:12:01.8
NGC 2345(59)	13.050	0.390	A0/B8	07:08:28.04	-13:15:35.8
NGC 2345(61)	13.360	0.430	A0/B9	07:08:29.85	-13:13:14.7
NGC 2345(X1)	*	*	*	07:07:58.15	-13:10:59.6
NGC 2345(X2)	*	*	*	07:08:12.50	-13:09:55.8
NGC 2414(1)	*	*	*	07:33:06.38	-15:26:35.8
NGC 2414(2)	*	*	*	07:33:20.44	-15:27:07.0
NGC 2421(1)	11.480	0.240	B3.5V	07:36:06.68	-20:37:57.5
NGC 2421(2)	12.465	0.262	B7V	07:36:02.96	-20:37:39.1
NGC 2421(3)	12.900	*	*	07:36:00.06	-20:38:46.0
NGC 2421(4)	12.240	0.260	B6.5V	07:36:21.95	-20:37:09.6
NGC 6649(1)	11.770	1.300	B1.5	18:33:28.27	-10:24:07.3
NGC 6649(2)	15.210	1.30	A0/1	18:33:26.16	-10:23:35.9
NGC 6649(3)	14.980	1.260	A0	18:33:23.95	-10:24:41.2
NGC 6649(4)	14.070	2.100	B7	18:33:36.29	-10:22:52.4
NGC 6649(5)	14.080	1.500	B7	18:33:25.34	-10:20:51.5
NGC 6649(6)	14.930	1.290	A0	18:33:34.10	-10:26:04.8
NGC 6649(7)	*	*	*	18:33:12.32	-10:25:13.5
NGC 6756(2)	14.299	0.965	B3.5	19:08:40.15	+04:43:51.2
NGC 6756(3)	14.052	0.947	B2.5	19:08:46.24	+04:40:23.2

Emission star	V mag	(B-V)	Spectral Type	RA	Dec
NGC 6823(1)	13.730	0.660	B6.5	19:43:04.38	+23:18:48.8
NGC 6834(1)	13.230	0.540	B7.5	19:52:06.48	+29:24:37.7
NGC 6834(2)	12.430	0.720	B5.5	19:52:09.53	+29:23:34.0
NGC 6834(3)	13.260	0.640	B8	19:52:21.21	+29:20:20.4
NGC 6834(4)	12.900	0.580	B6.5	19:52:16.62	+29:25:15.0
NGC 6910(A)	13.600	1.060	B9.5	20:23:11.74	+40:43:25.9
NGC 6910(B)	12.360	0.480	B6	20:23:09.74	+40:45:53.0
NGC 7039(1)	13.750	0.330	B0V	21:11:00.95	+45:39:41.4
NGC 7128(1)	13.210	0.800	B1V	21:44:02.92	+53:42:12.4
NGC 7128(2)	14.440	0.740	B2.5	21:44:05.25	+53:42:36.8
NGC 7128(3)	*	*	*	21:43:33.57	+53:45:32.3
NGC 7235(1)	12.150	0.800	B0.5	22:12:19.54	+57:16:04.1
NGC 7261(1)	*	*	*	22:19:51.44	+58:08:53.5
NGC 7261(2)	*	*	*	22:20:10.09	+58:06:34.3
NGC 7261(3)	*	*	*	22:20:13.31	+58:07:45.5
NGC 7380(1)	13.590	0.560	B9	22:47:42.62	+58:07:46.8
NGC 7380(2)	13.550	0.600	B9	22:47:40.12	+58:09:03.7
NGC 7380(3)	10.160	0.390	B0.5V	22:47:49.56	+58:08:49.6
NGC 7380(4)	14.720	1.550	A1	22:47:22.39	+58:01:21.5
NGC 7419(A)	14.340	1.640	B1.5	22:54:36.68	+60:48:35.2
NGC 7419(B)	14.770	1.530	B2	22:54:27.12	+60:48:52.2
NGC 7419(C)	14.060	1.430	B1	22:54:25.62	+60:49:01.4
NGC 7419(D)	15.560	1.500	B2.5	22:54:23.76	+60:49:31.0
NGC 7419(E)	16.560	1.700	B6	22:54:24.36	+60:47:36.2
NGC 7419(F)	*	*	*	22:54:24.28	+60:47:01.6
NGC 7419(G)	14.250	1.540	B1.5	22:54:20.49	+60:49:52.5
NGC 7419(H)	15.670	1.450	B2.5V	22:54:19.54	+60:48:52.0

Emission star	V mag	(B–V)	Spectral Type	RA	Dec
NGC 7419(I)	14.240	1.510	B1.5	22:54:19.65	+60:48:35.8
NGC 7419(I1)	*	*	*	22:53:53.24	+60:48:08.3
NGC 7419(J)	13.930	1.620	B1	22:54:15.34	+60:49:49.9
NGC 7419(K)	14.790	1.510	B2	22:54:20.47	+60:48:53.9
NGC 7419(L)	15.090	1.540	B2	22:54:17.86	+60:48:57.2
NGC 7419(M)	13.720	1.600	B0.5	22:54:14.55	+60:48:39.1
NGC 7419(N)	15.370	1.740	B2.5	22:54:15.90	+60:47:49.2
NGC 7419(O)	*	*	*	22:54:07.03	+60:48:18.0
NGC 7419(P)	15.360	1.630	B2.5	22:54:13.97	+60:46:20.4
NGC 7419(Q)	15.970	1.640	B4	22:54:14.83	+60:51:22.7
NGC 7419(R)	16.090	1.480	B4V	22:54:17.07	+60:51:37.6
NGC 7419(1)	15.730	1.530	B3	22:54:29.22	+60:49:08.0
NGC 7419(2)	15.350	1.380	B2.5	22:54:26.46	+60:49:06.3
NGC 7419(3)	14.190	1.620	B1	22:54:22.56	+60:49:53.1
NGC 7419(4)	14.170	1.620	B1	22:54:23.00	+60:50:04.4
NGC 7419(5)	15.400	1.870	B2.5	22:54:07.58	+60:50:22.9
NGC 7419(6)	16.260	1.590	B5	22:54:26.05	+60:47:57.1
NGC 7510(1A)	13.920	0.810	B2.5	23:10:57.76	+60:33:57.1
NGC 7510(1B)	14.750	0.880	B5	23:11:08.53	+60:35:03.9
NGC 7510(1C)	14.530	1.110	B4	23:10:47.75	+60:31:52.7
Roslund 4(1)	16.100	1.280	A1	20:04:50.44	+29:11:06.1
Roslund 4(2)	10.810	0.890	B0	20:04:47.07	+29:10:03.2

Table 2.3: Spectral lines identified in e-stars

Emission Star	Nature of H_{β}	FeII lines	OI lines	CaII triplet	Paschen lines	Other features
Berkeley 62(1)	$H_{\beta}(e)$	none	8446(e)	all in a	P11(eina),P12,P14, P19(a)	
Berkeley 63(1)	$H_{\beta}(eina)$	4e	7772(a),8446(e)	8662(a)	P11(eina),P12(a)	
Berkeley 86(9)	$H_{\beta}(a)$	2a,1e	7772(a), 8446(e)	all in a	P11,P12,P14,P19(a)	
Berkeley 86(26)	$H_{\beta}(e)$	4a,2e	7772(a), 8446(e)	all in e	7 in e	
Berkeley 87(1)	$H_{\beta}(eina)$	none	8446(e)	all in e	P11,P12,P17	
Berkeley 87(2)	$H_{\beta}(e)$	2e,1a	8446(e)	all in e	P11(a),P12(e),P14(e)	
Berkeley 87(3)	$H_{\beta}(\text{fill-in})$	none	7772(e), 8446(e)	all in e	5 in e	
Berkeley 87(4)	$H_{\beta}(e)$	7e,1a	7772(e), 8446(e)	all in e	8 in e	
Berkeley 90(1)	$H_{\beta}(e)$	6e	7772(e), 8446(e)	all in e	P14(e),P19(e)	
Bochum 2(1)	$H_{\beta}(\text{fill-in})$	5169(a)	7772(a), 8446(e)	8542(a),8662(a)	8 in a	SiII in a
Bochum 6(1)	$H_{\beta}(e)$	4 [FeII] in e, 5e	7772(e), 8446(e)	all in e	11 in e	SiII in a
Collinder 96(1)	$H_{\beta}(e)$	4e	7772(e), 8446(e)	all in e	5 in e	
Collinder 96(2)	$H_{\beta}(a)$	none	7772(a)	all in a	P11,P12,P14	
IC 1590(1)	$H_{\beta}(eina)$	11e	7772(a), 8446(e)	all in e	5 in e	SiII in a
IC 1590(2)	$H_{\beta}(eina)$	14e	7772(e), 8446(e)	all in e	4 in e	
IC 1590(3)	$H_{\beta}(a)$	none	7772(a)	all in a	P11,P12,P14(a)	

Emission Star	Nature of H_{β}	FeII lines	OI lines	CaII triplet	Paschen lines	Other features
IC 4996(1)	H_{β} (eina)	1e	8446(e)	8662(a)	P11,P12(eina),P14, P17(e)	
King 10(A)	H_{β} (eina)	2e	8446(e)	all in e	P11,P12,P14(e), P17(e),P19	6347(SiII)
King 10(B)	H_{β} (eina)	none	8446(e)	all in e	2e,3a	
King 10(C)	H_{β} (eina)	1e	8446(e)	all in e	P11,P12(eina),P14(e)	
King 10(E)	H_{β} (eina)	none	8446(e)	all in e	6e,2a	
King 21(B)	H_{β} (eina)	none	7772(a), 8446(e)	all in a	9a	
King 21(C)	H_{β} (a)	none	8446(e)	8542(e),8662(a)	7a,1e	
King 21(D)	H_{β} (eina)	none	8446(e)	all in a	6a	
NGC 146(S1)	H_{β} (eina)	11a,1e	7772(a), 8446(e)	all in e	8a,2e	SiII in a
NGC 146(S2)	H_{β} (eina)	1a	8446(e)	none	none	
NGC 436(1)	H_{β} (a)	none	7772(a), 8446(e)	all in a	7a	SiII in a
NGC 436(2)	H_{β} (eina)	9e	7772(e), 8446(e)	2e,8662(a)	4e,2a	
NGC 436(3)	H_{β} (a)	2a,1e	7772(a), 8446(a)	2a,8662(e)	7a,2e	
NGC 436(4)	H_{β} (a)	3a,1e	7772(a), 8446(e)	all in a	10a	SiII in a
NGC 436(5)	H_{β} (eina)	8e	7772(e), 8446(e)	all in e	8e	
NGC 457(1)	H_{β} (eina)	none	8446(e)	all in dpe	5e	

Emission Star	Nature of H_{β}	FeII lines	OI lines	CaII triplet	Paschen lines	Other features
NGC 457(2)	H_{β} (eina)	8a,2e	7772(a), 8446(e)	all in a	8a,1e	SiII in a
NGC 581(1)	H_{β} (eina)	2e	7772(e), 8446(e)	all in e	P14(e),P17(a)	
NGC 581(2)	H_{β} (eina)	4a,3e	7772(a), 8446(e)	all in e	8a,2e	SiII in a
NGC 581(3)	H_{β} (eina)	4e,1a	7772(e), 8446(e)	all in e	8e	
NGC 581(4)	H_{β} (a)	none	7772(a), 8446(e)	all in a	9a	SiII in a
NGC 637(1)	H_{β} (eina)	none	8446(e)	all in e	3e,3a	
NGC 654(2)	H_{β} (e)	9e,3a	7772(e), 8446(e)	all in e	5e	
NGC 659(1)	H_{β} (eina)	2dpe	7772(dpe), 8446(e)	all in dpe	P14(dpe)	
NGC 659(2)	H_{β} (eina)	none	7772(a), 8446(a)	all in a	4a	
NGC 659(3)	H_{β} (eina)	none	7772(e), 8446(e)	all in e	4e,1a	
NGC 663(1)	H_{β} (eina)	2a,1e	7772(e), 8446(e)	all in e	4e,5a	
NGC 663(2)	H_{β} (e)	5e,4a	7772(e), 8446(e)	all in e	9e,2a	
NGC 663(3)	H_{β} (fill-in)	6a,2e	7772(a), 8446(e)	all in a	12a	SiII in a
NGC 663(4)	H_{β} (eina)	5e	7772(e), 8446(e)	all in e	10e,2a	
NGC 663(5)	H_{β} (eina)	10e	7772(e), 8446(e)	all in e	10e,1a	6347(SiII,e)
NGC 663(6)	H_{β} (eina)	3e	none	all in a	2a,3e	6371(SiII)
NGC 663(7)	H_{β} (fill-in)	1e	7772(a), 8446(e)	all in a	5a,2e	6347(SiII)
NGC 663(9)	H_{β} (eina)	16e	7772(e), 8446(e)	all in e	9e,2a	

Emission Star	Nature of H_{β}	FeII lines	OI lines	CaII triplet	Paschen lines	Other features
NGC 663(11)	H_{β} (eina)	5e	7772(e), 8446(e)	all in e	8e,2a	
NGC 663(12)	H_{β} (eina)	7e	8446(e)	all in e	7e,3a	
NGC 663(12V)	H_{β} (e)	12e	7772(e), 8446(e)	all in e	7e,2a	
NGC 663(13)	H_{β} (a)	3a,1e	7772(a), 8446(e)	all in a	9a	SiII in a
NGC 663(14)	H_{β} (eina)	4e,2a	7772(e), 8446(e)	8662(eina)	6a	
NGC 663(15)	H_{β} (e)	13e	7772(e), 8446(e)	all in e	7e,2a	
NGC 663(16)	H_{β} (eina)	1e	8446(e)	all in e	4e,1a	
NGC 663(24)	H_{β} (a)	1a,1e	7772(a)	all in a	P11,P12,P14	
NGC 663(P5)	H_{β} (eina)	7e	7772(e), 8446(e)	all in e	8e	7896(MgII,e)
NGC 663(P6)	H_{β} (a)	1e	8446(e)	all in e	7e,1a	
NGC 663(P8)	H_{β} (eina)	2a,2e	8446(e)	all in e	7e,4a	
NGC 663(P23)	H_{β} (e)	6e	7772(e), 8446(e)	all in e	5e,4a	6371(SiII)
NGC 663(P25)	H_{β} (eina)	5e	7772(a), 8446(e)	all in e	10e	6371(SiII)
NGC 663(P151)	H_{β} (a)	3a	7772(a), 8446(e)	all in a	8a	6371(SiII)
NGC 869(1)	H_{β} (e)	19e	7772(e), 8446(e)	all in e	7e,1a	6347(SiII,e)
NGC 869(2)	H_{β} (eina)	7e,1a	7772(e), 8446(e)	all in e	7e,1a	
NGC 869(3)	H_{β} (eina)	2e	7772(e), 8446(e)	all in e	5e,1a	
NGC 869(4)	H_{β} (a)	5e	7772(a), 8446(e)	2a,8446(e)	3a	

Emission Star	Nature of H_{β}	FeII lines	OI lines	CaII triplet	Paschen lines	Other features
NGC 869(5)	H_{β} (a)	8e	7772(e), 8446(e)	all in e	3e,1a	
NGC 869(6)	H_{β} (e)	6a,3e	7772(a), 8446(e)	2a, 8662(e)	5a,2e	SiII in a
NGC 884(1)	H_{β} (eina)	none	8446(e)	all in e	5e	
NGC 884(2)	H_{β} (e)	25e	7772(e), 8446(e)	all in e	8e	SiII in e,7896(MgII,e)
NGC 884(3)	H_{β} (eina)	3e	7772(a)	all in a	4a,3e	
NGC 884(4)	H_{β} (eina)	5e	7772(e), 8446(e)	8498(e), 8542(e)	6e,2a	
NGC 884(5)	H_{β} (eina)	1e	7772(e), 8446(e)	all in e	8e,1a	SiII in e
NGC 884(6)	H_{β} (a)	6e,2a	7772(e), 8446(e)	all in a	7a,1e	
NGC 957(1)	H_{β} (e)	9e	7772(e), 8446(e)	all in e	7e,1a	SiII in e,7896(MgII)
NGC 957(2)	H_{β} (eina)	6e	7772(e), 8446(e)	all in e	6e	7896(MgII)
NGC 1220(1)	H_{β} (eina)	2e	7772(e), 8446(e)	all in e	5e	
NGC 1624(1)	H_{β} (e)	2e	8446(e)	all in e	3e	
NGC 1893(1)	H_{β} (e)	18e	7772(e), 8446(e)	all in e	5e	6347(SiII,e)
NGC 2345(2)	H_{β} (fill-in)	1e	7772(a), 8446(e)	all in a	4a	SiII in a
NGC 2345(5)	H_{β} (eina)	4e	none	none	none	6347(SiII)
NGC 2345(20)	H_{β} (eina)	3e	8446(e)	8662(a)	2a	
NGC 2345(24)	H_{β} (eina)	none	8446(e)	2e,1a	2a,1e	

Emission Star	Nature of H_{β}	FeII lines	OI lines	CaII triplet	Paschen lines	Other features
NGC 2345(27)	H_{β} (eina)	14e	7772(e), 8446(e)	all in e	5e,1a	6347(SiII)
NGC 2345(32)	H_{β} (fill-in)	none	8446(e)	8662(a)	2a	SiII in a
NGC 2345(35)	H_{β} (a)	none	8446(e)	2a,1e	2a,1e	SiII in a
NGC 2345(44)	H_{β} (fill-in)	none	7772(a), 8446(e)	8542(a), 8662(a)	2a,1e	6371(SiII)
NGC 2345(59)	H_{β} (eina)	4e	7772(e), 8446(e)	8498(e), 8542(e)	4e,2a	
NGC 2345(61)	H_{β} (a)	none	7772(a), 8446(e)	8542(a)	3a,2e	6347(SiII)
NGC 2345(X1)	H_{β} (eina)	1e,1a	8446(e)	8662(a)	3a,1e	6371(SiII)
NGC 2345(X2)	H_{β} (eina)	5e	7772(e), 8446(e)	all in e	4e	
NGC 2414(1)	H_{β} (eina)	4e,1a	7772(a), 8446(e)	8498(e), 8662(a)	3a	
NGC 2414(2)	H_{β} (eina)	2e	7772(e), 8446(e)	all in e	7e,1a	
NGC 2421(1)	H_{β} (eina)	11e	7772(e), 8446(e)	all in e	7e	
NGC 2421(2)	H_{β} (a)	none	7772(e), 8446(e)	8542(a), 8662(a)	4a	
NGC 2421(3)	H_{β} (eina)	4e	8446(e)	8542(e), 8662(a)	3a,2e	
NGC 2421(4)	H_{β} (eina)	5e	8446(e)	all in e	5e,2a	
NGC 6649(1)	H_{β} (e)	11e	7772(e), 8446(e)	all in e	9e,1a	
NGC 6649(2)	H_{β} (eina)	5e	8446(e)	all in e	5e,2a	
NGC 6649(3)	H_{β} (fill-in)	4e	7772(e), 8446(e)	2e,1a	5a,2e	6371(SiII)
NGC 6649(4)	H_{β} (eina)	5e	7772(a), 8446(e)	all in e	10e,2a	SiII in a

Emission Star	Nature of H_{β}	FeII lines	OI lines	CaII triplet	Paschen lines	Other features
NGC 6649(5)	H_{β} (fill-in)	2e	8446(e)	all in e	8e,2a	6371(SiII)
NGC 6649(6)	H_{β} (fill-in)	5e	8446(e)	2e,1a	5e,4a	6371(SiII)
NGC 6649(7)	H_{β} (eina)	14e	7772(e), 8446(e)	all in e	4a,4e	SiII in a
NGC 6756(2)	H_{β} (eina)	4e,1a	8446(e)	8542(a), 8662(a)	4a	
NGC 6756(3)	H_{β} (eina)	1e,1a	8446(e)	all in a	6a	5577([OI],e)
NGC 6823(1)	H_{β} (eina)	1a	7772(e), 8446(e)	all in e	5e	
NGC 6834(1)	H_{β} (eina)	18e	7772(e), 8446(e)	all in e	7e	5463(NII,e)
NGC 6834(2)	H_{β} (eina)	18e,2a	7772(e), 8446(e)	all in e	11e,1a	
NGC 6834(3)	H_{β} (a)	5e	8446(e)	8662(a)	3a,2e	
NGC 6834(4)	H_{β} (a)	2e	7772(a), 8446(e)	all in a	3a	
NGC 6910(A)	H_{β} (eina)	5e,4a	7772(a), 8446(e)	all in a	8a	7896(MgII,e),SiII in a
NGC 6910(B)	H_{β} (a)	2e	none	8662(a)	3a,1e	
NGC 7039(1)	H_{β} (eina)	16e	7772(e), 8446(e)	all in e	7e	
NGC 7128(1)	H_{β} (eina)	14e	7772(e), 8446(e)	all in e	8e	
NGC 7128(2)	H_{β} (a)	2a	7772(a), 8446(e)	all in a	7a	SiII in a
NGC 7128(3)	H_{β} (eina)	3a,1e	8446(e)	8542(a), 8662(a)	3a,2e	
NGC 7235(1)	H_{β} (ce)	16e	7772(e), 8446(e)	all in e	6e	
NGC 7261(1)	H_{β} (ce)	13e	7772(e), 8446(e)	all in e	10e	7896(MgII,e),SiII in e

Emission Star	Nature of H_{β}	FeII lines	OI lines	CaII triplet	Paschen lines	Other features
NGC 7261(2)	H_{β} (eina)	1e	8446(e)	all in e	6e	
NGC 7261(3)	H_{β} (eina)	13e	7772(e), 8446(e)	all in e	8e	7896(MgII,e),SiII in e
NGC 7380(1)	H_{β} (fill-in)	1e,2a	7772(a), 8446(a)	all in a	5a,5e	SiII in a
NGC 7380(2)	H_{β} (eina)	7e	7772(e), 8446(e)	8498(e), 8542(e)	8e,2a	
NGC 7380(3)	H_{β} (a)	16e	7772(e), 8446(e)	all in e	5a,4e	5942(NII,e)
NGC 7380(4)	H_{β} (e)	10e	7772(e), 8446(e)	all in e	11e	2NII(e),HeI(e),NaI(e),KI(e)
NGC 7419(A)	H_{β} (e)	13e	7772(e), 8446(e)	all in e	12e,2a	6371(SiII,e)
NGC 7419(B)	H_{β} (e)	10e	7772(e), 8446(e)	all in e	10e,2a	
NGC 7419(C)	H_{β} (a)	1e	7772(a), 8446(e)	all in a	5a,2e	5005(NII,e)
NGC 7419(D)	H_{β} (eina)	6e	7772(e), 8446(e)	all in e	11e,2a	6347(SiII,e),2MgII(e)
NGC 7419(E)	H_{β} (e)	4e	7772(e), 8446(e)	all in e	8e,1a	
NGC 7419(F)	H_{β} (a)	1e	8446(e)	8498(e), 8542(e)	none	
NGC 7419(G)	H_{β} (e)	11e	7772(e), 8446(e)	all in e	11e	
NGC 7419(H)	H_{β} (a)	4e	7772(a), 8446(e)	all in a	4a,1e	
NGC 7419(I)	H_{β} (eina)	9e	7772(e), 8446(e)	all in e	10e,1a	4131(SiII)
NGC 7419(II)	H_{β} (eina)	none	7772(a), 8446(e)	none	3a,1e	
NGC 7419(J)	H_{β} (eina)	5e	7772(e), 8446(e)	all in e	13e	
NGC 7419(K)	H_{β} (a)	3e	7772(a), 8446(e)	all in a	8a	

Emission Star	Nature of H_{β}	FeII lines	OI lines	CaII triplet	Paschen lines	Other features
NGC 7419(L)	H_{β} (e)	14e	7772(e), 8446(e)	all in e	9e,2a	6347(SiII,e),5530(NII,e)
NGC 7419(M)	H_{β} (e)	14e	7772(e), 8446(e)	all in e	11e,2a	6371(SiII)
NGC 7419(N)	H_{β} (e)	12e	7772(e), 8446(e)	all in e	11e,2a	7896(MgII)
NGC 7419(O)	H_{β} (a)	3e	7772(e), 8446(e)	all in e	12e,2a	7877(MgII,e)
NGC 7419(P)	H_{β} (a)	5e	7772(a), 8446(e)	all in a	11a,2e	5684(NII,e),6371(SiII),7896(MgII)
NGC 7419(Q)	H_{β} (e)	12e,1a	7772(e), 8446(e)	all in e	5e,5a	6347(SiII),7877(MgII)
NGC 7419(R)	H_{β} (e)	5e	7772(a), 8446(e)	8498(e),8542(dpe)		
NGC 7419(1)	H_{β} (e)	5e	7772(e), 8446(e)	all in e	7e,1a	7896(MgII)
NGC 7419(2)	H_{β} (a)	2e	7772(a), 8446(e)	all in e	8e,2a	
NGC 7419(3)	H_{β} (e)	9e	7772(e), 8446(e)	all in e	8e	7896(MgII)
NGC 7419(4)	H_{β} (e)	7e	8446(e)	8498(e), 8542(e)	6e,3a	
NGC 7419(5)	H_{β} (e)	6e,1a	7772(e), 8446(e)	all in e	12e,2a	5711(NII,e),SiII(e),7896(MgII)
NGC 7419(6)	H_{β} (e)	8e	8446(e)	all in e	6e	6347(SiII)
NGC 7510(A)	H_{β} (eina)	7e,3a	7772(a), 8446(e)	all in e	8e,1a	
NGC 7510(B)	H_{β} (eina)	5e,1a	7772(a), 8446(e)	all in e	8e,1a	
NGC 7510(C)	H_{β} (e)	12e	7772(a), 8446(e)	all in e	7e,3a	MgII(e),SiII(e)
Roslund 4(1)	H_{β} (a)	1e,2a	7772(a), 8446(e)	8498(e)	3a	5577([OI],e)
Roslund 4(2)	H_{β} (e)	17e,1a	7772(a), 8446(e)	all in e	7e	SiII(a), 7896(MgII,e)

e - emission profile, a - absorption, dpe - double-peaked emission

eina - emission in absorption, ce - core-emission

2.2.3 Photometry

In order to study the identified e-stars as well as the hosting cluster in detail, we have taken the photometric data from the references listed in WEBDA. For a few clusters like King 21, NGC 146, NGC 6756, NGC 6834 and NGC 7419, we have obtained the photometry using the HCT. After cross-correlating the e-stars from our R band image with the location given in the reference, the photometric parameters were taken. We have also taken the $E(B-V)$ and distance values listed in the reference to estimate the absolute magnitude M_V and $(B-V)_0$. The spectral type is determined from the estimated M_V and $(B-V)_0$ using Schmidt-Kaler (1982).

The optical data were combined with near-IR photometry to look for near-IR excess in e-stars. The near-IR photometric magnitudes in J, H, K_s bands for all the candidate stars are taken from 2MASS database. The $(J-H)$ and $(H-K_s)$ colours obtained were transformed to Koornneef (1983) system using the transformation relations by Carpenter (2001). For brevity, we have used $(H-K)$ throughout the text eventhough it means $(H-K_s)$ colour. The colours are de-reddened using the relation from Rieke and Lebofsky (1985), since the slope of the reddening vector matches with this extinction relation. For this purpose we have made use of the optical colour excess $E(B-V)$, which corresponds to the reddening of the cluster to which the e-star is associated.

2.3 Analysis of clusters with e-stars

Among the 207 clusters, 23 clusters do not have reliable age estimates. They are Basel 1, Basel 4, Basel 6, Basel 7, Basel 11b, Berkeley 6, Berkeley 43, Berkeley 45, Berkeley 63, Berkeley 84, Berkeley 90, Czernik 20, Kharchenko 1, Mayer 2, NGC 2364, NGC 3231, NGC 6525, NGC 6832, NGC 6882, NGC 7024, Roslund

18, Roslund 32, Roslund 36, Turner 3, Turner 4, Turner 8, vdB-Hagen 80 and vdB-Hagen 92. We have detected 2 e-stars in 2 clusters (Berkeley 63 and Berkeley 90), for which reliable age information is not available. The clusters without age information were picked up based on their young appearance with the presence of bright stars. Therefore the number of clusters with age estimation is 184. Thus 40 out of 184 clusters (22%) are found to have e-stars in them. 39 clusters are found to be older than 100 Myr and two among them have CBe stars. Hence out of the 207 clusters surveyed, 145 were found to have age less than 100 Myr, with 38 clusters housing e-stars (26%). The coordinate list of the surveyed clusters is given in table 2.1.

From the slitless spectra of 207 clusters, we identified 42 clusters to have e-stars. On the whole, we identified 157 e-stars. A detailed list of e-stars along with the coordinates, V magnitude, (B–V) colour and the spectral type are given in table 2.2. We have identified e-stars in 19 clusters, which were not in the Be star list of WEBDA. These 19 clusters are found to have 49 e-stars. Together with the new identifications from already known clusters with e-stars (5 clusters), we have found 54 new e-stars in 24 open clusters. Among the newly identified clusters with e-stars, NGC 2345 (12 stars), NGC 6649 (7 stars) and NGC 436 (5 stars) are noteworthy.

The clusters with e-stars are mostly younger than 50 Myr, whereas there are a few clusters, which are quite old to have these stars. The oldest clusters to have these stars are NGC 6756 and NGC 7039, where the age of the second cluster is debatable. NGC 6756, with an age of 125–150 Myr is thus the oldest cluster to house two CBe stars. NGC 6834, an 80 Myr cluster is found to house 4 CBe stars, but with our CCD photometry the age was re-estimated to be about 40 Myr. Another interesting cluster is the 60–100 Myr old NGC 2345, where we have detected 12 e-stars. No e-stars were known in this cluster. NGC 436 (40 Myr) is another

not-so-young cluster, where we have detected 5 CBe stars for the first time. NGC 6649 is a young 30 Myr cluster in which we have identified 7 CBe candidates for the first time. On the other extreme, there are some very young clusters (~ 4 Myr), where we have identified CBe candidates (NGC 1624, NGC 637 & IC 1590). In some clusters, CBe and HAeBe stars are found to co-exist (NGC 146, IC 1590, NGC 7380 & Roslund 4). The largest number of CBe stars is found in NGC 7419 (25 stars), closely followed by NGC 663 (22 stars).

We found that 37 clusters have proper optical photometric data, out of the 42 clusters and we have constructed optical CMD for them. The cluster members are shown as points while e-stars are shown as special symbols in the CMD. We have plotted ZAMS (Schmidt-Kaler, 1982) and isochrones of solar metallicity on the CMD (Padova isochrones, Bertelli et al. (1994)). The cluster parameters are not re-estimated but taken from the literature. In some cases, the fit is not found to be satisfactory. The position of the Be stars in the CMD is checked to look for the evolutionary effect, which has been quoted as one of the reasons for Be phenomenon in CBe stars. If the e-stars are preferentially located near the evolved region or turn-off of the cluster MS, it is an indication of evolutionary effect. The near-IR CCDm were plotted for the clusters to classify e-stars based on their IR excess. The location of the MS and reddening vectors are taken from Koornneef (1983) and the IR sources in the $10' \times 10'$ cluster field are shown as dots while the e-stars are shown in special symbols. This diagram is not dereddened for e-stars whose colour excess $E(B-V)$ is not known. A detailed analysis of the individual clusters which contain e-stars along with the optical CMDs and near-IR CCDm are provided in the following subsections. The description of clusters which harbour sure HAeBe stars, Bochum 6, IC 1590, NGC 6823 and NGC 7380, are given in chapter 5. Hence we have not included these clusters in this chapter.

Among the surveyed clusters which contain e-stars, we have studied NGC 7419

(Subramaniam et al., 2006), NGC 146 (Subramaniam et al., 2005) and 4 clusters (Berkeley 86, Berkeley 87, IC 4996, NGC 6910) in the Cygnus region (Bhavya et al., 2007) in detail. The turn-on age of these clusters (estimated by fitting PMS isochrones) was found to be different from the turn-off age, suggesting continued or multiple episodes of star formation in the above open clusters.

The spectra of e-stars in each cluster in the wavelength range 3800 – 9000 Å are shown with optical CMD and near-IR CCDm. The spectral lines are identified and marked for e-stars in clusters Berkeley 62, Berkeley 63 and Berkeley 86, which has been used to identify the features in remaining e-stars. The important spectral lines of total surveyed e-stars is listed in table 2.3. The lines which are in emission are indicated as ‘e’, those having emission in absorption profile as ‘eina’, double peaked emission profile as ‘dpe’ while others are in absorption only. The table lists the number of FeII lines present in each e-star while their wavelength is given in chapter 4. A discussion of individual clusters which harbour Be stars is given below.

2.3.1 Berkeley 62

Berkeley 62 belongs to Trumpler class III2m. Photoelectric UBV observations by Forbes (1981) showed the cluster ($RA = 01^h01^m00^s$, $Dec = +63^{\circ}57'$, $l = 123^{\circ}.982$, $b = 1^{\circ}.098$) to have a distance modulus (DM) of 11.56 ± 0.25 and a reddening of $E(B-V)=0.86 \pm 0.04$. At the corresponding distance of 2.05 ± 0.24 kpc, the cluster would lie near the inner edge of the Perseus spiral arm and is a possible member of the Cassiopeia OB7 association at 2.5 kpc. They estimated an age of 10 Myr, based on an early type star (B1) in the cluster. Phelps and Janes (1994) estimated an age of 10 Myr for the cluster along with an $E(B-V)$ of 0.82 and distance of 2704 pc.

well below the turn-off of the cluster MS.

The near-IR CCDm for the cluster is shown in figure 2.2(b). The e-star is found to show low IR excess, which puts it in CBe category. If we assume this CBe candidate to be a member of this cluster, we find the presence of a late B-type CBe star in a very young open cluster. The spectra of the e-star Berkeley 62(1) in the wavelength range 3800 – 9000 Å are shown in figure 2.2(c). We do not find any FeII lines in the spectrum while H_{β} , OI 8446 Å lines are in emission. The CaII triplet (8498, 8542, 8662 Å) and Paschen lines P12, P14 and P19 are in absorption while P11 shows ‘eina’ profile.

2.3.2 Berkeley 63

The cluster Berkeley 63 lies in the Perseus arm with Galactic coordinates $l = 132^{\circ}.506, b = 2^{\circ}.496$. Not much information is available for this cluster, in the literature. The cluster is found to have an e-star. Since the optical data was not available for the cluster we were unable to estimate the age of the cluster.

The near-IR CCDm for the cluster is given in figure 2.3(a) and the candidate is found to have near-IR excess. But after dereddening, the e-star may lie close to the MS which puts them in CBe category. No nebulosity is associated with the e-star. The spectra of the e-star Berkeley 63(1) in the wavelength range 3800 – 9000 Å are shown in figure 2.3(b). The spectra is found to have 4 FeII lines in emission while OI 7772 Å line is in absorption and 8446 in emission. Among the CaII triplet members only 8662 is present, which is in absorption. The Paschen lines P11 shows ‘eina’ profile while P12 shows absorption profile.

contents of this cluster. They found the PMS stars to be distributed in two age groups. The younger group is found to be younger than 1 Myr, while the older group is as old as or older than 5 – 7 Myr. Star 9 is found to lie on the 0.25 Myr PMS isochrone and 26 is located on the 0.5 Myr isochrone. Thus these stars could be younger than 1 Myr, which makes them as candidate HAeBe stars. Otherwise, these stars could be 5 Myr old or slightly older, which would make them as candidate CBe stars. These stars are found to show considerable IR excess in near-IR CCDm. The spectra of the e-stars in the wavelength range 3800 – 9000 Å are shown in figure 2.4(c). The star Berkeley 86(9) is found to have H_{β} , CaII triplet and Paschen lines in absorption while they are in emission in Berkeley 86(26).

2.3.4 Berkeley 87

Berkeley 87 (Dolidze 7, $RA = 20^h 21^m 42^s$, $Dec = 37^{\circ}.22$), located at $l = 75^{\circ}.71$, $b = +0^{\circ}.31$ is a sparse grouping of early-type stars lying in a heavily obscured region of the Cygnus. Turner and Forbes (1982) derived a distance of 946 ± 26 pc and an age of 1–2 Myr for the cluster from UVB photometry of 105 stars. The age as reported in WEBDA is 14 Myr. The distance was estimated to be 0.9 kpc from the interstellar line depth of the cluster members (Polcaro et al., 1989). It is part of the star formation region ON 2, which harbours many compact HII regions, strong OH masers and CO, ammonia molecular clouds. Diffuse emission in C IV 5802-12 Å doublet and X-ray emission in 2–6 keV range have been detected in the cluster, which is interpreted as due to the interaction of the strong wind from a Wolf Rayet star (ST 3) of velocity 5200 km s^{-1} with the cluster members. A high energy γ -ray source 2CG 075+00 (≤ 100 Mev) has been found to be associated with this cluster. Berkeley 87 contains a peculiar emission-line B super giant HDE 229059 (Hiltner, 1956), two faint objects (VES 203 and VES 204) which show H_{α} in emission (Coyne et al., 1975), the red super giant BD +37 39 03 and the faint

variable star V439 Cygni. According to WEBDA the cluster contains 5 B type e-stars.

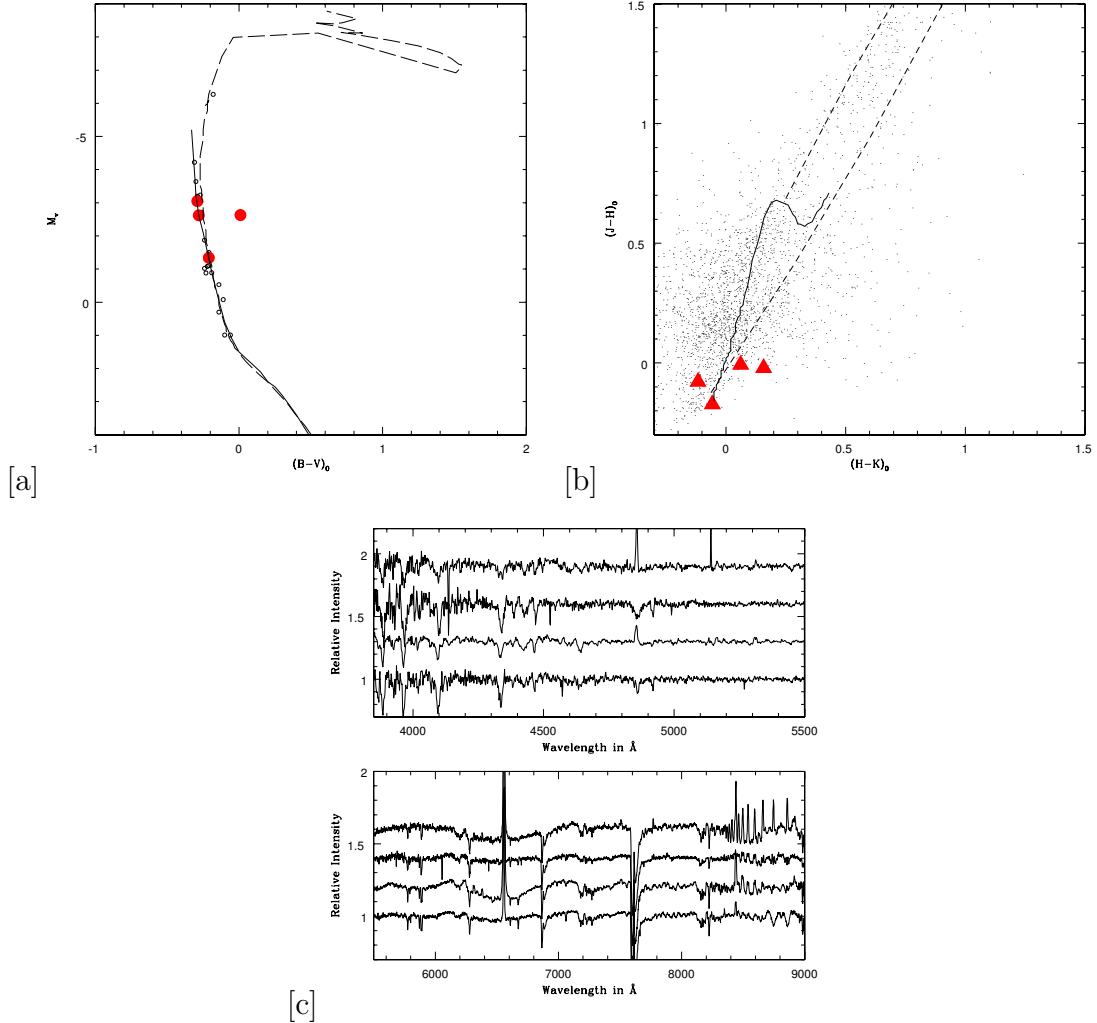


Figure 2.5: (a) Optical CMD of the cluster Berkeley 87 is shown with the e-stars shown as solid circles. (b) The near-IR CCDm is shown with e-stars shown as filled triangles. (c) The spectra of the e-stars Berkeley 87(1), Berkeley 87(2), Berkeley 87(3) and Berkeley 87(4) are shown in order from bottom to top.

We identified 4 e-stars in this cluster. Stars 9(2), 15(4), 38(1) and 68(3) (Turner and Forbes, 1982) are stars with H_α emission, shown as filled circles (figure 2.5(a)). The numbers given in brackets are the ones followed in this paper. The CMD is shown in figure 2.5(a) fitted with 8 Myr isochrone. Three stars are earlier than B2

and one star is B4 spectral type, located on the MS of the cluster CMD. Bhavya et al. (2007) estimated the turn-on age of the cluster to be less than 1 Myr, which is consistent with the recent star formation activity in the cluster vicinity. The cluster has a turn-off age of 14 Myr, as indicated in WEBDA. On the other hand, the age of 2 Myr as estimated by Turner and Forbes (1982), is in good agreement with our estimation of the turn-on age. The e-stars in this cluster are very young. The stars Berkeley 87(1) and Berkeley 87(4) (figure 2.5(b)) show near-IR excess compared to Berkeley 87(2) and Berkeley 87(3) and hence can be considered as candidate HBe stars. There is significant differential reddening in this cluster. No nebulosity is associated with the e-stars. Therefore, the above classification should be taken with some caution. From PMS isochrone fitting it has been found that if they are HAeBe stars, then they are as young as 0.15 Myr. If they are CBe stars, then they are ≤ 2 Myr old. Thus, if these stars are CBe stars, these might be one of the very young CBe stars known. The spectra of the e-stars in the wavelength range 3800 – 9000 Å are shown in figure 2.5(c). The spectral lines OI 8446 Å and CaII triplet are found to be in emission for all e-stars.

2.3.5 Berkeley 90

The cluster Berkeley 90 is found to be located near Cygnus region ($l= 84^{\circ}.877$ and $b= 3^{\circ}.784$). Not much information is found in the literature about this cluster. The e-star is found to be highly reddened as shown in near-IR CCDm (figure 2.6(a)). This e-star is associated with nebulosity. Hence it may be a candidate HBe star. The spectra of the e-star in the wavelength range 3800 – 9000 Å are shown in figure 2.6(b). The spectral lines H_{β} , OI, CaII triplet, Paschen lines (P14 & P19) are in emission.

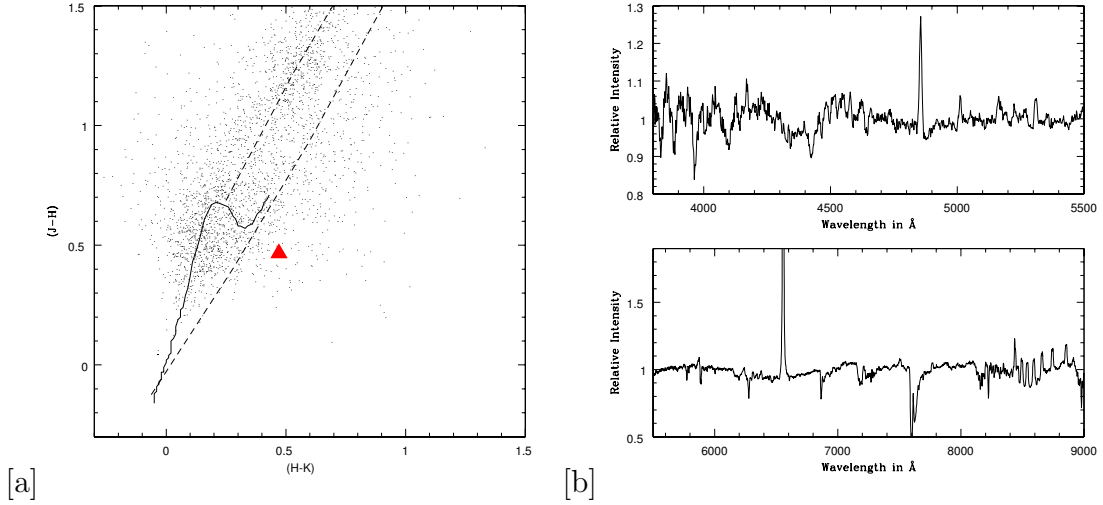


Figure 2.6: (a) The near-IR CCDm of the cluster Berkeley 90 is shown with e-stars shown as filled triangles. (b) The spectra of the e-star are shown in the wavelength range 3800 – 9000 Å.

2.3.6 Bochum 2

Bochum 2 ($RA = 06^h 48^m 54^s$, $Dec = +00^{\circ} 23'$, $l = 212^{\circ}.302$, $b = -0^{\circ}.390$) lies in the Galactic anti-centre direction and therefore seems to be important for investigations of the spiral structure, dynamics and chemistry of the outer disk of our Galaxy. Turbide and Moffat (1993) used the cluster for the same and found that the galactic rotation curve is flat or slightly rising out to the limit at $R = 16$ kpc. Moffat and Vogt (1975) obtained UBV photoelectric photometry for eight stars in the cluster and came to the conclusion that the cluster lies at a distance of 5.5 kpc with a mean $E(B-V) = 0.89$. Moffat et al. (1979) determined a reddening of 0.84 and distance of 4.8 kpc from spectroscopic observations of three bright stars.

Munari and Carraro (1995) used UBV(RI) $_C$ H α CCD photometry and Grism spectroscopy and found the cluster to be young (7 Myr) with a DM of 14.0 and a reddening of 0.80. The cluster exhibits differential reddening. Munari and Tomasella (1999) found a trapezium system (BD +00 16 17) associated with the cluster and the high resolution spectra showed variations in neutral helium absorp-

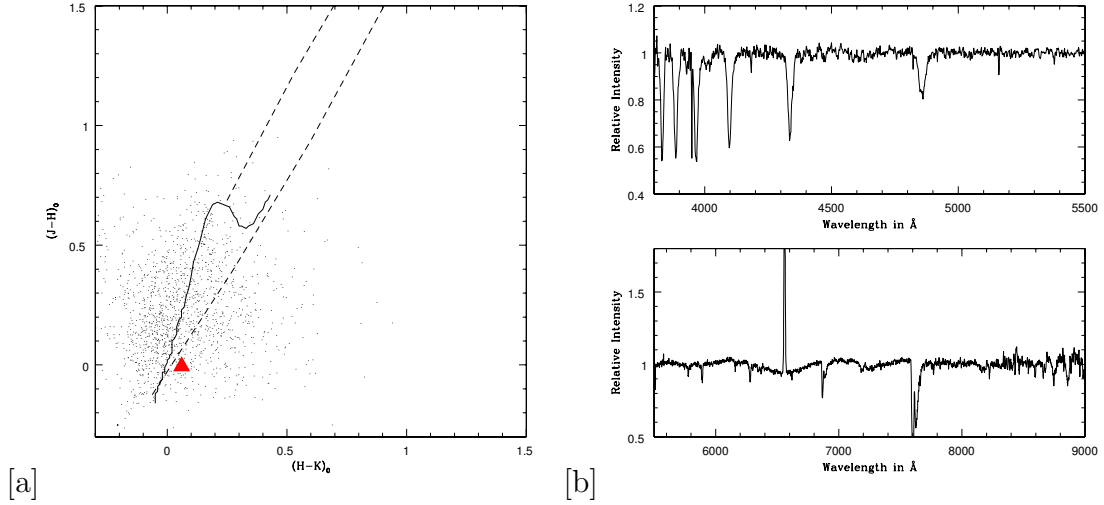


Figure 2.7: (a) The near-IR of the cluster Bochum 2 is shown with e-stars shown as filled triangles. (b) The spectra of the e-star are shown in the wavelength range 3800 – 9000 Å.

tion lines in binaries. A distance of 2661 pc and reddening of 0.831 mag have been given in WEBDA.

The e-star is located outside the UBV CCD photometric field. Hence we have not given the optical CMD. We have taken the $E(B-V)$ value of 0.89 from Turbide and Moffat (1993) to deredden the near-IR CCDm (figure 2.7(a)). It is likely to be a CBe candidate, again in a young cluster. The e-star is not associated with nebulosity. The spectra of the e-star in the wavelength range 3800 – 9000 Å are shown in figure 2.7(b). The He I lines are found to be weak and Si III lines 6347 and 6371 Å are in absorption.

2.3.7 Collinder 96

Collinder 96 ($RA = 06^h30^m18^s$, $Dec = +02^{\circ}52'$) is a young open cluster located in the Monoceros region ($l = 207^{\circ}.964$, $b = -3^{\circ}.386$).

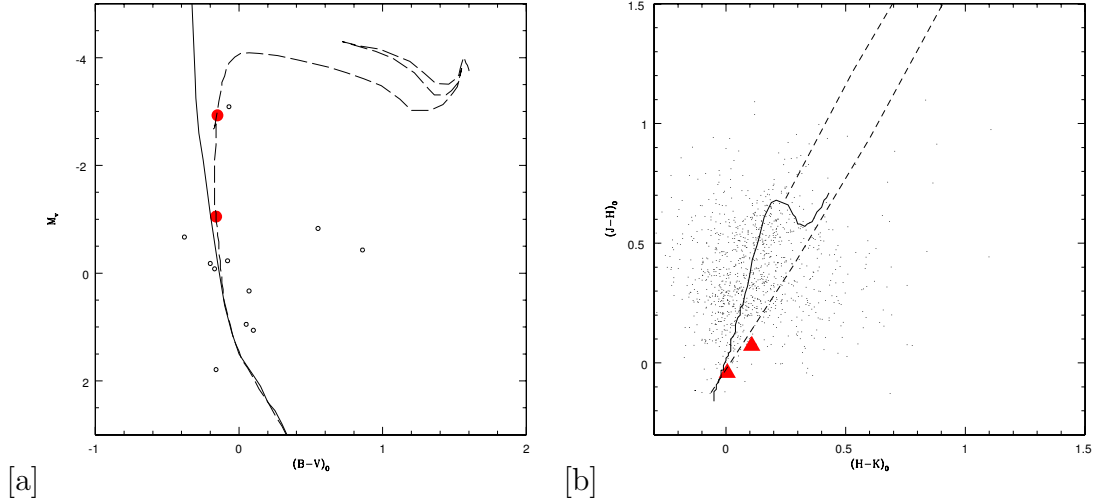


Figure 2.8: (a) Optical CMD of the cluster Collinder 96 is shown with the e-stars shown as solid circles. (b) The near-IR CCDm is shown with e-stars shown as filled triangles.

Moffat and Vogt (1975) indicated that the cluster contains 4 B-type stars with similar reddening from $UBV H_\beta$ photoelectric photometry. They estimated the mean reddening of the cluster to be 0.48 ± 0.06 and DM as 11.8, from which the distance is estimated as 1.1 kpc. They identified a Be star from the small beta value and relatively blue $U-B$ index. WEBDA has reported a value of 0.510 mag as reddening value, a distance of 962 pc and an age of 10.7 Myr.

The UBV data are taken from Moffat and Vogt (1975) and the stars 1 and 4 listed in their catalogue are found to show emission. The spectral type of star 1 is found to be B1 while star 4 is B5.5. Even though a younger age is quoted in WEBDA, an isochrone of 63 Myr fits the turn-off region well, as shown in figure 2.8(a). Photometry is available only for a few stars and hence the age estimation is quite unreliable. Hence deep field CCD photometry is necessary to estimate an accurate age to this cluster. The e-stars are located close to the MS in near-IR CCDm (figure 2.8(b)) without much reddening. Hence they can be considered as CBe stars. The spectra of the e-stars in the wavelength range $3800 - 9000 \text{ \AA}$ are shown in figure 2.9. The spectral lines H_β , $O\text{I}$, CaII triplet and Paschen lines

are found to be in emission for Collinder 96(1) while they are in absorption for Collinder 96(2).

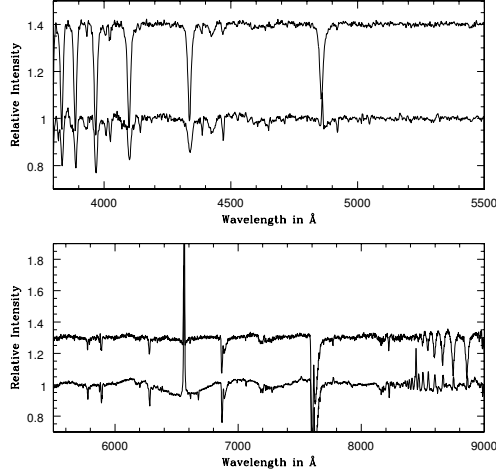


Figure 2.9: The spectra of the e-stars Collinder 96(1) and Collinder 96(2), in the wavelength range 3800 – 9000 Å, are shown from bottom to top.

2.3.8 IC 4996

IC 4996 is located ($RA = 20^h14^m24^s$, $Dec = +37^{\circ}29'$, $l = 75^{\circ}.36$, $b = 1^{\circ}.31$) in the direction of the Cygnus and is part of a star forming region. IRAS map of the region (Lozinskaya and Repin, 1990) shows the presence of a dusty shell around the cluster. Zwintz and Weiss (2006) performed time series CCD photometry in Johnson B and V filters to find 40 stars to lie in the classical instability strip, of the 113 stars analysed in the cluster. They have discovered two δ Scuti-like PMS stars in the cluster. The parameters obtained by Delgado et al. (1998) for the cluster are $E(B-V)=0.71 \pm 0.08$ mag, $DM = 11.9$ mag and age of 7.5 ± 3 Myr. They suggested a number of PMS stars in the cluster, which are located at 0.5 and 1 magnitude above the MS in the V vs (B–V) CMD, around the location of spectral types A–F. Delgado et al. (1999) estimated the spectral types and heliocentric radial velocities for 16 stars in the cluster and the mean radial velocity was found

to be $-12 \pm 5 \text{ kms}^{-1}$. Vansavicius et al. (1996) estimated the distance and age of the cluster to be 1620 pc and 9 Myr respectively, using BVRI CCD photometry. Pietrzynski (1996) performed variability studies on the cluster and found an RR Lyrae type variable and another eclipsing system. WEBDA lists 2 Be stars in this cluster.

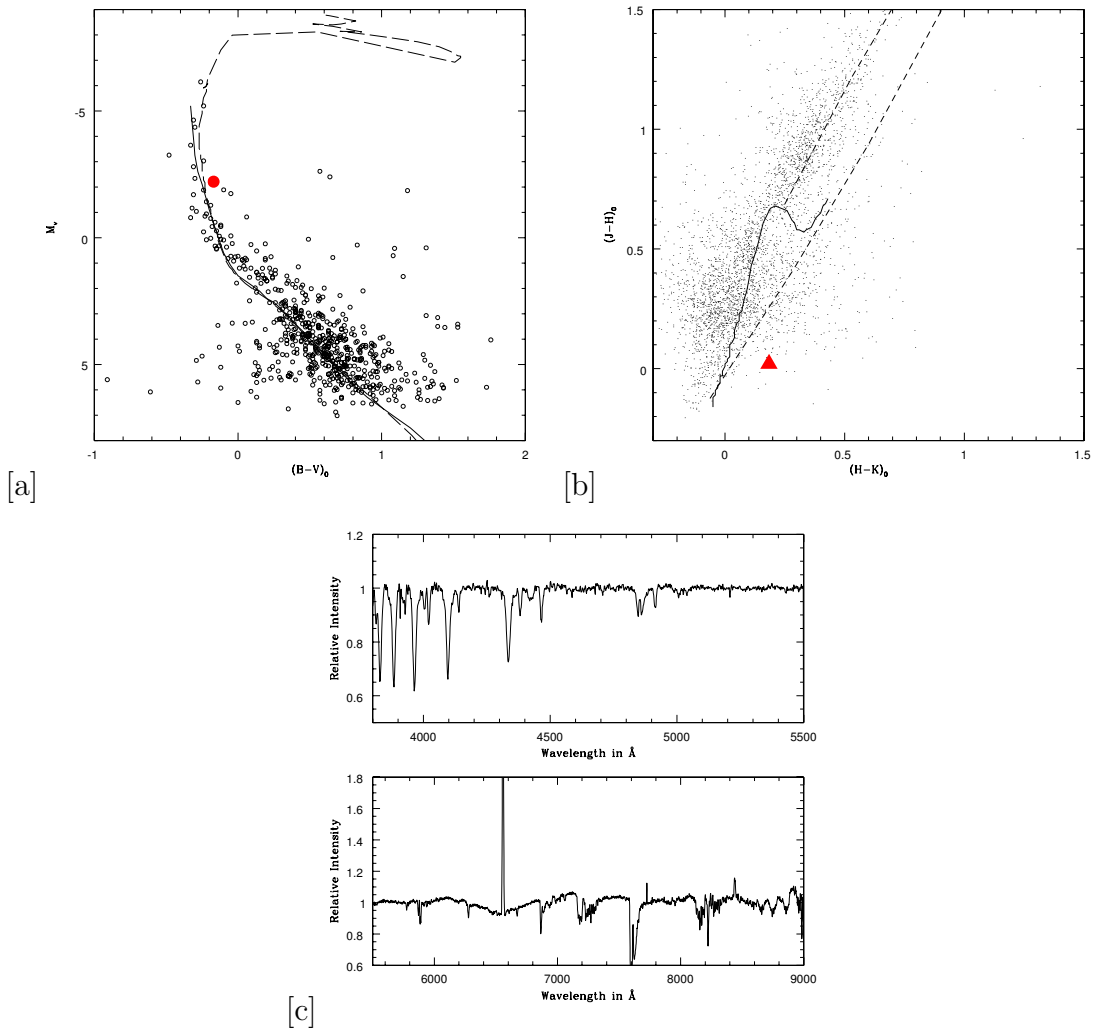


Figure 2.10: (a) Optical CMD of the cluster IC 4996 is shown with the e-stars shown as solid circles. (b) The near-IR CCDm is shown with e-stars shown as filled triangles. (c) The spectra of the e-star are shown in the wavelength range 3800 – 9000 Å.

We identified one e-star in this cluster. Star numbered 23 in Delgado et al.

(1998) is found to have H_α emission and shown as filled circle in optical CMD, fitted with 8 Myr isochrone (figure 2.10(a)). The spectral type is found to be B2. The star is found to be located close to the evolved part of the CMD. Bhavya et al. (2007) studied the cluster in an attempt to understand the star formation in Cygnus region. They found that the cluster has been forming stars for the last 7 Myr. Also, the presence of PMS stars near the tip of the MS indicates that some of the high mass stars could be very young and the star formation stopped very recently. The e-star is not much reddened in near-IR CCDm (figure 2.10(b)) and hence can be considered as a CBe star, near the MS turn-off. The spectra of the e-star in the wavelength range 3800 – 9000 Å are shown in figure 2.10(c).

2.3.9 King 10

King 10 ($RA = 22^h54^m54^s$, $Dec = +59^\circ10'00''$, $l = 108^\circ.481$, $b = -0^\circ.396$) is classified as Trumpler class II1m (Lynga, 1987). UBVRI CCD photometry of the cluster was carried out by Mohan et al. (1992) down to 19.5 mag in V band and estimated a distance of 3.2 kpc, mean $E(B-V)$ of 1.16 mag and an age of 50 Myr. The age given in WEBDA is 30 Myr and indicates the presence of 6 Be stars.

The cluster is found to contain four e-stars. We have taken UBVR CCD data from Mohan et al. (1992). But this data set do not contain the magnitudes of e-stars. So while plotting the CMD, we have used UBVR photographic data of Handschel (1972) for e-stars. The e-stars are found to be 931(A), 309(B), 459(C) and 806(E). The numbers from Handschel (1972) are given with our designations in brackets. The stars A and B are of B1 spectral type while C and E are of B2.5 and B2 type respectively. The 50 Myr isochrone is plotted on the CMD, as shown in figure 2.11(a). The earlier spectral types are found to be near the turn-off. All the e-stars are found to be of CBe nature, as seen from their location in near-IR

CCDm (figure 2.11(b)), though one star (star B) shows relatively large reddening and IR excess.

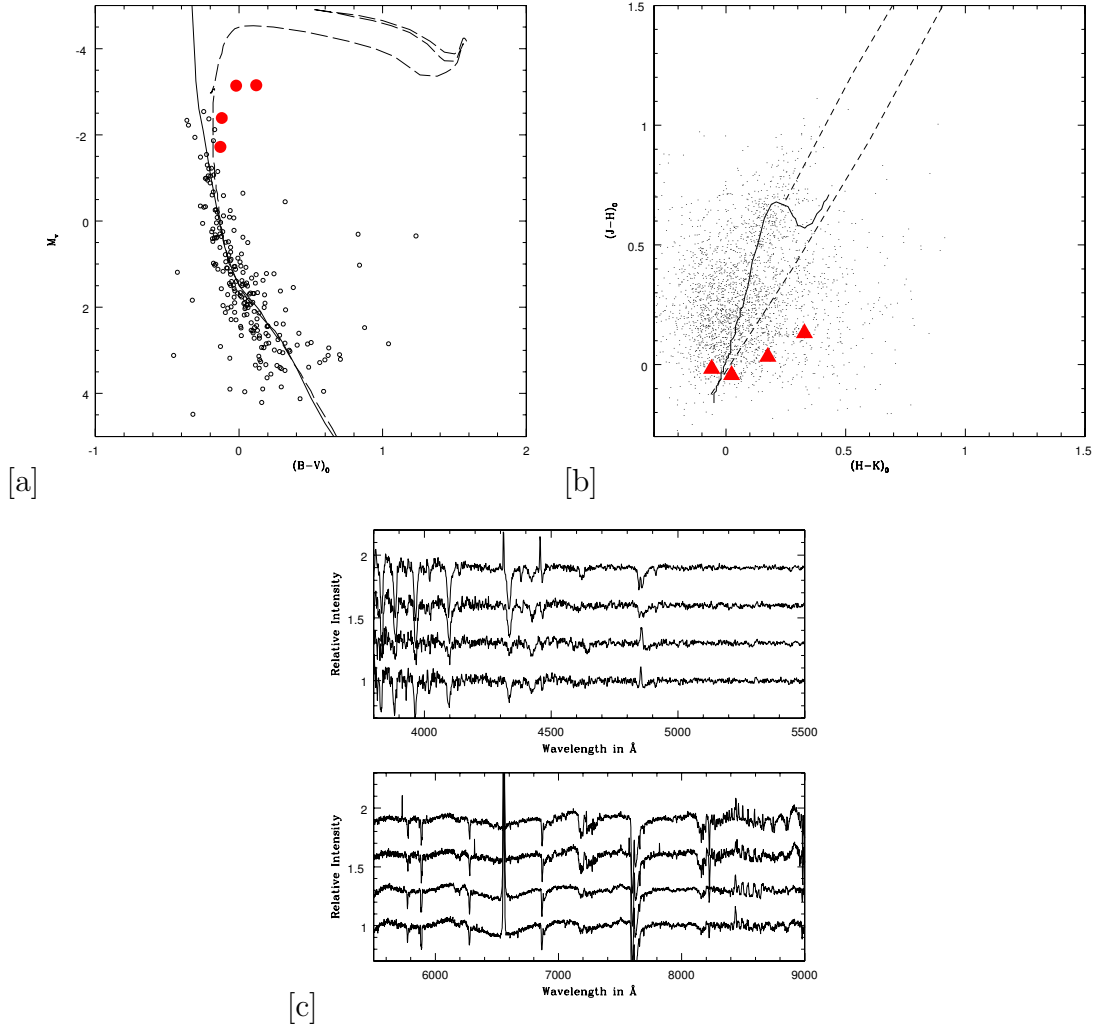


Figure 2.11: (a) Optical CMD of the cluster King 10 is shown with the e-stars shown as solid circles. (b) The near-IR CCDm is shown with e-stars shown as filled triangles. (c) The spectra of the e-stars King 10(A), King 10(B), King 10(C), King 10(E), in the wavelength range 3800 – 9000 Å, are shown from bottom to top.

The spectra of the e-stars in the wavelength range 3800 – 9000 Å are shown in figure 2.11(c). The e-star King 10(A) is found to have SiII line 6347 Å in absorption while H_β , OI 8446 Å, CaII triplet and Paschen lines are in emission for all e-stars.

2.3.10 King 21

The open cluster King 21 is of Trumpler class III3m with coordinates $RA = 23^h49^m56^s$, $Dec = +62^{\circ}41'54''$ (Ruprecht, 1966). The cluster lies very close to the Galactic plane with longitude of $115^{\circ}.946$ and latitude of $0^{\circ}.664$.

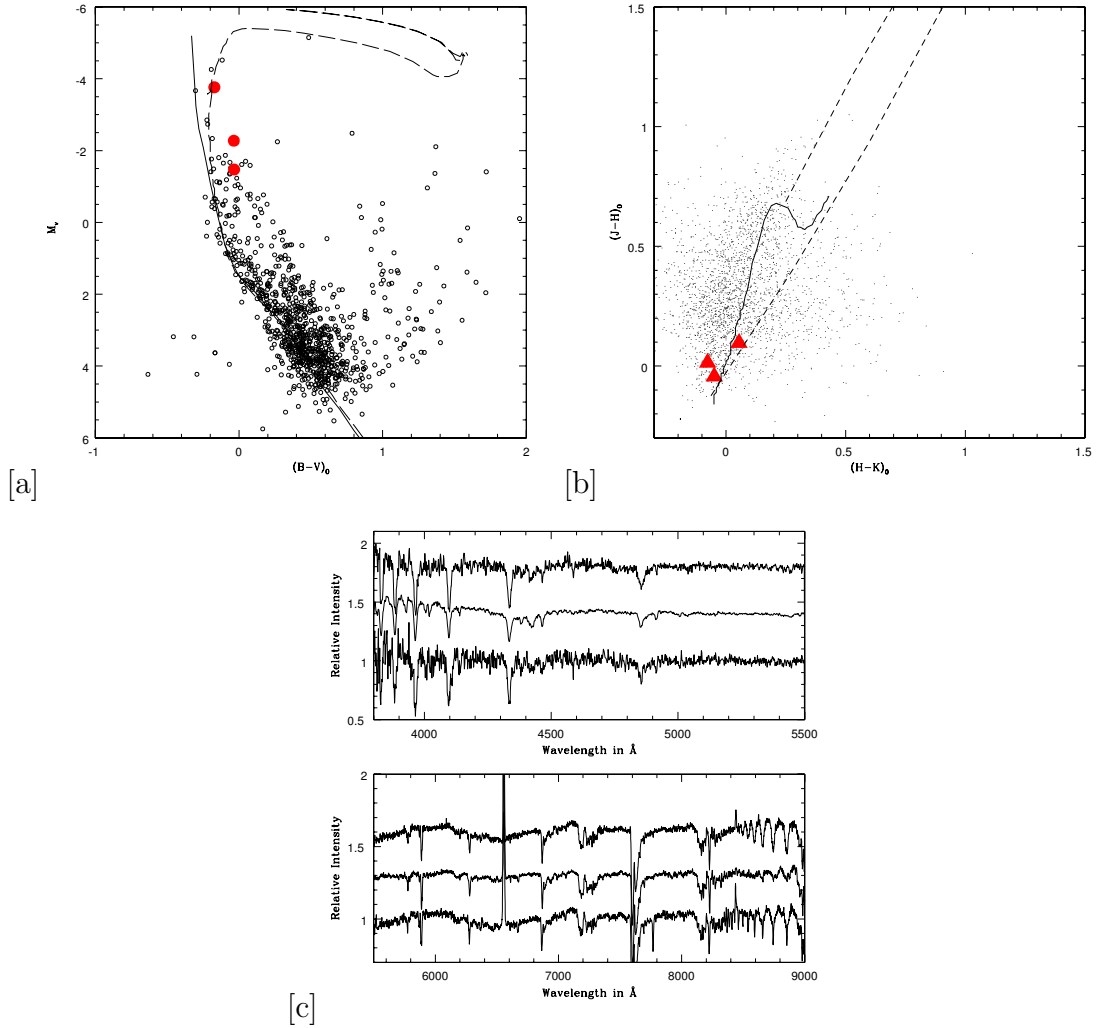


Figure 2.12: (a) Optical CMD of the cluster King 21 is shown with the e-stars shown as solid circles. (b) The near-IR CCDm is shown with e-stars shown as filled triangles. (c) The spectra of the e-stars King 21(B), King 21(C), King 21(D), in the wavelength range 3800 – 9000 Å, are shown from bottom to top.

Haug (1970) obtained photometric magnitudes of four stars in the cluster field. From the photoelectric magnitudes of 26 stars in the cluster field, Mohan and

Pandey (1984) estimated a distance of 1.91 kpc. The cluster exhibits a differential reddening of 0.21 mag with a mean $E(B-V)$ of 0.89 mag.

We have done the UBV CCD photometry of the cluster and the cluster parameters estimated are $E(B-V) = 0.80$ mag, distance = 3.5 kpc and age = 30 Myr. We have identified 3 e-stars in the cluster (labelled B,C and D in our catalogue) which are of spectral types B3.5, B0.5 and B2.5 respectively. The optical CMD of the cluster is given in figure 2.12(a) fitted with a 30 Myr isochrone. The e-star C is found to be in the evolved part of the isochrone and hence may be a giant. The stars B and D seems to be displaced by 0.3 mag in $(B-V)$ from the MS, which might be due to gravity darkening effect in CBe stars.

From near-IR CCDm (figure 2.12(b)) the e-stars show low near-IR excess and hence can be considered as CBe stars. The spectra of the e-stars in the wavelength range 3800 – 9000 Å are shown in figure 2.12(c). We do not find FeII lines in any of the e-stars while Paschen lines are present in absorption and OI 8446 Å in emission.

2.3.11 NGC 146

NGC 146 ($RA = 00^h33^m03^s$, $Dec = +63^\circ18'06''$, $l = 120^\circ.868$, $b = 0^\circ.504$) is a young open cluster located in the direction of the Perseus spiral arm. The cluster was studied by Hardorp (1960) using RGU photometry and Jasevicius (1964) using UBV photographic photometry. From the CCD photometry, Phelps and Janes (1994) estimated a distance of 4786 pc along with an $E(B-V)$ value of 0.70 mag and an age of 10 Myr.

Subramaniam et al. (2005) studied the cluster using UBV CCD photometry down to a limiting magnitude of 20. From the UBV CCD photometry of 434 stars they estimated an excess $E(B-V)$ of 0.55 ± 0.04 mag and with BV photometry

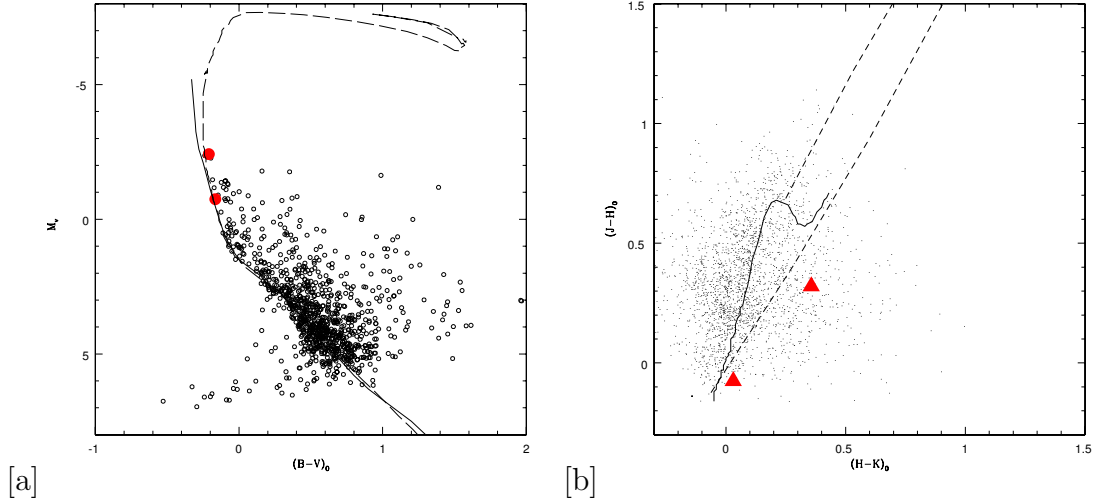


Figure 2.13: (a) Optical CMD of the cluster NGC 146 is shown with the e-stars shown as solid circles. (b) The near-IR CCDm is shown with e-stars shown as filled triangles.

of 976 stars they estimated a distance of 3470 ± 300 pc. The turn-off age of the cluster was found to be 10–16 Myr while the turn-on age is about 3 Myr, which was estimated from the isochrone fitting of 54 PMS stars with near-IR excess. From the slitless spectra of the cluster we found 2 e-stars, of which one is found to be a HBe star from its location in near-IR CCDm.

The UBV CCD data were taken from Subramaniam et al. (2005) and the e-stars correspond to star number 563 and 502 which are of spectral type B2V and B6.5V respectively. These stars are numbered as S1 and S2 in our catalogue. The CMD of the cluster is shown in figure 2.13(a) with a 10 Myr isochrone. S1 is located near, but below the turn-off, whereas S2 is located well below the turn-off. The star S1 may be a candidate HBe star since it is found to be heavily reddened in near-IR CCDm (figure 2.13(b)), whereas S2 is a candidate CBe star. The spectra of the e-stars in the wavelength range $3800 - 9000 \text{ \AA}$ are shown in figure 2.14. The e-star NGC 146(S1) is rich in spectral lines with 11 FeII lines and 10 Paschen lines. SiIII lines are present in absorption while CaII triplet and OI 8446 \AA are in emission.

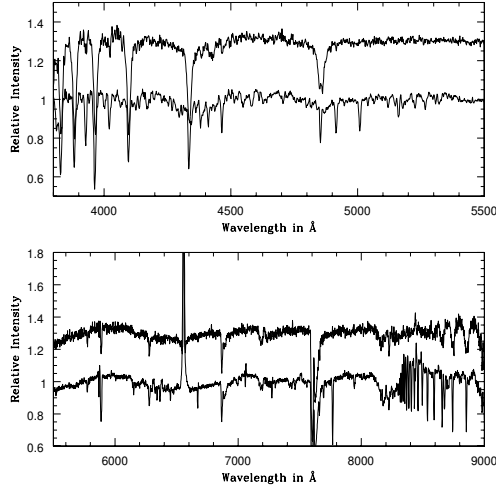


Figure 2.14: The spectra of the e-stars NGC 146(S1) and NGC 146(S2), in the wavelength range 3800 – 9000 Å, are shown from bottom to top.

2.3.12 NGC 436

NGC 436 ($RA = 01^h15^m58s$, $Dec = +58^\circ48'42''$) is located in the Cassiopeia-Perseus spiral arm ($l = 126^\circ.111$, $b = -3^\circ.909$). The cluster was observed photoelectrically by Huestamendia et al. (1991) and photographically by Alter (1944) and Boden (1950). Becker and Stock (1958) studied the cluster in RGU system. Phelps and Janes (1994) found the cluster to be 42 Myr old at a distance of 3236 pc with an $E(B-V)$ value of 0.50, using UBV CCD photometry. Huestamendia et al. (1991) found the cluster to be 63 Myr old at a distance of 2600 pc and $E(B-V)$ of 0.48 mag. WEBDA gives an age of 90 Myr.

The e-stars were identified using UBV CCD data from Phelps and Janes (1994) and photoelectric photometry of Huestamendia et al. (1991). There are 5 e-stars and star 3 does not have optical data. The spectral types range from B3 to B7. The CMD of the cluster is shown in figure 2.15(a) fitted with a 40 Myr isochrone. All the e-stars are located below the turn-off. The star 3 do not have any optical data and its location in near-IR CCDm (figure 2.15(b)) is a puzzle even though

the flag of 2MASS data is good. All the e-stars are candidate CBe stars, as seen from their location in the optical and near-IR CCDm.

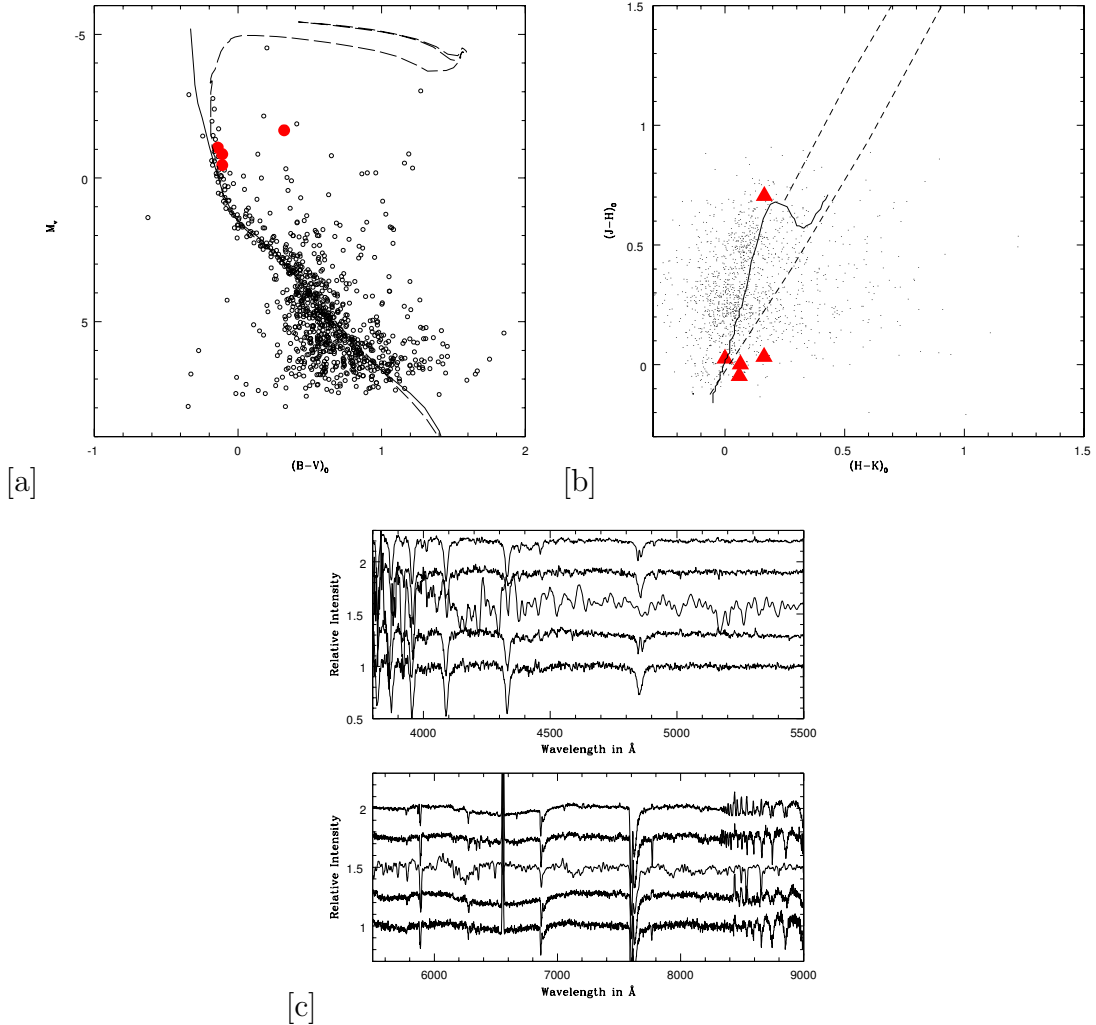


Figure 2.15: (a) Optical CMD of the cluster NGC 436 is shown with the e-stars shown as solid circles. (b) The near-IR CCDm is shown with e-stars shown as filled triangles. (c) The spectra of the e-stars NGC 436(1), NGC 436(2), NGC 436(3), NGC 436(4), NGC 436(5) in the wavelength range 3800 – 9000 Å, are shown from bottom to top.

The spectra of the e-stars in the wavelength range 3800 – 9000 Å are shown in figure 2.15(c). Si III lines are found in absorption for NGC 436(1) and NGC 436(4). The spectrum of NGC 436(3) is found to be different from the other spectra.

2.3.13 NGC 457

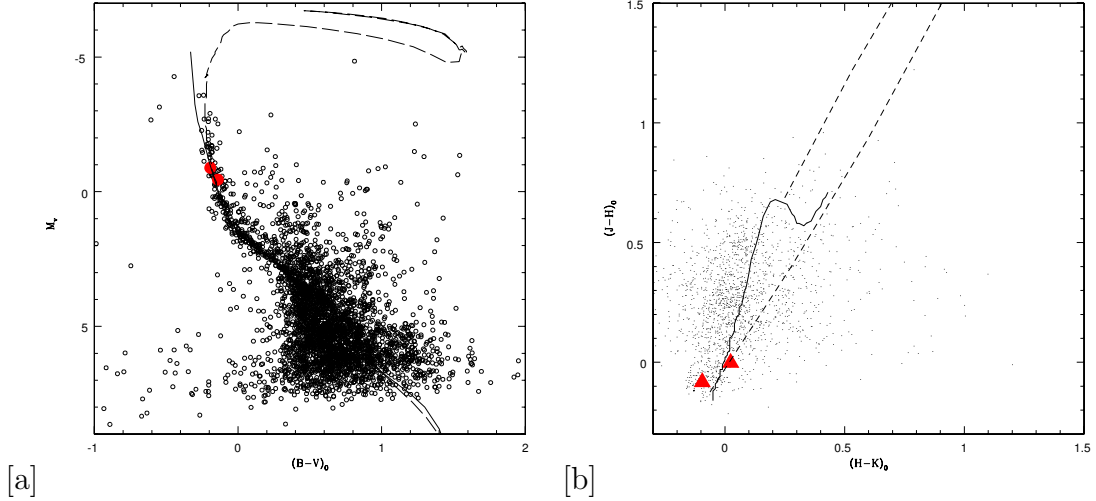


Figure 2.16: (a) Optical CMD of the cluster NGC 457 is shown with the e-stars shown as solid circles. (b) The near-IR CCDm is shown with e-stars shown as filled triangles.

NGC 457 is located in Cassiopeia with coordinates $RA = 01^h19^m35s$, $Dec = +58^\circ17'12''$, $l = 126^\circ.635$ and $b = -4^\circ.383$. Pesch (1959) estimated a reddening of 0.50 mag and a distance of 2880 pc from UBV photoelectric observations and identified supergiants of spectral types B6 Ib, F0 Ia and M0 Ib-II. Phelps and Janes (1994) found an age spread of 12 Myr in the cluster with a turn-off of 20 Myr. They estimated an $E(B-V)$ value of 0.49, a distance of 3020 pc from UBV CCD photometry.

The UBV data are taken from Phelps and Janes (1994) and the e-stars are those numbered 17 and 31 in their catalogue. We have found their spectral types to be B6 and B7 respectively.

The CMD of the cluster is shown in figure 2.16(a) with a 20 Myr isochrone. The e-stars are located on the MS, well below the turn-off and hence they may be candidate CBe stars. This is also supported by their location in the near-IR CCDm (figure 2.16(b)), since they are not much reddened like HBe stars. The spectra of the e-stars in the wavelength range 3800 – 9000 Å are shown in figure

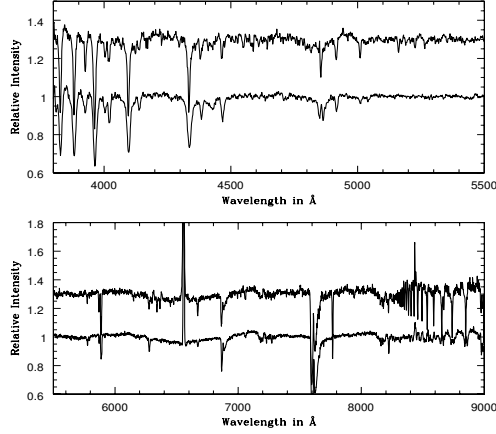


Figure 2.17: The spectra of the e-stars NGC 457(1) and NGC 457(2), in the wavelength range 3800 – 9000 Å, are shown from bottom to top.

2.17. We found deep OI 7772 Å absorption profile for NGC 457(2), which is similar to NGC 146(S1). The spectral lines are also similar (figure 2.17). Most of the lines including SiII are in absorption for NGC 457(2).

2.3.14 NGC 581

NGC 581 (M103, $RA = 01^h33^m23s$, $Dec = +60^\circ39'00''$, $l = 128^\circ.053$, $b = -1^\circ.804$) is a young open cluster of Trumpler type II3m which lies near ϵ Cassiopeia. Photographic UBV studies were done by Hoag et al. (1961), McCuskey and Houk (1964), Moffat (1974) and Osman et al. (1984). Sagar and Joshi (1978) estimated the age of the cluster to be 40 Myr and a distance modulus of 12.16 mag. Steppe (1974) estimated a distance of 3110 pc for the cluster using RGU photographic photometry. Phelps and Janes (1994) used UBV CCD photometry to find the cluster to lie at a distance of 2692 pc with an $E(B-V)$ value of 0.44 and an age range of 10 – 22 Myr. Sanner et al. (1999) performed CCD photometry and found it to be 16 ± 4 Myr old, at a distance of 3 kpc. The proper motion studies identified 77 stars of $V=14.5$ mag or brighter as the cluster members.

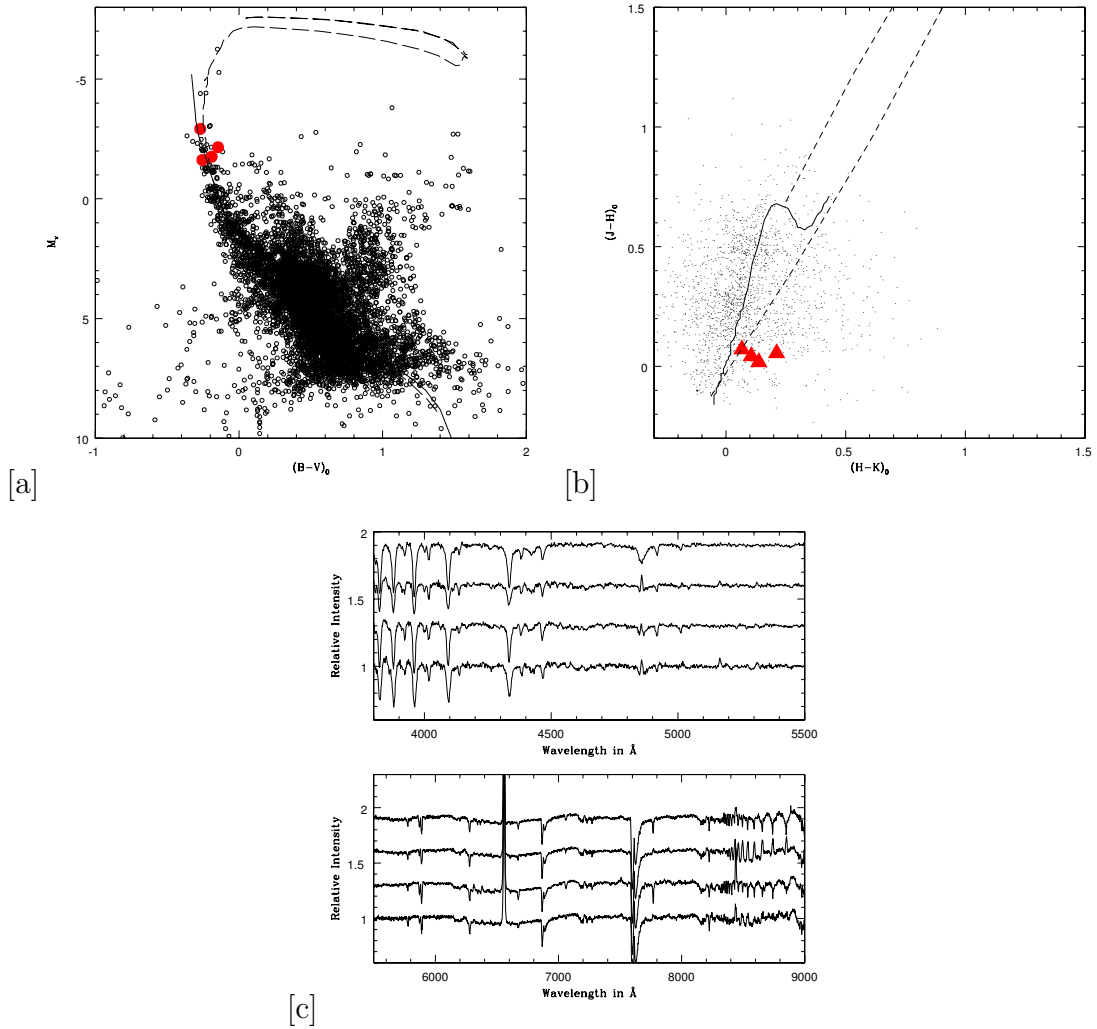


Figure 2.18: (a) Optical CMD of the cluster NGC 581 is shown with the e-stars shown as solid circles. (b) The near-IR CCDm is shown with e-stars shown as filled triangles. (c) The spectra of the e-stars NGC 581(1), NGC 581(2), NGC 581(3), NGC 581(4), in the wavelength range 3800 – 9000 Å, are shown from bottom to top.

The UBV CCD data were taken from Phelps and Janes (1994) and the e-stars are found to be the stars numbered 87, 7540, 7834 and 49. The CMD of the cluster is shown in figure 2.18(a) with a 12.5 Myr isochrone. All the four e-stars are below the MS turn-off. All the e-stars belong to the location of the CBe stars in near-IR CCDm (figure 2.18(b)) indicating that all the stars are candidate CBe stars. The spectra of the e-stars in the wavelength range 3800 – 9000 Å are shown in fig-

ure 2.18(c). There is a similarity between the line features of e-stars NGC 581(1) and NGC 581(3) while SiII lines are present for stars NGC 581(2) and NGC 581(4).

2.3.15 NGC 637

NGC 637 ($RA = 01^h43^m04^s$, $Dec = +64^\circ02'24''$, $l = 128^\circ.546$, $b = 1^\circ.732$) is a young open cluster located in the Perseus arm. Grubissich (1975) estimated the distance to the cluster to be 2.45 kpc from three-colour RGU photometry.

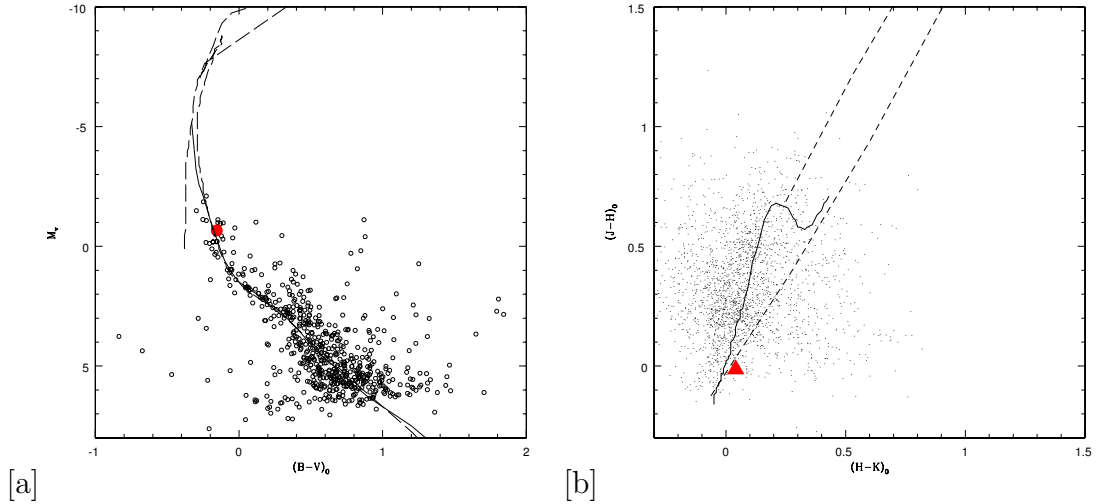


Figure 2.19: (a) Optical CMD of the cluster NGC 637 is shown with the e-stars shown as solid circles. (b) The near-IR CCDm is shown with e-star shown as filled triangle.

From UVB photoelectric photometry Huestamendia et al. (1991) found an $E(B-V)=0.66$ mag, a DM of 11.89, which corresponds to a distance of 2.5 kpc and an age of 15 Myr. In an effort to determine the stellar and molecular velocities of six young open clusters, Liu et al. (1988) made a CO-13 map of the cluster. The observations show strong CO emission in certain regions of the cluster which indicated the presence of molecular gas. Phelps and Janes (1994) estimated a distance of 2884 pc, $E(B-V)$ of 0.65 and age of 1–4 Myr for the cluster. Using UVBRI CCD and 2MASS JHK photometry, Yadav et al. (2008) estimated the radius of

the cluster as 4.2 arcmin, a distance of 2.5 ± 0.2 kpc and an age of 10 ± 5 Myr. The mass function slope for the cluster is found to be 1.65 ± 0.20 . The cluster was found to be dynamically relaxed due to the dynamical evolution of the cluster.

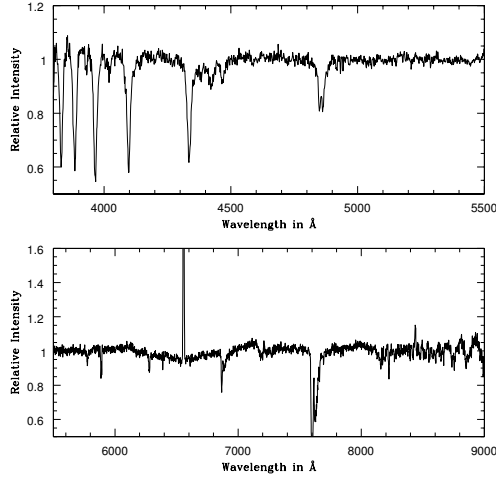


Figure 2.20: The spectra of the e-star in the cluster NGC 637 are shown in the wavelength range 3800 – 9000 Å.

The UBV CCD photometric data was taken from Phelps and Janes (1994). The star 27 was identified as an e-star and belongs to B6.5V spectral type. A 4 Myr isochrone is fitted and the resulting CMD is shown in figure 2.19(a). The e-star belongs to CBe category, as inferred from its location in the optical CMD and near-IR CCDm (figure 2.19(b)). This is also another very young CBe candidate. The spectra of the e-star in the wavelength range 3800 – 9000 Å are shown in figure 2.20.

2.3.16 NGC 654

The young open cluster NGC 654 ($RA = 01^h44^m00^s$, $Dec = +61^{\circ}53'06$, $l = 129^{\circ}.082$, $b = -0^{\circ}.357$) is in the Cassiopeia region and classified as type I2p by

Trumpler (1930). The cluster was studied by Pesch (1960), Hoag et al. (1961), McCuskey and Houk (1964), and Moffat (1974).

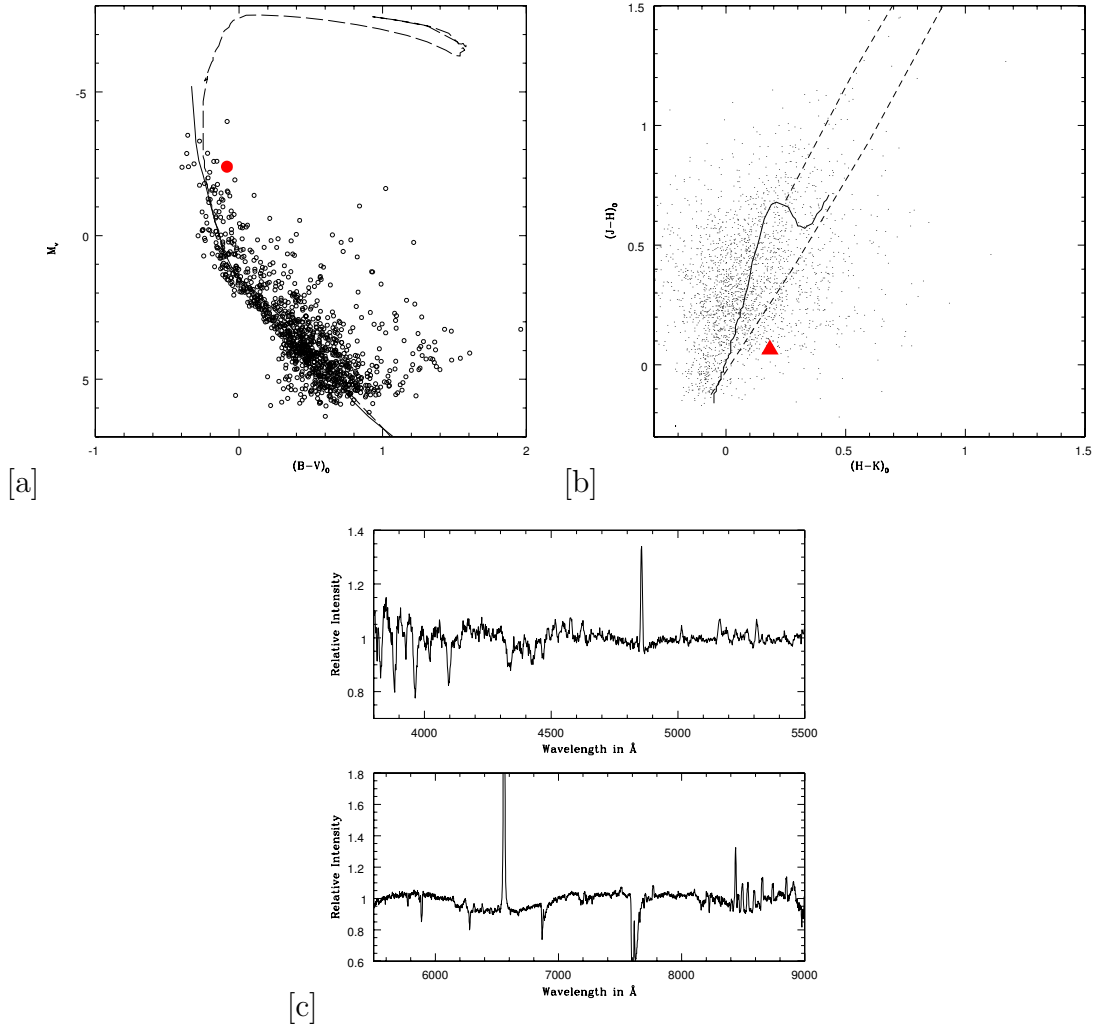


Figure 2.21: (a) Optical CMD of the cluster NGC 654 is shown with the e-star shown as solid circle. (b) The near-IR CCDm is shown with e-star shown as filled triangle. (c) The spectra of the e-star in the cluster NGC 654 are shown in the wavelength range 3800 – 9000 \AA .

Using photoelectric UBV magnitudes, Joshi and Sagar (1983) found the reddening to vary from 0.74 to 1.16 magnitudes. This is interpreted as due to residual material from the cluster’s formation by Samson (1975) or due to a local cloud in the direction of the cluster by Stone (1977), and McCuskey and Houk (1964). From UBV CCD photometry, Phelps and Janes (1994) estimated an $E(B-V)$ of

0.90, a distance of 2692 pc and an age range of 8–25 Myr for the cluster. The cluster is found to have variable reddening with values ranging from 0.75 to 1.15 mag (Pandey et al., 2005; Phelps and Janes, 1994). Pandey et al. (2005) estimated the cluster age to be in the range of 15–20 Myr and is located at a distance of 2.41 ± 0.11 kpc.

The UBV CCD data were taken from Pandey et al. (2005). Star numbered 221 in their catalogue shows emission and is of B2V type. A 10 Myr isochrone is fitted and the resulting CMD is shown in figure 2.21(a). The star is reddened with respect to the cluster MS and is located below the turn-off. Since the e-star is close to the MS in near-IR CCDm (figure 2.21(b)), it is a candidate CBe star. The spectra of the e-star in the wavelength range 3800 – 9000 Å are shown in figure 2.21(c). Many of the spectral lines like FeII, CaII, OI and Paschen series are present in emission.

2.3.17 NGC 659

The cluster NGC 659 ($RA = 01^h44^m24^s$, $Dec = +60^\circ40'24''$, $l = 129^\circ.375$, $b = -1^\circ.534$) was studied using UBV photometry by McCuskey and Houk (1964), RGU photometry by Steppe (1974), BVRI and H_α photometry by Coyne et al. (1978). Alter (1944) obtained a distance of 3 kpc for this cluster. Phelps and Janes (1994) estimated a distance of 3.5 kpc and an age of 22 Myr from CCD photometry. Pietrzynski et al. (2001) found three Be stars in the cluster when they monitored it for photometric variability over 35 nights. Apart from Be stars they found three pulsating variables of γ -Dor type and one detached binary.

The UBV CCD data were taken from Phelps and Janes (1994) and the stars numbered 193, 11, 109 are e-stars. The spectral types of these stars are B2.5, B0

and B2 respectively. The CMD of the cluster is shown in figure 2.22(a) with a 20 Myr isochrone. The star 2 is found to be in the evolved part of the isochrone while the other two stars are on the MS. All the 3 e-stars are CBe candidates as seen from their location in the optical CMD and near-IR CCDm (figure 2.22(b)). The spectra of the e-stars in the wavelength range 3800 – 9000 Å are shown in figure 2.22(c).

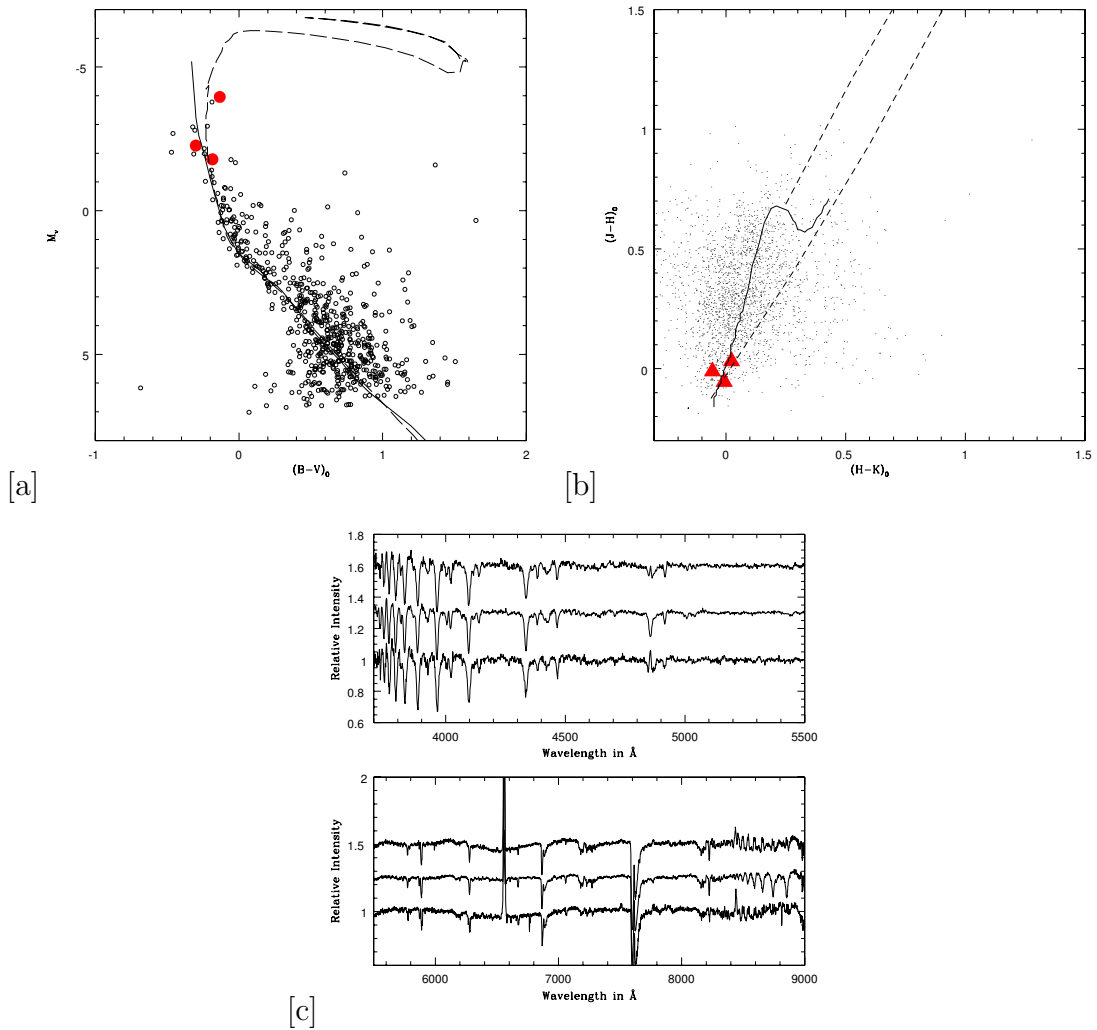


Figure 2.22: (a) Optical CMD of the cluster NGC 659 is shown with the e-stars shown as solid circles. (b) The near-IR CCDm is shown with e-stars shown as filled triangles. (c) The spectra of the e-stars NGC 659(1), NGC 659(2), NGC 659(3), in the wavelength range 3800 – 9000 Å, are shown from bottom to top.

2.3.18 NGC 663

The open cluster NGC 663 ($RA = 01^h 46^m 09^s$, $Dec = +61^\circ 14' 06''$, $l = 129^\circ.467$, $b = -0^\circ.941$, Trumpler class II3r) is rich in e-stars and is located in the Cassiopeia region in the Perseus arm. Sanduleak (1979) observed the cluster using objective-prism plates during a period from 1946 to 1975 and found 27 e-stars with most of the Be stars confined to a spectral type earlier than B5. The number got updated, during an observation in 1981-1990 in high-resolution mode, to 24 with 12 stars showing variability in H_α emission on a timescale of years to several decades (Sanduleak, 1990). Moffat (1972) obtained the cluster parameters as distance = 2.29 kpc, $E(B-V) = 0.86$ and earliest spectral type to be B0 along with some B super giants.

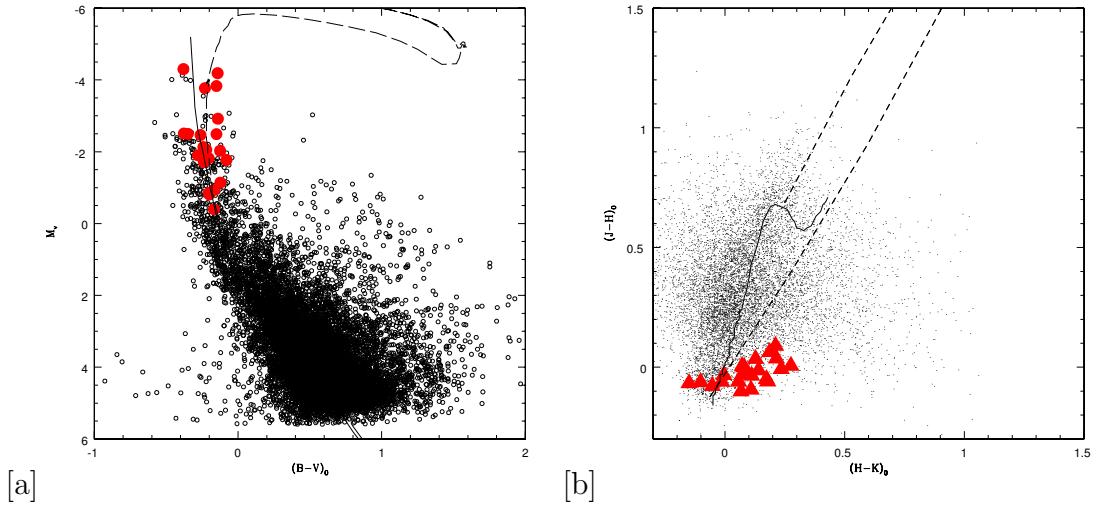


Figure 2.23: (a) Optical CMD of the cluster NGC 663 is shown with the e-stars shown as solid circles. (b) The near-IR CCDm is shown with e-stars shown as filled triangles.

Van den Bergh and de Roux (1978) estimated $E(B-V)$ to vary from 0.8 to 1.0 using photographic UBV photometry with a DM of 11.55 ± 0.04 . Tapia et al. (1991) estimated a distance of 2.5 kpc, $A_V = 1.98 \pm 0.04$ mag, $R_v = 2.73 \pm 0.20$ and an age of 9 Myr from near-IR JHK and Stromgren uvby and H_β photometry. Phelps and Janes (1991) found that the cluster lies in front of a molecular cloud using UBV photometric analysis which was identified earlier by Leisawitz (1989)

from a CO map of this region. Phelps and Janes (1991) estimated a mean reddening of $E(B-V) = 0.80$ mag and a distance of 2.8 kpc. They also found a large deficiency of low mass stars in the cluster relative to the number expected from the field star IMF. As part of an effort to study the star formation history and mass function of open clusters, Pandey et al. (2005) conducted a wide field UBVRI CCD photometry and found a variable reddening from 0.62 to 0.95. Using Bertelli isochrones for $Z = 0.02$, they estimated a distance of 2.42 ± 0.12 kpc and $\log(\text{age}) = 7.4$.

Fabregat and Capilla (2005) performed CCD $uvby\beta$ photometry to estimate a variable reddening of $E(b-y) = 0.639 \pm 0.032$ in the central region to $E(b-y) = 0.555 \pm 0.038$ in the south-east region and a DM of 11.6 ± 0.1 mag. The estimated age of the cluster ($\log t = 7.4 \pm 0.1$) favoured their interpretation of Be phenomenon to be an evolutionary effect. Pigulski et al. (2001b) identified 26 Be stars in the cluster using $BV(RI)_c H_\alpha$ photometry down to a magnitude of $R_c = 15.4$ mag. They detected Be stars over a range of spectral type with the majority falling in between B0 and B3. About 70 % of the observed Be stars showed photometric variability with certain members showing up to 0.4 magnitude variations in Cousins I band (Pigulski et al., 2001a). Pietrzynski (1997) found two Be stars to show variability along with RR Lyrae candidates.

From the slitless survey we found 22 e-stars in the cluster. Stars numbered 13, 24 and P151 have been newly detected. We did not find emission for 4 stars in the cluster, which are identified as Be in SIMBAD (<http://simbad.u-strasbg.fr/simbad/>). This may be due to spectroscopic variability, which seems to be associated with most of the Be stars. The UVB CCD photometric data are from Pandey et al. (2005). The CMD of the cluster along with an isochrone corresponding to a turn-off age of 25 Myr is shown in figure 2.23(a).

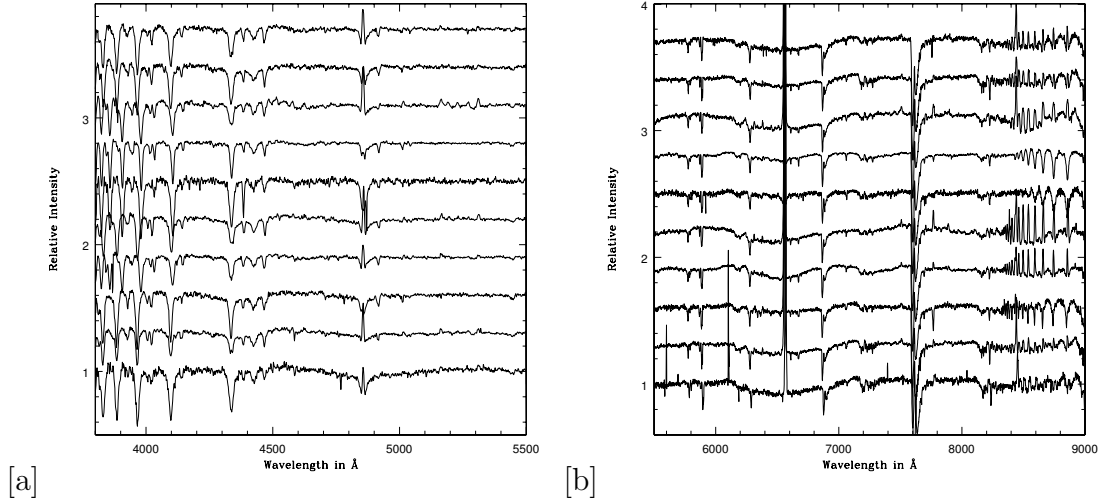


Figure 2.24: The spectra of the e-stars NGC 663(1), NGC 663(2), NGC 663(3), NGC 663(4), NGC 663(5), NGC 663(6), NGC 663(7), NGC 663(9), NGC 663(11) and NGC 663(12), in the wavelength range 3800 – 9000 Å, are shown from bottom to top.

The stars 7, 16, P6 and 12V are found to be at the turn-off of the MS in the optical CMD. The rest of the e-stars are below the turn-off. Thus in this cluster, the e-stars are distributed throughout the MS between the spectral types B0 - B8. The star P6 (V977 Cas) has been quoted as of B2 IV spectral type in SIMBAD while 7 (V985 Cas) is of B3V, 16 (V972 Cas) is of B3III and 12V (V981 Cas) is of B3 type with no information on luminosity class. Our estimates of the spectral types of the above stars seems to be off from the above values quoted in SIMBAD which could be due to different methods used for classification. From the near-IR CCDm (figure 2.23(b)) we can see that all the e-stars are not much reddened, which puts them in CBe category. The spectra of 22 e-stars in the wavelength range 3700 – 9000 Å are given in figures 2.24 & 2.25. The e-stars NGC 663(3), NGC 663(5), NGC 663(7) and NGC 663(13) are found to have 6347 Å SiII line while NGC 663(6), NGC 663(P23), NGC 663(P25) and NGC 663(P151) have 6371 Å line in absorption. The MgII line 7896 Å is present in emission in NGC 663(P5). The lines of FeII, CaII, OI and Paschen series are present in the spectra of all e-stars.

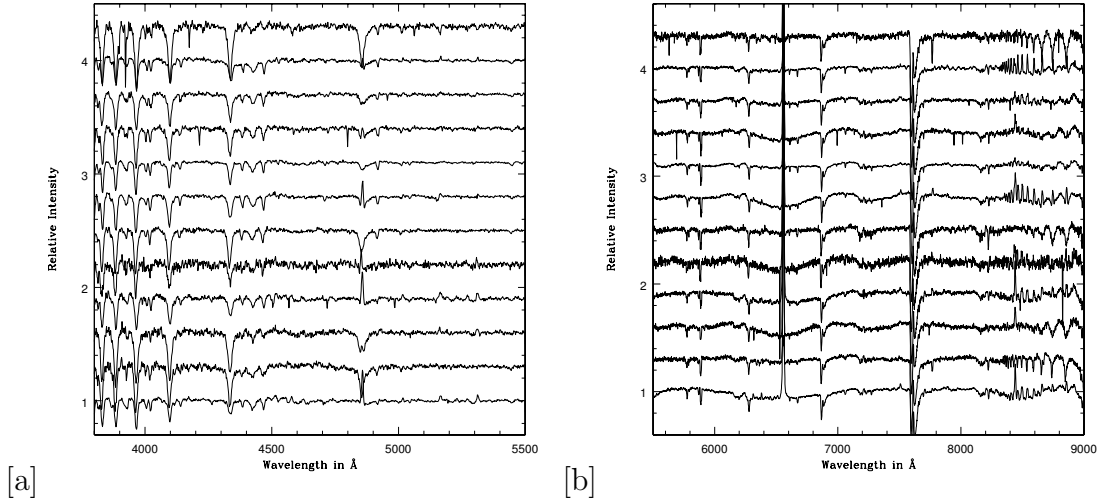


Figure 2.25: The spectra of the e-stars NGC 663(12V), NGC 663(13), NGC 663(14), NGC 663(15), NGC 663(16), NGC 663(24), NGC 663(P5), NGC 663(P6), NGC 663(P8), NGC 663(P23), NGC 663(P25) and NGC 663(P151) in the wavelength range 3800 – 9000 Å, are shown from bottom to top.

2.3.19 NGC 869

NGC 869 (h Persei, $RA = 02^h19^m00^s$, $Dec = +57^\circ07'42''$, $l = 134^\circ.632$, $b = -3^\circ.741$) is a part of the twin cluster h & χ Persei. While searching for B-type pulsators in h Persei, Krzesiński et al. (1999) discovered two β Cephei stars and one SPB star along with three eclipsing binaries and one λ Eri star. They estimated the average reddening to be 0.52 mag with a dispersion of 0.1 mag throughout the cluster from UBV photometry of 258 stars in the field. The cluster parameters listed in WEBDA are distance = 2079 pc, $E(B-V) = 0.575$ and age = 11.72 Myr. Slesnick et al. (2002) found the cluster parameters as $E(B-V) = 0.56 \pm 0.01$, $DM = 11.85 \pm 0.05$, and age = 12.8 ± 1.0 Myr using UBV CCD photometry. They derived a mass of $3700 M_\odot$ for the cluster by integrating the present-day mass function from 1 to $120 M_\odot$. They derived an initial mass function slope to be $\Gamma = -1.3 \pm 0.2$ which is normal for high-mass stars and close to the Salpeter value.

The UBV CCD photometric data of 3461 stars in the cluster are taken from

Slesnick et al. (2002). The cluster is found to contain 6 e-stars in the central region. The CMD of the cluster along with isochrone for a turn-off age of 12.5 Myr is shown in figure 2.26(a). The e-stars 1 (BD+56 534, B2IIIe), 3 (B3IVe) and 4 (BD+56 511, B3III) are reported to be in the evolved phase, as given in SIMBAD. All the e-stars are located well below the MS turn-off.

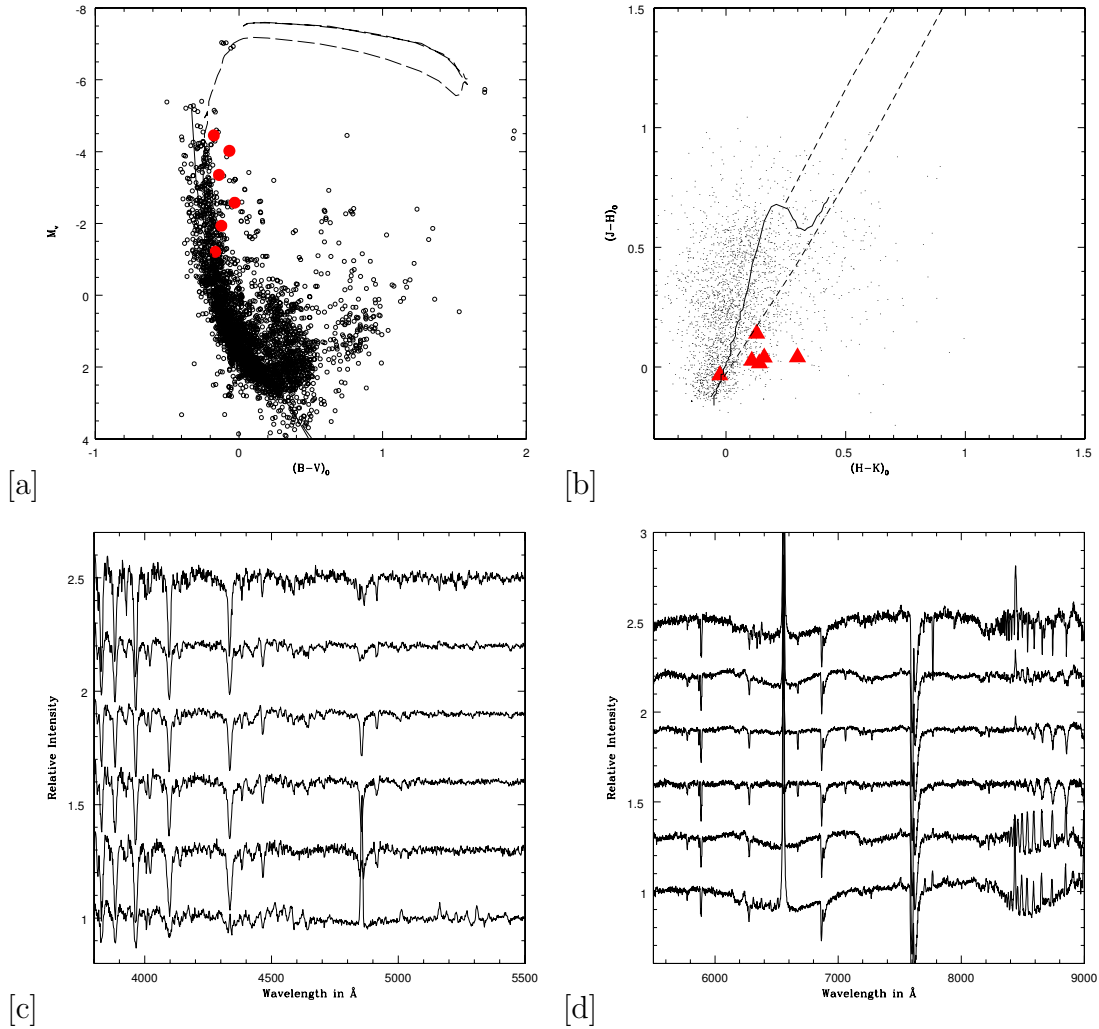


Figure 2.26: (a) Optical CMD of the cluster NGC 869 is shown with the e-stars shown as solid circles. (b) The near-IR CCDm is shown with e-stars shown as filled triangles. (c) & (d) The spectra of the e-stars NGC 869(1), NGC 869(2), NGC 869(3), NGC 869(4), NGC 869(5) and NGC 869(6), in the wavelength range 3800 – 9000 Å, are shown from bottom to top.

The stars are found to lie in the CBe location in the near-IR CCDm (figure

2.26(b)). The stars 2, 3 and 5 seems to be clubbed together and hence show similar reddening values. All the e-stars are found to be CBe candidates. The spectra of the e-stars in the wavelength range 3800 – 9000 Å are shown in figure 2.26(c & d). The SiII line 6347 Å is found to be in emission for NGC 869(1) while it is in absorption for NGC 869(6). OI 8446 Å is found in emission for all e-stars.

2.3.20 NGC 884

NGC 884 (χ Persei, $RA = 02^h22^m18^s$, $Dec = +57^\circ08'12''$, $l = 135^\circ.052$, $b = -3^\circ.582$) is the younger of the double cluster h & χ Persei, located in the Perseus arm of the Galaxy. Fletcher (1988) suggested the presence of M-type red super giants in the cluster. Krzesinski and Pigulski (1997) performed a photometric search for B-type pulsators in the central region of χ Persei cluster and found two β Cephei stars, apart from nine other variables which contains two eclipsing stars. They found the Be stars in the cluster to be variable and redder than B stars of the same spectral type. The cluster parameters as given in WEBDA are distance = 2345 pc, reddening = 0.560, age = 10.76 Myr.

Slesnick et al. (2002) found the cluster parameters as $E(B-V) = 0.56 \pm 0.01$, $DM = 11.85 \pm 0.05$ and age = 12.8 ± 1.0 Myr using UBV CCD photometry. They derived a mass of 2800 M_\odot for the cluster by integrating the present-day mass function from 1 to 120 M_\odot . They derived an initial mass function slope to be $\Gamma = -1.3 \pm 0.2$ which is normal for high-mass stars and close to the Salpeter value.

The UBV CCD photometric data of 3144 stars in the cluster were taken from Slesnick et al. (2002). The cluster is found to contain 6 e-stars in the central region. The optical CMD of the cluster along with an isochrone for a turn-off age of 12.5 Myr is shown in figure 2.27(a). The star 2 (BD+56 573) is found to be of B2III-IVe spectral type. The star 5 (V506 Per) has been reported as a variable

in SIMBAD and found to be of B1IIIe spectral type. All the e-stars are located below the turn-off.

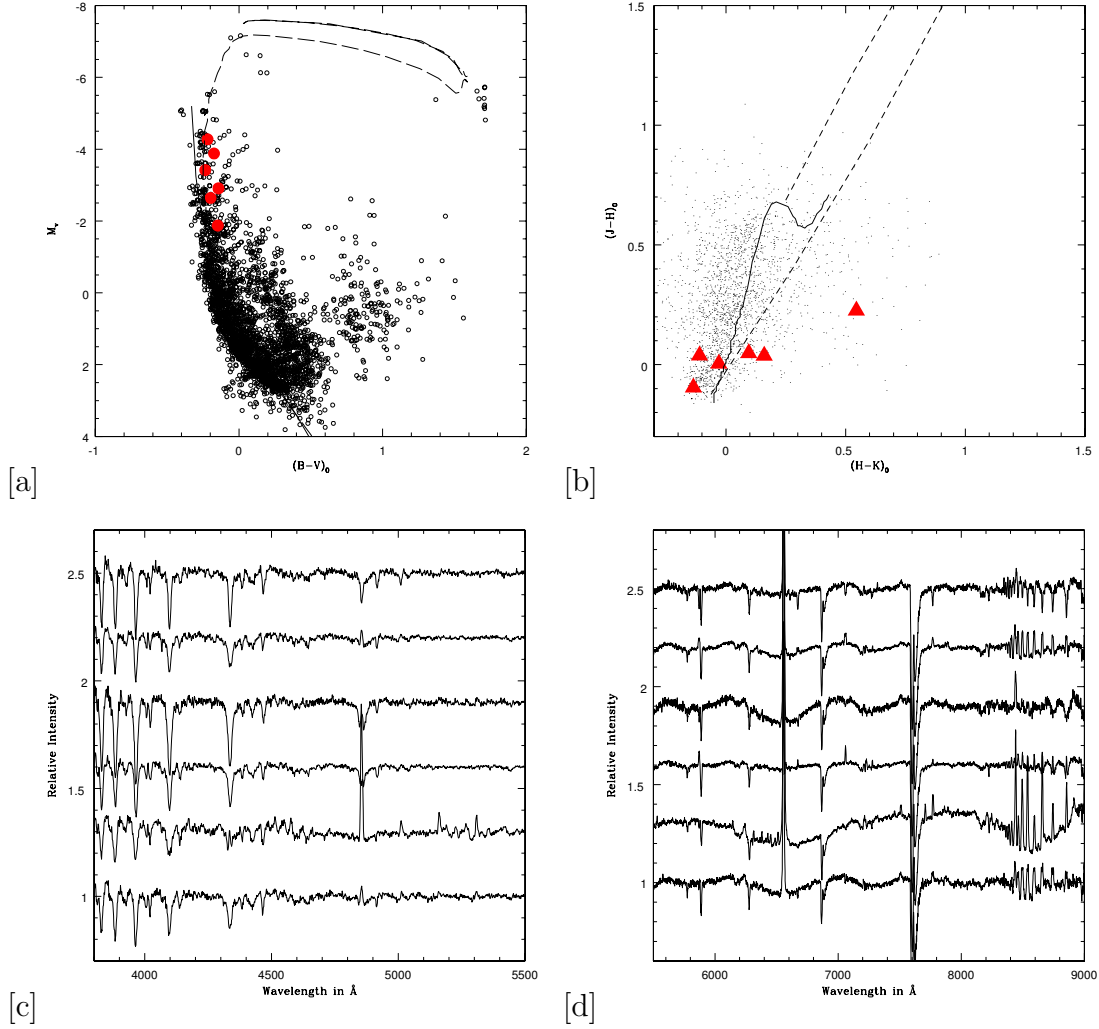


Figure 2.27: (a) Optical CMD of the cluster NGC 884 is shown with the e-stars shown as solid circles. (b) The near-IR CCDm is shown with e-stars shown as filled triangles. (c) & (d) The spectra of the e-stars NGC 884(1), NGC 884(2), NGC 884(3), NGC 884(4), NGC 884(5) and NGC 884(6), in the wavelength range 3800 – 9000 \AA , are shown from bottom to top.

It can be seen that all the e-stars in near-IR CCDm (figure 2.27(b)) have relatively less reddening suggesting that they belong to CBe category. Star 2 has large IR excess, may be due to the presence of a large amount of circumstellar material. The spectra of the e-stars in the wavelength range 3800 – 9000 \AA are shown in

figure 2.27 (c & d). We found HeI 5876, 6678, 7065 Å in emission for NGC 884(5) with SiII 6347 and 6371 Å lines. NGC 884(2) is found to have 25 FeII emission lines along with SiII and MgII 7896 Å lines in emission.

2.3.21 NGC 957

NGC 957 is an open cluster of Trumpler class III3r with coordinates $RA = 02^h33^m21^s$, $Dec = +57^{\circ}33'36''$, $l = 136^{\circ}.287$, $b = -2^{\circ}.645$ and is located in the Perseus spiral arm. This cluster lies near to the double cluster η & χ Persei. Using photographic photometry for 250 stars brighter than $V=14.5$ mag, in the Morgan-Johnson UBV system, Gerasimenko (1991) estimated a distance of 1.82 kpc, a colour excess of 0.90 and an age of 3.8 Myr. Gimenez and Garcia-Pelayo (1980) investigated the cluster using RGU photographic photometry and found a reddening of $E(G-R) = 1.12$ and a distance of 1850 pc. Using UBVR CCD and 2MASS JHK photometry Yadav et al. (2008) estimated the radius of the cluster as 4.3 arcmin at a distance of 2.2 ± 0.2 kpc and age of 10 ± 5 Myr. The mass function slope for the cluster is found to be 1.31 ± 0.50 by correcting field star contamination and data incompleteness. The cluster was found to be dynamically relaxed due to the dynamical evolution of the cluster.

The UBV photoelectric data for the cluster were taken from Hoag et al. (1961) and the e-stars are 94 and 188 in their catalogue. Star 94 belongs to B2 and star 188 belongs to B2.5 spectral type. The CMD of the cluster is shown in figure 2.28(a) with a 10 Myr isochrone. The e-stars are located well below the MS turn-off. From the location of stars in optical CMD and near-IR CCDm (figure 2.28(b)) it can be inferred that both are CBe candidates. The spectra of the e-stars in the wavelength range 3800 – 9000 Å are shown in figure 2.28(c). Both e-stars are found to have MgII line 7896 Å, OI 7772 & 8446 Å and CaII triplet in emission.

NGC 957(1) has SiII lines in emission.

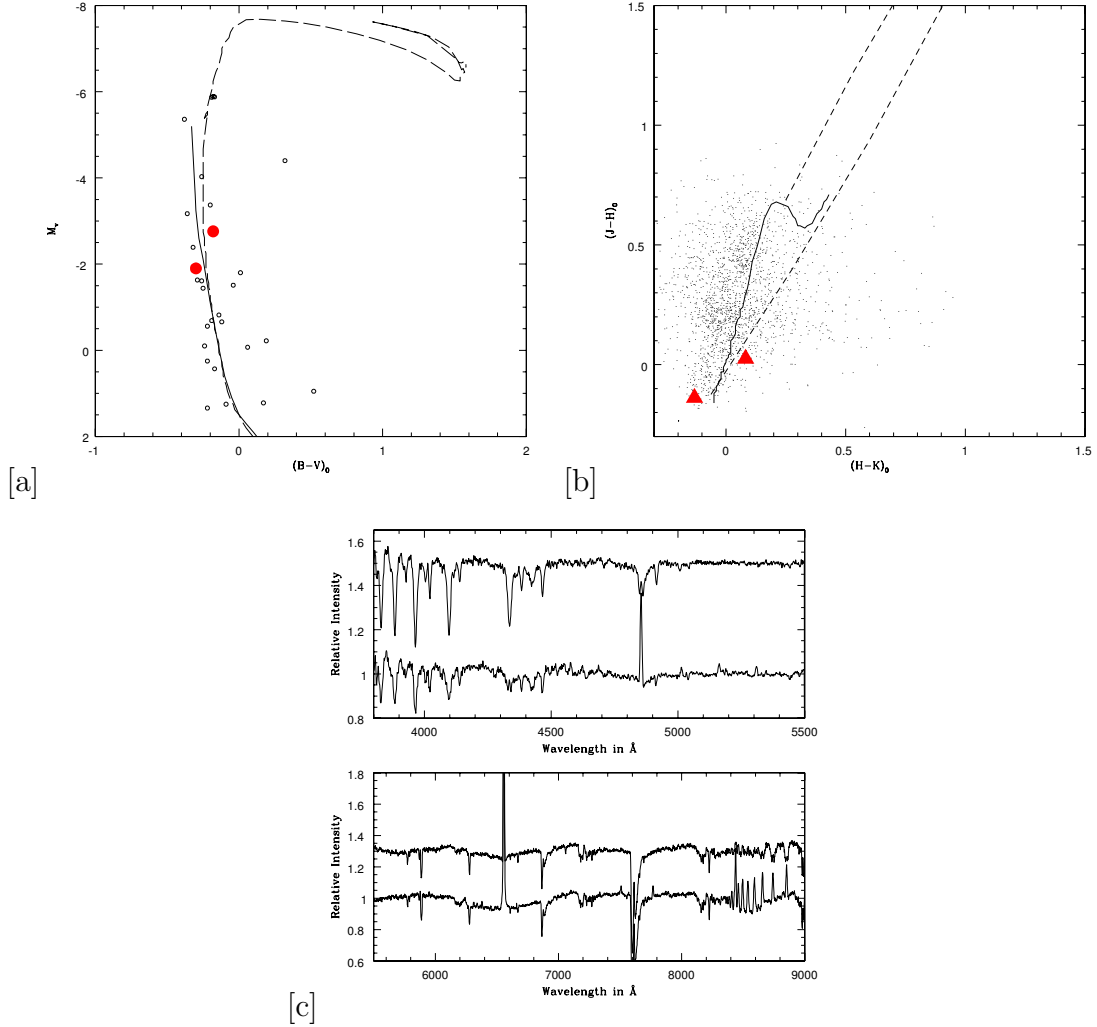


Figure 2.28: (a) Optical CMD of the cluster NGC 957 is shown with the e-stars shown as solid circles. (b) The near-IR CCDm is shown with e-stars shown as filled triangles. (c) The spectra of the e-stars NGC 957(1) and NGC 957(2), in the wavelength range 3800 – 9000 Å, are shown from bottom to top.

2.3.22 NGC 1220

NGC 1220 ($RA = 03^h 11^m 40^s$, $Dec = +53^\circ 20' 42''$, $l = 143^\circ.036$, $b = -3^\circ.963$) is a young compact open cluster with a core radius of 1.5–2.0 arcmin. Ortolani et al.

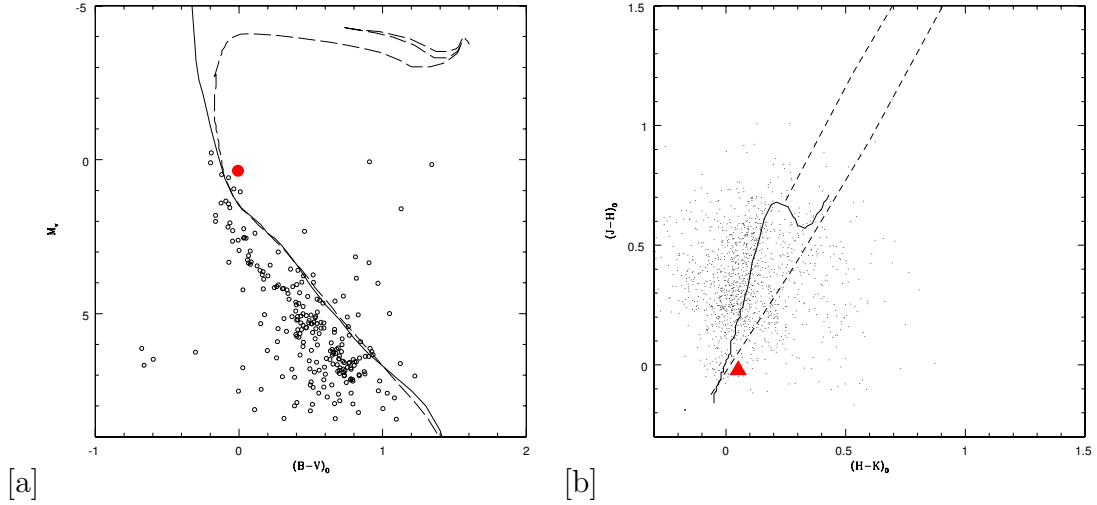


Figure 2.29: (a) Optical CMD of the cluster NGC 1220 is shown with the e-star shown as solid circles. (b) The near-IR CCDm is shown with e-star shown as filled triangle.

(2002) estimated the reddening $E(B-V) = 0.70 \pm 0.15$ mag, distance = 1800 ± 200 pc and an age of 60 Myr using UBV CCD observations. They found the cluster to lie at 120 pc above the galactic plane which is relatively high for its age. From the location of stars in $(B-V)$ vs $(U-B)$ plane, they inferred that the cluster members are between B5 and A5 spectral types.

The UBV CCD data were taken from Ortolani et al. (2002) for 234 stars. The star numbered 25 is found to show emission and is of B9.5 type. A 60 Myr isochrone is fitted and the resulting CMD is shown in figure 2.29(a). Both the ZAMS and isochrone fit do not look impressive. As mentioned in the beginning, we have used the parameters in the reference for fitting. Re-estimation of the parameters will be done using fresh photometric observations. From the location of the e-star in near-IR CCDm (figure 2.29(b)), the e-star is inferred to be CBe star with low IR excess. This cluster thus hosts one of the oldest CBe stars. The spectra of the e-star in the wavelength range $3800 - 9000 \text{ \AA}$ are shown in figure 2.30.

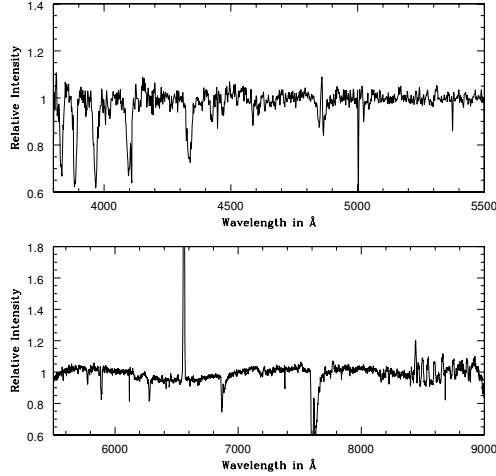


Figure 2.30: The spectra of the e-star in NGC 1220 are shown in the wavelength range 3800 – 9000 Å.

2.3.23 NGC 1624

NGC 1624 (OC1 403, Cr 53; $RA = 04^h 40^m 38^s$, $Dec = +50^\circ 28' 04''$, $l = 155^\circ.356$, $b = 2^\circ.616$) is a young cluster of Trumpler class I2p. Sujatha and Babu (2006) obtained UBVRI CCD photometry and found it to be 6.025 ± 0.5 kpc distant. It shows a differential reddening with $E(B-V)$ ranging from 0.70 to 0.90 mag, which might be due to the presence of an HII region within which the cluster is embedded. The cluster is young with an age of 3.98 Myr and has an initial mass function slope of 1.65 ± 0.25 , which is close to the Salpeter value.

The UVB CCD data were taken from Sujatha and Babu (2006) for 206 stars in the cluster. The star 101 is an e-star and is of B1 spectral type. This e-star is found to be associated with nebulosity. A 4 Myr isochrone is fitted and the resulting CMD is shown in figure 2.31(a). The e-star is located near the top of the MS, but below the turn-off. The star belong to CBe category as inferred from its location in the optical CMD and near-IR CCDm (figure 2.31(b)).

The spectra of the e-star in the wavelength range 3800 – 9000 Å are shown in

figure 2.31(c). HeI 4471 Å absorption line profile is found to be thin while 5876, 6678 and 7065 lines are in emission. The HeII lines 4541 and 5412 Å are found to be in absorption while 4687 Å is in emission. The candidate is found to be of O6 spectral type in SIMBAD. But high ionization lines of elements like silicon are not present. Moreover features like P-Cygni are not associated with line profiles.

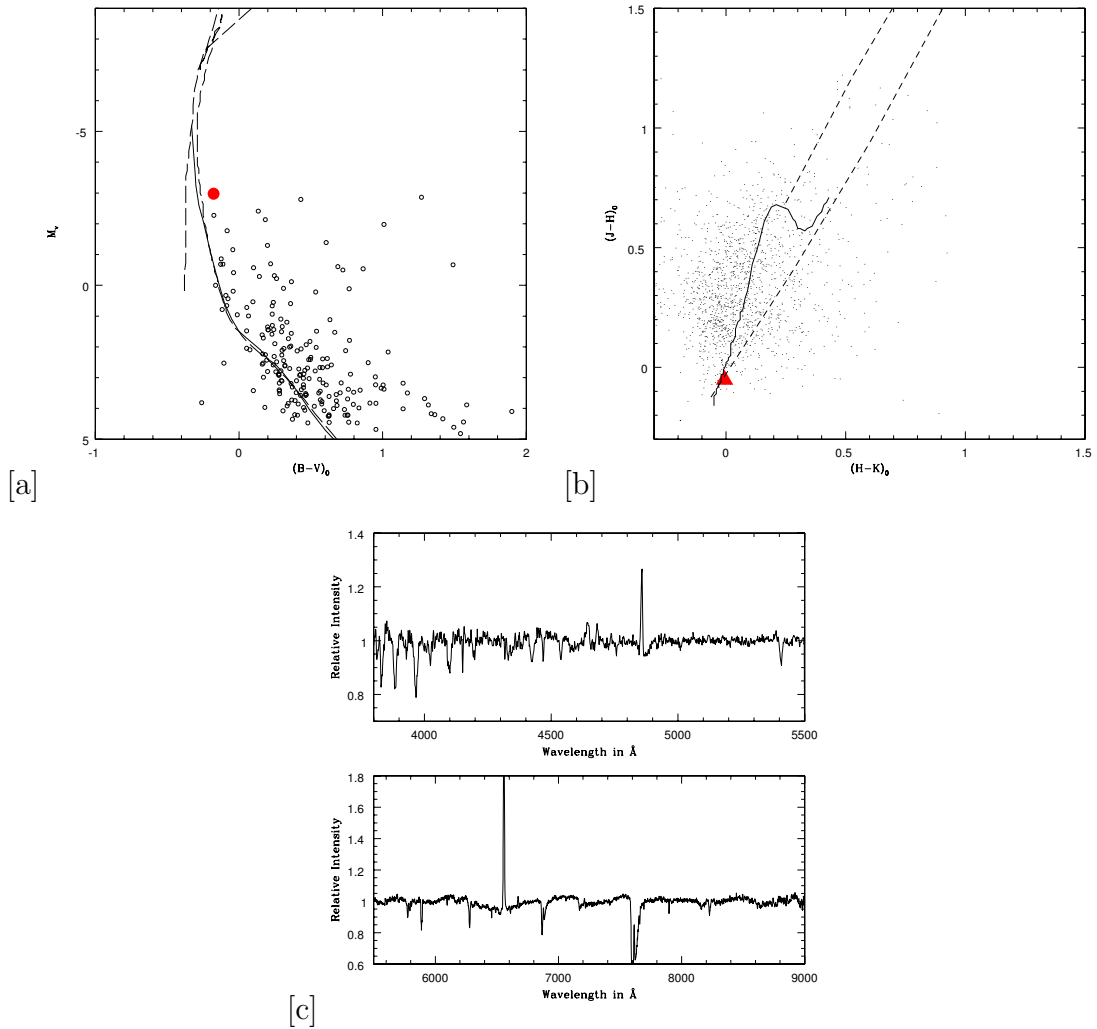


Figure 2.31: (a) Optical CMD of the cluster NGC 1624 is shown with the e-star shown as solid circle. (b) The near-IR CCDm is shown with e-star shown as filled triangle. (c) The spectra of the e-stars in the cluster are shown in the wavelength range 3800 – 9000 Å.

We found a probable companion at about 10 arc-second distance from the star. We plan to check for binarity by monitoring the variability of HeII and HeI lines

through repeated observations.

2.3.24 NGC 1893

NGC 1893 ($RA = 05^h22^m44^s$, $Dec = +33^{\circ}24'42''$, $l = 173^{\circ}.58$, $b = -1^{\circ}.680$) is a very young cluster associated with the bright diffuse nebulosity, IC 410 and obscured by several conspicuous dust clouds. UBV photometry has been carried out by Cuffey (1973) and Massey et al. (1995). Massey et al. (1995) found a mean $E(B-V)$ of 0.53 ± 0.02 for the cluster along with a distance of 2057 pc and an age of 2–3 Myr, estimated using massive stars. Moffat (1972) found an O5 type star as a cluster member at a distance of 3.98 kpc and reddening of 0.55 mag using faint stars. Some of the early-type stars in the cluster are responsible for the photo ionization of the IC 410 nebula. Tapia et al. (1991) performed near-IR and Strömgen photometry of 50 stars down to $K = 12$ mag. They estimated an age of 4 Myr along with a total extinction of 1.68 in V band and a distance of 4325 pc. The distance and age obtained by Fitzsimmons (1993) match with Tapia et al. (1991). Vallenari et al. (1999) studied about 700 stars down to $K \sim 17$ in J and K bands and estimated an age of 4 Myr and reddening value of 0.35 mag. Marco and Negueruela (2003) carried out a search for emission-line PMS stars using slitless spectroscopy in the cluster NGC 1893 and found 19 stars between B-type and G-type. They suggested that all the PMS stars are confined to the outer rim of the molecular cloud associated with the HII region IC 410 and the bright emission cometary nebulae Sim 129 and Sim 130. From the spatial distribution of PMS stars, they came up with the possibility of star formation in NGC 1893 triggered by the O-type stars in the cluster.

From the co-existence of HAeBe stars and B-type MS stars along with O-type stars, Marco and Negueruela (2002) concluded that massive star formation is still

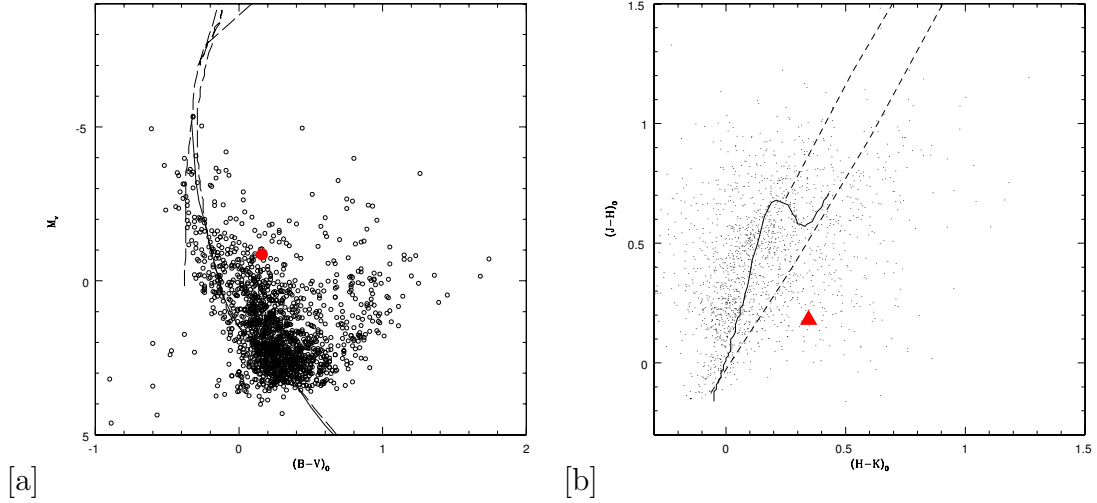


Figure 2.32: (a) Optical CMD of the cluster NGC 1893 is shown with the e-star shown as solid circle. (b) The near-IR CCDm is shown with e-star shown as filled triangle.

ongoing in NGC 1893 and has been taking place over a relatively long timescale. Marco et al. (2001) estimated a color excess $E(b-y)=0.33 \pm 0.03$ and a DM of 13.9 ± 0.2 from $uvby\beta$ photometry. Yadav and Sagar (2001) found a non-uniform extinction in the cluster with the $E(B-V)$ value varying from 0.39 to 0.63 mag. Sharma et al. (2007) have used near-IR colours, slitless spectroscopy and narrow-band H_α photometry to explore the effects of massive stars on low-mass star formation. They identified the candidate YSOs to have an age spread between 1 and 5 Myr using V versus $(V-I)$ CMD. This indicated a non-coeval star formation in the cluster. They found a shallower value of mass function for PMS stars compared to a value of -1.71 ± 0.20 for MS stars in the cluster.

The UBV CCD data for 1591 stars in the cluster were taken from Massey et al. (1995). The star 35 is an e-star of B6 spectral type. A 4 Myr isochrone is fitted and the resulting CMD is shown in figure 2.32(a). From the fitting of PMS isochrones to the optical CMD, the star is likely to be as young as 0.1 Myr. The e-star is found to be reddened by 0.3 mag in $(J-H)$ and 0.4 mag in $(H-K)$ (figure 2.32(b)). But the e-star is not associated with nebulosity. Since it is found to be of late spectral

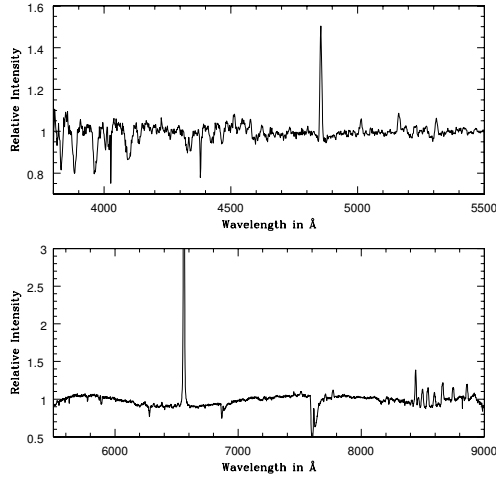


Figure 2.33: The spectra of the e-star in the cluster NGC 1893 are shown in the wavelength range 3800 – 9000 Å.

type and the cluster as a whole is young, it may be a HBe candidate, when coupled with information from near-IR excess and PMS isochrone fitting. The cluster has been reported to be located in a young star forming region and this HBe star is found to be in a location close to the core of the cluster. The spectra of the e-star in the wavelength range 3800 – 9000 Å are shown in figure 2.33. All the major lines are in emission including SiIII 6347 Å line. A total of 18 FeII lines are seen in emission with a shell line at 4233 Å.

2.3.25 NGC 2345

NGC 2345 ($RA = 07^h08^m18^s$, $Dec = -13^{\circ}11'36''$, $l = 226^{\circ}.580$, $b = -2^{\circ}.314$) is supposed to be a moderately young open cluster located in Canis Major. Moffat (1974) estimated a distance of 1.75 kpc from photoelectric UBV and spectroscopic observations. He found that the cluster contains two A-type and 5 K-type giants and the earliest spectral type detected is B4. WEBDA quotes an age of 71 Myr and a reddening of 0.616 mag.

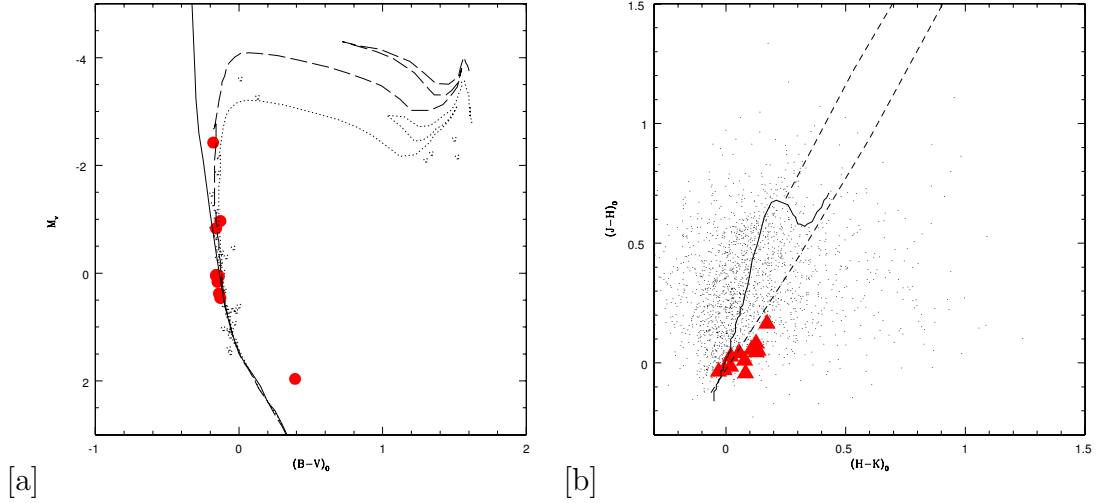


Figure 2.34: (a) Optical CMD of the cluster NGC 2345 is shown with the e-stars shown as solid circles. (b) The near-IR CCDm is shown with e-stars shown as filled triangles.

This cluster is not known to have any e-stars. We report the detection of 12 e-stars in this cluster. The UBV photoelectric data were taken from Moffat (1974) for 59 stars in the cluster. Out of the total list of 64 stars, 5 are left out for not having $E(B-V)$ value. Since the photometry is available only for a few stars in this cluster, we have obtained UBV CCD observation to estimate the cluster parameters accurately. Since we have not finished the analysis we are presenting the values obtained by Moffat (1974). The stars NGC 2345(X1) and NGC 2345(X2) do not have any photometric data. An isochrone of age 63 Myr is fitted to the cluster data (dashed line in figure 2.34(a)) considering the position of e-stars. We have fitted a 100 Myr isochrone (dotted line in figure 2.34(a)) considering giants as members of this cluster and to accommodate them in the fit. Hence the cluster seems to be in the age range 60–100 Myr.

The star 35 is found near the turn-off of the MS in the CMD and has been quoted as of spectral type B4 III in the literature (SIMBAD). The star 32 is found to be of A5 spectral type. All the remaining e-stars belongs to late B spectral type (B5–B9). All the stars are found to be in CBe location in the near-IR CCDm

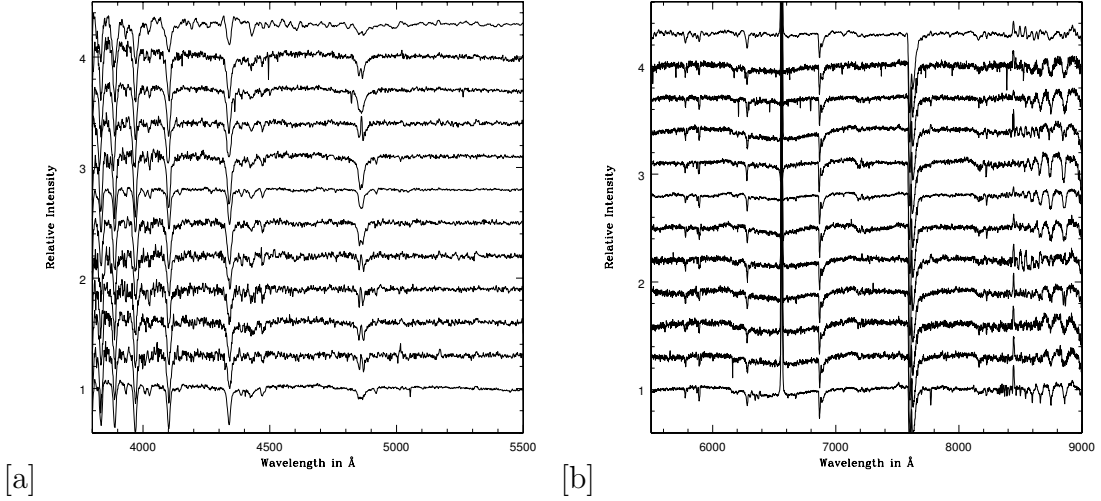


Figure 2.35: (a) & (b) The spectra of the e-stars NGC 2345(2), NGC 2345(5), NGC 2345(20), NGC 2345(24), NGC 2345(27), NGC 2345(32), NGC 2345(35), NGC 2345(44), NGC 2345(59), NGC 2345(61), NGC 2345(X1) and NGC 2345(X2), in the wavelength range 3800 – 9000 Å, are shown from bottom to top.

(figure 2.34(b)). This is one of the oldest cluster to have a large number of e-stars. This cluster is very interesting due to the presence of large number of e-stars and giants. The spectra of the e-stars in the wavelength range 3800 – 9000 Å are shown in figure 2.35. All the e-stars except NGC 2345(20), NGC 2345(24), NGC 2345(59) and NGC 2345(X2) are found to have SiIII lines in the spectra.

2.3.26 NGC 2414

Vogt and Moffat (1972) found a constant reddening across the cluster NGC 2414 ($RA = 07^h33^m12^s$, $Dec = -15^{\circ}27'12''$, $l = 231^{\circ}.412$, $b = 1^{\circ}.946$) with a mean value of $E(B-V) = 0.55$ mag and a distance of 4.15 kpc. They have used only 10 stars as cluster members and the earliest one was of B1 spectral type. As a part of analysing the luminous stars in $l = 231^{\circ}$ region, Fitzgerald and Moffat (1980) found the cluster to lie at a distance of 4.15 kpc and colour excess of 0.55 ± 0.03 mag. From the significant lack of stars beyond 4.2 kpc they suggested that the

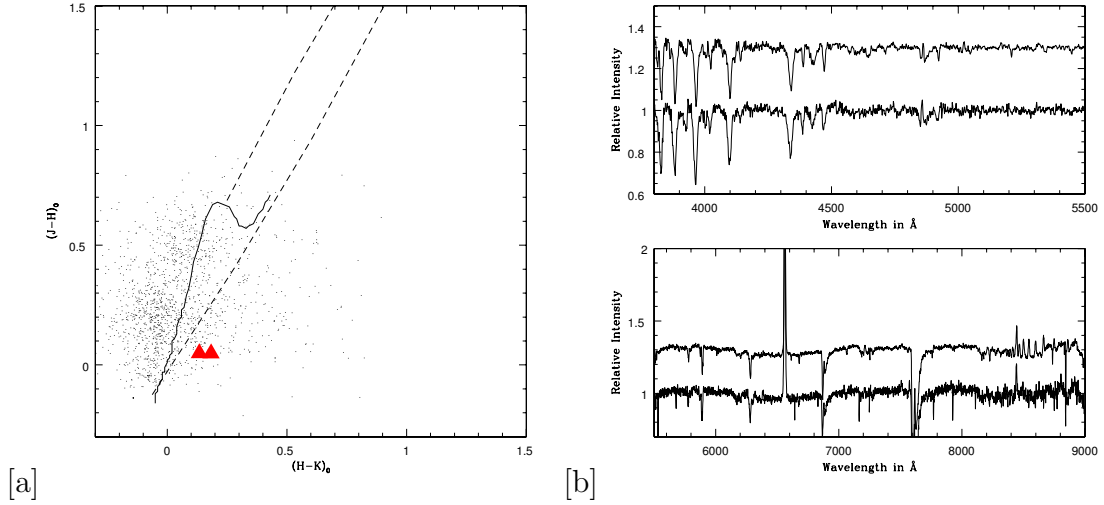


Figure 2.36: (a) The near-IR CCDm of the cluster NGC 2414 is shown with e-stars shown as filled triangles. (b) The spectra of the e-stars NGC 2414(1) and NGC 2414(2), in the wavelength range 3800 – 9000 Å, are shown from bottom to top.

Orion arm does not extend beyond this distance in this direction. WEBDA alerts that this may not be a true cluster.

No photometric data is available for the e-stars in this cluster. The e-stars are found to be of B1.5 and B0 spectral types from spectral line matching. The 2MASS photometric data of the cluster was de-reddened using $E(B-V)$ value of 0.55, as given in Vogt and Moffat (1972). The near-IR CCDm of the cluster is shown in figure 2.36(a). The Be stars show low near-IR excess. The cluster is not associated with nebulosity. Hence both of them belong to CBe category. The spectra of the e-stars in the wavelength range 3800 – 9000 Å are shown in figure 2.36(b).

2.3.27 NGC 2421

The open cluster NGC 2421 ($RA = 07^h36^m13^s$, $Dec = -20^{\circ}36'42''$, $l = 236^{\circ}.271$, $b = 0^{\circ}.069$) was classified as Trumpler class I2m by Ruprecht (1966). Moffat and Vogt (1975) used UB V , H β photoelectric photometry to study the cluster and estimated

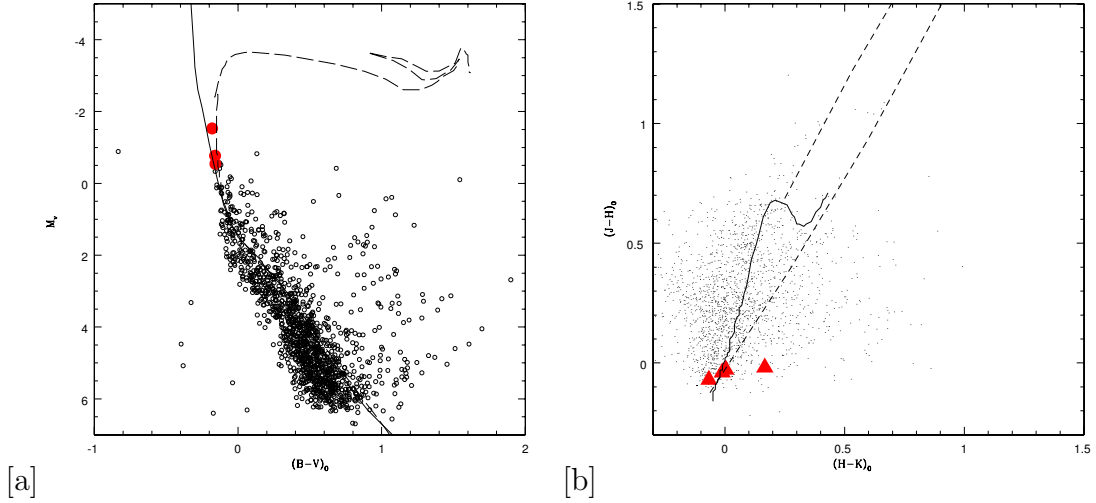


Figure 2.37: (a) Optical CMD of the cluster NGC 2421 is shown with the e-stars shown as solid circles. (b) The near-IR CCDm is shown with e-stars shown as filled triangles.

the cluster parameters as $E(B-V) = 0.47 \pm 0.05$, distance = 1.87 kpc with an earliest spectral type of B0.5 in the cluster. Ramsay and Pollaco (1992) observed the central region of the cluster of size 2.2×3.3 arcmin, using $UBVI_c$ photometry. They estimated a distance of 2.75 kpc, reddening of $E(B-V) = 0.49 \pm 0.03$ and an age less than 300 Myr. Yadav and Sagar (2004) studied the cluster using $UBVRI$ CCD photometry and determined the radius of the cluster to be 3 arcmin using stellar density profile. The cluster exhibits a colour excess of $E(B-V) = 0.42 \pm 0.05$ mag and an age of 80 ± 20 Myr. A distance of 2.2 ± 0.2 kpc has been obtained from ZAMS fitting and the metallicity was found to be $Z \sim 0.004$. The cluster is dynamically relaxed with a relaxation time of 30 Myr.

The UBV CCD data and XY positions for 1285 stars are taken from Yadav and Sagar (2004). We detected 4 e-stars in this cluster using slitless spectroscopy. Stars numbered 873(2) of Yadav and Sagar (2004), 1436(1), 1452(4) from Moffat and Vogt (1975) and 32(3) from Babu (1983) are found to show emission. The numbers given in brackets are our identification numbers. The stars belong to the spectral type B7V, B3.5V, B6.5V and B8 respectively. The star numbered 3 does

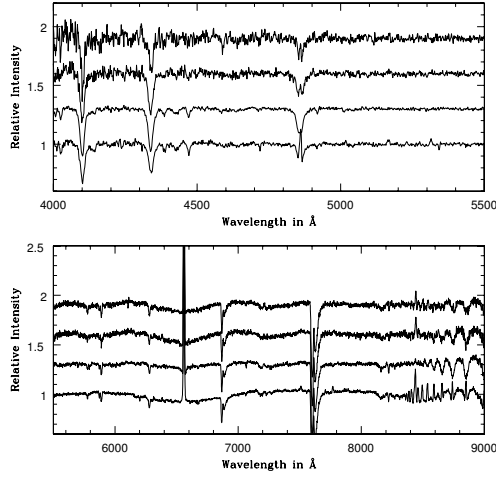


Figure 2.38: The spectra of the e-stars NGC 2421(1), NGC 2421(2), NGC 2421(3) and NGC 2421(4), in the wavelength range 3800 – 9000 Å, are shown from bottom to top.

not have $(B-V)$ value and hence cannot be represented in the optical CMD. All the Be stars seem to be located close to the evolved part of the cluster sequence. An 80 Myr isochrone is fitted to the MS and the resulting CMD is shown in figure 2.37(a). Since the data for e-stars are taken from different references and the ZAMS and isochrone fit is poor, re-estimation of parameters is necessary using new CCD data. The e-stars 2, 3 and 4 are clubbed together at the tip of the MS while star 1 is more reddened in $(H-K)$ colour as shown in near-IR CCDm (figure 2.37(b)). Since star 1 looks like more evolved compared to other stars in the cluster CMD, it might be a Be star in giant phase with circumstellar dust. The spectra of the e-stars in the wavelength range 3800 – 9000 Å are shown in figure 2.38. OI 8446 Å is found to be in emission for all e-stars while CaII triplet is in emission for NGC 2421(1) and NGC 2421(4).

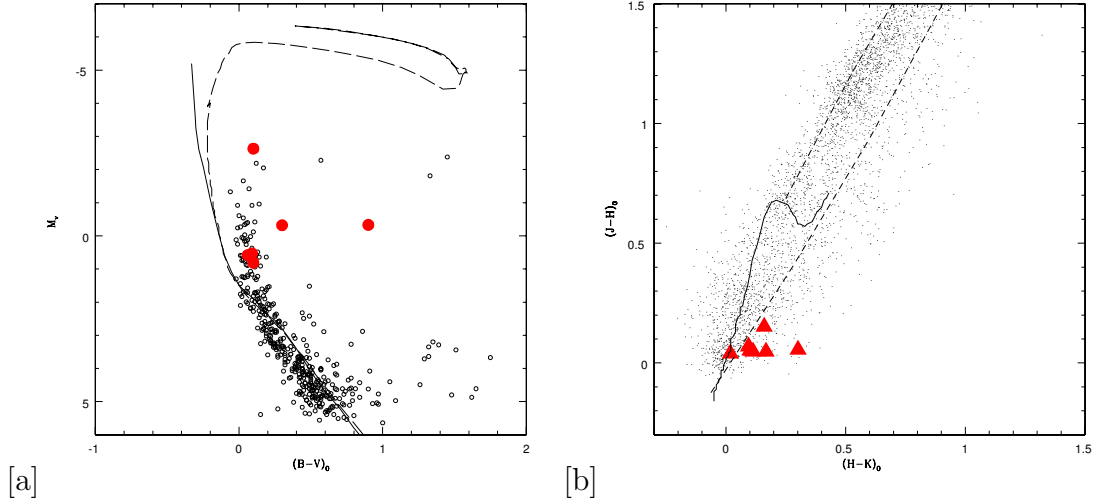


Figure 2.39: (a) Optical CMD of the cluster NGC 6649 is shown with the e-stars shown as solid circles. (b) The near-IR CCDm is shown with e-stars shown as filled triangles.

2.3.28 NGC 6649

NGC 6649 ($RA = 18^h33^m27^s$, $Dec = -10^{\circ}24'12''$) is a relatively rich, compact cluster lying in the galactic plane ($l = 21^{\circ}.635$, $b = -0^{\circ}.785$) behind a dusty region, producing more than four magnitudes of visual absorption. The cluster was studied by The and Roslund (1963), Talbert (1975) and Barrell (1980). Walker and Laney (1987) estimated a distance of 1585 pc from UB V CCD photometry. The cluster is heavily reddened with a variable reddening of 0.3 mag over 5 arc-minute diameter of the cluster. The cluster is found to contain a Cepheid variable V367 Scuti with $M_v = -3.80$. Madore and van den Bergh (1975) estimated a DM of 15.4 and an $E(B-V)$ of 1.37 for the cluster using UB V photoelectric photometry. An age of 37 Myr is given in WEBDA.

The UB V photometric data for 400 stars were taken from Walker and Laney (1987). There are 7 e-stars in this cluster as identified from the slitless spectra. Stars numbered 16(2) in Talbert (1975), 65(6) in Walker and Laney (1987), 09(1) and 20(3) in Madore and van den Bergh (1975), stars 59(4) and 81(5) in The and Roslund (1963) are found to show emission. The numbers given in brackets are our

catalogue numbers and star number 7 in our catalogue does not have photometric data.

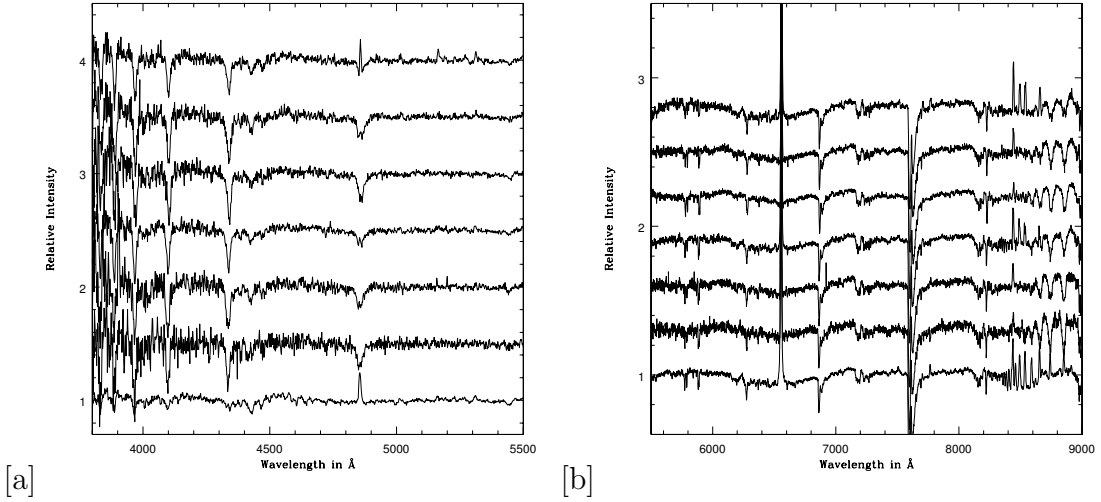


Figure 2.40: (a) & (b) The spectra of the e-stars NGC 6649(1), NGC 6649(2), NGC 6649(3), NGC 6649(4), NGC 6649(5), NGC 6649(6) and NGC 6649(7), in the wavelength range 3800 – 9000 Å, are shown from bottom to top.

An isochrone for 25 Myr is fitted to the cluster data and the resulting CMD is shown in figure 2.39(a). The isochrone fit does not look satisfactory. Moreover the magnitudes of e-stars are taken from different references. Hence we are planning to estimate the parameters using new UBV CCD photometry. The e-star numbered 1 seems to be near the turn-off, whereas others are well below the turn-off point of the isochrone. The same star separates out in IR excess from other stars in near-IR CCDm (figure 2.39(b)). It may be a CBe giant with a dusty envelope around it since the excess in (H–K) is higher than in (J–H) colour. The e-stars are found to belong to CBe category since all of them are clustered near the hot end of MS showing a little excess. Star 4 is very reddened in the optical CMD, such a large reddening is not seen in the near-IR CCDm, the (B–V) value of this star may be unreliable. The spectra of the e-stars in the wavelength range 3800 – 9000 Å are shown in figure 2.40. All e-stars except NGC 6649(1) and NGC 6649(2) show Si III

lines in the spectra.

2.3.29 NGC 6756

NGC 6756 ($RA = 19^h08^m42^s$, $Dec = +04^{\circ}42'18''$, $l = 39^{\circ}.089$, $b = -1^{\circ}.682$) is a moderately young open cluster belonging to Trumpler type I2r. Using CCD Strömgren Photometry of 368 stars in the cluster, Delgado et al. (1997) estimated an age of 131 Myr, $E(B-V)$ of 0.91 and DM of 12.60 mag. Paunzen et al. (2003) searched for peculiar stars in the cluster using narrow band photometric system. They estimated the uvby indices for two peculiar stars and found that it matches with a typical B8 star and a late type star respectively. Svolopoulos (1965) used RGU system to estimate a distance of 1.65 kpc, linear diameter of the cluster as 1.9 pc, reddening values $E(G-R) = 1.64$, $E(U-G) = 1.15$ mag and the earliest spectral type as B3. Different authors estimate a range of cluster diameter (3 – 11 arcmin) and distance (1270 – 5250 pc) values. Similarly, a large range in age is found in the literature, from 63 Myr (WEBDA) to 130 Myr (Delgado et al., 1997).

We have obtained UBV photometry of the cluster using HCT. The reddening has been obtained as $E(B-V) = 1.1$ (Ranges between 1.1–1.2) and a DM of 15.8, which translates to a distance of 3 kpc. The age is estimated to be in the range 125 – 150 Myr. The isochrones corresponding to 125 Myr and 150 Myr are fitted in the CMD (figure 2.41(a)). The e-stars are close to the evolved region of the isochrone. They belong to B3.5 and B2.5 spectral types respectively. Even though the e-stars are reddened, they lie within the reddening vector in near-IR CCDm (figure 2.41(b)). Hence both of the e-stars may be CBe stars.

Thus, NGC 6756 is one of the few clusters which has crossed the survey category of 100 Myr and one of the old clusters to have CBe stars. The spectra of the

e-stars in the wavelength range 3800 – 9000 Å are shown in figure 2.41(c). The e-star NGC 6756(3) is found to have 5577 [OI] line in emission.

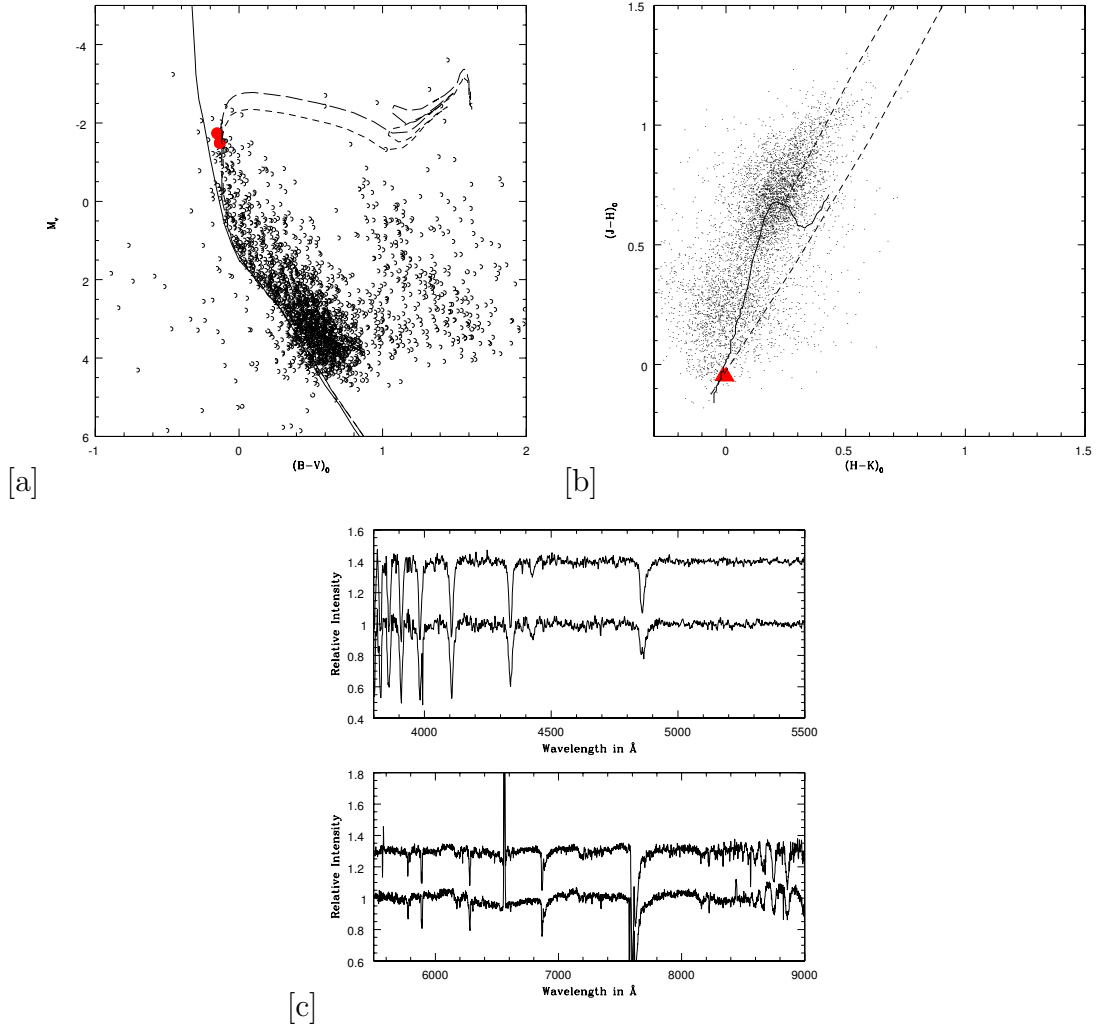


Figure 2.41: (a) Optical CMD of the cluster NGC 6756 is shown with the e-stars shown as solid circles. (b) The near-IR CCDm is shown with e-stars shown as filled triangles. (c) The spectra of the e-stars NGC 6756(2) and NGC 6756(3), in the wavelength range 3800 – 9000 Å, are shown from bottom to top.

2.3.30 NGC 6834

NGC 6834 ($RA = 19^h52^m12^s$, $Dec = +29^\circ24'30''$, $l = 65^\circ.698$, $b = 1^\circ.189$) is a cluster of Trumpler type II2m. Miller et al. (1996) observed this cluster as part of a CCD photometric survey for Be stars using B, V filters and two narrow-band interference filters at H_α and H_α continuum. By fitting Geneva isochrones with solar metallicity to the cluster population, they found an age of ~ 50 Myr, a mean reddening of $E(B-V) \sim 0.7$ mag, and a DM of 12.2 mag (i.e. a distance of ~ 2750 pc). They used $(H_\alpha \text{ continuum} - H_\alpha)$ index and $(B-V)$ color index to find six Be star candidates in the cluster. Fünfschilling (1967) estimated a distance of 2100 pc and a color excess of $E(B-V) = 0.61$ from photographic observations. Paunzen et al. (2006) determined the cluster parameters as $\log(\text{age}) = 7.9$, $E(B-V) = 0.70$ and $m_v - M_v = 13.6$. Moffat (1972) estimated a DM of 11.65, distance of 2.14 kpc, mean reddening of 0.72 and an age of 80 Myr using UBV photographic data from Hoag et al. (1961) and Fünfschilling (1967). He mentioned the existence of a partly disrupted dust ring of diameter $49'$, corresponding to 3.1 pc, associated with the cluster. Johnson (1961) estimated a distance of 3030 pc for the cluster. The evolved stars numbered 32 (WEBDA no.) and 129, showing a possible emission, were investigated spectroscopically by Sowell (1987), classified as G0/5 III/V and F2 Ib, respectively.

We have obtained UBV CCD photometric data and estimated the parameters of the cluster based on this photometry. We found 4 e-stars in the cluster which are of spectral type B7.5, B5.5, B8 and B6.5 respectively. An isochrone of 40 Myr is fitted and resulting CMD is shown in figure 2.42(a). The star 2 is displaced away from the optical CMD while the remaining candidates lie closer to the MS. The e-stars are devoid of any nebulosity. They all lie near the tip of the MS in near-IR CCDm (figure 2.42(b)) and hence do not show considerable near-IR excess. Hence all the 4 e-stars belong to CBe category. The spectra of the e-stars in

the wavelength range 3800 – 9000 Å are shown in figure 2.42(c).

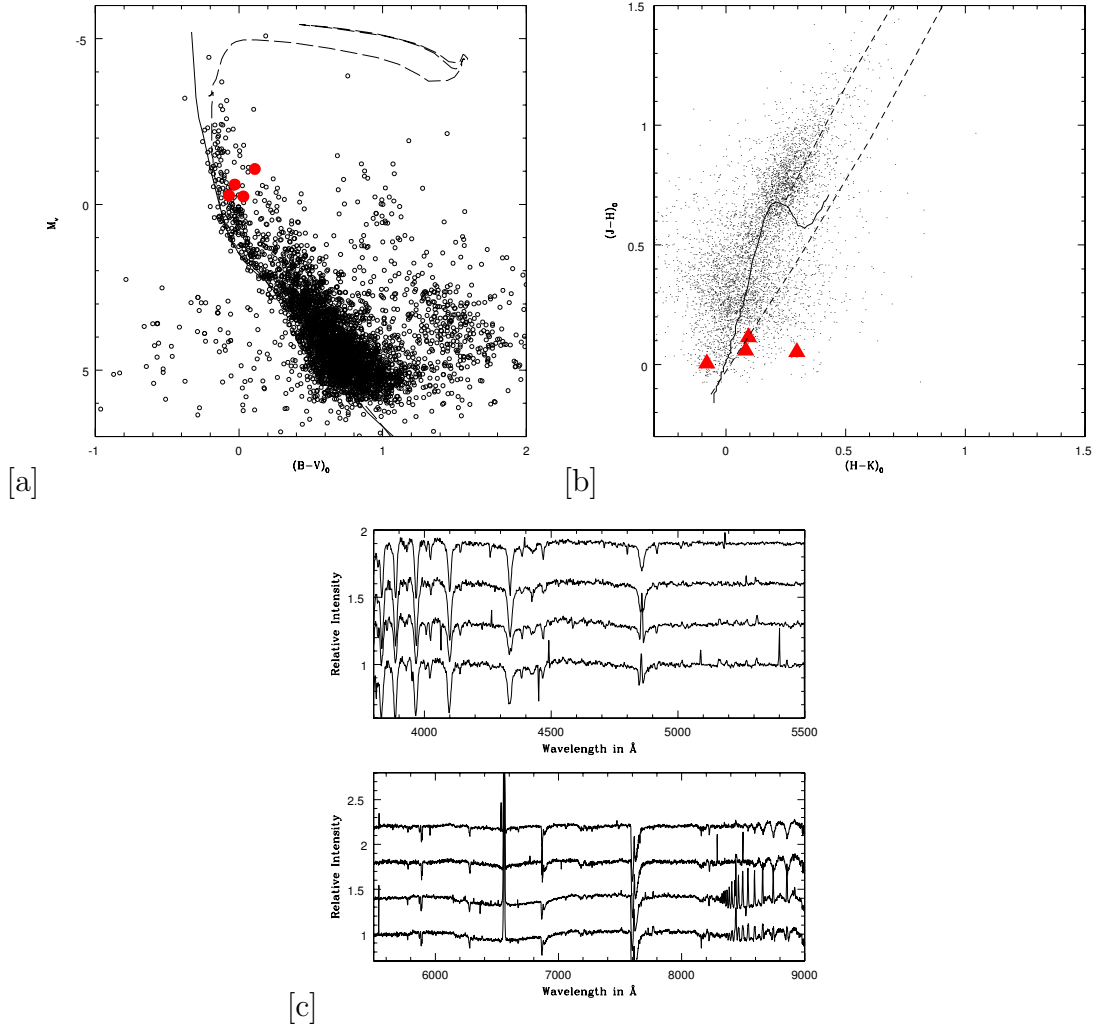


Figure 2.42: (a) Optical CMD of the cluster NGC 6834 is shown with the e-stars shown as solid circles. (b) The near-IR CCDm is shown with e-stars shown as filled triangles. (c) The spectra of the e-stars NGC 6834(1), NGC 6834(2), NGC 6834(3) and NGC 6834(4), in the wavelength range 3800 – 9000 Å, are shown from bottom to top.

2.3.31 NGC 6910

NGC 6910 ($RA = 20^h21^m18^s$, $Dec = +40^\circ37'$, $l = 78^\circ.66$, $b = 2^\circ.03$) is a young open cluster located in the Cygnus region and is a part of the Cygnus OB9 associ-

ation. This cluster is located in the core of the star forming region, 2 Cygni. It is surrounded by a series of gaseous emission nebulae which resemble Barnard's loop in the Orion. From UBV CCD observations down to $V = 18$ mag of 206 stars in the cluster, Delgado and Alfaro (2000) found eleven PMS stars of spectral type A to G. They estimated the cluster parameters to be $E(B-V) = 1.02 \pm 0.13$, $DM = 11.2 \pm 0.2$ and $\text{age} = 6.5 \pm 3$ Myr. Kolaczowski et al. (2004) found four β Cep-type stars along with three e-stars, while searching for variable stars in the cluster. They suggest a possibility of finding a large number of β Cep stars in the cluster due to higher metallicity of the cluster. Using VI_c and H_α photometry, they have determined an age of 6 ± 2 Myr, DM of 11.0 ± 0.3 mag and an $E(B-V)$ value varying from 1.0 to 1.4 mag.

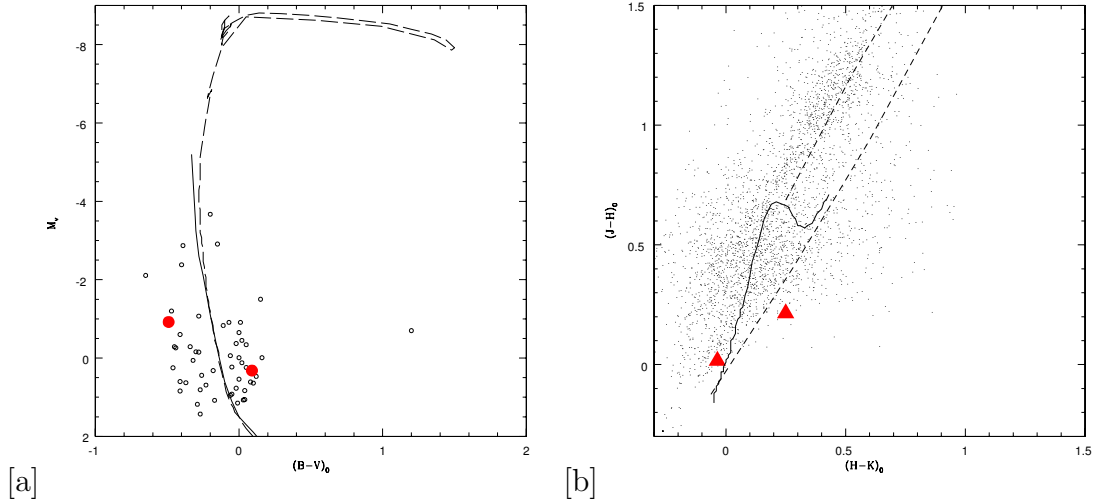


Figure 2.43: (a) Optical CMD of the cluster NGC 6910 is shown with the e-stars shown as solid circles. (b) The near-IR CCDm is shown with e-stars shown as filled triangles.

Shevchenko et al. (1991) studied the cluster using UBVR photoelectric photometry. From the photometry of 132 stars, they found the HAeBe stars BD +40 41 24 and BD +41 37 31 to be associated with it. The extinction is high in the region with a value of $E(B-V) = 1.2$ mag and the value of $R = 3.42 \pm 0.09$. Using intermediate-band photoelectric photometry for 16 cluster members, Crawford

et al. (1977) obtained a reddening value of $E(b-y)=0.75$ mag and a DM of 10.5 mag. They found that a type Ia super giant star of $M_v = -6.9$ to be associated with the cluster. WEBDA has not recorded any e-star in the cluster.

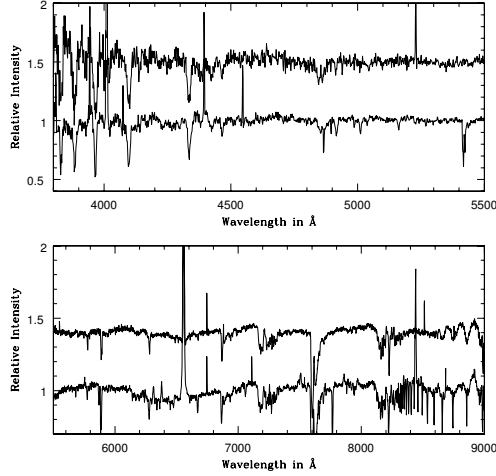


Figure 2.44: The spectra of the e-stars NGC 6910(A) and NGC 6910(B), in the wavelength range 3800 – 9000 Å, are shown from bottom to top.

Since no CCD photometry is available for the e-stars, we have used the UB V photographic photometry of Hoag et al. (1961). The e-stars 26(B) and 181(A) are located very close to each other. The labels for e-stars given in brackets are followed in this work. These stars are shown as dark filled circles in the optical CMD. We have fitted a 6.3 Myr isochrone and the resulting CMD is shown in figure 2.43(a). Bhavya et al. (2007) found that this cluster has been forming stars till recently. The e-star NGC 6910(A) is found to be located near the 0.5 Myr PMS isochrone, indicating that this could also be a candidate HBe star. The star NGC 6910(B) is located to the left of the MS, hence we do not discuss the nature of this star based on the photometry. The peculiar location may be due to two reasons - we used the photographic data for these two stars and there may be some error in the data of this star, or, the reddening is very different for this star. If these two stars belong to the CBe class, then these stars are ≤ 7 Myr old. We

plan to estimate the cluster and Be star parameters using new photometric data. The near-IR CCDm of the e-stars is shown in figure 2.43(b) and we can see that star A is reddened and hence can be considered as a HBe candidate while star B belongs to CBe category. We conclude the star A to be HBe star of spectral type B9.5 and star B to be CBe star of spectral type B6. The spectra of the e-stars in the wavelength range 3800 – 9000 Å are shown in figure 2.44. The e-star NGC 6910(A) shows 7896 MgII line in emission while SiII lines are in absorption.

2.3.32 NGC 7039

The open cluster NGC 7039 ($RA = 21^h 10^m 48^s$, $Dec = +45^\circ 37' 00''$, $l = 87^\circ.879$, $b = -1^\circ.705$) lies in a low density region in Cygnus and is of Trumpler type III2p. Collinder (1931) obtained a distance of 900 pc while Schöneich (1963) estimated a distance of 700 pc for this cluster with 13 members from spectral type B5 to K0. Hassan (1973) determined the cluster parameters as $E(B-V) = 0.19$, distance = 1535 pc and an age of 1 billion years from photographic photometry. Schneider (1987) observed the cluster using Strömgren and H_β photometry and estimated a distance of 675 pc along with a color excess of $E(b-y) = 0.056$. They pointed out the possibility of the existence of another cluster in the background, at a distance of 1500 pc. The cluster parameters as given in WEBDA are, age = 66 Myr, distance = 951 pc and $E(B-V) = 0.131$ mag.

The UBV photographic data are taken from Hassan (1973). An isochrone of 1000 Myr is fitted and resulting CMD is shown in figure 2.45(a). The photometric data is found to have a scatter and hence the spectral type of A6 estimated photometrically is not reliable. The near-IR CCDm of the cluster shows that the Be star is reddened compared to the cluster members (figure 2.45(b)). Hence it may be an Ae star. Better photometry is needed to estimate the parameters of

this cluster, such as reddening, distance and age. The spectra of the e-star in the wavelength range 3800 – 9000 Å are shown in figure 2.45(c). We found 16 FeII lines in emission along with OI, CaII and Paschen lines.

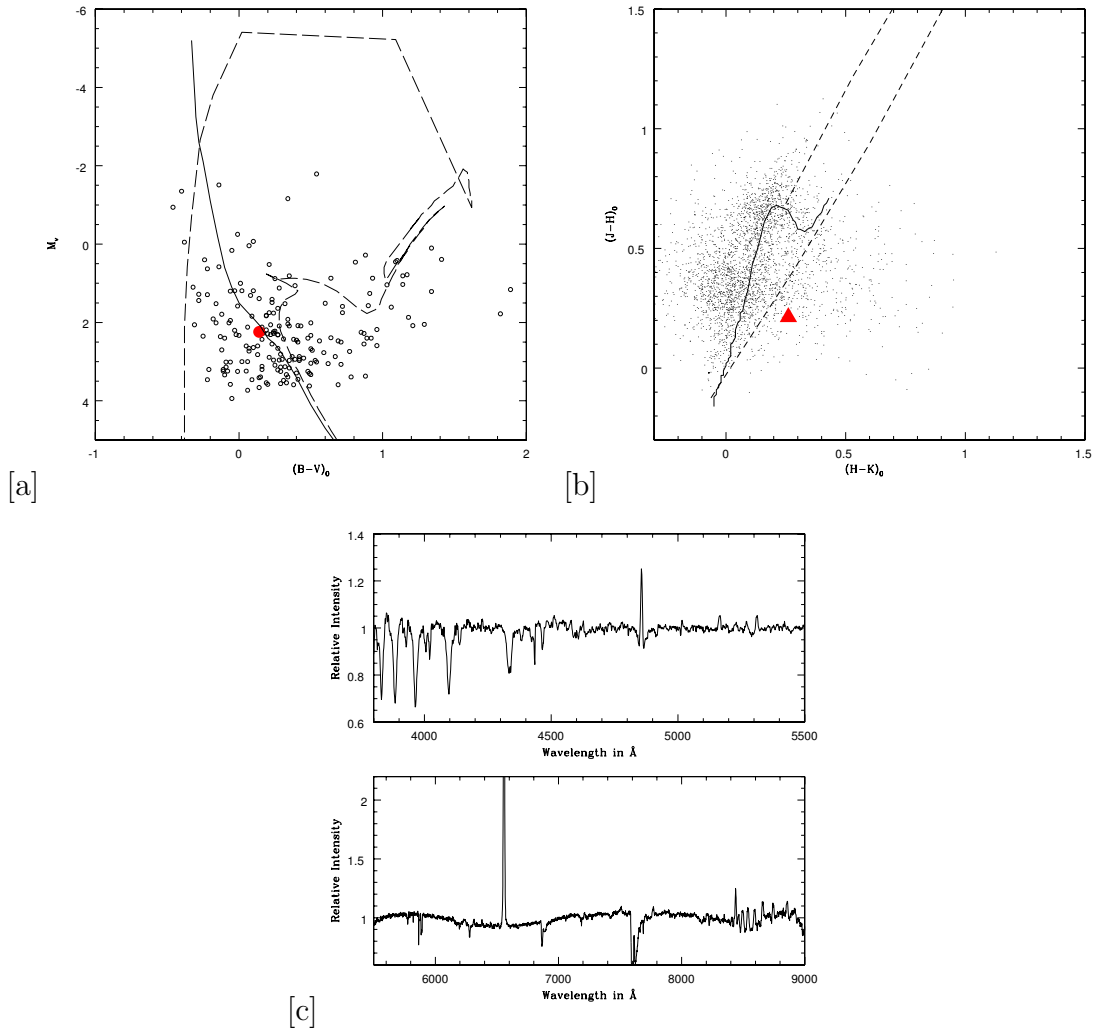


Figure 2.45: (a) Optical CMD of the cluster NGC 7039 is shown with the e-stars shown as solid circles. (b) The near-IR CCDm is shown with e-stars shown as filled triangles. (c) The spectra of the e-star in the cluster are shown in the wavelength range 3800 – 9000 Å.

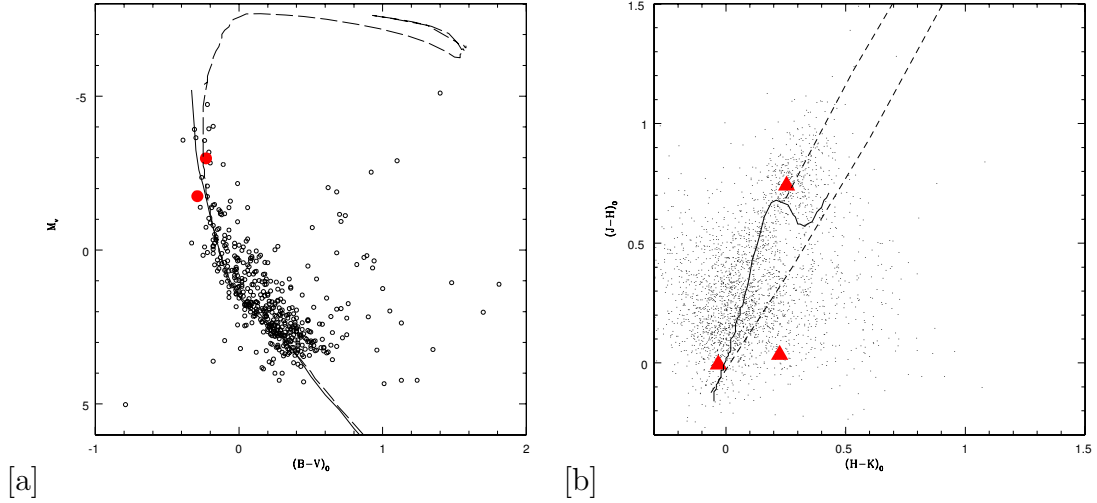


Figure 2.46: (a) Optical CMD of the cluster NGC 7128 is shown with the e-stars shown as solid circles. (b) The near-IR CCDm is shown with e-stars shown as filled triangles.

2.3.33 NGC 7128

NGC 7128 ($RA = 21^h43^m57s$, $Dec = +53^\circ42'54''$) is a Trumpler-type II3m cluster situated in the second galactic quadrant ($l = 97^\circ.4$, $b = 0^\circ.4$), close to the direction of the Cygnus star formation complex. An average distance of 3 kpc and an age of 10 Myr were obtained by various authors (Johnson, 1961; Barbon, 1969). Balog et al. (2001) studied the cluster using Johnson UBV CCD photometry, Strömgren uvby photometry and medium resolution spectroscopy. They found two obvious and one probable Be star in the cluster. From an analysis of the photometric diagrams they estimated a colour excess of $E(B-V) = 1.03 \pm 0.06$ mag, DM of 13.0 ± 0.2 mag and an age above 10 Myr. In a search for variable stars using CCD photometry, Jerzykiewicz et al. (1996) discovered two eclipsing binaries, one irregular red variable and three small-amplitude periodic variables in the cluster.

The UBV CCD photometric data for 452 stars were taken from Balog et al. (2001). The stars 1081 and 12 are found to show emission which are numbered as 1 and 2 respectively in our catalogue. Star 1 is of B1.5 type and star 2 is of B2.5V type. The third e-star's UBV magnitudes are not estimated but found to

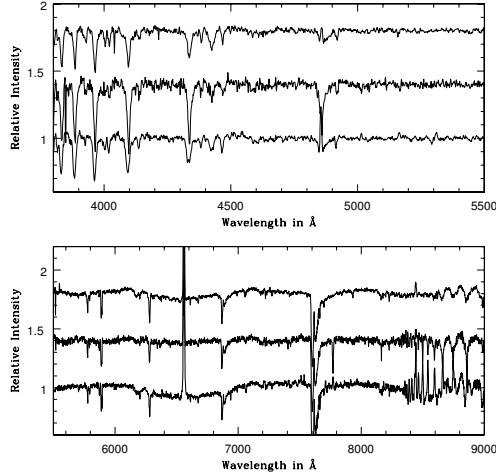


Figure 2.47: The spectra of the e-stars NGC 7128(1), NGC 7128(2) and NGC 7128(3), in the wavelength range 3800 – 9000 Å, are shown from bottom to top.

be of B0V from spectral line analysis. A 10 Myr isochrone is fitted to the cluster data and the resulting CMD is shown in figure 2.46(a). The stars are located on the MS and below the turn-off. The star 1 is found to be in an odd position in the near-IR CCDm (figure 2.46(b)). But the quality flag of the 2MASS data is DEE, which means the magnitudes are unreliable. The e-stars are not associated with any nebulosity. Hence the three e-stars are CBe candidates. The spectra of the e-stars in the wavelength range 3800 – 9000 Å are shown in figure 2.47. The e-star NGC 7128(1) is found to have all major lines in emission, as presented in table 2.3. NGC 7128(2) has SiII lines in absorption.

2.3.34 NGC 7235

NGC 7235 ($RA = 22^h 12^m 25^s$, $Dec = +57^\circ 16' 12''$, $l = 102^\circ.701$, $b = 0^\circ.782$) is a small cluster of Trumpler type III2p in Cepheus. The cluster has an angular diameter of about 5' and contains about 30 B-type stars. Hoag et al. (1961) carried out UBV photometry of the cluster. Becker (1965) performed photographic observations and photoelectric observations of nine faint stars were done by Garcia-

Pelayo and Alfaro (1984).

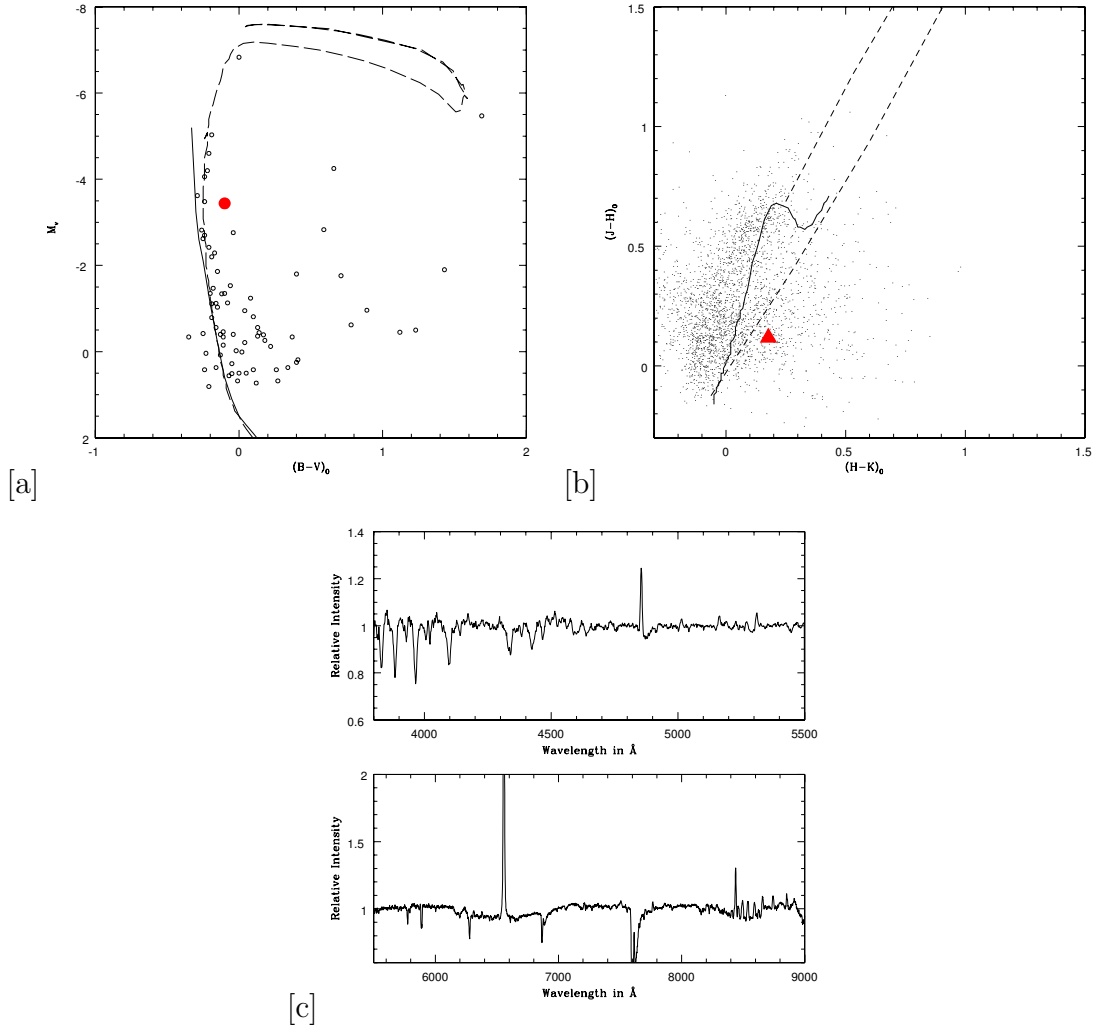


Figure 2.48: (a) Optical CMD of the cluster NGC 7235 is shown with the e-star shown as solid circle. (b) The near-IR CCDm is shown with e-star shown as filled triangle. (c) The spectra of the e-star in the cluster are shown in the wavelength range 3800 – 9000 Å.

Moffat (1972) used photographic UBV data to estimate the cluster parameters as distance = 3.16 kpc and $E(B-V) = 0.96$. He found the earliest spectral type to be B0.5 along with B0 II and B9 Iab super giants. Using BVR I_H $_{\alpha}$ CCD photometry Pigulski et al. (1997) found a β Cep star, a Be short-period variable (period= 0.862 days, star 1 in our catalogue) of λ Eri type, a Mira variable, a W UMa eclipsing binary, a candidate α Cyg variable and a probable eclipsing binary in the

cluster. They have agreed the age of the cluster to be between the age estimated by Lindoff (1968) and Stothers (1972), which is 10–25 Myr.

The UBV CCD data were taken from Pigulski et al. (1997) for 75 stars in the cluster. The e-star is numbered as 9 in their list and we have found it to be of B0.5 spectral type. A 12.5 Myr isochrone is fitted to the cluster data and the resulting CMD is shown in figure 2.48(a). The e-star is located below the turn-off, slightly reddened with respect to the MS location. The near-IR CCDm of the cluster is shown in figure 2.48(b). Both the diagrams indicate that this e-star is a CBe candidate. The spectra of the e-star in the wavelength range 3800 – 9000 Å are shown in figure 2.48(c).

2.3.35 NGC 7261

NGC 7261 ($RA = 22^h20^m11^s$, $Dec = 58^{\circ}07'18''$, $l = 104^{\circ}.037$, $b = 0^{\circ}.910$) is located at a distance of 1681 parsec with a reddening value of 0.969 mag and an age of 46.8 Myr, as mentioned in WEBDA.

We identified 3 e-stars in this cluster. No photometry is available for e-stars in this cluster. An $E(B-V)$ value of 0.969 mag is used to de-redden the JHK_s magnitudes taken from 2MASS catalogue. The resultant near-IR CCDm is shown in figure 2.49(a). The e-stars 1 and 2 are more reddened compared to the third star. No nebulosity is found to be associated with the e-stars. All the three stars may belong to CBe category. The spectra of the e-stars in the wavelength range 3800 – 9000 Å are shown in figure 2.49(b).

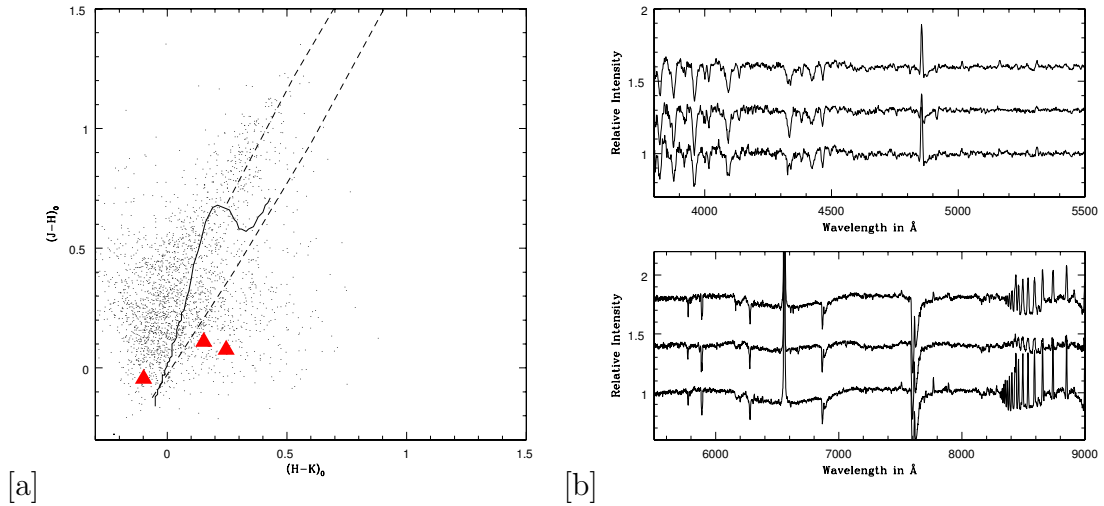


Figure 2.49: (a) The near-IR CCDm of the cluster NGC 7261 is shown with e-stars shown as filled triangles. (b) The spectra of the e-stars NGC 7261(1), NGC 7261(2) and NGC 7261(3), in the wavelength range 3800 – 9000 Å, are shown from bottom to top.

2.3.36 NGC 7419

NGC 7419 ($RA = 22^h 54^m 20^s$, $Dec = +60^\circ 48' 54''$) is a moderately populated galactic star cluster in Cepheus, lying along the Galactic plane $l = 109^\circ.13$, $b = 1^\circ.14$ with an unusual number of giants and super giants (Fawley and Cohen, 1974). Blanco et al. (1955) identified the giants/super giants from objective prism infrared spectroscopy and estimated a visual absorption of 5.0 mag and a distance of 6.6 kpc. van de Hulst et al. (1954) estimated a distance of 3.3 kpc, whereas Moffat and Vogt (1973) estimated the distance to be 6.0 kpc. Photometric observations of the central region of this cluster was made by Bhatt et al. (1993). They found a differential reddening of 1.54 – 1.88 mag with a mean value of 1.71 mag, a cluster distance of 2.0 kpc and age about 40 Myr.

Beauchamp et al. (1994) estimated a younger age of 14 Myr and indicated higher A_v as reported by majority of authors. General interstellar absorption is found to be higher in this direction. Pandey and Mahra (1987) and Neckel and Klare (1980) found an absorption of 2.0 – 3.0 mag at 2 kpc in this direction. H_α

emission stars in NGC 7419 were discovered by Gonzalez and Gonzalez (1956) and Dolidze (1959, 1975). Furthermore, Kohoutek and Wehmeyer (1999) updated this list with more such stars.

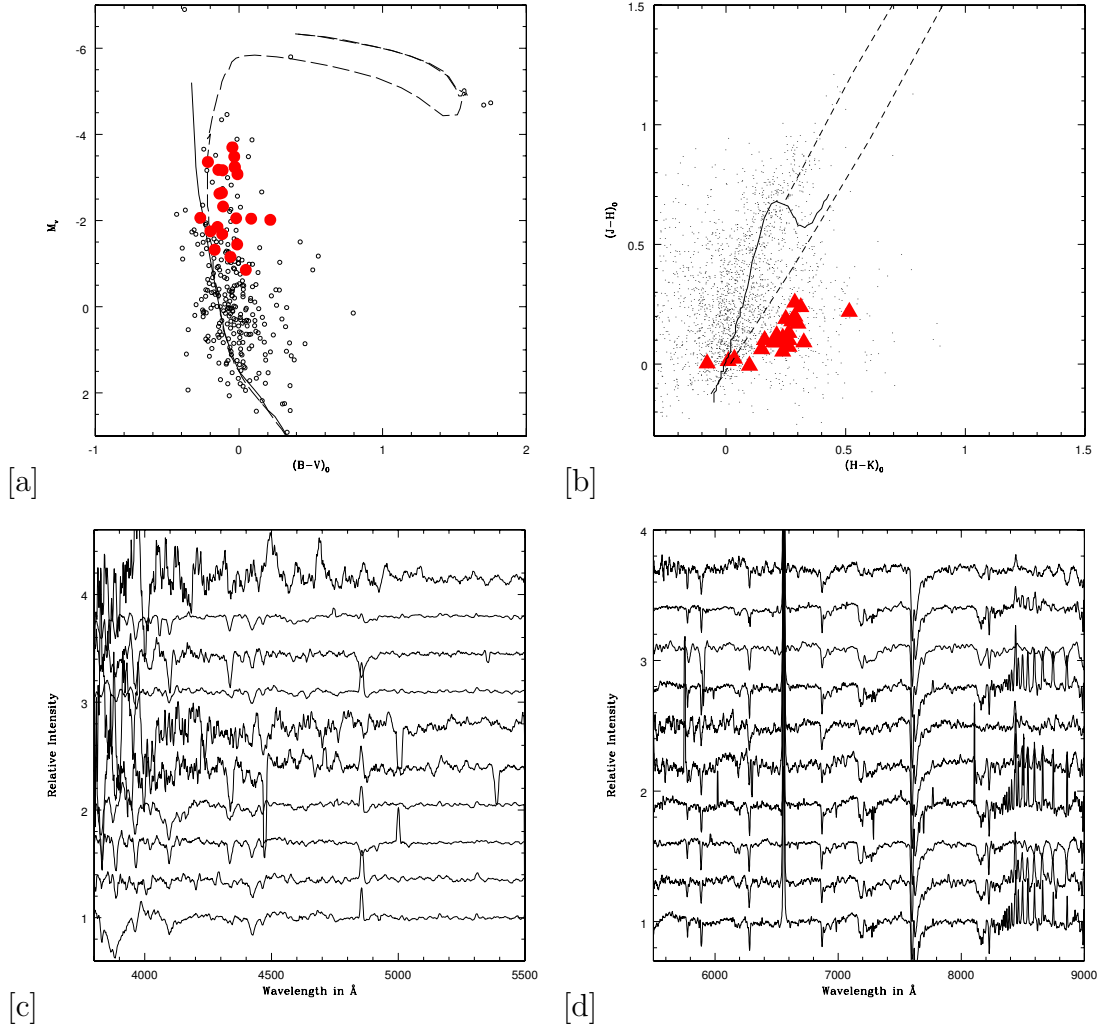


Figure 2.50: (a) Optical CMD of the cluster NGC 7419 is shown with the e-stars shown as solid circles. (b) The near-IR CCDm is shown with e-stars shown as filled triangles. (c) & (d) The spectra of the e-stars NGC 7419(A), NGC 7419(B), NGC 7419(C), NGC 7419(D), NGC 7419(E), NGC 7419(F), NGC 7419(G), NGC 7419(H), NGC 7419(I) and NGC 7419(II), in the wavelength range 3800 – 9000 Å, are shown from bottom to top.

Pigulski and Kopacki (2000) reported that NGC 7419 contains a relatively large number of CBe stars. From CCD photometry in narrow-band H_α and broad-band

R and I (Cousin) filters, they identified 31 such stars. The fraction of CBe stars found in this cluster puts it along with NGC 663, which is the richest in CBe stars among the open clusters in our Galaxy. NGC 7419 also contains a low blue-red giants ratio (Beauchamp et al., 1994). Caron et al. (2003) indicated a direct relation between the relative frequency of red super giant (RSG) stars and CBe stars.

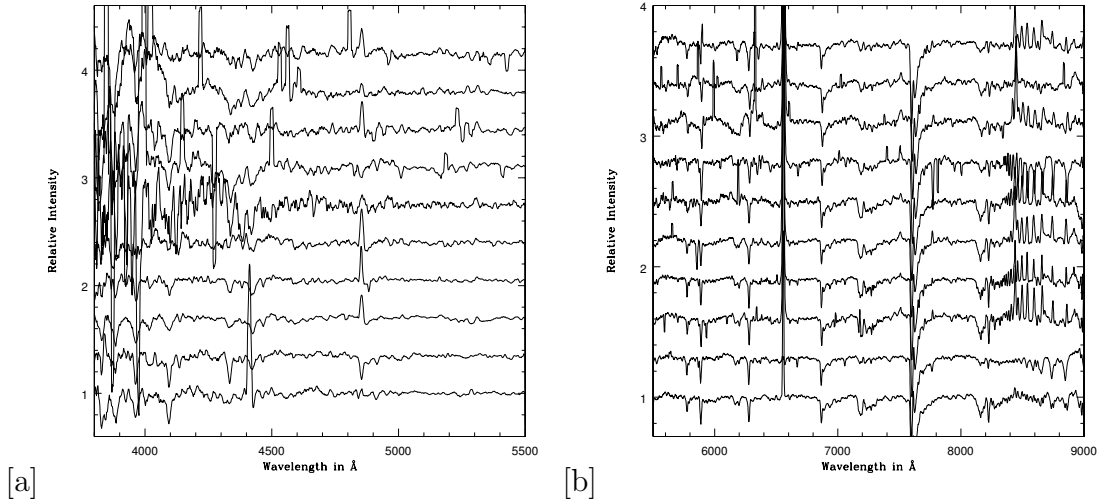


Figure 2.51: (a) & (b) The spectra of the e-stars NGC 7419(J), NGC 7419(K), NGC 7419(L), NGC 7419(M), NGC 7419(N), NGC 7419(O), NGC 7419(P), NGC 7419(Q), NGC 7419(R) and NGC 7419(1), in the wavelength range 3800 – 9000 Å, are shown from bottom to top.

Based on the CCD photometric observations of 327 stars in UB V passbands, Subramaniam et al. (2006) estimated the cluster parameters as reddening, $E(B-V) = 1.65 \pm 0.15$ mag, distance = 2900 ± 400 pc and a turn-off age of 25 ± 5 Myr. The turn-on age of the cluster has been found to be in the range 0.3 – 3 Myr from isochrone fits. About 42% of the stars are found to show near-IR excess which, from their position in the near-IR CCDm, which indicates that they are intermediate mass PMS stars. From slitless spectra we have identified 27 stars showing H_{α} in emission, from which slit spectra of 25 stars were taken in the wavelength region 3700 – 9000 Å. From the spectral features and their location in the near-IR CCDm (figure 2.50(b)) the e-stars are found to fit the HBe properties rather than those

of CBe stars. Better techniques are required to prove the HBe nature of these stars. For the present study, we consider the e-stars as CBe candidates and assign an age of 25 Myr. The analysis has been done for 25 stars since 2 stars are out of the photometric field of the cluster. The spectral type of the 25 e-stars in the cluster is given in table 2.2. A 25 Myr isochrone is fitted to the cluster data and the resulting CMD is shown in figure 2.50(a).

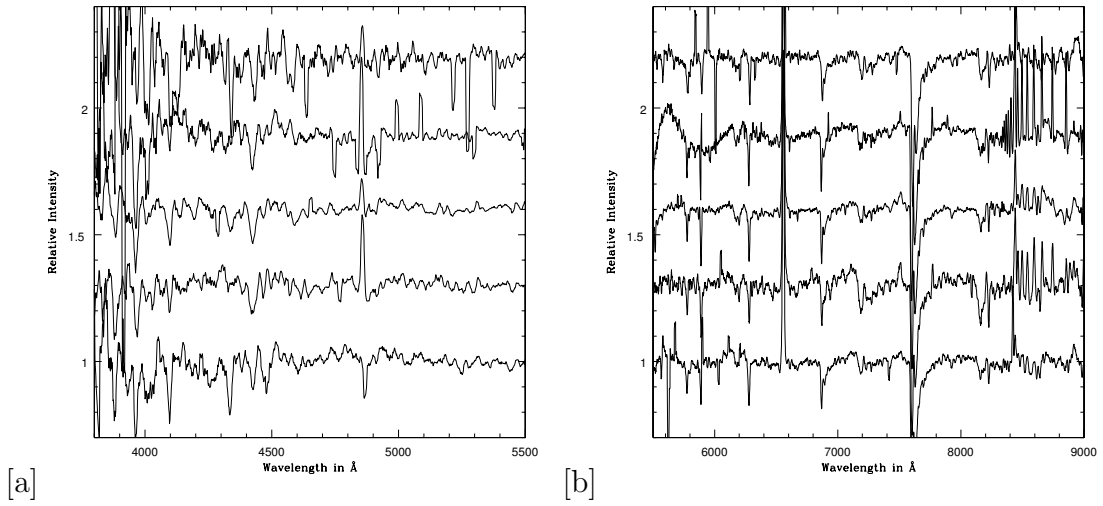


Figure 2.52: (a) & (b) The spectra of the e-stars NGC 7419(2), NGC 7419(3), NGC 7419(4), NGC 7419(5) and NGC 7419(6), in the wavelength range 3800 – 9000 Å, are shown from bottom to top.

The spectra of the e-stars in the wavelength range 3800 – 9000 Å are shown in figure 2.50(c & d), 2.51 and 2.52. MgII line 7877 Å is present in the spectra of NGC 7419(D), NGC 7419(O), NGC 7419(Q) and 7896 Å in NGC 7419(D), NGC 7419(N), NGC 7419(P), NGC 7419(1), NGC 7419(3) and NGC 7419(5). CaII triplet is found in emission for 16 e-stars. NII lines 5005, 5530, 5684, 5711 Å are found in the spectra of NGC 7419(C), NGC 7419(L), NGC 7419(P) and NGC 7419(5) respectively.

2.3.37 NGC 7510

NGC 7510 ($RA = 23^h11^m03^s$, $Dec = +60^\circ34'12''$, $l = 110^\circ.903$, $b = 0^\circ.064$) is a young open cluster of Trumpler type II2m, located in Cepheus.

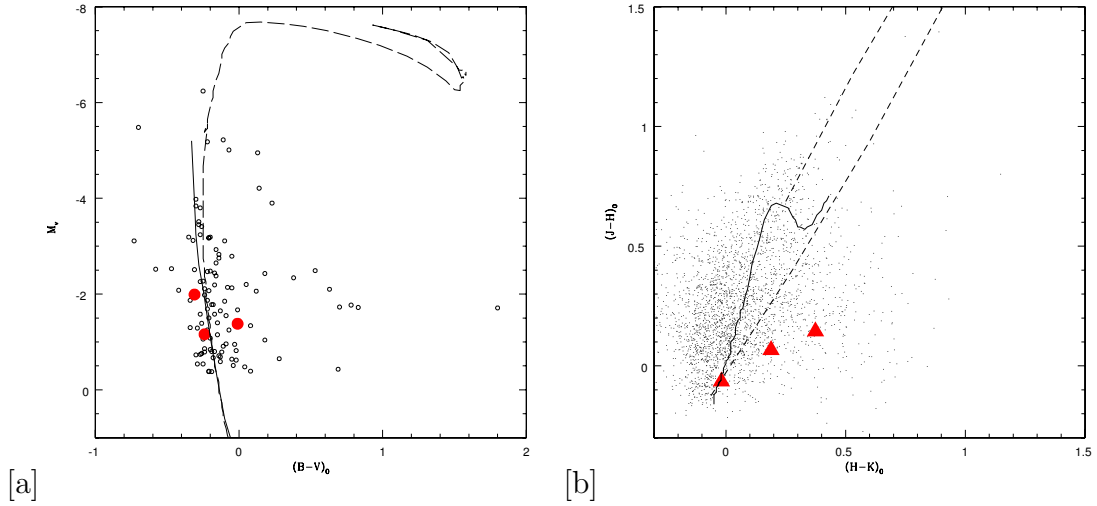


Figure 2.53: (a) Optical CMD of the cluster NGC 7510 is shown with the e-stars shown as solid circles. (b) The near-IR CCDM is shown with e-stars shown as filled triangles.

From UBV photographic photometry of the cluster, Barbon and Hassan (1996) estimated a mean color excess $E(B-V) = 1.12$, distance of 3.09 kpc and age of 10 Myr. Sagar and Griffiths (1991) obtained CCD observations of the cluster in B, V and I passbands down to $V \sim 21$ mag. The cluster has a colour excess, $E(B-V)$ in the range 1.0 to 1.3 mag. From an analysis of V vs $(B-V)$ and V vs $(V-I)$ CMDs, they found a DM of 12.5 mag and an age of 10 Myr. Paunzen et al. (2005) detected two Be stars using narrow band, three filter photometric system. From the derived cluster parameters $E(B-V) = 0.90 \pm 0.02$, distance = 3480 ± 420 pc, age = 22.3 Myr, they found the cluster to be part of the Perseus arm of the Milky way.

The UBV photographic data were taken from Barbon and Hassan (1996) and the stars 18, 77 and 25 are found to show emission. They are numbered as 1A, 1B and 1C by us and are found to be of B2.5, B5 and B4 spectral type respectively. A

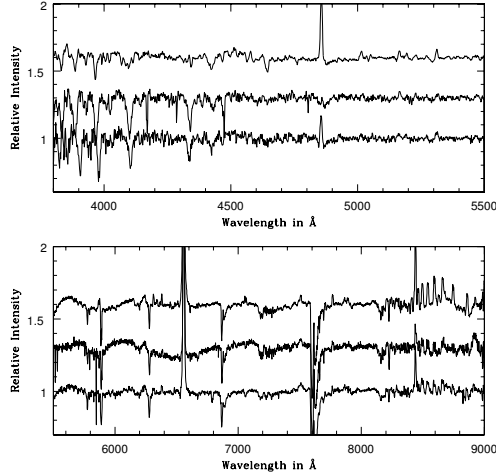


Figure 2.54: The spectra of the e-stars NGC 7510(1A), NGC 7510(1B) and NGC 7510(1C), in the wavelength range 3800 – 9000 Å, are shown from bottom to top.

10 Myr isochrone is fitted to the cluster data and the resulting CMD is shown in figure 2.53(a). Comparing optical CMD and near-IR CCDm (figure 2.53(b)) the e-star NGC 7510(1C), shows relatively large reddening and IR excess, and could be a HBe candidate. But the absence of nebulosity may cause doubt to the candidature. The stars NGC 7510(1A) and NGC 7510(1B) belong to CBe category. The spectra of the e-stars in the wavelength range 3800 – 9000 Å are shown in figure 2.54. NGC 7510(1A) and NGC 7510(1B) show similar spectral features with CaII triplet, Paschen lines and FeII lines in emission while NGC 7510(C) shows MgII and SiII lines also in emission. The OI 7772 Å line is present in absorption while 8446 is present in emission in all the e-stars.

2.3.38 Roslund 4

Delgado et al. (2004) obtained photometric and spectroscopic observations of the cluster Roslund 4 ($RA = 20^h04^m54^s$, $Dec = +29^\circ13'00''$, $l = 66^\circ.984$, $b = -1^\circ.270$) and estimated a colour excess of 1.1 ± 0.2 , DM of 11.7 ± 0.5 , age of 15.8 Myr and a heliocentric radial velocity of -15.7 ± 5.2 km/s. They found that the emissions

seen in H_α and forbidden lines are of nebular origin except in the case of three stars of spectral type earlier than A0. They suggested the cluster to be associated with two nebulae IC 4954 and IC 4955 along with two Herbig-Haro objects.

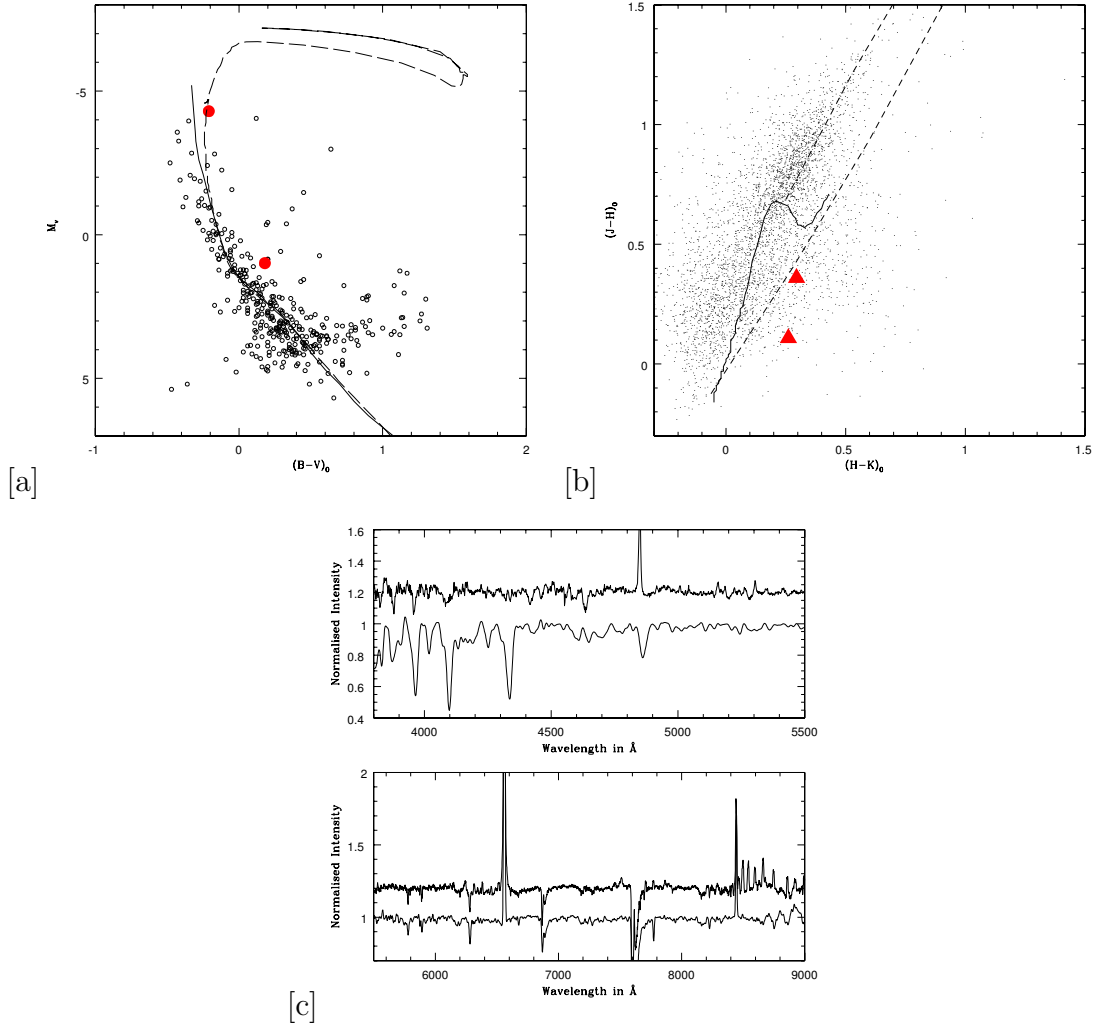


Figure 2.55: (a) Optical CMD of the cluster Roslund 4 is shown with the e-stars shown as solid circles. (b) The near-IR CCDm is shown with e-stars shown as filled triangles. (c) The spectra of the e-stars Roslund 4(1) and Roslund 4(2), in the wavelength range 3800 – 9000 \AA , are shown from bottom to top.

Racine (1969) used photoelectric photometry to study the cluster and estimated a distance of 2900 ± 300 pc using thirteen cluster members. Phelps (2003) used B and V band CCD data and $[SII]$ emission-line imaging to study the cluster and obtained an age of 4 Myr, which explains shocked gas features in the region, and

a distance of 1700–2000 pc.

The photometric data were taken from Delgado et al. (2004). The cluster data is fitted with 15.8 Myr isochrone and resulting CMD is shown in figure 2.55(a). The cluster is found to have 2 e-stars of spectral type A1 and B0 respectively. The B0 star is located very close to the turn-off, whereas the other e-star is located on the MS, well below the turn-off. The star 1 (A1) has been found to be associated with nebulosity. Using PMS isochrone fitting, the age of the star has been estimated in the range 1.5–3 Myr. From the near-IR CCDm, this star is found to have a considerable near-IR excess of 0.5 mag in (J–H) (figure 2.55(b)). These evidences suggest that the star can be a HAe candidate. Hence out of the 2 e-stars in the cluster, Roslund 4(1) is HAe star while Roslund 4(2) is a CBe candidate. The spectra of the e-stars in the wavelength range 3800 – 9000 Å are shown in figure 2.55(c). Roslund 4(1) shows [OI] 5577 Å in emission and the spectrum resembles NGC 6756(3). Roslund 4(2) has 6347 Å SiII line in absorption and 7896 Å MgII line in emission.

2.4 Conclusion

- We performed slitless spectroscopy to search for e-stars in open clusters. We identified 157 e-stars in 42 open clusters from a survey of 207 open clusters.
- We have used UBV photometric data, most of which were taken from WEBDA, to construct optical CMDs. These were fitted with ZAMS and isochrones using the age and distance values taken from data references. These values have been used for the comparative analysis of the photometric parameters of e-stars, which is given in next chapter. The location of e-stars in these diagrams have been used to understand their evolutionary phase.

- From the above cluster analysis, we found that new photometric data are needed for the clusters Berkeley 63, Berkeley 90, Collinder 96, NGC 1220, NGC 2414, NGC 2421, NGC 6649, NGC 6910, NGC 7039, NGC 7261 and NGC 7510. This will help in re-estimating the CBe parameters from the modified cluster parameters. The clusters Bochum 2, NGC 2414, NGC 7261 do not have the data corresponding to the e-stars.
- The near-IR JHK_s magnitudes for the cluster region are used to construct near-IR CCDm. The position of e-stars in near-IR CCDm, which is corrected for cluster reddening, is used as a method to classify CBe stars from HAeBe candidates.
- The spectra of 157 e-stars, taken with a resolution of 4.41 \AA in the wavelength range $3800 - 5500 \text{ \AA}$ and 3.75 \AA in the wavelength region $5500 - 9000 \text{ \AA}$, are presented. The spectral features identified for each e-star is given in table 2.3. The spectra of e-stars in each cluster is compiled with optical CMD and near-IR CCDm. A comprehensive analysis of the stellar properties using measured spectral parameters is given in chapter 4.
- The clusters Bochum 6, IC 1590, NGC 6823 and NGC 7380 which were found to have HAeBe stars are not described here. They will be presented in chapter 5.

Chapter 3

Be phenomenon in open clusters: results from a survey of emission-line stars in young open clusters

3.1 Introduction

A collective analysis of the properties of 157 e-stars, identified from slitless survey, is presented in this chapter. We estimated their distance, age and spectral type from the optical CMD of open clusters to which they are associated. We also identified their evolutionary phase by finding their location in the cluster MS. We looked for nebulosity around the e-stars in addition to the location in optical CMD and near-IR CCDm, to separate possible HBe stars from CBe stars. A detailed analysis of e-stars treating them as members of the parent cluster is given in chapter 2. To classify e-stars based on near-IR excess, we have compared the 2MASS colours of the known catalogued HBe stars (The et al., 1994) and CBe stars (Jaschek and Egret, 1982) along with our candidate stars. The B and V band photometric magnitudes were taken from Tycho-2 Catalog (Høg et al., 2000), which along with the known spectral types were used to determine colour excess $E(B-V)$. This was used to estimate $E(J-H)$ and $E(H-K)$ using the relations by

Rieke and Lebofsky (1985), which in turn were used to deredden the (J–H) and (H–K) colours. The distribution of clusters which have Be stars were studied in Galactic coordinates with respect to the clusters which do not contain e-stars to look for any preferential location for clusters with e-stars.

3.2 Results and Discussion

As mentioned earlier, the technique used here only identifies definite e-stars and thus the statistics presented here are lower limits. Since this survey has covered a large number of clusters, we have done statistical analysis of the fundamental parameters of the e-stars and the clusters which house them. The following sections discuss these facts. Most of the identified e-stars are CBe candidates (145 stars, $\sim 92\%$), whereas some are HBe candidates (10 stars, $\sim 6\%$). A very few (2, $\sim 2\%$) HAe candidates are also present (table 3.1). In order to study the identified e-stars as well as the hosting cluster in detail, we have taken the photometric data from the references listed in table 3.1.

3.2.1 Colour-Magnitude Diagram of the e-stars

The M_v versus $(B-V)_0$ CMD of the e-stars in all the clusters is shown in figure 3.1. From the distribution of stars in the diagram we can see that a few could belong to HBe stars. Stars brighter than $M_v \sim -3.0$ are located to the right of the ZAMS. There are about 20 stars in this group and this might be due to reddening or due to evolution away from the MS. From the analysis of the CMDs of 37 clusters, we identified only about 12 stars to be located close to the MS turn-off and probably evolving away from the MS. Thus, the deviation from the MS is likely to be due to both evolution and reddening. In the range, $M_v = -3 - 0.0$, most of the CBe stars

are located very close to the ZAMS with some located to the right, probably due to reddening. This figure and also the summary given below show that most of the CBe stars are still in the MS evolutionary phase. Thus, the emission mechanism is not connected with the core-contraction at the MS turn-off for a majority of the identified e-stars.

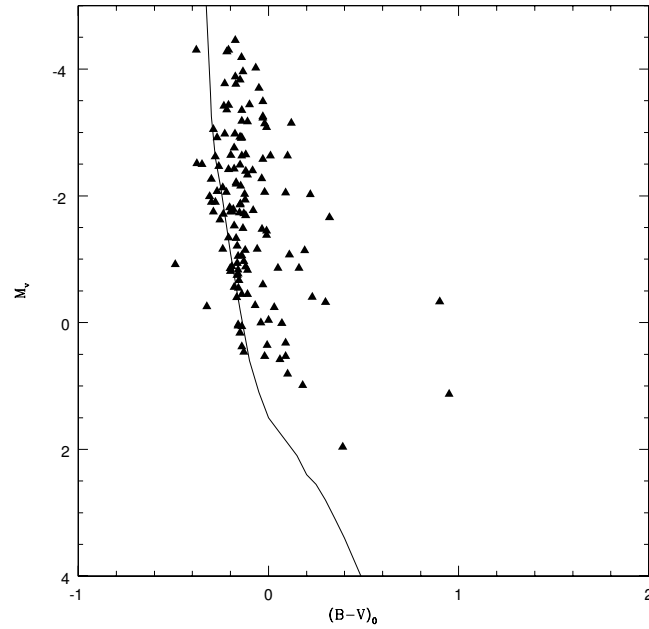


Figure 3.1: The CMD of the e-stars is shown in figure with Y-axis being the absolute magnitude and X-axis being the reddening corrected colour.

From the 40 clusters with ages known, we found 9 clusters younger than 10 Myr to harbour e-stars. These clusters contain 15 e-stars out of which 10 belong to CBe category while five belong to HBe class. We have found the cohabitation of both classes of e-stars in the clusters IC 1590 and NGC 6910. The clusters IC 1590, NGC 637 and 1624 are found to have young CBe stars whose age is about 4 Myr. We have observed 16 clusters to be in the age range 10–19 Myr which contain a total of 42 e-stars out of which 35 belong to CBe category, five HBe stars and two HAe stars. We have found seven clusters to be in 20–40 Myr age

bin which contain a total of 65 e-stars, all of which are CBe stars. This age bin contains rich clusters like NGC 663, 6649 and 7419 which contribute 22, 7 and 25 CBe stars to the total sample. Since the remaining clusters in this group have at least three Be stars, we can infer that this age range favours a rich environment for the formation of Be stars. From a spectral type evolution point of view, B-type stars earlier than B5 are found to be in and around MS phase during this period.

The clusters King 10, NGC 6834 and 7261 are found in 40–50 Myr age range which contain 11 CBe stars. We have four clusters in the age bin 60–100 Myr which have a total of 19 CBe stars, out of which 12 are from the cluster NGC 2345. We have a couple of clusters with age greater than 100 Myr: NGC 6756 and 7039. NGC 6756 is found to have an age range of 125–150 Myr, which is found to have two CBe stars with spectral types B3.5 and B2.5, respectively. Even though we have fitted an age of 1000 Myr to the cluster NGC 7039, the presence of e-star makes the age estimation suspicious. Hence, deeper and new UBV CCD observations are needed to have any say about this cluster.

From the analysis of the individual cluster CMDs with e-stars, 12 are found to be near the turn-off in the CMD. They are IC 4996(1, B2), King 10(B, B1), King 10(E, B2), King 21(C, B0.5), NGC 659(2, B0), NGC 663(7, B0), NGC 663(16, B0), NGC 663(P6, B0.5), NGC 663(12V, B0.5), NGC 2421(1, B3.5), NGC 6649(1, B1.5), Roslund 4(2, B0). Our catalogue number and spectral type are given in brackets. Hence majority of the e-stars are not in the evolved part of the MS. Thus our result does not favour core contraction scenario as the only mechanism for the Be phenomenon.

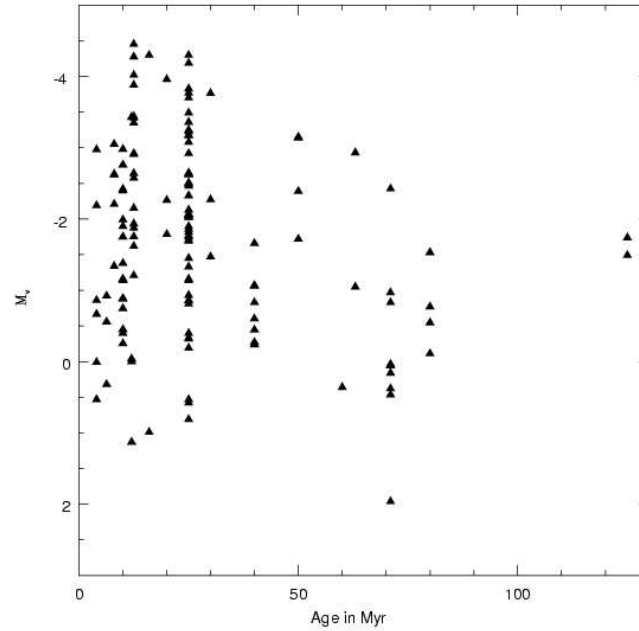


Figure 3.2: A plot of M_v versus the age in Myr of the e-stars is shown. The e-star belonging to cluster NGC 7039 is not plotted due to uncertainty in age estimation.

3.2.2 M_v versus age of the e-stars

A plot of M_v with respect to age of the e-stars is shown in figure 3.2. Stars in the age range 0–10 Myr are distributed between $M_v = 0.5$ and -3.0 . That is, these clusters lack CBe stars of spectral type earlier than B1. On the other hand, these very early spectral types as well as the later spectral types are seen in the age range 10–30 Myr. A trend is seen for the e-stars to shift to late B spectral type with age, especially for the stars in 40–80 Myr, due to massive stars evolving away. This trend is deviated by the two stars in the cluster NGC 6756, which is older than 100 Myr.

The trend which is noteworthy is the absence of very early CBe spectral types in clusters younger than 10 Myr. This suggests that the spectral types earlier than B1 show Be phenomenon after 10 Myr. If this is true, this suggests that the Be phenomenon in spectral types earlier than B1 is due to evolutionary effect. The

existence of this younger age limit is only indicative here. Search and identification of CBe stars in more clusters in this age range are required to confirm this result.

3.2.3 Distribution of e-stars versus cluster Age

We have surveyed 207 open clusters, out of which 145 were younger than 100 Myr, 39 clusters were older than 100 Myr while the age of 23 clusters is unknown. Out of the total number of clusters surveyed, 22% have been found to have e-stars. The fraction of clusters which have e-stars with respect to total surveyed clusters as a function of age is shown as histograms in figure 3.3. We find that the maximum fraction of clusters which house CBe stars fall in the age bin 0–10 and 20–30 Myr ($\sim 40\%$). There seems to be a dip in the fraction of CBe clusters in the 10–20 Myr age bin. For older clusters, the estimated fraction ranges between 10 and 25%. The reduction in the fraction from 0–10 Myr age bin to 10–20 Myr age bin could be due to evolutionary effects and also due to the MS evolution of the probable HBe stars. Also, the fraction in the 10–20 Myr age bin is similar to the value found for older clusters. There seems to be an enhancement in the cluster fraction with Be stars in the 20–30 Myr age bin.

In table 3.2, we have also shown the results from McSwain and Gies (2005b), in parenthesis. They have a good number of clusters younger than 40 Myr and there are only a few older clusters. The CBe cluster fraction from their data indicates that the largest fraction (0.71) is in the 10–20 Myr, with lesser fractions in the 0–10 and 20–30 age bins. Thus McSwain and Gies (2005b) data set indicates that the fraction of clusters with Be stars increases after 10 Myr, whereas our data set shows the rise after 20 Myr. The striking result is that both the sets indicate a rise in the age bin, 10–30 Myr, from the initial fraction. It should be noted that these two data sets have sampled different part of the galactic disk. This result is

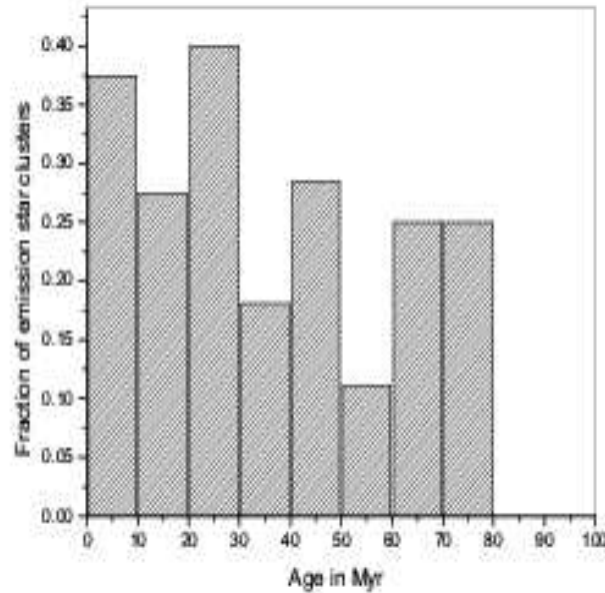


Figure 3.3: Fraction of clusters which have e-stars with respect to the total number of clusters surveyed is shown in the figure.

similar to that reported by Wisniewski and Bjorkman (2006).

When we estimate the fraction of CBe stars observed in various age bins, the statistics is dominated by the CBe-rich clusters. Out of the 155 e-stars (ages of two stars is not known), distributed in 40 clusters, 19.3% (30 of 155) of the stars are found to belong to 1–10 Myr group, with the 10 Myr clusters belonging to this group. About 61.9% (96) are in the 10–40 Myr age group including the candidates of 40 Myr old clusters. We have found seven e-stars (4.5%) in the 40–50 Myr age group. The surprising aspect is the presence of 19 stars in 50–100 Myr group (12.2%), which are the stars from the clusters Collinder 96, NGC 1220, 2345 and 2421. For the sake of completion, we have to include the clusters older than 100 Myr like NGC 6756 and 7039 (2% contribution to the total list of e-stars) to this list of old clusters.

We find that Be phenomenon is pretty much prevalent in clusters younger than 10 Myr, $\sim 40\%$ of clusters in this age range house CBe stars and about 20% CBe stars are younger or as old as 10 Myr. McSwain and Gies (2005b) also find a good fraction of young clusters to have CBe stars. Thus, using a much larger sample, we confirm similar results obtained by Wisniewski and Bjorkman (2006); Wisniewski et al. (2007) and McSwain and Gies (2005b). Thus, these CBe stars are born as CBe stars, rather than evolved to become CBe stars. Since we do not find any CBe stars earlier than B1 in clusters of this age range, our results mildly suggest that this happens mainly for spectral types later than B1.

We also find that the fraction of clusters with CBe stars significantly increases in the age range 20–30 Myr, similar to the result found by Wisniewski and Bjorkman (2006) (10–25 Myr) and McSwain and Gies (2005b) (10–20 Myr). All these results put together indicate that there is an enhancement in the 10–30 Myr age range. These suggest that stars in these clusters evolve to become CBe stars. Thus, there could be two mechanisms responsible for the Be phenomenon. Rapid rotation is generally considered as the reason for the Be phenomenon. First mechanism is where the stars start off as CBe stars early in their lifetime, as indicated by CBe stars in very young clusters. These probably are born fast-rotators. These type of stars are found in all age groups of clusters. These types of stars are likely to be later than B1, as indicated by the paucity of very early type CBe stars in young clusters. The second mechanism is responsible for the enhanced appearance of Be stars in the 10–30 Myr age group clusters. This is likely to be an evolutionary effect on the MS. As seen in figure 3.3, the 10–30 Myr age range has a large number of CBe stars in the spectral type earlier than B1. This component is probably due to the structural or rotational changes in the early B-type stars, in their second half of the MS life time (Fabregat and Torrejón, 2000).

Recently Martayan et al. (2009b) gave explanation to the above plot in terms

of the evolution of angular velocity as follows. In massive Be stars, the threshold value of ω/ω_c for Be phenomenon (0.7) is acquired during the beginning of main sequence lifetime. Here ω_c is critical angular velocity. The value of ω/ω_c is dropped below 0.7 due to wind-driven mass loss which results in the reduction of angular momentum. Hence the Be phenomenon disappears after 5–10 Myr. Intermediate-mass Be stars seem to retain the value of ω/ω_c above the threshold value during their entire main sequence lifetime. The Be phenomenon vanishes when the star evolves to reach TAMS in 40 Myr, which explains the lower fraction in this age-bin. Low-mass B stars appear as Be at the beginning of main sequence phase but will switch back to B star by reorganisation of the internal angular momentum. Eventually the threshold value of 0.7 is achieved during an age of 40–50 Myr, which is visible in the increment of the number of open clusters with Be stars at an age of 40 Myr. Then the low mass stars reaches TAMS and the fraction of clusters with Be stars decreases with age. However, this explanation do not account for the presence of massive Be stars in clusters older than 10 Myr.

3.2.4 Distribution of e-stars as a function of spectral type

Out of the total 157 e-stars, spectral types of 140 have been estimated based on available photometric data. The photometric UBV magnitudes available from the literature have been corrected for reddening and distance to determine the spectral type using Schmidt-Kaler (1982). Mermilliod (1982) studied the distribution of Be stars as a function of spectral types, which is found to show maxima at types B1–B2 and B7–B8. The positions of these maxima are identical to those of gaps already noticed in the (U–B) vs (B–V) plane at exactly B1–B2 and B7–B8. Our analysis shows bimodal peaking of the distribution in B1–B2 and B5–B7 spectral bins (figure 3.4).

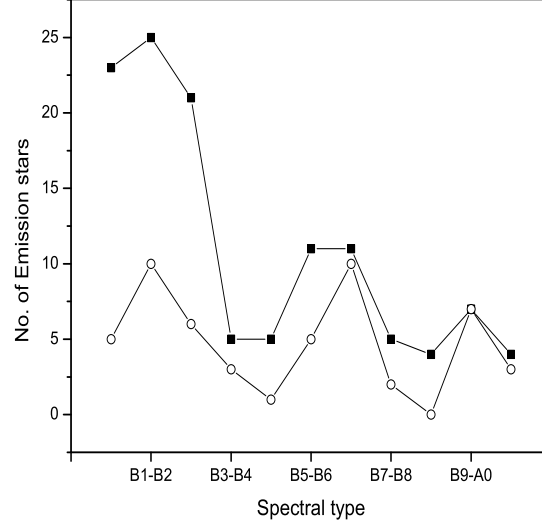


Figure 3.4: The distribution of the surveyed e-stars with respect to the spectral type is given in figure. The solid squares show the total candidates while the open circles show the number of candidates after removing the contribution from 5 rich clusters.

Fabregat (2003) studied the Be star frequency as a function of the spectral subtype for Galactic and Magellanic cloud clusters in the 14–30 Myr age interval, and found that Be stars of the earlier subtypes are significantly more frequent than in the Galactic field, and late Be stars are less. Our results indicate that about 32% of the e-stars belong to spectral type later than B5. We have found 26 stars in B0–B1 spectral bin, 23 in B1–B2 bin, 20 in B2–B3 bin, six in B3–B4 and five in B4–B5 spectral bin (figure 3.4). In this analysis also, the statistics is dominated by the clusters rich in CBe stars. It can be seen that most of the CBe stars in rich clusters belong to early B type. Thus, the enhanced peak seen in the B0–B1 bin is due to rich clusters. The distribution obtained after removing the contribution from rich clusters like NGC 7419, 2345, 663 and h & χ Persei is also shown in figure 3.4. It can be seen that the B0–B1 enhancement is substantially reduced. The distribution is more or less even with peaks in B1–B2 and B6–B7 spectral

bins.

3.2.5 Be star fraction

The Be phenomenon has always been connected with the question that whether all B-type stars pass through the Be phase or not. Jaschek and Jaschek (1983) estimated the mean frequency of Be stars to be around 11% from Bright Star Catalogue considering all spectral type and luminosity classes. In order to address this question we have found the ratio of Be stars to total B-type stars $[N(\text{Be})/N(\text{Be}+\text{B})]$ in the surveyed clusters. We have estimated this fraction in 37 clusters for which reliable photometry was available. The ratio is found to be less than 0.1 (10%) for 29 clusters. The rich clusters NGC 7419, 663 and 2345, which are having more than 10 e-stars, are found to be well separated from the rest (figure 3.5).

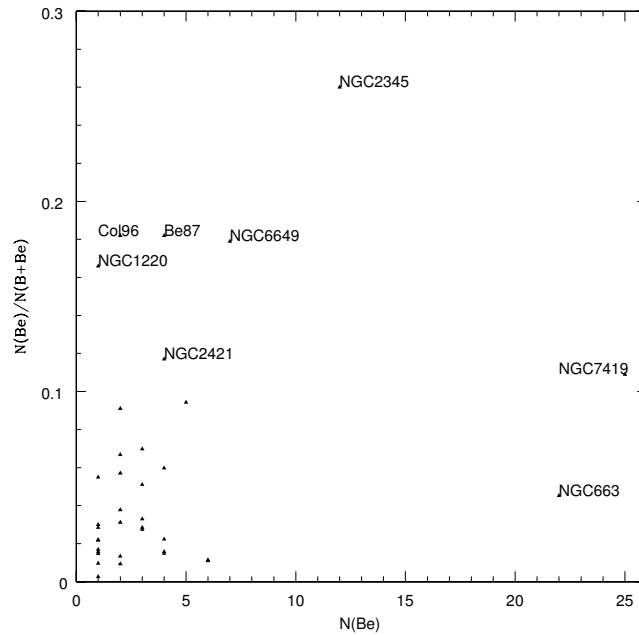


Figure 3.5: The figure shows the ratio of Be stars with respect to all B type stars in the surveyed clusters.

The Be star fraction of NGC 2345 is highest among the surveyed clusters (26%) while the rich clusters like NGC 7419 (11%) and NGC 663 (4.5%) shows a lesser value. The clusters which stand out from the rest are labelled in figure 3.5. These include clusters having multiple e-stars like NGC 6649 (Be star fraction of 17.9%), Berkeley 87 (18.2%), NGC 2421 (11.7%), Collinder 96 (18.2%) and NGC 1220 (16.6%). McSwain and Gies (2005b) also found the Be star fraction to be $\leq 10\%$ for most of the clusters. Fabregat and Gutierrez-Soto (2005) have estimated Be star fraction in NGC 663 and h& χ Persei to be around 9.5 and 6.8%, respectively. They have found 188 B-type stars in NGC 663 out of which 18 are Be stars while we have found a total of 486 B-type stars including 22 Be candidates. For h& χ Persei, they have estimated a total of 218 stars among which 15 showed emission while we have found 1065 B stars out of which 12 showed emission, which results in a Be fraction of 1.1%.

3.2.6 Distribution of e-stars in near-IR CCDm

The near-IR CCDm of the cluster e-stars along with the catalogued CBe and HAeBe stars is shown in figure 3.6. The diagram also shows the MS and the reddening line (Koornneef, 1983). The cluster e-stars which are displaced from the CBe location, where all the catalogued CBe stars lie, are discussed below. The e-stars NGC 7380(4)(1.005,0.855), IC 1590(1)(0.953,0.500), IC 1590(2)(0.999,0.790) and NGC 6823(1)(1.045,0.767) are located in the HAeBe location. Some stars like Bochum 6(1)(0.596,0.295), NGC 884(2) (0.545, 0.226), NGC 7419(1) (0.515, 0.219), NGC 146(S1)(0.356,0.320) and Roslund 4(1)(0.296,0.359) are located in the region between the HAeBe and CBe distribution. The stars NGC 436(3)(0.165,0.705) and NGC 7128(1)(0.254,0.741) are found to be beyond the reddening vector. In the former case, it might be due to the variation of colour excess around the star while in the latter case the quality of the data is poor with a flag of DEE. Thus,

this comparison confirms that most of the cluster e-stars are CBe type of stars, and only a few stars are HBe candidates.

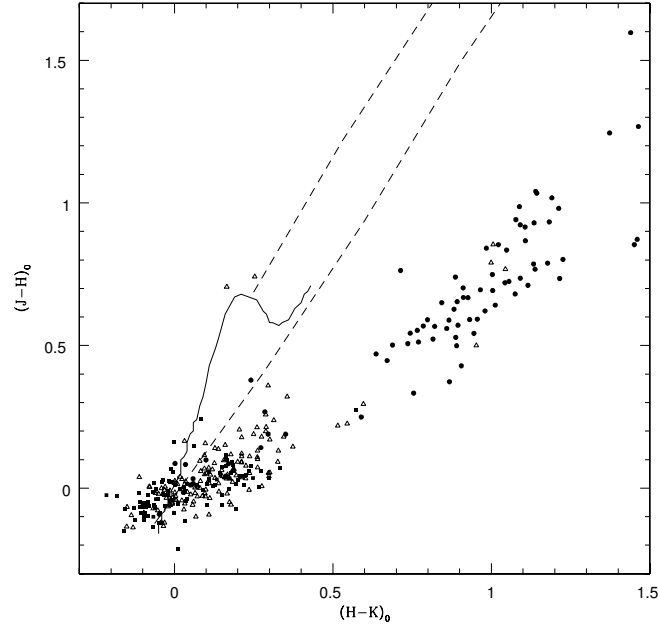


Figure 3.6: Extinction corrected near-IR CCDm of e-stars (open triangles) in open clusters with MS (bold curve) and reddening vectors (dashed lines). The field CBe stars (filled squares) and HBe stars (filled circles) from the catalogue are also shown in figure.

Some of the catalogued Herbig stars (The et al., 1994) like HBC 334(0.286,0.268), V374 Cep(0.351,0.189), HD 35929 (0.296, 0.190), HD 130437 (0.273, 0.142), V361 Cep (0.170, 0.085), HD 37490 (0.100, 0.099), HBC 324 (0.059, 0.016), CPD-613587 (0.029, -0.016), HD 76534(-0.040,-0.121), HD 53367(-0.050,-0.092), HD 141569(0.004,0.020), V599 Car(0.035,0.083), HD 141569(-0.004,0.020), are found to be in the CBe location while LkH $_{\alpha}$ 208(0.589,0.249) and TY CrA(0.241,0.379) are found to be in the transition region in between the two zones. Out of the catalogued CBe stars (Jaschek and Egret, 1982) only BD +56573(0.573,0.274) is found to be in the transition zone between HAeBe stars and CBe stars. The presence of HAeBe stars in CBe location may be due to the evolutionary scenario in which a

HAeBe star can lose disk and de-redden to a CBe location. This type of HAeBe stars may be spun up candidates since CBe stars are high rotators. We have found a few cluster candidates in this transition phase. The rotation velocity of these stars could progressively increase as we come down along the reddening vector, from HAeBe location to CBe location. We are doing extensive analysis of the rotation velocity information from spectral line analysis of our candidate stars as well as field stars.

3.2.7 Location of clusters with e-stars in the Galaxy

We have plotted the surveyed clusters in the Galactic plane (Galactic longitude - latitude, $l-b$ plane), as shown in figure 3.7(a). The total surveyed clusters are shown as open triangles while the clusters which harbour e-stars are shown as filled triangles. It can be seen that most of the e-stars lie within a longitude range of $120^\circ - 130^\circ$, which correspond to Perseus arm of the galaxy. Most of the rich clusters like NGC 7419 ($l = 109^\circ$), NGC 663 ($l = 129^\circ$) and $h \ \& \ \chi$ Persei (NGC 869 and NGC 884; $l = 135^\circ$) are found to lie in this region, which point to vigorous star formation activities. The rich cluster NGC 2345 ($l = 226^\circ$) is found in Monoceros region of the Galaxy along with the clusters like Bochum 2, Bochum 6, Collinder 96 and NGC 2421.

We were not able to survey clusters in the Carina, Crux and Norma spiral arm of the Galaxy since they are southern objects which are not accessible using our observation facility. Most of the surveyed clusters lie along the galactic plane, as expected, while some like IC 348 ($b = -17^\circ.8$), NGC 1758 ($b = -10^\circ.5$), NGC 2355 ($b = 11^\circ.8$), NGC 2539 ($b = 11^\circ.1$) lie away from the plane. The location of clusters in the Galactic plane is shown in figure 3.7(b). This also suggests a preferential occurrence of clusters with CBe stars in the second Galactic quadrant.

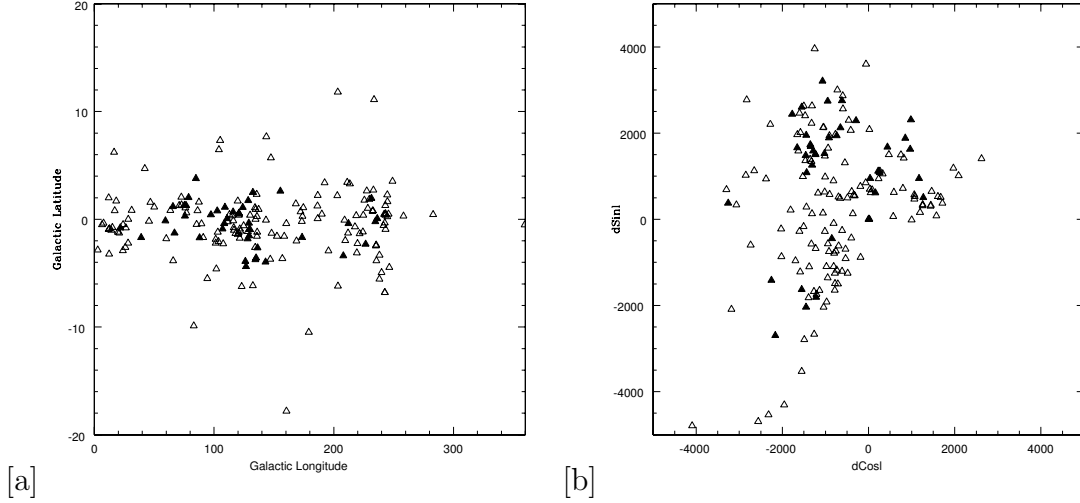


Figure 3.7: (a) Distribution of clusters with e-stars (filled triangles) and clusters without e-stars (open triangles) is shown in the figure. (b) The figure shows the distribution of clusters with e-stars (filled triangles) and without e-stars (open triangles). The axes are given in units of kilo parsecs.

Only a few clusters are found to have Be stars in the third quadrant. These plots indicate that regions with vigorous star formation are coincident with clusters containing CBe stars.

3.3 Conclusion

- We have searched for e-stars in 207 clusters out of which 42 has been found to have at least one. This can be a lower limit, considering the variability of e-stars and detection limit of the instrument.
- A total of 157 e-stars were identified in 42 clusters. We have found 54 new e-stars in 24 open clusters, out of which 19 clusters are found to house e-stars for the first time.
- The fraction of clusters housing e-stars is maximum in both the 0–10 and 20–30 Myr age bin ($\sim 40\%$ each) and in the other age bins; this fraction

ranges between 10 and 25%, up to 80 Myr.

- Most of the e-stars in our survey belong to CBe class ($\sim 92\%$) while a few are HBe stars ($\sim 6\%$) and HAe stars ($\sim 2\%$).
- The youngest clusters to have CBe stars are IC 1590, NGC 637 and 1624 (all 4 Myr old) while NGC 6756 (125 – 150 Myr) is the oldest cluster to have CBe stars.
- The CBe stars are located all along the MS in the optical CMDs of clusters of all ages, which indicates that the Be phenomenon is unlikely only due to core contraction near the turn-off.
- The distribution of CBe stars as a function of spectral type shows peaks at B1–B2 and B6–B7. Rich clusters like NGC 7419, 2345, 663 and h & χ Persei are found to favour the formation of early-type Be stars.
- Among 37 surveyed clusters, 29 are found to have Be star fraction to be less than 10% while rich clusters like NGC 2345 (26%) and NGC 6649 (17.9%) have more than 15%.
- Be phenomenon is very common in clusters younger than 10 Myr, but there is an indication that these clusters lack CBe stars of spectral type earlier than B1. The fraction of clusters with CBe stars shows an enhancement in the 20–30 Myr age bin, which indicates that this could be due to evolution of some B stars to CBe stars. The above two findings suggest that there could be two mechanisms responsible for Be phenomenon. The first mechanism is where some stars are born CBe stars. Our results mildly suggest that this happens mainly for spectral types later than B1. The second mechanism is where the B stars evolve to CBe stars, likely due to evolution on the MS, enhancement of rotation or structural changes. This is likely to happen in early B spectral types.

- We have made an effort to classify e-stars on the basis of IR excess using near-IR CCDm. Using the catalogued field CBe and HBe stars, we have found that CBe stars are strictly confined to the location prescribed to them in terms of IR excess, while HBe stars are seen to migrate from HBe location to CBe location. Some of the cluster stars are also found to belong to this category. Detailed spectral analysis is done to understand these stars.
- Most of the clusters which contain e-stars are found in Cygnus, Perseus & Monoceros region of the Galaxy, which are locations of active star formation.

Table 3.1: Details of e-stars in surveyed clusters. Clusters with ‘*’ in the last column are those with Be stars identified for the first time from this survey.

Cluster Name	No.of e-stars	Age in Myr	CBe/HBe	Reference	WEBDA
Berkeley 62	1	10	1 CBe	17	*
Berkeley 63	1		1 CBe		*
Berkeley 86	2	10	2 CBe	6	3
Berkeley 87	4	8	4 CBe	26	5
Berkeley 90	1		1 HBe		*
Bochum 2	1	4.6	1 CBe		*
Bochum 6	1	10	1 HBe	27	*
Collinder 96	2	63	2 CBe	14	*
IC 1590	3	4	1 CBe,1 HAe, 1HBe	8	4
IC 4996	1	8	1 CBe	4	2
King 10	4	50	4 CBe	17	6
King 21	3	30	3 CBe	22	*
NGC 146	2	10–16	1 CBe,1 HBe	20	*
NGC 436	5	40	5 CBe	17	*
NGC 457	2	20	2 CBe	17	7
NGC 581	4	12.5	4 CBe	17	4
NGC 637	1	4	1 CBe	17	*
NGC 654	1	10	1 CBe	16	6
NGC 659	3	20	3 CBe	17	5
NGC 663	22	25	22 CBe	16	34
NGC 869	6	12.5	6 CBe	19	28
NGC 884	6	12.5	6 CBe	19	25
NGC 957	2	10	2 CBe	10	5
NGC 1220	1	60	1 CBe	15	*

Cluster Name	No.of e-stars	Age in Myr	CBe/HBe	Reference	WEBDA
NGC 1624	1	4	1 CBe	23	*
NGC 1893	1	4	1 HBe	12	4
NGC 2345	12	60–100	12 CBe	13	*
NGC 2414	2	10	2 CBe		*
NGC 2421	4	80	4 CBe	1, 14, 28	*
NGC 6649	7	25	7 CBe	11, 24, 25, 29	*
NGC 6756	2	125–150	2 CBe	22	*
NGC 6823	1	6.3	1 HBe	7	5
NGC 6834	4	40	4 CBe	22	3
NGC 6910	2	6.3	1 CBe	10	*
NGC 7039	1	1000	1 CBe	9	*
NGC 7128	3	10	3 CBe	2	2
NGC 7235	1	12.5	1 CBe	18	1
NGC 7261	3	46	3 CBe		2
NGC 7380	4	10–12	1CBe, 2HBe, 1HAe	12	3
NGC 7419	25	25	25 CBe	21	37
NGC 7510	3	10	2CBe, 1HBe/CBe	3	2
Roslund 4	2	16	1CBe, 1HAe	5	3

Reference: **1.**Babu(1983) **2.**Balog et al.(2001) **3.**Barbon et al.(1996) **4.**Delgado et al.(1998) **5.**Delgado et al.(2004) **6.**Forbes et al.(1992) **7.**Guetter(1992) **8.**Guetter et al.(1997) **9.**Hassan(1973) **10.**Hoag et al.(1961) **11.**Madore(1975) **12.**Massey et al.(1995) **13.**Moffat(1974) **14.**Moffat et al.(1975) **15.**Ortolani et al.(2002) **16.**Pandey et al.(2005) **17.**Phelps & Janes(1994) **18.**Pigulski et al.(1997) **19.**Slesnick et al.(2002) **20.**Subramaniam et al.(2005) **21.**Subramaniam et al.(2006) **22.**Subramaniam et al.(in prep.) **23.**Sujatha et al.(2006) **24.**Talbert(1975) **25.**The et al.(1963) **26.**Turner(1982) **27.**Yadav et al.(2003) **28.**Yadav et al.(2004) **29.**Walker et al.(1987)

Table 3.2: The list of clusters with and without e-stars in various age bins. For comparison, values obtained by McSwain & Gies (2005) are given in parenthesis.

Age Bin in Myr	Non-Emission star clusters	Emission star clusters	Total clusters surveyed	Fraction of e-star clusters
0–10	30(6)	18(11)	48(17)	0.375(0.647)
10–20	21(4)	8(10)	29(14)	0.275(0.714)
20–30	6(4)	4(4)	10(8)	0.4(0.5)
30–40	9(3)	2(1)	11(4)	0.181(0.25)
40–50	5	2	7	0.285
50–60	8	1	9	0.111
60–70	3	1	4	0.25
70–80	6	2	8	0.25
80–90	5	0	5	0
90–100	9	0	9	0
>100	37	2	39	0.051

Chapter 4

Spectroscopic characteristics of Classical Be stars in open clusters: Evidence for bimodal origin

4.1 Introduction

Following the survey (Mathew et al., 2008), the spectra of the identified e-stars were obtained to study their spectral properties. The survey identified a large number of stars covering a wide spectral and age range, thus making the sample ideal for statistical analysis of various spectral characteristics. In order to compare these cluster e-stars with those in the field, spectra of field CBe as well as HAeBe stars were also obtained. Thus this study aims to understand spectral characteristics of CBe stars in clusters and compare their properties with those in the field. In particular, the sample presented here is used to understand the angular momentum distribution of the star-disk system as a function of spectral type. We also attempt to detect any evolution of the angular momentum of the disk and star over an age range.

Mathew et al. (2008) suggested that certain B stars evolve to become CBe while others are born as CBe stars. Martayan et al. (2009a) confirmed the above finding from the H_α spectroscopic survey of Be stars in the SMC clusters. McSwain et al. (2008) found that Be stars are not associated with a particular stage of MS evolution, from the investigation of long-term variability of Be stars in the cluster NGC 3766. From the measurement of changing disk sizes they confirmed the idea of NRP contributing to the formation of variable disks. McSwain et al. (2009) found 12 new transient Be stars and confirmed 17 additional Be stars with relatively stable disks from H_α spectroscopy of 296 stars in eight open clusters. Martayan et al. (2007a) studied 131 Be stars in the SMC cluster NGC 330. They found that early type Be stars with large H_α EW is higher in the SMC than in the LMC and the Milky way. They identified short-term variability in 13 Be stars of which 9 are multiperiodic. From the spectroscopic study of e-stars in NGC 330, Hummel et al. (1999) suggested that the rotation axis of Be stars are not aligned. Using Balmer line spectroscopy of 58 stars in 8 open clusters and associations, Torrejon et al. (1997) identified the spectroscopic behaviour to be similar in both field and cluster Be stars. Using high and medium resolution spectroscopy of Be stars and binary stellar systems in young open clusters, Malchenko and Tarasov (2008) found that CBe stars mostly appear at an age of 10 Myr and their concentration reaches the maximum at 12–20 Myr.

The chapter is arranged as follows. Section 4.2 explains the major results from the spectral line analysis. In this section, a comparative analysis of the spectral lines of 152 surveyed CBe stars is presented with the studies known in literature. The distribution of Balmer decrement (D_{34}), correlation between OI and Balmer line profiles, distribution of H_α EW, its variation with age and spectral type are presented. The line profiles are not corrected for stellar absorption while measuring the EW and FWHM. We plan to estimate accurate stellar parameters using a grid of synthetic spectra, in the future.

The Be phenomenon is closely linked with the stellar rotation velocity. We estimated the stellar rotation velocity from HeI 4471 Å absorption line profile and disk velocity from H $_{\alpha}$ emission-line profile. The rotation velocity measurements are used to understand the stellar and disk velocity distribution and its evolution in surveyed stars. We discuss the results in section 4.3 followed by conclusions in section 4.4.

4.2 Results: Spectral line analysis

A comparative analysis of the spectral lines of 152 surveyed stars is presented with the studies found in literature.

Among the Balmer lines, H $_{\alpha}$ is present in emission in all the stars, while H $_{\beta}$ shows emission or filled-in profile. The higher order lines like H $_{\gamma}$, H $_{\delta}$ are either filled-in or in absorption. All the major helium (HeI) lines like 4026 Å, 4471 Å, 5016 Å, 5876 Å, 6678 Å and 7065 Å are present in the spectra with varying intensity depending on the spectral type.

Using photometric and spectroscopic analysis we confirmed that 5 out of the total sample of 157 e-stars belong to HAeBe category. These are excluded from present study. The following analysis uses a sample of 152 CBe stars.

4.2.1 Distribution of H $_{\alpha}$ equivalent width

We estimated the distribution of H $_{\alpha}$ EW among the observed stars (figure 4.1(a)). The H $_{\alpha}$ EW distribution is found to show an initial rise, which peaks in $-10 \text{ \AA} - -20 \text{ \AA}$ bin and steadily decreases beyond.

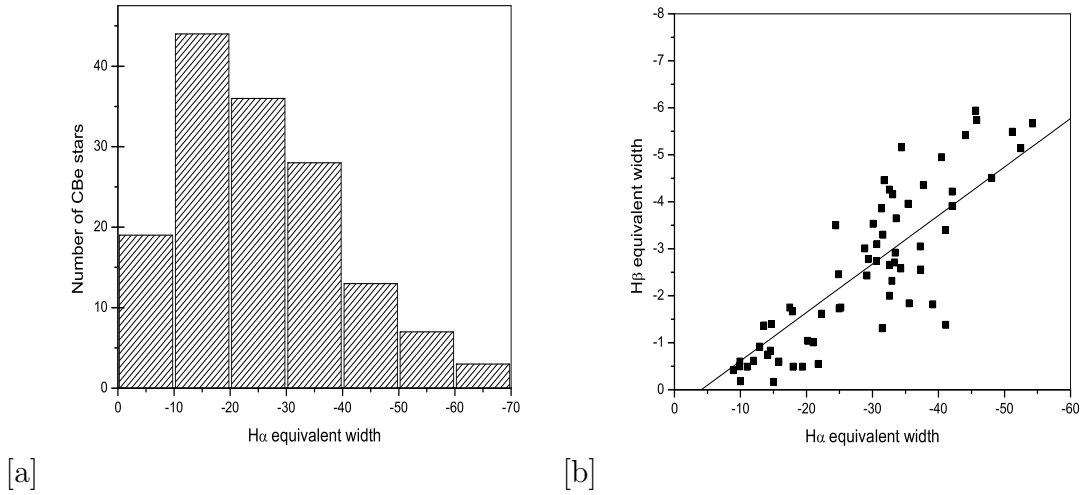


Figure 4.1: (a) H_α EW distribution of surveyed stars. (b) The correlation between H_α and H_β EWs.

In order to study the correlation between emission in prominent Balmer lines, a plot between H_α and H_β EWs is shown in figure 4.1(b). We obtained a relation between the EWs from a linear fit as

$$EW(H_\beta) = 0.10 * EW(H_\alpha) + 0.42 \quad (4.1)$$

with a correlation coefficient of 0.93. The slope of the fit is 0.103 ± 0.005 . This gives an H_α to H_β EW ratio of 9.7.

4.2.2 Correlation between OI lines

Jaschek et al. (1993) found OI 7772 Å line (unresolved triplet line at 7772, 7774, 7775 Å) in emission for all CBe stars, with stars of spectral type earlier than B5 showing clear emission and that of later spectral type showing filled-in emission. Jaschek et al. (1993) estimated the emission region of 7772 Å line as 1.78 stellar radius, which is the smallest radius found for any element. Here the emission radius was calculated by assuming angular momentum conservation of rotating disk, which is a non-Keplerian hypothesis. The emission radius is 3.6 stellar radius for OI 8446 Å line and 2.21 for FeII 7712 Å line. There is no match between the

emission regions of OI 8446 Å and 7772 Å lines. The emission region of OI 8446 Å matches with the average emission region of hydrogen lines, which is around 4 stellar radius. This correlation is reflected through the well known Lyman β fluorescence. They found good correlation between the emission strengths of OI 8446 Å and 7772 Å lines with the former being four times stronger. In one third of the stars earlier than B6, FeII 7712 Å line is seen in emission whereas in late-type stars the line is either absent or appear in shell stars in absorption. They found that the emission line of FeII 7712 Å line is always associated with OI 7772 Å line. The emission intensities of OI 8446 Å and lower order Balmer lines are found to be well correlated (Briot, 1981).

The spectra of all but three stars in our sample show 8446 Å line. Only 116 stars have both 7772 Å and 8446 Å oxygen lines in their spectra, where 71 stars (47%) have both lines in emission. Collisional excitation is the likely mechanism for the production of OI 8446 Å line if 7772 Å line is also present. On the other hand, 36 stars (24%) show only 8446 Å oxygen line in their spectra. Here OI 8446 Å line is likely to be produced by Bowen fluorescence mechanism in Lyman β radiation (Lyman β fluorescence). To verify the findings of Jaschek et al. (1993) we checked whether FeII 7712 Å line is always associated with OI 7772 Å line in our candidate stars. We found 45 stars to show both lines in emission while 9 stars have OI 7772 Å line in absorption with FeII 7712 Å line in emission. Also there are 4 candidates where OI line is absent while FeII is seen in emission. The star NGC 436(3) is found to have both lines in absorption. We have found 14 candidates among the surveyed candidates not agreeing with the predictions of Jaschek et al. (1993). To summarise, 30% of the surveyed candidates show OI 7772 Å and FeII 7712 Å lines in emission. About 9% of stars have either of these lines in emission. The remaining stars do not have both lines in spectrum. Even if filled-in profiles are included in emission category, these results suggests only a mild correlation between the nature of FeII 7712 Å and OI 7772 Å line profiles. Larger fraction

of stars show evidence for collisional excitation mechanism than the fluorescence mechanism for line formation in the disk.

4.2.3 Iron and metallic lines

A list of the metallic lines FeII, SiII, MgII, CaII, OI and NII observed in the spectra of surveyed stars is shown in table 4.1. 131 (86%) CBe stars are found to show FeII lines in their spectra. Among these, 92 have FeII only in emission, while 5 have FeII absorption lines. We identified 49 different FeII spectral lines including 4 forbidden lines. Bochum 2(1) and NGC 146(S2) have only 1 FeII absorption line while NGC 7128(2) has 2 and NGC 663(P151) has 3 lines. These stars have the least number of FeII lines among the surveyed candidates. On the other hand, NGC 884(2) have 25 FeII emission lines and NGC 869(1) show 19 lines.

Either of the SiII lines 6347 Å and 6371 Å is seen in 25% of the spectra in absorption or emission. For 27 stars these SiII lines are seen together either in emission or absorption. The SiII line 4131 Å is seen in absorption in the star NGC 7419(I). The prominent MgII lines in the spectra are of wavelengths 7877 Å and 7896 Å which are present in 4 stars. The MgII line 4481 Å appears in the wing of HeI 4471 Å and hence difficult to isolate due to low resolution. The NII 5005 Å line is present in emission in NGC 7419(C), 5463 Å in NGC 6834(1), 5530 Å in NGC 7419(L), 5684 Å in NGC 7419(P) and 5942 Å in NGC 7380(3). The star NGC 7380(3) (PS Cep) has been quoted as an eclipsing binary in the literature.

4.2.4 CaII and P14 lines

The CaII triplet (8498 Å, 8542 Å, 8662 Å) is found to be blended with Paschen lines (P16, P15 and P13 respectively) in the spectra of surveyed stars. We have not

removed their contribution from the spectra of our candidate stars. CaII triplet is seen together either in absorption or emission for 130 stars. 92 (60%) stars show CaII triplet in emission in their spectra. We found 100 stars to show Paschen 14 line (P14, 8598 Å) in emission while 144 have this line either in emission or absorption. Stars which have P14 line do not exhibit full Paschen series in their spectra. 117 candidates are found to show more than 5 Paschen series lines in their spectra. The CaII K absorption line (3933 Å) is found in almost all the spectra.

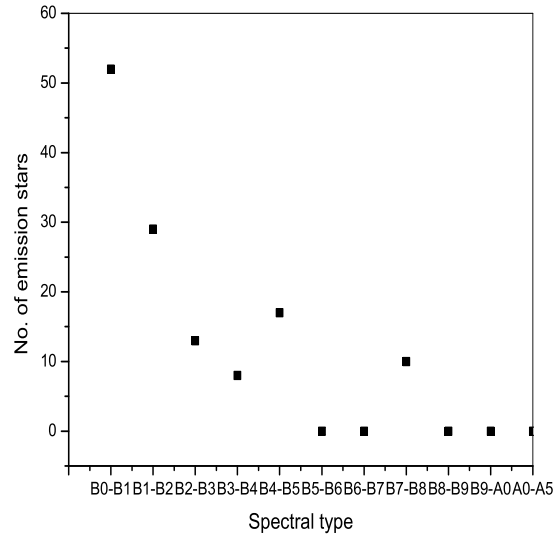


Figure 4.2: Distribution of emission stars with respect to Spectral type.

4.2.5 Spectral type estimation

We tried to estimate the spectral type of candidate stars by comparing Balmer lines in the blue region (3970 Å, 4100 Å, 4340 Å) and the helium lines (4026 Å, 4471 Å) with the standard spectral library (Jacoby et al., 1984). The resulting plot in each spectral bin is shown in figure 4.2. Most of the e-stars are crowded in

B0–B1 spectral bin. About 17 stars are found in B4–B5 spectral bin while 10 are in B7–B8 bin. Using photometric data we found the spectral type distribution of e-stars peaked in B1–B2 and B6–B7 spectral bins (figure 3.4). Hence estimation of spectral type from spectroscopy show bias to early type in comparison with photometry. This is expected since Be stars are found to show filled-in emission in higher order Balmer lines. Hence we have used the photometric spectral types estimated in chapter 2 for the rest of the analysis.

4.2.6 The distribution of Balmer decrement (D_{34})

The Balmer decrement ($I(H_\alpha)/I(H_\beta)$, D_{34}) of Be stars have been studied extensively by several authors (Slettebak et al., 1992; Burbidge and Burbidge, 1953; Dachs et al., 1990) and they all agree with the theoretical value of nebular region, even though the Be star envelopes have different density and temperature structure than nebulae. For nebular region, the peak emission strength ratio of H_α to H_β is given as 2.7 for a typical electron density of 10^6 cm^{-3} and a temperature of 20,000 K, which is mentioned as Case B transition in nebulae (Brocklehurst, 1971; Hummer and Storey, 1987). Briot (1971) found the mean value of D_{34} to increase from flat decrement at spectral type B0 (~ 1.5) to steep decrement for Be stars later than B5 (~ 5). Dachs et al. (1990) found the D_{34} value in the range 1.2 to 3.2 from an analysis of 26 equatorial and southern Be stars. They found that weak Be stars are often characterized by relatively flat D_{34} while shell Be stars show very steep decrements. They commented that the main parameter governing the value of D_{34} appears to be the mean electron density in the circumstellar envelope. They found D_{34} values of majority of Be stars agree with the standard nebular value for Be stars with H_α EW in excess of -25 \AA . Ashok and Banerjee (2000) identified deviation from Case B values for Brackett lines which has been interpreted as due to the effect of optical depth.

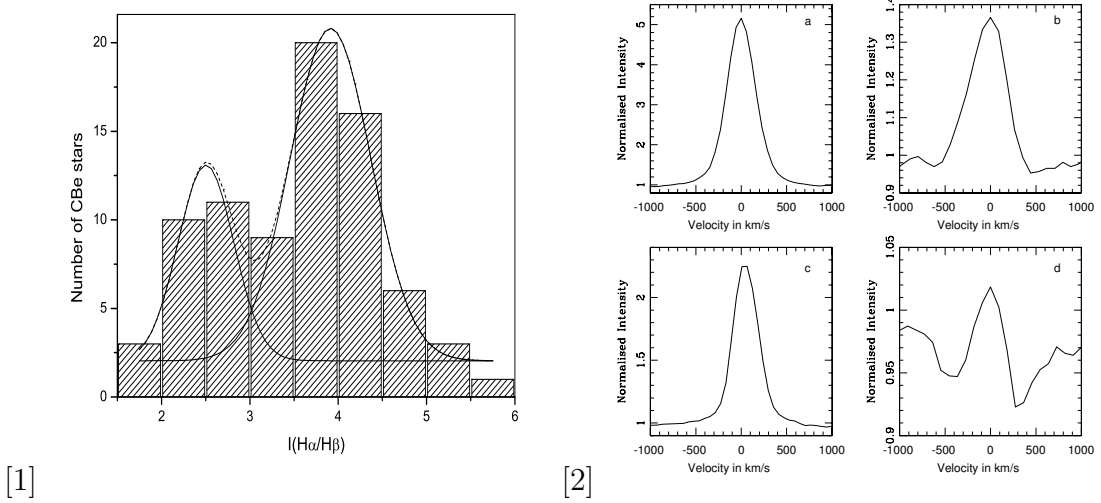


Figure 4.3: (1) The Balmer decrement distribution of surveyed stars. (2) The H_α and H_β line profiles of Berkeley 87(4) are given in (a) and (b) while those of NGC 663(P25) are given in (c) and (d).

The Balmer decrement was calculated for 88 CBe stars, which show emission in both H_α and H_β line profiles. The D_{34} values of 67 candidates (76%) were found to be more than the standard nebular value of 2.7. We have plotted the histogram of D_{34} (with bin size of 0.5) in figure 4.3(a). The values of D_{34} were calculated from the normalised, continuum fitted spectra. The estimated intensities are not corrected for the fill up of the respective absorption profiles. We do not expect a significant change in the result even after the correction. We plan to include this and re-estimate the values in the future. Also we do not use the D_{34} values to estimate any quantitative parameter. Our candidate stars were found to have values ranging from 1.5 to 6.5 with a mean around 3.5 as shown in figure 4.3(1). We fitted Gaussians for the 2 peaks seen in the distribution and they are found to peak at 2.5 and 3.9 respectively. The population in the first peak are found to have an emission in absorption (or filled-in) profile for H_β line, while H_α profile showed emission above the continuum. The population in the second peak are found to have emission above the continuum in H_α and H_β with no

filled-in features. Moreover, the peak emission strength of H_α is found to be lower for the candidates having filled-in H_β profiles so that the lower value of Balmer decrement is related to the reduction in intensities of both profiles. The H_α and H_β line profiles of a representative candidate belonging to each group is given in figure 4.3(2). The star Berkeley 87(4) is found to have a high D_{34} value of 3.84 while NGC 663(P25) is found to have a low value of 2.18. The maximum value of H_α peak emission strength measured among our candidate stars is 7.52 and the corresponding H_β value is 1.55, for the star NGC 884(2). The minimum peak emission strength values measured for H_α and H_β are 1.82 and 0.97 respectively, for the star NGC 6910(B). Since we address the relative intensities with respect to the origin of intensity axis, the deblending of stellar absorption component is unlikely to change the values of D_{34} . Hence the bimodal distribution of Balmer decrement and its deviation from the nebular value needs to be addressed in detail.

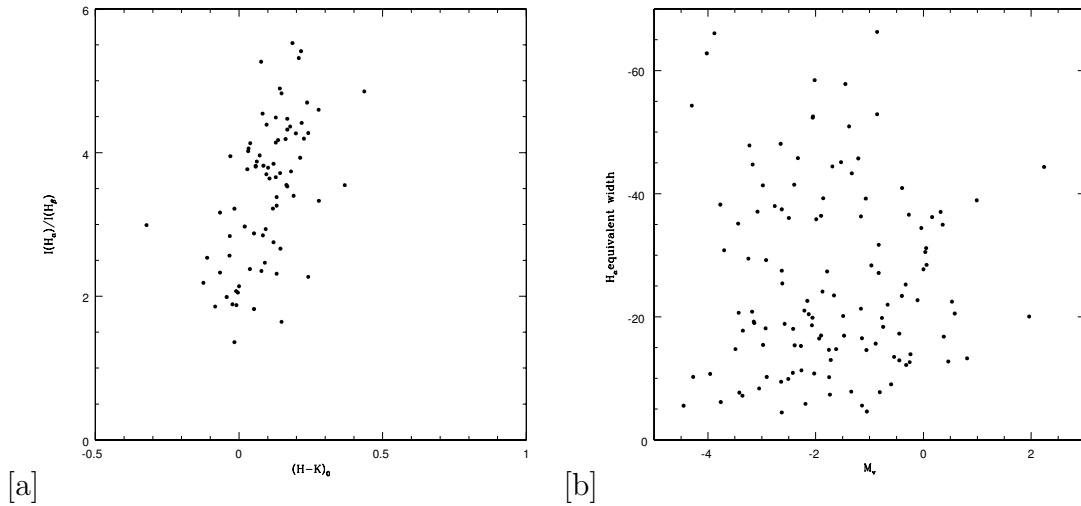


Figure 4.4: (a) The variation of Balmer Decrement with respect to the near-IR colour $(H-K)_0$. (b) The variation of H_α EW with respect to spectral type.

Another interesting finding is that the stars belonging to the first group (with a peak of 2.5) have less number of spectral lines (especially FeII lines) compared to the candidates in the second group. Moreover CaII triplet and Paschen lines

are found to be structured, absent or in absorption in the first group while they appear as single peak emission profiles in the other group. These suggest that the stars belonging to first bin, with low Balmer decrement, may have an optically and geometrically thin disk while those with higher Balmer decrement might have a thick disk.

To check the correlation between the extent of disk and opacity, we plotted D_{34} with near-IR colour excess $(H-K)_0$, as shown in figure 4.4(a). It can be seen that D_{34} is directly proportional/linearly correlated with $(H-K)_0$. The Balmer decrement (correlated to line optical thickness) is high for a geometrically thick and extended circumstellar disk (higher value of $(H-K)_0$). The fact that a large fraction of stars seem to possess thick/extended disks, as contrary to what is seen in the field CBe stars might suggest a difference in disk properties for CBe stars in cluster environment.

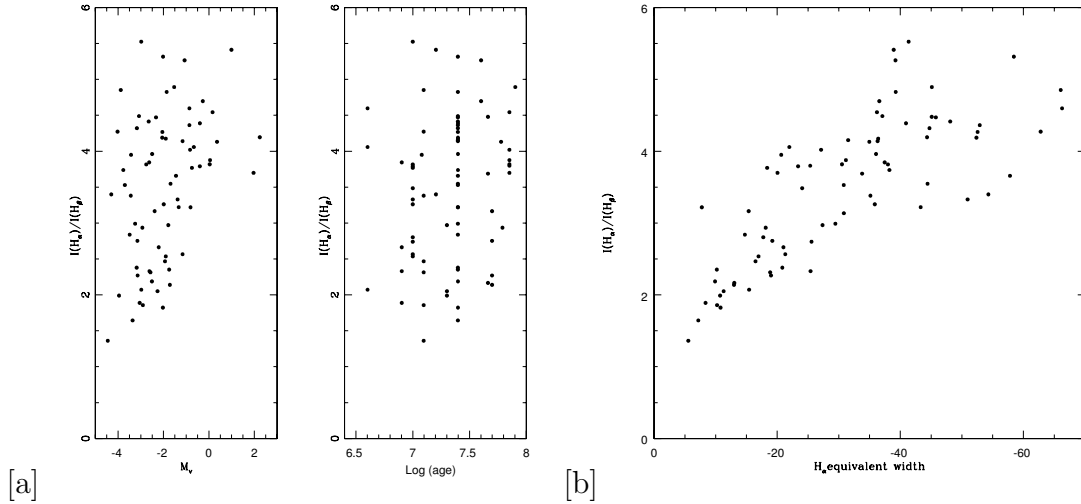


Figure 4.5: (a) The variation of D_{34} with respect to spectral type is shown in left panel while the variation of D_{34} with age is shown in right panel. (b) A plot of D_{34} with respect to H_α EW of CBe stars.

It has been observed by some authors (Briot, 1971; Briot and Zorec, 1981) that

along the spectral sequence (B0–B8) the H_α emission EW decreases while the Balmer decrement D_{34} increases. Our studies show that H_α emission EW do not show any trend with respect to spectral type (figure 4.4(b)). The Balmer decrement is found to show a rising trend with respect to spectral type as shown in figure 4.5(a). The variation of D_{34} with respect to the age of the stars is shown in figure 4.5(a). It can be seen that late type stars show a higher value of D_{34} . The same trend can be seen in D_{34} versus age plot keeping in mind that only late type stars are present in older clusters. The early type stars are found to have a range of D_{34} values. This suggests that the formation and evolution of circumstellar disks in late type stars may be different from those of early type stars.

We found a correlation between the Balmer decrement D_{34} and H_α EW as shown in figure 4.5(b). The correlation is linear and is tight at low values of H_α EW. We have checked for the correlation between higher value of D_{34} and the presence of OI lines 7772 and 8446 Å, since both requires high electron density environment. From a sample of 88 surveyed stars, which have clean H_α and H_β measurements (removing filled-in profiles), 67 have D_{34} above 2.7. Among these 48 (72%) stars have both OI lines while 16 have only 8446 Å line present in the spectra. Among the remaining 21 stars having D_{34} less than 2.7, 12 (57%) have both OI lines while 8 have only 8446 Å line. To summarise, a good fraction of the surveyed stars (76%) may have optically thick disks, identified by the presence of large D_{34} , high H_α EW, metallic lines and high $(H-K)_0$ values.

4.2.7 Relationship between OI(8446) and Balmer line profiles

The OI 8446 Å line is produced by Lyman β fluorescence since it is a cascade product of 1025.76 Å OI line. Since H_α is a cascade product of Lyman β line, a

correlation is expected between the line intensities of OI 8446 Å and H_α . Kitchin and Meadows (1970) found a strong correlation between the emission strength of OI and H_α spectral lines.

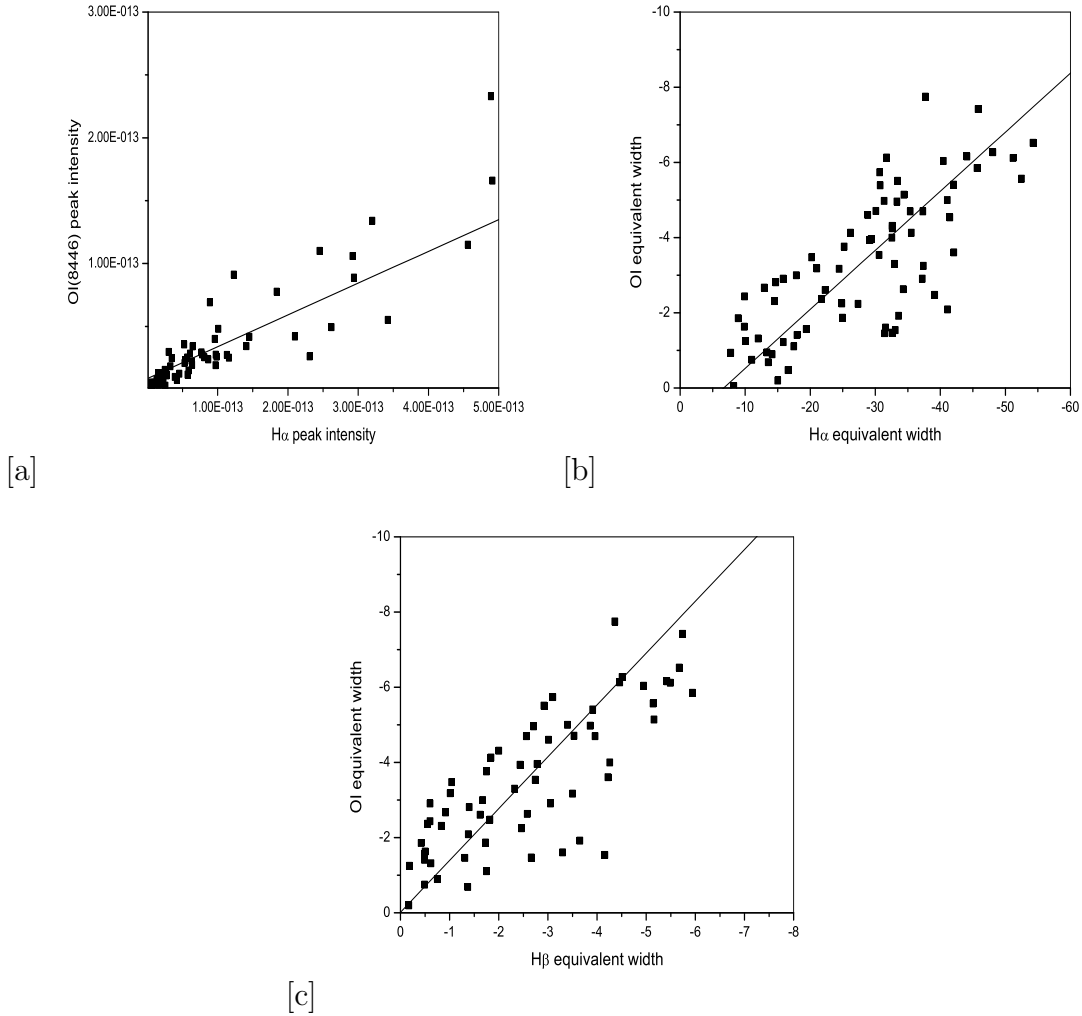


Figure 4.6: (a) The OI(8446) emission strength is plotted with respect to H_α emission strength. (b) A plot of EW of OI(8446) against H_α EW. (c) A plot of EW of OI(8446) against H_β EW.

We found a correlation between peak emission strengths of OI 8446 Å and H_α spectral lines for our candidate stars, as shown in figure 4.6(a). The ratio of peak emission strengths ($I(\text{OI})/I(\text{H}_\alpha)$) is found to have a range of values between 0.1

and 1, with a mean value of 0.4. The relation obtained from a linear fit is given as

$$I(8446) = 0.25 * I(H_\alpha) + 8.5 * 10^{-15} \quad (4.2)$$

The correlation coefficient obtained is 0.96. Slettebak (1951) found the equivalent widths of OI 8446 Å and H_β to be better correlated when compared to OI and H_α, as predicted by Bowen (1947). Briot (1981) supported the prediction of Bowen (1947) from a study of the line profiles of 15 Be stars. Andrillat et al. (1988) found a linear correlation between the EWs of OI 8446 Å and H_α for a sample of 23 CBe stars. But the correlation was not convincing since the measurements of both lines were not simultaneous. Jaschek et al. (1993) also quoted a relation between OI 7772 Å and 8446 Å lines along with the relation between OI 7772 Å and H_α line EWs. From this we derived a relation between the line EWs of OI 8446 Å line and H_α which is found to be

$$EW(8446) = 0.067 * EW(H_\alpha) + 0.61 \quad (4.3)$$

We plotted the EW values of OI 8446Å line with H_α in figures 4.6(b). From the linear fit we have the relation

$$EW(8446) = 0.157 * EW(H_\alpha) + 1.05 \quad (4.4)$$

with a correlation coefficient of 0.92.

The plot between OI 8446 Å line and H_β is given in figure 4.6(c). A linear fit to the data points gives the relation

$$EW(8446) = 1.37 * EW(H_\beta) - 0.01 \quad (4.5)$$

with a correlation coefficient of 0.90. The error in slope estimated for the former correlation is 0.007 while it is 0.005 for the latter. From the above relations it can be seen that OI 8446 Å line correlates fairly well with H_α, as well as H_β.

4.2.8 The variation of H_α EW as a function of age

The H_α EW of surveyed stars are plotted as a function of their age in figure 4.7(a). Clusters younger than 30 Myr are found to have e-stars with a range of H_α EW. For older clusters there is an absence of stars with EWs greater than -40 \AA except two stars. The measure of EW is correlated with the number of emitting atoms which again corresponds to the extend of the circumstellar disk (as explained in the subsection on Balmer decrement). The plot also suggests that the H_α EW peaks at about 10 Myr. This is supportive of the reported enhancement of the Be phenomenon at ~ 10 Myr (Mathew et al., 2008) for early type stars.

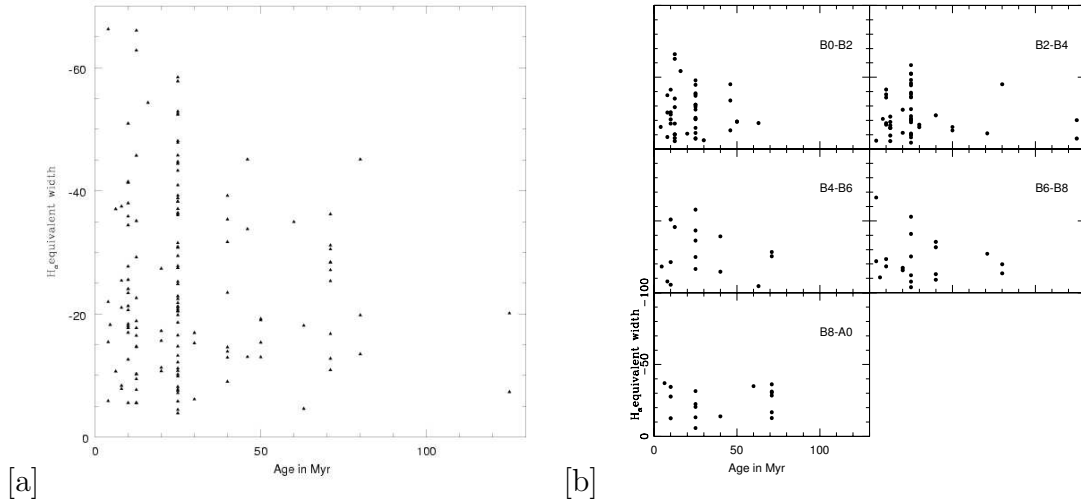


Figure 4.7: (a) The H_α EW of the surveyed e-stars are plotted with respect to the age of the cluster to which they are associated. (b) The H_α EW of e-stars is shown with respect to age for various spectral bins.

We looked for the evolution of H_α EW with age for each spectral type as shown in figure 4.7(b). For the spectral bin B0–B2, the H_α EW is found to peak at 12.5 Myr with rich cluster candidates NGC 869(1) and NGC 884(2) topping the plot with values -63 \AA and -66 \AA respectively. A similar rising and decaying trend in EW is found in B2–B4 spectral bin with a peak at 25 Myr. The peak is dominated by e-stars in rich clusters like NGC 7419(5) (-58 \AA), NGC 7419(N) (-52

Å) and NGC 663(9)(-52 Å). The star NGC 2421(1) stands out from the decaying trend in EW with a value of -45 Å. An age shift of 12.5 Myr to 25 Myr for a spectral type shift of B0–B2 to B2–B4 is worth noticing. This also supports the contribution of evolutionary effect to Be phenomenon. Stars in the spectral bins B4–B6, B6–B8 and B8–A0 do not show any clear trend. The H_α EW shows a marginal enhancement for younger stars and then remains at a lower value without any change with respect to age. The stars of the cluster NGC 2345 in the spectral bin B8–A0 have quite a number of high EW candidates which do not correlate with their old age. We are in the process of re-estimating the parameters of this cluster. To summarise, massive Be stars of spectral type B0–B4 show enhanced H_α emission at the end of their MS lifetime, as inferred from the enhancements observed at 12.5 and 25 Myr. No such trend is observed in later spectral types (B4–A0).

4.2.9 Estimation of H_α emission radius

Emission lines of Be stars are typically double peaked, with the peak separation correlated to the observed line width (Struve, 1931; Hanuschik, 1996). Slettebak et al. (1992) assumed a Keplerian geometry for the circumstellar disk and used H_α profile to find the radius of the emitting region, which is found to be in the range 7–15 stellar radius (R_s). Using strong lines of H_α , H_β and H_γ , the outer radii of emitting envelopes, in terms of R_e/R_s , were found to be 18.9, 12.2 and 10.7 respectively. Using weak lines ($EW \leq 20$ Å) they were found to be 7.3, 4.6 and 5.3.

We used H_α emission line profile to estimate the disk rotation velocity $v \sin i(d)$ while the stellar rotation velocity $v \sin i$ was estimated using HeI 4471 Å line. We measured FWHM and EW using routines in IRAF with an error of 3% and 4% respectively about the mean values. The FWHM of H_α is corrected for instrument

line width using FeAr and FeNe arc spectra, taken along with the objects. The rotation velocity was calculated using the formula

$$v \sin i = c * FWHM / [2\lambda_0 * (\ln 2)^{1/2}] \quad (4.6)$$

where c is the velocity of light, λ_0 is the central wavelength of the spectral line. The H_α emission region is calculated, in terms of stellar radius, using the formula,

$$R_e/R_s = (2v \sin i / \delta V_p)^2 \quad (4.7)$$

assuming the region to be in Keplerian orbit around the star (Huang, 1972). Here, δV_p is the velocity difference between the peaks of a double-peaked emission profile. For a non-Keplerian orbit, the equation changes to

$$R_e/R_s = (2v \sin i / \delta V_p) \quad (4.8)$$

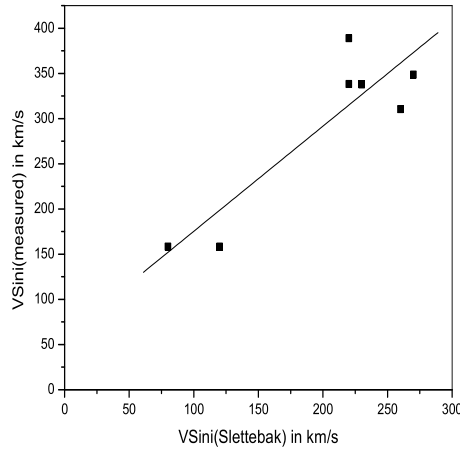


Figure 4.8: Presently estimated $v \sin i$ values of field CBe stars is shown against those estimated by Slettebak. The linear fit which gives the best correlation is also shown.

For calibrating the $v \sin i$ values, we correlated our observed $v \sin i$ values with those estimated by Slettebak (1982) for some field CBe stars. We observed the field

CBe stars using the same setup which we used for our candidate stars. The CBe stars which were used for calibration are 10 Cas, γ Cas, omi Cas, HD 18552, HD 23552, HD 6811 and HD 83953. The plot between the $v \sin i$ values estimated by us using the above procedure and those given in Slettebak(1982) is shown in figure 4.8. We used a linear fit which gives 90% correlation between the data points. The resulting relation is

$$v \sin i(\text{measured}) = 59 + 1.16 * v \sin i(\text{Slettebak}) \quad (4.9)$$

where the $v \sin i$ values are in km/s. The error in the estimation of slope is 0.266. We have calibrated our $v \sin i$ values using this relation.

Stars with double-peaked H_α emission profiles are used to find emission radius. The calculated parameters, $v \sin i$ and R_e are given in table 4.2. The emission region for H_α profile is found to be around 15 stellar radii, with a range of 7–30 stellar radii excluding the extreme values. The mean H_α emission radius will be around 4 stellar radii, if we consider a non-Keplerian disk.

4.2.10 Rotation velocity estimation

The stellar rotation velocity of the surveyed stars were estimated from HeI 4471 Å absorption line. The measurements were corrected for instrumental broadening and were converted to the Slettebak system using the relation derived in the previous section. Only 120 stars were found to have a clean profile since HeI gets faded out for late spectral types. We plotted the histogram of the stellar rotation velocities of these stars in velocity bins of width 50 km/s, over a range of 550 km/s (figure 4.9(a)).

The distribution is found to peak in the velocity bin 250–300 km/s with 28 candidates belonging to that group while 22 are found in 200–250 km/s bin. We

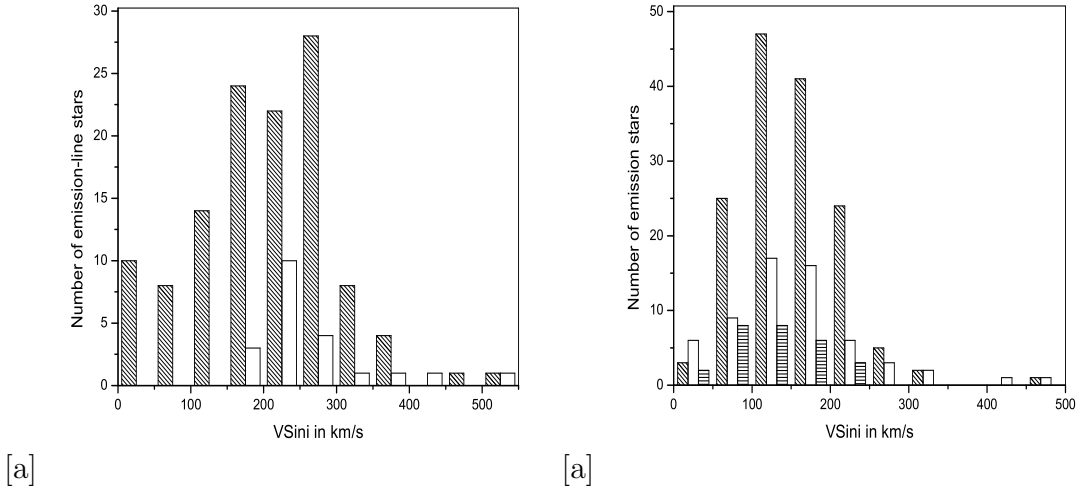


Figure 4.9: (a) The histograms show the $vsini$ distribution of our candidates (oblique shaded histograms) and field CBe stars (open histograms), estimated from HeI 4471 Å line profile. (b) The $vsini(d)$ distribution estimated from H_{α} line profile is shown with candidate stars as oblique shaded histograms, field CBe stars as unshaded ones and HAeBe stars as horizontally shaded histograms.

found 24 stars in 150–200 km/s bin while 14 are in 100–150 km/s velocity bin. 73% are found to have stellar rotation velocities in the range 100–300 km/s. For comparison, we also included the velocity distribution of field CBe stars in the same figure. We only have 21 field CBe stars with valid HeI measurements. Most of the field CBe stars (10 out of 21) are found to have rotation velocity in the range 200–250 km/s while 3 are in 150–200 and 4 in 250–300 velocity bin. Even though it is difficult to draw any conclusion from small number statistics, it can be seen that about 81% of field CBe stars have stellar rotation velocities in the range 150–300 km/s. Hence the range of stellar rotation velocities derived for our candidate stars matches with those derived for field CBe stars. Our result suggests that the CBe stars in clusters have a similar distribution of $vsini$, when compared to the field CBe stars.

The disk rotation velocity, $vsini(d)$ is estimated from H_{α} emission-line profile. The velocities are calibrated using the same method as for HeI 4471 Å spectral

line. For calibration purpose we also plotted the field HAeBe stars and CBe stars which were observed using the same setup. It can be found from figure 4.9(b) that 47 stars among our candidates fall in 100–150 km/s velocity bin while 41 are in 150–200 velocity bin. There are only 3 candidates with velocity greater than 300 km/s with 2 in 300–350 velocity bin and 1 in 450–500 velocity bin. About 92% of the candidates are found to have disk velocity distributed in the range 50–250 km/s and 58% fall in the 100–200 km/s bin. From a sample of 27 HAeBe stars, taken from the catalog by The et al. (1994), 8 stars are found in 50–100 and 8 in 100–150 velocity bin. None of the stars are found to have velocity greater than 250 km/s. We have taken a sample of 61 field CBe stars from Be star catalogue of Jaschek and Egret (1982). Out of these 17 are found in 100–150 km/s velocity bin, closely followed by 16 in 150–200 velocity bin. We have 4 candidates with velocity greater than 300 km/s with 2 in 300–350 velocity bin and 1 each in 400–450 and 450–500 velocity bin. The field CBe stars show a surprisingly large number in 1–50 km/s age bin with 6 stars, while there are only 2 HBe and 3 candidate stars in this bin. About 54% of the field CBe stars are distributed in 100–200 km/s velocity bin which agrees well with the statistics of our surveyed stars.

Comparing the stellar and disk velocity distributions of our candidate stars, we find that, former peaks in 150–300 km/s velocity bin, while the latter peaks in 100–200 km/s bin. Hence the stellar velocity is found to be higher than the disk velocity. This means that the disk is not in synchronised rotation with the star, but lags behind by 50–100 km/s.

4.2.11 The evolution of rotation velocity as a function of age

We studied the variation of rotation velocity of disk with respect to age for various spectral bins, as shown in figure 4.10. We binned the stars belonging to two adjacent spectral classes together. For the spectral bin B0–B2 the rotation velocity is found to peak in the age range 10–20 Myr after an initial rise. The upper limit of the velocity reduces progressively for older stars in the age range 50–60 Myr. In this spectral bin, the velocity of B0 is found to peak at 12.5(250 km/s), 16(210) and 25 Myr(220), for B0.5 it is 12.5(158), 25(165) and 30 Myr (230), for B1 it is 12.5(224) and 25 Myr(179) while for B1.5 it is 8(269), 10(219) and 25 Myr(226). The values in brackets correspond to the peak velocity values of the stars in that spectral bin.

If we estimate the average of the velocity values of all stars corresponding to same age and spectral type, we can see that B0 spectral type stars have the distribution like 130 km/s (10 Myr), 180(12.5 Myr), 210(16 Myr), 150(25 Myr) while B1 shows the distribution like 132(8 Myr), 190(12.5 Myr), 120(25 Myr). Hence high rotation velocity disks around stars in the spectral range B0–B2 are found to be absent in the ~ 10 Myr age bin. The rotation velocity of the disk seems to increase and peak at about 10–20 Myr and then decrease again. Thus, our results suggest that disks of stars in the B0–B2 spectral bin are found to be spun up towards the end of their MS life time, which is 10–20 Myr. This supports the results presented in section 4.2.8 and Mathew et al. (2008).

A large amount of scatter can be seen in the disk velocity distribution in B2–B4 age bin (figure 4.10). The general trend is that the disk rotation decreases from an initial high value with an increase in the age of the star. A similar trend is seen in the distribution for stars in B4–B6 spectral bin. The stars in the spectral bins

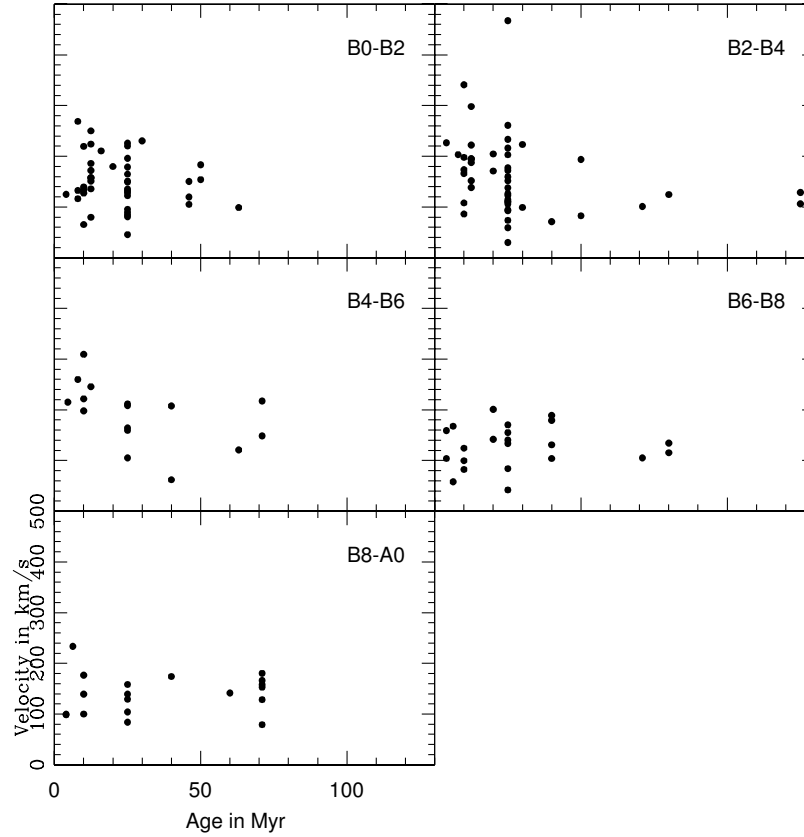


Figure 4.10: The disk rotation velocity is shown with respect to age for different spectral bins.

B6–B8 and B8–A0 show a flat distribution in disk rotation velocities. We can see crowding of stars in the 25 Myr age range for all the spectral bins, especially B0–B2 and B2–B4. This corresponds to the age of rich clusters NGC 663, NGC 6649 and NGC 7419 which contribute a total of 54 stars to the total sample. But the interesting fact is the change in $v \sin i$ value of a CBe star of same spectral type from cluster to cluster. Even though this trend is prominent in early spectral bins, it can be observed in other bins also. A similar trend can be found for the double cluster (NGC 869, NGC 884) and NGC 581 which fall in 12.5 Myr age bin and contribute a total of 16 stars to the total sample. The cluster NGC 2345 shows a spread in the velocity distribution in B8–A0 spectral bin. To summarise,

disk rotation as a function of spectral type suggest lack of fast rotating disks for B0–B2 spectral types younger than 10 Myr. Some fast rotating disks are found in the spectral bin B4–B6. From B4 onwards we find that the disk rotation is not dependent on the age of the stars. Thus, our results suggest spin up of the disk of early type stars, but no spin up or spin down is found for stars later than B4.

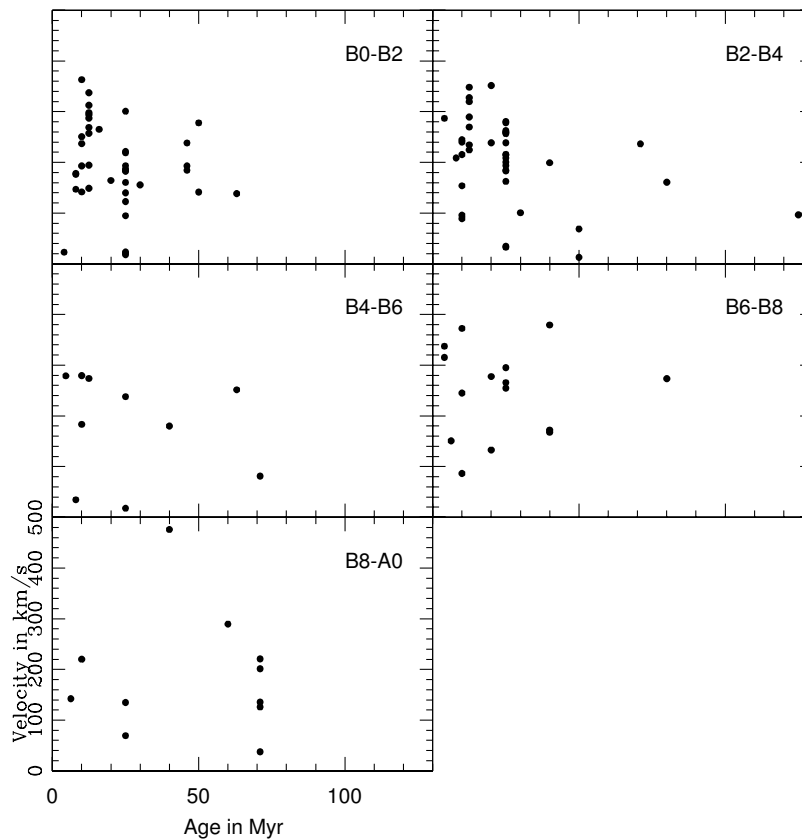


Figure 4.11: The stellar rotation velocity is shown with respect to age for different spectral bins.

In order to study the angular momentum evolution in stars, a plot between the stellar rotation velocity of Be stars with respect to age in various spectral bins is shown in figure 4.11. The stellar velocity is estimated from HeI 4471 Å absorption line profiles. The HeI line fades towards late B spectral type and hence we have

not taken A0 stars while averaging in B8–A0 bin. The distribution looks more or less the same like disk velocity distribution, with increased scatter. The spectral bins B0–B2 and B2–B4 show a decrement in the stellar rotation with age. An initial spin up at 10 Myr is only suggestive, due to less number of stars in the 0–10 Myr age bin. The later bins B4–B6, B6–B8 and B8–A0 show that the stellar rotation does not vary with age. To summarise, the spectral rotation velocity analysis seems to confirm the bimodal origin of Be stars. The early type CBe stars (B0–B4) behave differently from the (B4–A0) stars. The rich clusters are found to have a range in the distribution of stellar rotation velocity which has to be dealt closely with the star formation in rich environment scenario. The range in rotation velocity observed in these clusters is to some extent due to variation in inclination resulting in a range in $v\sin i$.

4.2.12 Variability of H_α profile

Be stars are known to show spectroscopic variability over a period of months to years, which gives an idea about the activity of the circumstellar disk. We observed H_α lpv for a number of candidate stars, whose variability is due to the activity in the disk environment (figure 4.12). Baade (1982) proposed that the short term lpv , on timescales between 0.5 and 2 days, can be due to NRP phenomenon. However, Balona (1990, 1995) argued on statistical grounds that the periods were better explained by stellar rotation and attributed the lpv to stellar spots, and later to corotating clouds.

We obtained repeated observations for most of the candidate stars and those which show considerable changes in H_α profile are listed below. Also quoted are the $v\sin i$ and R_e values estimated for stars which have double-peak profile. The candidates which are used for estimating $v\sin i$ and R_e are tabulated in table 4.2 with the estimated values.

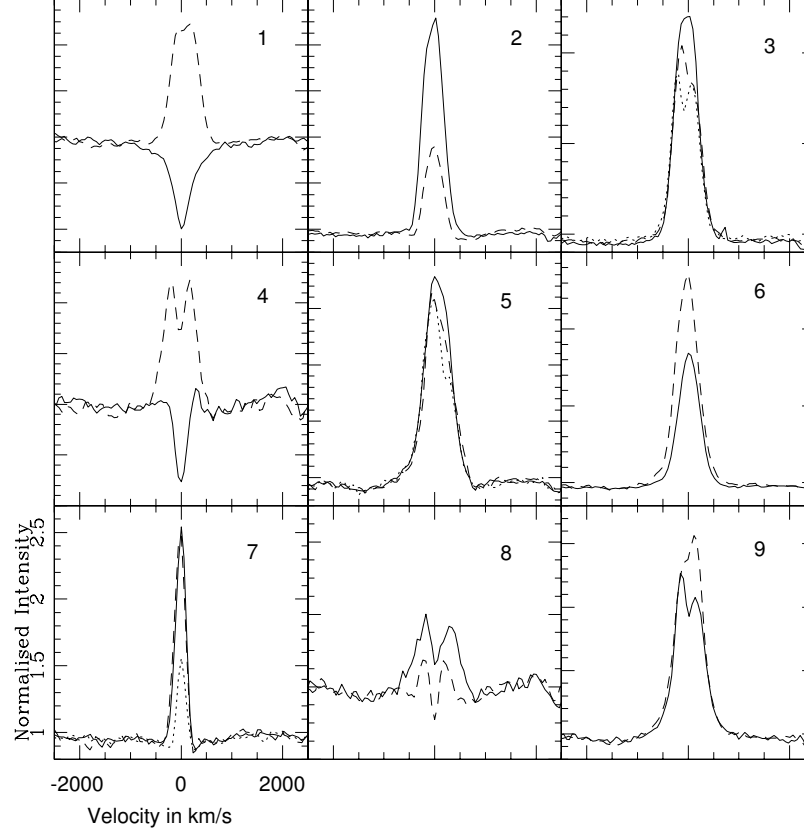


Figure 4.12: The variation in H_{α} profile for e-stars (1) Berkeley 87(3), (2) NGC 659(2), (3) NGC 663(3), (4) NGC 663(13), (5) NGC 869(4), (6) NGC 884(1), (7) NGC 7419(H), (8) NGC 7419(K), (9) NGC 7419(P) are shown. Initial observation is shown as solid line followed by repeated observations in dashed and dotted lines respectively.

Berkeley 87(3): The observations of this star were made in 08-10-2005 and 25-10-2005. The profile changed from absorption to emission during this period. The disk rotation velocity ($V\sin i(d)$) has been estimated to be 259 km/s and the H_{α} emission radius is found to be 12 stellar radii.

NGC 659(2): The H_{α} profile changed from normal state when observed on 21-11-2005 to core-emission on 30-09-2006 with a significant reduction in emission strength.

NGC 663(3): The H_α profile had normal emission when observed on 07-10-2005 which changed to asymmetric emission on 09-10-2006. When observed on 24-10-2007 the profile was found to show double-peak feature.

NGC 663(13): The H_α emission profile of the star changed from P-Cygni (the emission part is weak), when observed in 22-11-2005 to double-peaked profile on 09-10-2006. The estimated rotation velocity ($v \sin i(d)$) is 552 km/s. This also can be a shell star due to the extended emission wings. The profile variability suggests that the star might have strong wind/outflow (inferred from P-Cygni profile) with a geometrically thin disk which subsided down over a period of 1 year.

NGC 869(4): The H_α changed from a symmetric emission profile when observed on 22-01-2006 to an asymmetric profile on 24-10-2007 and 16-12-2007 with reduction in emission strength.

NGC 884(1): The emission strength of H_α profile was enhanced when observed on 15-12-2007 compared to that on 22-01-2006.

NGC 7419(H): The H_α profile is of inverse P-Cygni nature when observed on 15-07-2005, which changed to single-peak profile on 08-08-2005. The profile again changed to core-emission on 09-10-2006.

NGC 7419(K): The profile resembled that of a typical Be shell star, since the absorption component over the emission dips below the continuum level. The H_α profile was double-peaked when observed on 21-01-2006 and the absorption component on emission deepened and fell below the continuum in the normalised spectra of 09-10-2006. The rotation velocity values changed from 833 km/s to 504 km/s while the H_α emission radius changed from 23 to 12 stellar radius.

NGC 7419(P): The profile was double-peaked when observed on 08-10-2005 with the violet part of the double profile fading in intensity to a single profile on 10-10-2006. Both the $v \sin i$ and (R_e/R_s) values reduced from 476 km/s and 25 to 260 km/s and 9 respectively.

The variation in H_α emission line profile will give an idea about the circumstellar environment. In the case of Berkeley 87(3), circumstellar disk is formed during a short period of time (17 days), which suggest the wind compressed disk model as a favourable scenario for disk formation. This can be considered as an example of short-term variability. The star NGC 663(13) is another interesting candidate which was in disk formation process by stellar wind (inferred from P-Cygni profile) during initial observation. This star exhibited double-peaked profile on repeated observation after a period of 1 year. The V/R ratio of NGC 663(P151) and NGC 869(6) were found to change over a period of time, suggesting a turbulent nature of the circumstellar disk. The star NGC 7419(H) showed inverse P-Cygni in H_α line which is an indication of accreting disk. But the activity stops over a span of 3 weeks. We have found NGC 7419(K) as a typical Be shell star from H_α line profile analysis. The shell episodes can appear over a period of time when observed regularly. The fast rotating candidates among our program stars (as shown in table 4.2) may be shell stars which can be confirmed through continuous profile monitoring.

4.3 Discussion

This survey of CBe stars in young open clusters was effectively used to address a number of issues connected with Be phenomenon. Unlike the field CBe stars, the age and distance to these stars can be accurately estimated. Thus, properties

of Be phenomenon as a function of age and stellar mass are addressed using this sample. The present sample consists of 157 stars, of which only 5 stars were found to be probable HAeBe candidates using various proxys. Thus this study uses the statistically significant sample of 152 CBe stars to address the properties of the Be phenomenon. The stars studied here belong to clusters and hence there could be effects in the observed phenomenon due to the denser environment in clusters. In order to compare the observed properties with the field CBe stars, a good number of field CBe stars were observed with the same set up and the line profiles were also analysed similarly. We do not find any significant difference between the cluster and field CBe stars, in terms of stellar or disk property, as observed in the H_α EW, disk and stellar rotation velocities. In rich clusters like NGC 7419, NGC 663, NGC 869 and NGC 884, Be stars of the same spectral type are found to have a range of rotation velocities. This has to be addressed with star formation in dense environment and the presence of binaries. In order to explore this issue in detail, we plan to study the rotation statistics of B and Be stars in clusters with and without e-stars.

As suggested above, the surveyed sample can be used to trace the evolution of angular momentum in the star as well as in the disk. Since this could also be a function of stellar mass, the large number sample allowed us to bin in spectral type as well. The results from the study on stellar and disk angular momentum evolution and the evolution of H_α EW suggest that there could be two types of Be phenomenon. The early type stars (B0–B2/B3) tend to rotate faster with an increase in H_α EW, in the 10–30 Myr range, suggesting that these stars evolve to become Be stars. It also suggests that the activity is probably at its peak near the end of its MS evolution. This result confirms such a suggestion by Mathew et al. (2008) using photometric analysis. Fabregat and Torrejón (2000) suggested that the Be phenomenon will start to develop only in the second half of a B star’s MS lifetime, because of structural changes in the star. The early type stars

(B0–B2/B3) seem to follow the above trend. Such a trend is not seen in the later type stars (B4–B9/A0). These stars do not show any evolutionary effect on the above mentioned parameters. Thus, the suggestion by Fabregat and Torrejón (2000) is not satisfied by the late type stars.

The role of binarity to understand Be phenomenon is one of the often discussed topics. Among the surveyed stars only NGC 7380(3) (PS Cep) has been reported as part of a binary in literature. Another interesting candidate is NGC 1624(1), whose detailed analysis of time series spectra and orbital parameters is underway. Apart from these candidates, others are found to be single. This might be very low number taking into account of the fact that about 30% of Be stars exists as binaries (Porter and Rivinius, 2003). So a final say about the presence of the companion can be done from a detailed time series spectral analysis of our surveyed candidates.

4.4 Conclusion

From the spectroscopic survey of 152 CBe stars, various spectral and evolutionary properties of Be stars and their disk are studied. The results are summarised below:

- Apart from the Balmer lines in emission, spectra of most of the stars show FeII, Paschen and OI lines in emission while HeI is seen in absorption. About 86% of the surveyed emission stars show FeII lines in their spectra. We have found Lyman β fluorescence as the mechanism for the production of 8446 Å line in 24% of the surveyed stars and 47% show line formation (OI 8446 Å & 7772 Å lines) due to collisional excitation. Of the total stars, 14 do not show correlation in FeII 7712 Å and OI 7772 Å line profiles. We found 60% of stars having CaII triplet in emission.

- The Balmer decrement (D_{34}) of Be stars is found to range between 1.5 and 6.5 with a mean value of 3.5 unlike the typical nebular value of 2.7. Gaussians were fitted to the 2 observed peaks seen in the distribution and the peak values were estimated to be 2.5 and 3.9 respectively. The Be star population in first peak were found to have a filled-in profile for H_β line, while stars in the second peak showed H_β with no filled-in features and more number of FeII lines. The Balmer decrement D_{34} was found to increase with H_α EW for the surveyed stars. The higher value of Balmer decrement probably corresponds to (correlated to line optical thickness) a geometrically thick and extended circumstellar disk (higher value of $(H-K)_0$).
- The estimated H_α EW distribution of the surveyed stars peak in the range -10 \AA to -20 \AA . The H_α and H_β EWs are correlated giving an H_α to H_β EW ratio around 10.
- The H_α emission line profile is found to show short (few days) and long term variability (\sim years). We found the profile of Berkeley 87(3) to change from absorption to emission in 17 days while V/R ratio changes over a period of 1 year for a few stars. The H_α emission profile of the star NGC 663(13) changed from P-Cygni to double-peaked profile during a span of \sim 1 year. We found NGC 663(13) and NGC 7419(K) belong to shell star category from the analysis of H_α line profiles.
- The clusters younger than 30 Myr are found to have stars with a range of H_α EWs. For clusters older than 30 Myr, there is an absence of stars with EWs greater than -40 \AA .
- We calibrated our stellar velocity ($v \sin i$) values with the Slettebak system using HeI 4471 \AA profile of 7 field CBe stars. The same calibration relation is used to standardise the disk rotation velocity which was obtained using H_α profiles. The average emission region for H_α profile is found to be around 15

stellar radii, with a range of 7–30 stellar radii, assuming the circumstellar disk to be Keplerian.

- The rotation velocity of candidate stars is found to be in the range 150–300 km/s, which matches with the values of field CBe stars. The rotation velocity of the disks were found to range between 50–250 km/s, thus the circumstellar disk is found to lag behind the star by 50–100 km/s.
- The angular momentum evolution of stars and disk as a function of age and spectral type also suggest a bimodal origin of Be stars. Our results suggest that stars in the B0–B2 spectral bin are found to spin up towards the end of their MS life time, which is 10–20 Myr. Stars in the B0–B4 bin show enhanced H_α emission at the end of their MS lifetime, as inferred from the enhancements observed at 12.5 and 25 Myr. All the above results indicate that the activity in early type Be stars gets accelerated towards the end of the MS evolution. Thus early type stars evolve to become Be stars. Similar variation in properties were not found for stars in the later spectral types (B4–A0), suggesting that the Be phenomenon differs in early and late type stars.

Table 4.1: Spectral lines identified in the surveyed e-stars, with the number of emission and absorption profiles in brackets.

FeII				
4173(17e,7a)	4233(8e,4a)	4287([FeII],1e)	4303(2e,2a)	4352(3a)
4358([FeII],1e)	4385(2e)	4413([FeII],1e)	4417(2e,1a)	4515(6e,1a)
4520(8e,2a)	4523(3e,3a)	4549(7e,1a)	4556(5e,3a)	4584(30e,6a)
4629(23e,1a)	4924(4e)	5018(51e,1a)	5159([FeII],1e)	5169(65e,19a)
5197(23e,1a)	5235(34e,10a)	5276(28e,7a)	5316(79e,7a)	5363(11e,1a)
5425(8e,1a)	5480(4e)	5496(1a)	5535(7e,1a)	5814(1a)
5957(1e)	5991(4e)	6084(1e)	6103(1a)	6148(12e,1a)
6248(9e)	6317(60e,4a)	6384(79e,3a)	6417(2e)	6432(1e)
6456(32e,7a)	6483(2e)	6516(35e)	7222(3e)	7308(1e)
7321(1e)	7462(8e)	7513(68e,2a)	7712(56e,1a)	
OI				
5577([OI],1e)	7772(71e,45a)	8446(145e,3a)		
Ca II				
8498(103e,33a)	8542(104e,39a)	8662(98e,48a)		
Si II				
4131(1a)	6347(11e,28a)	6371(6e,33a)		
Mg II				
7877(3e,1a)	7896(8e,7a)			
N II				
5005(1e)	5463(1e)	5530(2e)	5535(2e)	5684(1e)
5711(1e)	5942(1e)			

e - emission, a - absorption

Table 4.2: The estimated H_α emission region, in terms of stellar radius, for e-stars which showed double-peak profile.

Star	Observed on	$v \sin i$ (km/s)	R_e/R_s
Berkeley 86(9)	27-06-2005	309	16
Berkeley 87(2)	09-10-2005	268	130
Berkeley 87(3)	25-10-2005	259	12
NGC 663(13)	09-10-06	552	19
NGC 663(24)	09-10-05	381	15
	10-10-06	415	70
NGC 663(P151)	25-10-05	439	19
	10-10-06	435	12
NGC 869(6)	22-01-2006	256	29
NGC 6834(4)	07-10-2005	178	14
NGC 6910(A)	29-07-2005	232	7
NGC 7128(2)	14-10-2005	164	2
NGC 7419(K)	21-01-06	833	23
	09-10-06	504	12
NGC 7419(P)	08-10-05	476	25
	10-10-06	260	9

Chapter 5

Spectroscopic study of a few Herbig Ae/Be stars in Young Open Clusters

5.1 Introduction

The survey to search for Be stars in young open clusters using slitless spectroscopy was explained in chapter 3. Even though the aim was to study ‘Be phenomenon’ in CBe stars, a few HAeBe candidates were also found among the surveyed stars. Most of the e-stars in the survey belonged to CBe class ($\sim 92\%$), while $\sim 6\%$ are HBe stars and $\sim 2\%$ belong to HAe category. In chapter 3, we identified Berkeley 90(1), Bochum 6(1), IC 1590(1), NGC 146(S2), NGC 1893(1), NGC 6823(1), NGC 7380(1), NGC 7380(2), NGC 7510(1C) as possible HBe stars and IC 1590(2), NGC 7380(4), Roslund 4(1) as possible HAe stars from optical CMD, near-IR CCDm and nebulosity. In this chapter we have compiled the spectroscopic information of these candidate stars, along with their photometric details, to identify the most likely HAeBe candidates.

Marco and Negueruela (2002) identified four PMS stars in the field of cluster NGC 1893 from low-resolution spectroscopy and photometry. The early-type PMS stars are found in the rim of the molecular cloud and in the vicinity of nebulae

Sim 129 and Sim 130. They found possible cohabitation of HBe and CBe stars in the cluster, whose age is around 3 Myr. Testi et al. (1999) found clustering of low mass stars around early HBe stars while HAe stars are never associated in groups. They proposed that the formation of high-mass stars is influenced by dynamical interaction in a young cluster environment. Subramaniam et al. (2006) found 42% of the stars in the rich cluster NGC 7419 to have near-IR excess, which were confirmed to be PMS candidates. From a fit of PMS isochrones the turn-on age of the cluster is found to be 0.3–3 Myr, which indicates a recent episode of star formation. Bhavya et al. (2007) studied recent star formation history in the Cygnus region using the clusters Berkeley 86, Berkeley 87, Biurakan 2, IC 4996 and NGC 6910. They proposed that Cygnus region has been actively forming stars for the last 7 Myr. Similarly, in this study we have identified PMS stars in clusters with HAeBe stars and estimated the duration of star formation. The ages of the identified HAeBe stars were also estimated. The locations of PMS stars and HAeBe stars were compared to identify the presence of any clustered star formation around the HAeBe stars.

In the following sections we have described the techniques used to classify HAeBe candidates from the observed list of e-stars. The candidates are identified through the correlation between H_{α} , OI EW with near-IR excess, followed by the identification of PMS stars, duration of star formation and discussion.

5.2 Observations

The near-IR photometric magnitudes in J, H, K_s bands for all the candidate stars are taken from 2MASS (<http://vizier.u-strasbg.fr/cgi-bin/VizieR?-source=II/246>) database. The 2MASS colors (J–H) and (H– K_s) are de-reddened using the relation from Bessell and Brett (1988) and near-IR CCDm is plotted for the identified

stars in the cluster. The main sequence track and giant star location are taken from Bessell and Brett (1988) which is transformed to 2MASS photometric system using the relations from Carpenter (2001). The HAeBe star location is taken from Hernández et al. (2005) while CBe star location is taken from Dougherty et al. (1994). The reddening bands are shown which limits the reddening due to normal interstellar dust. The stars which have near-IR excess are located to the right of reddening vector and are considered to be candidate PMS stars. The PMS stars shows near-IR excess due to the presence of a dusty circumstellar disk. The near-IR CCDm also helps to identify CBe and HAeBe stars separately, in which both of them occupy distinct regions (Lada and Adams, 1992). HAeBe stars are found to show dust excess in addition to free electron excess in near-IR colours due to the presence of a thick circumstellar disk.

For determining the age of candidate PMS stars, optical CMD is plotted after correcting for cluster excess. The cluster mean reddening value ($E(B-V)$) is used to de-redden near-IR CCDm and optical CMD. The ZAMS (Schmidt-Kaler (1982)) is fitted and DM is estimated. PMS isochrones of various ages (Siess et al., 2000) are plotted and the ages of candidate PMS stars are estimated. Their relative spatial distribution of PMS and Be stars is used to look for clustering.

For the construction of spectral energy distribution (SED), we have taken the photometric magnitudes from following database. U magnitudes from Homogeneous Means in the UBV System (Mermilliod, 1994), B, V, R magnitudes from NOMAD Catalog (Zacharias et al., 2005), I from DENIS database (DENIS Consortium, 2005) and J, H, K_s magnitudes from 2MASS database. We have taken the V magnitudes from NOMAD instead of using the values quoted in chapter 2 to keep all B, V, R magnitudes on the same system. We have verified the values in both cases and found to match well. The extinction corrected magnitudes have been converted to fluxes and the resulting plot between $\log(\lambda f_\lambda)$ and $\log(\lambda)$

is shown separately for e-stars in each clusters. The SED has been normalised in V magnitude to look for the excess in near-IR bands. The excess flux in K_s band due to dust emission have been used to separate HAeBe stars from CBe stars.

5.3 Results and Discussion

In the following subsections, correlation between H_α , Paschen, CaII and OI lines with near-IR excess are presented. We used these correlations to confirm HAeBe candidates among the surveyed stars.

5.3.1 Correlation of H_α EW with Near-IR Colour excess

Feinstein (1982) found a correlation between H_α EW and (K–L) colour suggesting that stars with high H_α EW also show large IR excess. Neto and de Freitas-Pacheco (1982) found a linear correlation between H_α flux and the infrared flux at $3.8\mu\text{m}$. These results suggest that the same region of Be star envelope produces IR excess and Balmer line emission.

A plot between the colour excess $E(V-K_s)$ and H_α EW of e-stars is shown in figure 5.1(a). The identified CBe stars among the surveyed candidates are shown as open circles while the suspected HAeBe stars (Mathew et al., 2008) are shown as filled circles. We have not included Berkeley 90(1) and Bochum 6(1) in the plot since former do not have optical photometry while the latter has high H_α EW. The photometric V magnitudes are taken from the references given in chapter 2, while K_s magnitude is taken from the 2MASS database. Usually $(V-K_s)$ has been used to find excess from circumstellar medium over the photospheric continuum since the emission from circumstellar medium starts dominating from V magnitude

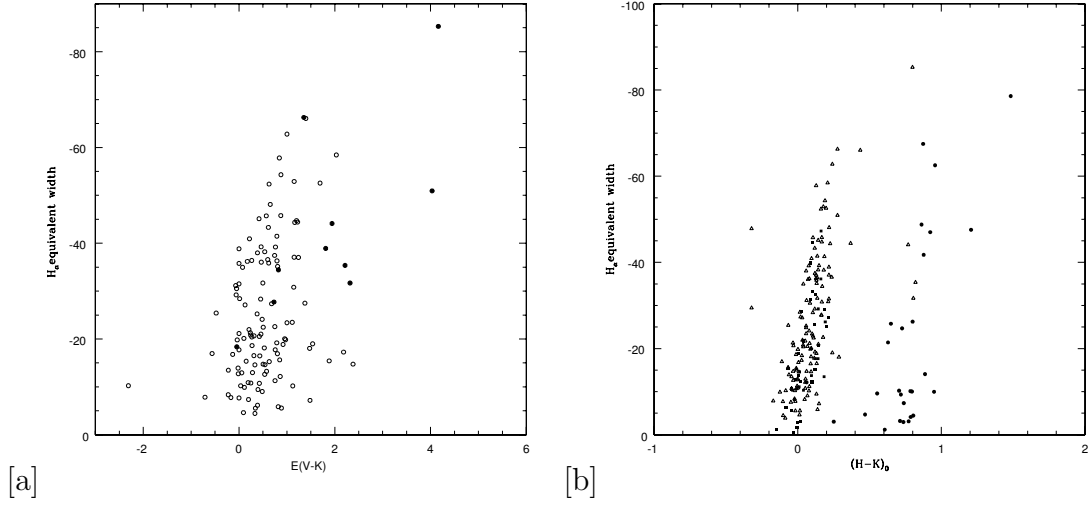


Figure 5.1: (a) Correlation between H_α EW and $E(V-K_s)$ for all e-stars. The candidate CBe stars are shown as open circles while the suspected HAeBe stars are shown as filled circles. (b) Correlation between H_α EW and $(H-K_s)_0$ for all e-stars. Our candidate e-stars are shown as open triangles while the Herbig Be stars from The et al. (1994) is shown as filled circles and CBe stars from Jaschek and Egret (1982) as filled squares.

onwards. To quantify the contribution from the circumstellar medium, we have deducted the colour excess of cluster from $(V-K_s)$ using the $E(B-V)$ value of the cluster. We have estimated the colour excess $E(V-K_s)$ using the relation

$$E(V - K_s) = (V - K_s)_0 - (V - K_s)_S \quad (5.1)$$

where $(V-K_s)_0$ is the corrected (for cluster excess) $(V-K_s)$ colour and $(V-K_s)_S$ is the standard colour corresponding to the spectral type of candidate stars, taken from Koornneef (1983). Hence $E(V-K_s)$ indicates the colour excess due to circumstellar material since we have removed the contribution from the interstellar medium. As seen from figure 5.1(a), the disk excess $E(V-K_s)$ is found to be correlated with H_α EW. Eventhough 6 stars are separated from the remaining candidates, this plot do not clearly distinguish HAeBe stars from surveyed CBe stars. This might be due to the fact that HAeBe stars do not show optical excess along with near-IR excess for all candidates.

We propose that the plot between H_α EW and $(H-K_s)_0$ colour as a tool to differentiate HAeBe stars from CBe stars. The near-IR colour $(H-K_s)$ has been corrected for cluster reddening using the relations by Rieke and Lebofsky (1985). We have plotted our surveyed stars with the catalogued field HAeBe stars (The et al., 1994) and CBe stars (Jaschek and Egret, 1982) in figure 5.1(b). A clear offset can be found between the distribution of field HAeBe and CBe stars. This is expected since HAeBe stars are found to have an extended circumstellar disk with more dust content than CBe stars. The near-IR excess in CBe stars is due to free electrons while this adds up with dust excess in HAeBe stars. The stars Bochum 6(1), IC 1590(1), IC 1590(2), NGC 6823(1), NGC 7380(4) have been found along with catalogued HAeBe stars and hence they agree with their previous identification as HAeBe stars (Mathew et al., 2008). We have not included Bochum 6(1) in this plot due to the high value of EW. The stars Bochum 6(1), IC 1590(1), NGC 6823(1) belong to HBe class while IC 1590(2) and NGC 7380(4) belong to HAe category. Berkeley 90(1) is not included in this analysis since $E(B-V)$ is not available. The e-stars NGC 146(S2), NGC 1893(1), NGC 7380(1), NGC 7380(2), NGC 7510(1C) and Roslund 4(1) were identified as HAeBe by Mathew et al. (2008), but are found to be along with catalogued CBe stars in this plot.

The stars which have missed detection in this plot (7 stars) might be the ones which are losing disk and hence showing less H_α EW and near-IR excess. They might belong to Group III category, which is a classification of HAeBe stars done by Hillenbrand et al. (1992) based on SED. Hence from the photometric and spectroscopic estimates we conclude that out of 157 surveyed e-stars 3 are HBe candidates while 2 are sure HAe candidates. The H_α EW shows a striking correlation with $(H-K_s)_0$ colour, which implies that the presence of dusty regions favours the production of H_α by creating an environment to produce recombination radiation.

5.3.2 Correlation of OI, P14 and CaII triplet EW with $(H-K_s)_0$ colour

It has been pointed out by Briot (1977, 1981) that Be stars with CaII and Paschen lines are found to show high near-IR excess compared to other Be stars. We have searched for this trend in our surveyed 157 candidate e-stars. The presence of ionized calcium in emission for some Be stars was found by Hiltner (1947). Andrillat et al. (1988) observed that if CaII lines are in emission, Paschen lines are also in emission with a similar dependence for absorption profiles also. Polidan and Peters (1976) connected the presence of CaII triplet in emission to the binary nature of the star. They found no correlation between the line properties and the star-disk parameters.

Out of 157 candidate stars, 100 show P14 line in emission and 92 show CaII triplet, while 146 show OI 8446 Å lines in emission. We have looked for the correlation of the EW of these line profiles with $(H-K_s)_0$, which is indicative of near-IR excess. The e-stars which were found to belong to HAeBe category are shown as solid circles while all the other e-stars are shown in open circles. We have used line profiles which have good signal and unblended for this correlation studies. The EW of CaII 8498 Å profile is found to be correlated with $(H-K_s)_0$ for the surveyed e-stars (figure 5.2(a)). The e-stars NGC 6823(1) and NGC 7380(4) seem to move away from the total candidate stars, with former showing a low EW of -0.64 Å while latter having a strong emission of -32 Å. We have not deblended the contribution of Paschen line from CaII line while measuring the EW. The EW of P14 line seems to show a sparse correlation with $(H-K_s)_0$ (figure 5.2(b)).

Of the 5 classified HAeBe candidate stars, 4 stars seem to be away from the general trend. Bochum 6(1) is found to have P14 EW of -5.7 Å, which is the highest among the group of surveyed stars. Since the correlation of Paschen lines

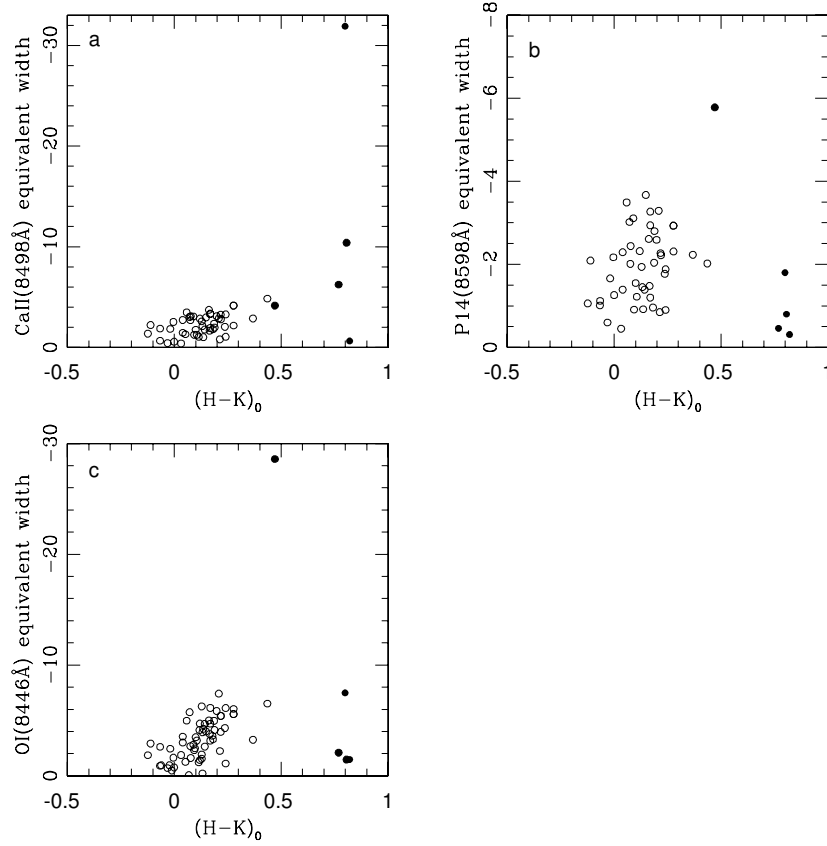


Figure 5.2: A plot of $(H-K_s)_0$ vs EW of CaII (a), P14 (b) and OI (c) are shown. The e-stars which were found to belong to HAeBe category are shown as solid circles while all the other e-stars are shown as open circles.

with $(H-K_s)_0$ is sparse, correlation observed here can be assumed to be mainly due to CaII line. The Be stars which have Paschen emission lines do not have near-IR excess when compared to other Be stars, which does not support the results by Briot (1981). Our results seems to be statistically sound compared to 15 stars used in their analysis.

All the 5 classified HAeBe stars are found to be well separated from the group of surveyed e-stars in the plot between OI 8446 Å and near-IR colour $(H-K_s)_0$ (figure 5.2(c)). The star Bochum 6(1) is found to have the highest value of OI

Table 5.1: Photometric parameters of identified HAeBe stars

HAeBe star	U mag	B mag	V mag	J mag	H mag	K_s mag	Sp. type	Age Myr
Bochum 6(1)	13.880	13.890	13.300	11.330	10.832	10.223	B6	0.5
IC 1590(1)	13.620	13.820	13.430	12.214	11.638	10.807	B8.5	2
IC 1590(2)	14.200	14.250	13.950	12.493	11.620	10.752	A0	3
NGC 6823(1)	*	14.390	13.730	11.556	10.530	9.546	B6.5	0.5–1
NGC 7380(4)	16.780	16.270	14.720	10.797	9.763	8.847	A1	≤ 0.25

EW (-28.6 \AA) among the surveyed stars. This plot correlates well with H_α EW versus $(H-K_s)_0$ colour distribution of e-stars. Hence this plot can also be used as a criteria to differentiate CBe stars from HAeBe stars.

5.4 HAeBe stars as members of parent clusters

In this section we put up all the evidences (optical CMD with PMS isochrones fitted, near-IR CCDm and optical spectra) along with SED to test the above classification.

Previous studies about the cluster have been included to understand the cluster environment and the cluster parameters used for deducing the stellar parameters. Hence in the following subsections we also describe the star formation scenario in the parent clusters with which these e-stars are associated. For the clusters Bochum 6, IC 1590, NGC 6823 & NGC 7380 optical and near-IR data are combined to detect the PMS candidates. This also helps to check whether the star formation process in the cluster is continuous or due to a single burst. The coordinates, photometric magnitudes (U, B, V, J, H, K_s), age and distance estimated for the e-stars treating them as members of corresponding clusters are given in table

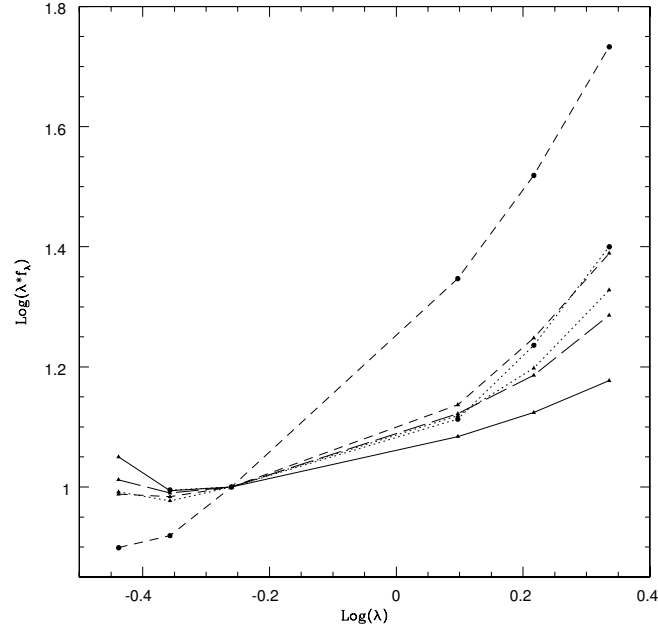


Figure 5.3: The Spectral Energy Distribution for e-stars IC 1590(3) (bold-line + triangle), IC 1590(1) (dot line + triangle), IC 1590(2) (short-dash + triangle), Bochum 6(1) (long-dash + triangle), NGC 6823(1) (dot-line + circle) and NGC 7380(4) (short-dash + circle) are shown. The CBe star IC 1590(3) is shown as reference.

5.1. Of the 4 clusters described here as hosting e-stars, Bochum 6, NGC 6823 and NGC 7380 are found to have single e-star. The open cluster IC 1590 is found to have a CBe, HAe and HBe candidate each. The combined SED of all the e-stars is shown in figure 5.3. A detailed list of the spectral lines is tabulated in table 5.2.

5.4.1 Bochum 6

The open cluster Bochum 6 ($RA = 07^h 32^m 00^s$, $Dec = -19^{\circ} 25'$, $l = 234^{\circ}.745$, $b = -0^{\circ}.218$) was observed by Moffat and Vogt (1975) for the first time and concluded that this is a group of 5 OB stars. They estimated a reddening value of 0.70 mag and distance of 4 kpc from photoelectric observations. They suggested that the cluster appears to coincide with the HII region S309, whose photometric distance

and kinematic distances are 6.30 kpc and 2.24 ± 0.36 kpc respectively.

Table 5.2: Spectral lines identified in HAeBe stars

HAeBe star	H $_{\alpha}$ EW in Å	H $_{\beta}$ EW in Å	OI 8446 EW	CaII 8498 EW	Special lines
Bochum 6(1)	-206	-16.28	-28.6	-4.16	[FeII] (4287, 4358, 4413 and 5159 Å) in emission, SiII 6347 Å & 6371 Å in absorption
IC 1590(1)	-44.12	-1.38	-2.09	-6.24	FeII lines (4549, 4584, 4924, 5018, 5169, 5235, 5276, 5316, 5363 Å) in emission
IC 1590(2)	-31.70	-1.31	-1.46	-10.4	H $_{\alpha}$ & FeII(5018) P-Cygni profile
NGC 6823(1)	-35.38	-2.66	-1.47	-0.64	HeI in emission
NGC 7380(4)	-85.29	-14.10	-7.48	-32	NaI, KI, NII(5530, 5535 Å) in emission

From deep UBVRI CCD photometry, Yadav and Sagar (2003) determined an $E(B-V)$ of 0.71 ± 0.13 and distance of 2.5 ± 0.4 kpc. They estimated an age of 10 ± 5 Myr by fitting Schaller et al. (1992) isochrones of Solar metallicity. We have identified a peculiar e-star, Bochum 6(1), in this cluster from our survey. The e-star corresponds to star 2143 in Yadav and Sagar (2003) and is found to be of B6 spectral type.

We have taken UBVR CCD photometric data of 1459 stars from Yadav and Sagar (2003) which were cross correlated with 2MASS photometric data. Thus 146

stars were found to have UBV CCD and JHK_s magnitudes. After de-reddening the $(J-H)$ and $(H-K_s)$ colors using $E(B-V) = 0.71$ (Yadav and Sagar, 2003), near-IR CCDm is plotted as shown in figure 5.4(a). There are 20 stars (including e-star) located below the reddening vector, of which 2 stars occupy same location in near-IR CCDm. The e-star is highly reddened in near-IR CCDm and found to be located inside the HAeBe location. There is also nebulosity associated with this e-star. The SED (figure 5.3) shows a sharp rise in J, H, K_s magnitudes due to near-IR excess. This is due to the circumstellar dust around this candidate HBe star.

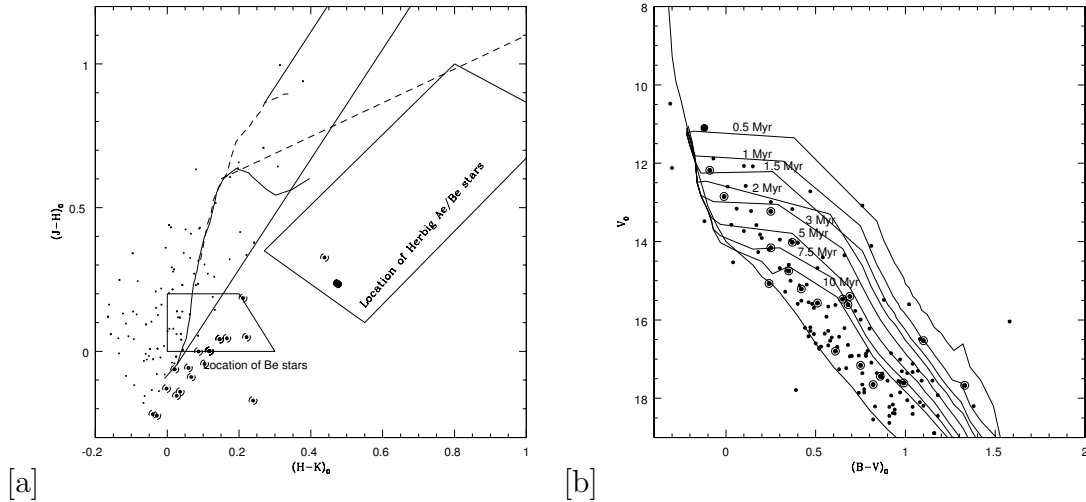


Figure 5.4: (a) Near-IR CCDm of Bochum 6. The normal stars in cluster are shown as small circles. Encircled ones are candidate PMS stars and filled circle represents e-star. (b) Optical CMD of Bochum 6. PMS isochrones of ages 0.5–10 Myr are plotted. The e-star is found to occupy 0.5 Myr isochrone.

For the identified stars, optical CMD is plotted (figure 5.4(b)) after reddening correction. ZAMS is fitted for a DM of 12.5 (corresponding to a distance of 3.16 kpc). Yadav and Sagar (2003) estimated the distance as 2.5 ± 0.5 kpc. The PMS stars are found to be located in all the 1 to 10 Myr isochrones giving the cluster an age range of more than 10 Myr. The e-star is located near the MS. Yadav and Sagar (2003) found an age of 10 ± 5 Myr for Bochum 6, in which case both high

mass and low mass stars have formed together. Their studies did not consider stars fainter than $V = 14.5$ as cluster members. They assumed that the probability of forming the faint stars are negligible in OB associations. In our study we include stars up to a limit of 19 magnitude and low mass stars are also taken into account. The candidate PMS stars are located along the boundary of the cluster (figure 5.5(a)). The PMS stars are located in a ring like structure and none are located near the cluster center. The HBe star is also located in the ring-like structure. We do not find any evidence of any significant clustering around this star.

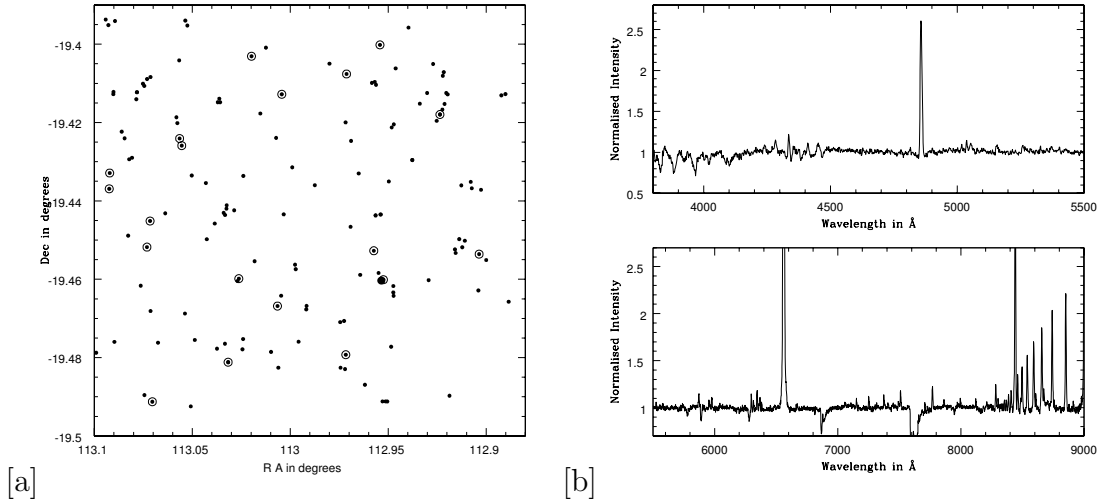


Figure 5.5: (a) Location of PMS stars and e-stars are shown in the field of Bochum 6. (b) The spectra of the e-star Bochum 6(1) in the wavelength range 3800 – 9000 Å.

This HBe star, Bochum 6(1) is peculiar due to the presence of intense Balmer lines with H_α EW of -206 \AA and H_β EW of -16.28 \AA along with OI 8446 Å line having a line width of -28.6 \AA (figure 5.5(b)). The unusually high value of H_α EW (which is quite high compared to the mean H_α EW of -40 \AA for surveyed stars) might be having contribution from the HII region S 309. The spectra of Bochum 6(1) shows 5 FeII lines in emission while SiII lines 6347 Å and 6371 Å are seen in absorption. It also shows 4 forbidden FeII ([FeII]) lines (4287, 4358, 4413 and 5159 Å) in emission, which corresponds to B[e] star. Hence from photometric and spec-

troscopic analysis it is deduced that Bochum 6(1) could be a HBe star in B[e] phase.

5.4.2 IC 1590

The young cluster IC 1590 ($l = 123^{\circ}.1, b = -6^{\circ}.2$) contains a group of stars clustered about the O-type trapezium system HD 5005 (Sharpless, 1954; Abt, 1986). The cluster is embedded in the nebulosity of NGC 281, which is also an HII region, Sharpless 184, of diameter 20 arc minutes. The HII region is surrounded by an extensive HI cloud which contains several dark Bok globules. The HII region seems to be associated with two CO molecular clouds NGC 281A and NGC 281B which were mapped in CO¹² and CO¹³ by Elmegreen and Lada (1978). Guetter and Turner (1997) used photoelectric and CCD photometry for 279 stars in the cluster region and estimated a distance of 2.94 ± 0.15 kpc. They estimated an age of 3.5 Myr using 63 identified probable members of the cluster with not much evidence for age spread. The cluster appears to have a high R_v value of 3.44. A value of -1.00 ± 0.21 is estimated for the initial mass function from the luminosity function of the cluster members. The e-stars are numbered as 215, 151 and 214 in Guetter and Turner (1997) while it is given in order 1, 2, 3 in this work. The star 214 is of B2 spectral type while the stars 215 and 151 are found to be of B8.5 and A0 respectively. We found nebulosity associated with stars 1 and 2.

The UB_v values and coordinates (B1950 coordinates) of 246 stars were taken from Guetter and Turner (1997). These were matched with 2MASS database and for 56 stars both JHK_s and UB_v magnitudes were found. After de-reddening the (J–H) and (H–K_s) colors using mean cluster reddening value, $E(B–V) = 0.37$ (Guetter and Turner, 1997), near-IR CCDm is plotted. In the near-IR CCDm, 12 stars were found to be located below the reddening vector of which 2 occupy the same position. They are considered to be candidate PMS stars, as shown in figure

5.6(a). Out of 3 e-stars, stars numbered 1 and 2 are located inside the HAeBe location and the star 3 is located inside the CBe star location.

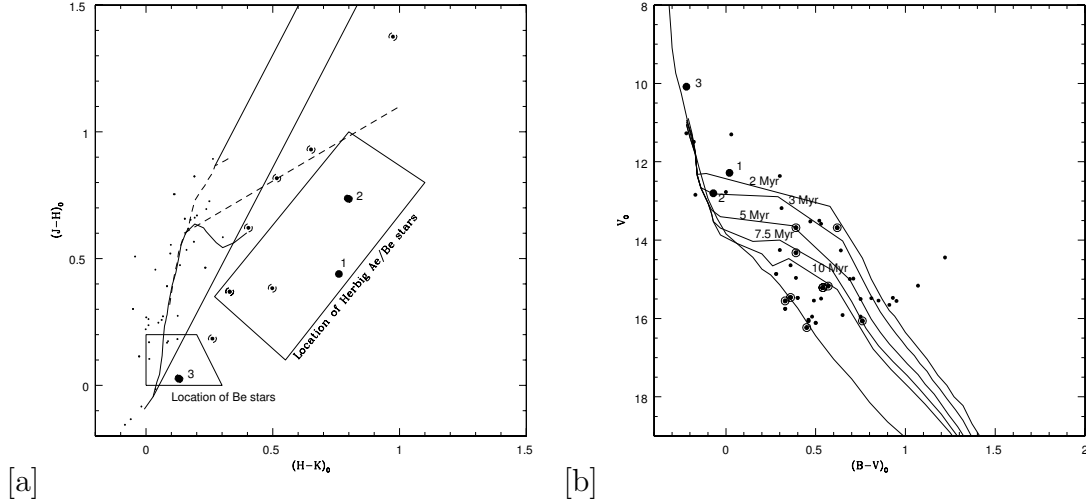


Figure 5.6: (a) The near-IR CCDm of the cluster IC 1590 is shown with PMS candidates as encircled symbols and e-stars as filled circles. (b) Optical CMD of IC 1590. PMS isochrones of ages 2–10 Myr are plotted. IC 1590-1 and IC 1590-2 occupy 2 Myr and 3 Myr PMS isochrones respectively.

In the optical CMD (figure 5.6(b)), ZAMS is fitted for a DM of 12.34. PMS isochrones of ages 2–10 Myr are plotted. It can be seen that all the candidate PMS stars are located in the 2–10 Myr isochrones, suggesting that star formation is a continuous process in the cluster. There are low mass members in the cluster which are older than the estimated age 3.5 ± 0.2 Myr (Guetter and Turner, 1997). The e-stars 1 and 2 are located along 2 and 3 Myr isochrones respectively, while e-star 3 is located along the main sequence track. By looking into the position of these e-stars, we can assume that stars 1 and 2 are of HAeBe nature and star 3 is a CBe star. In the cluster field all the e-stars are found to be located close to the center, as shown in figure 5.7(a). No significant clustering is found near the HAeBe stars. The cluster seems to have formed stars for a duration of at least 8 Myr.

All the Balmer lines except H_α and H_β are found in absorption/filled-in for the e-stars IC 1590(1), IC 1590(2) and IC 1590(3) (figure 5.7(b)). The emission profile of H_α shows P-Cygni nature for star 2 and double-peak for star 3 while it is normal single peak profile for star 1. The P-Cygni profile indicates that the H_α line might be formed in wind/outflow, which is characteristic of HAeBe stars. The double-peak H_α profile is usually indicative of the CBe star. H_β is found to have an asymmetric emission in absorption profile for stars 1 and 2 while it is in absorption for 3.

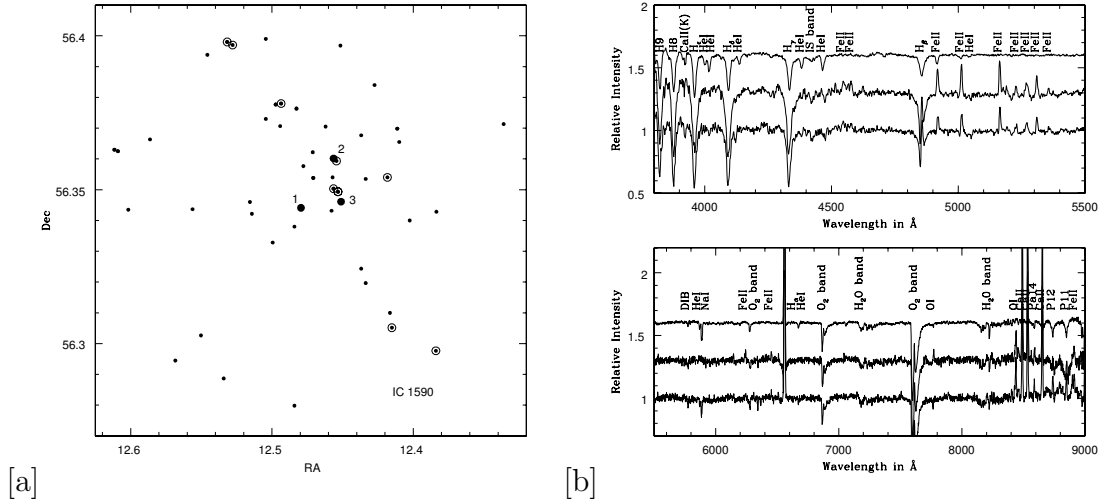


Figure 5.7: (a) Location of PMS stars and e-stars are shown in the field of IC 1590. (b) The spectra of e-stars IC 1590(1), IC 1590(2) and IC 1590(3), in the wavelength range 3800 – 9000 Å, is given from bottom to top.

As seen in figure 5.7(b), quite a number of FeII lines (4549, 4584, 4924, 5018, 5169, 5235, 5276, 5316, 5363 Å) are found in emission for the stars 1 and 2 while no such feature is seen for star 3. The 5018 Å FeII profile is found to show P-Cygni feature for stars 1 and 2, which is a signature of wind/outflow associated with the star. In the red region of the spectrum, CaII triplet is found in emission along with the Paschen lines (8467 (P17), 8598 (P14), 8750 (P12), 8862 (P11)) for stars 1 and 2 while they are found to be in absorption for star 3. The helium lines (4026, 4471,

5876, 6678, 7065 Å) are found to be visibly present in star 3 which matches with early spectral type estimated for the star from photometry. OI 8446 Å line shows intense emission for stars 1 and 2 while it is absent in 3. Hence the spectral line features confirms our prediction from optical and near-IR photometry that stars 1 and 2 are PMS HAeBe stars. To support our argument we have shown the SED for the e-stars in figure 5.3. It can be seen that the distribution shows a rising trend in H and K_s bands for stars 1 and 2, when compared to star 3.

5.4.3 NGC 6823

The cluster NGC 6823 is of Trumpler class IV3p, $RA = 19^h43^m09^s$, $Dec = +23^{\circ}18'$, $l = 59^{\circ}.402$, $b = -0^{\circ}.144$, surrounded by the reflection nebula NGC 6820. This cluster is associated with Vul OB1 association and this complex is similar to the star formation complex in Orion. The cluster contains O and early B-type stars and is situated in an HII region with several Bok globules. Stone (1988) divided the cluster into a central trapezium system, a nucleus of radius in between 0.6 to 3.5 arcmin and a corona of radius greater than 3.5 arcmin using Kholopov's criteria (Kholopov, 1969). From UBV photometric study Stone (1988) found that the luminosity function for the stars in the inner region is similar to initial luminosity function while the outer region appears to have an excess of bright cluster stars. Many of the stars in the outer region are found to be PMS objects. Guetter (1992) used CCD UBV photometry to observe the nuclear region and photoelectric photometry to study the coronal region of the cluster. He estimated a distance of 2.1 ± 0.1 kpc and age in the range 2–11 Myr. The trapezium stars are found to be younger compared to coronal stars with nuclear objects falling in between.

UBV CCD values of 440 stars were taken from Massey et al. (1995). After cross correlation with 2MASS values, only 253 stars were identified to have UBV

and JHK_s magnitudes. $(J-H)$ and $(H-K_s)$ colors were de-reddened using mean cluster reddening value 0.89 (Massey et al., 1995) and the resulting near-IR CCDm is plotted (figure 5.8(a)). 27 stars are taken as candidate PMS stars since they are located below the reddening vector. The e-star is considerably reddened (around 1 magnitude) as shown in the near-IR CCDm and hence can be considered as a candidate HBe star.

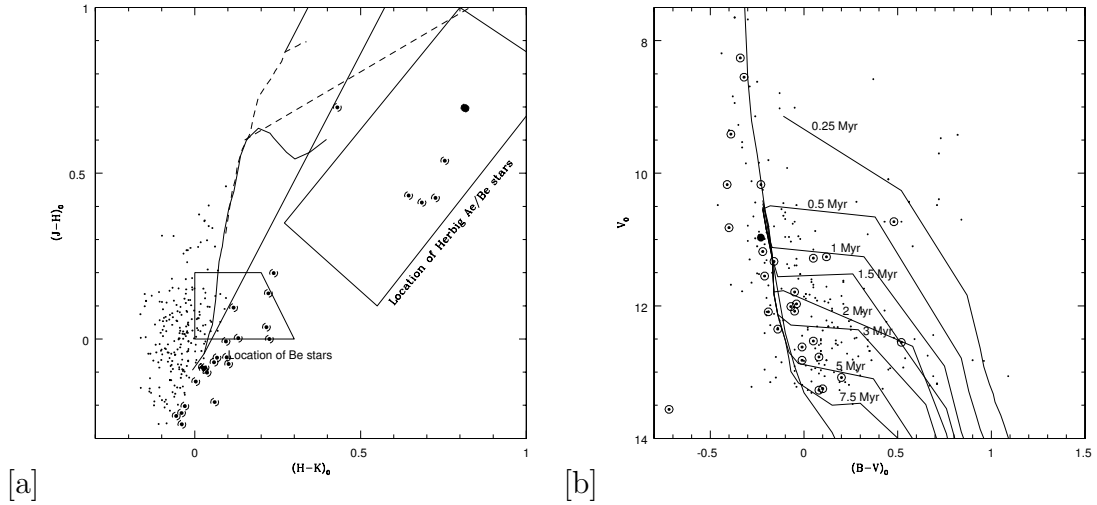


Figure 5.8: (a) The near-IR CCDm of the cluster NGC 6823 is shown in figure with e-stars shown as filled triangles. (b) Optical CMD of NGC 6823. PMS isochrones of ages 0.25–7.5 Myr are plotted. The e-star is found to lie between 0.5 and 1 Myr isochrone.

In the CMD (shown in figure 5.8(b)), ZAMS is fitted for a DM of 11.81 (Massey et al., 1995). Most of the candidate PMS stars are located in the isochrones of ages 0.25 to 7.5 Myr. Massey et al. (1995) suggested that there is age spread of 5 Myr in this cluster. The number of PMS stars are more in the center of the cluster, suggesting an ongoing star formation (figure 5.9(a)). The UBV CCD photometric data for e-star, NGC 6823(1), is taken from Guetter (1992) and it is found to be of B6.5 spectral type. The cluster sequence is not clearly defined even though we have used the best available CCD data. Eventhough the e-star looks like on the main sequence, a redefined sequence through the bluer stars shows the star to be

in PMS phase. From PMS isochrone fitting the age of the star is found to be in between 0.5 and 1 Myr. Even though no clear nebulosity is found around e-star, the cluster is associated with HII regions and star forming regions. The e-star is located close to the cluster center, as can be seen from figure 5.9(a). Again, the duration of star formation in this cluster is at least 10 Myr.

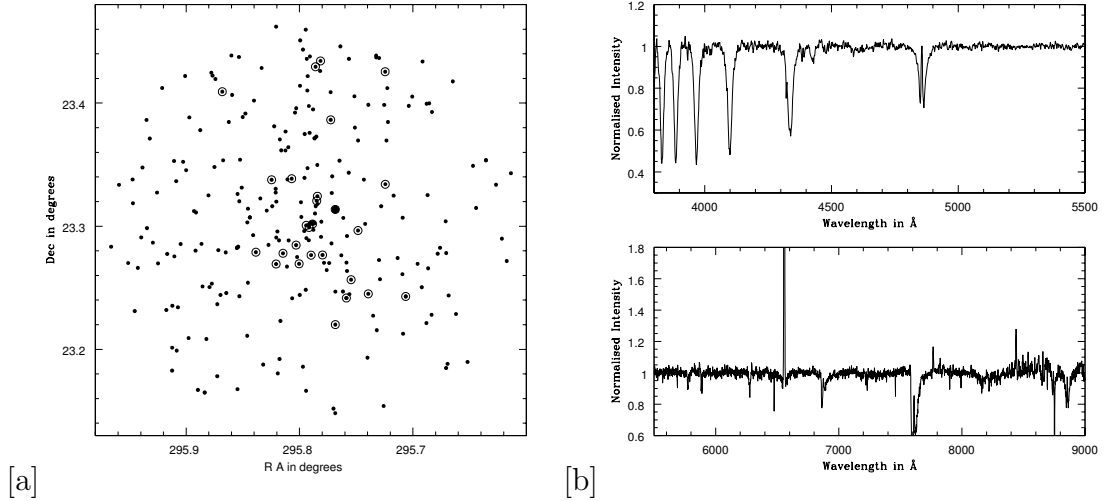


Figure 5.9: (a) Location of PMS stars and e-stars are shown in the field of NGC 6823. (b) The spectra of the e-star NGC 6823(1) in the wavelength range 3800 – 9000 Å.

The spectrum of NGC 6823(1) is interesting due to the presence of neutral helium (HeI) lines in emission. The HeI lines 4026, 4388 and 4471 Å show emission in absorption profiles while 5876 Å shows emission above the continuum, which is indicative of HBe stars. The higher order Balmer lines are seen in absorption, H_{β} has emission in absorption profile while H_{α} shows emission (figure 5.9(b)). Both the OI lines 7772 Å and 8446 Å are in emission along with CaII triplet lines. All the major Paschen lines like P11, P12, P14, P17, P19 are in emission. The SED (figure 5.3) shows a rising trend in J, H, K_s magnitudes which is indicative of circumstellar dust in HBe stars. Hence the e-star is likely to belong to HBe category.

5.4.4 NGC 7380

Moffat (1971) studied the cluster NGC 7380 ($RA = 22^h 47^m 21^s$, $Dec = 58^\circ 07' 54''$, $l = 107^\circ.141$, $b = -0^\circ.884$) using photographic UBV photometry down to $V \sim 16$ mag, and found a distance of 3.6 ± 0.7 kpc and an age of 2 Myr. He found a deficit of faint stars in the central region ($r \leq 3'$) and two dust shells at central radius $r = 6.5'$ and $r = 10.4'$. Massey et al. (1995) have estimated a distance of 3732 pc and an average $E(B-V)$ of 0.64 ± 0.03 from spectroscopy.

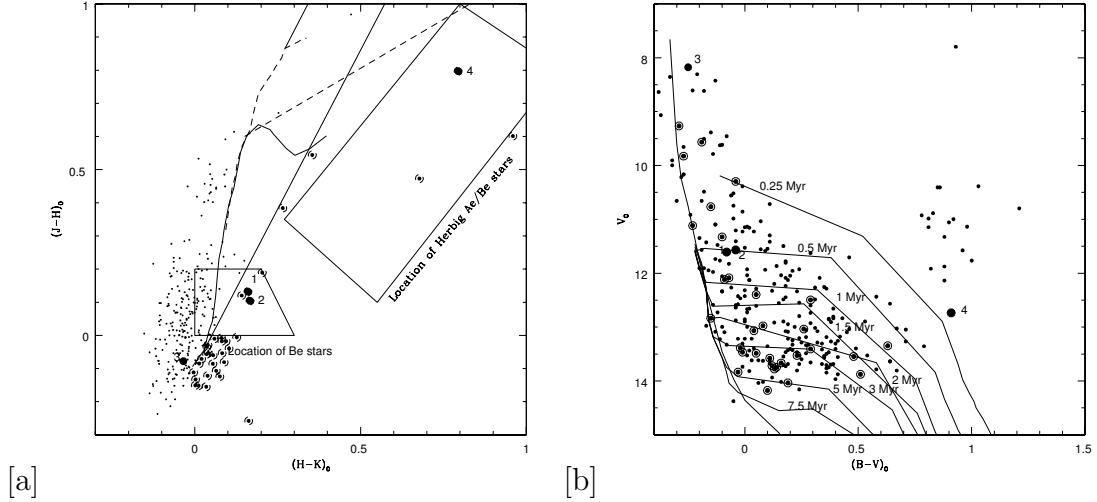


Figure 5.10: (a) The near-IR CCDm of the cluster NGC 7380 is shown with e-stars as filled circles and PMS as encircled symbols. (b) Optical CMD of NGC 7380. PMS isochrones of ages 0.25–7.5 Myr are plotted. The star NGC 7380(4) seems to be young than 0.25 Myr since it is found to lie beyond 0.25 Myr isochrone.

From our survey we found the stars numbered 1130, 55, 4 and 2249, as given in Massey et al. (1995), are found to show emission. The spectral types of the 4 e-stars has been estimated to be B9, B9, B0.5V and A1 respectively. The photometric UBV CCD values of 893 stars, taken from Massey et al. (1995), were cross correlated with 2MASS values and 277 stars were identified as having both UBV and JHK_s magnitudes. The near-IR colours are de-reddened using the mean cluster reddening value of 0.64 (Massey et al., 1995) and near-IR CCDm is plotted as

shown in figure 5.10(a). We identified 34 stars in PMS category from their location in the near-IR CCDm. The e-stars 1 and 2 are located inside the CBe location while 3 is below and star 4 is in HAeBe location (reddened by about 1 mag). The stars 1, 3 and 4 are found to be associated with nebulosity.

In the optical CMD, ZAMS is fitted for a DM of 12.86 (Massey et al., 1995). Massey et al. (1995) determined the age of the cluster as 2 Myr taking massive stars (above $25 M_{\odot}$) only. Our study shows that there are low mass stars having the age range 0.25 to 10 Myr (figure 5.10(b)). The e-stars 1 and 2 are located on the 0.5 Myr isochrone and star 3 is located at the top of MS. The star 4 is fitted with ≤ 0.25 Myr PMS isochrone and it is found to be located away from other e-stars (figure 5.10(b)). In the cluster field, the e-stars 1, 2 and 3 are located close to the center (figure 5.11(a)).

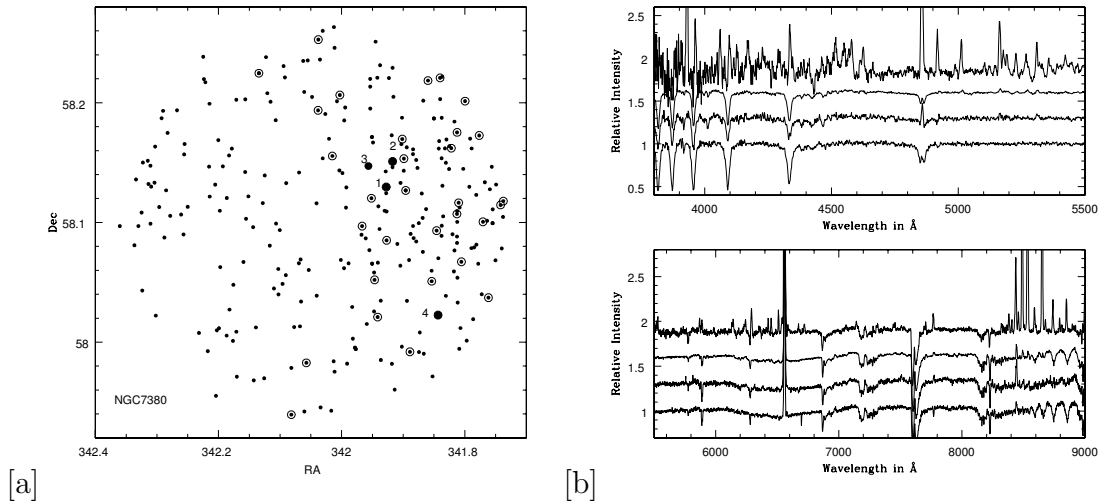


Figure 5.11: (a) Location of PMS stars and e-stars are shown in the field of NGC 7380. (b) The spectra of the e-stars NGC 7380(1), NGC 7380(2), NGC 7380(3) and NGC 7380(4), in the wavelength range 3800 – 9000 Å, is given from bottom to top.

Most of the PMS candidates are found to be crowded around the e-stars suggesting it to be an active star forming region. The PMS stars are located in a

crescent like structure on the western side of the cluster. Also, the PMS stars are beyond a radius of about 6 arcmin, which coincides with the location of the inner dust shell. Thus, recent star formation has taken place in the western region, which coincides with the location of the dust shells. The duration of star formation estimated for this cluster is also 10 Myr.

The spectra of e-stars are shown in figure 5.11(b) in the wavelength range 3800 – 9000 Å. The spectrum of star 4 is special among the list of surveyed stars due to the presence of NaI (5890, 5896 Å), KI (7699 Å) and NII (5530, 5535 Å) lines in emission. The OI lines 7772 Å and 8446 Å are seen in emission along with CaII triplet and Paschen lines P11, P12, P14, P17 and P19. The CaII triplet lines are strongest among the surveyed e-stars with 8498 Å line showing an EW of -32 Å. About 21 FeII lines are seen in emission. From SED (figure 5.3) we can see that the flux of the e-star NGC 7380(4) is rising in the near-IR region which seems to confirm that it belongs to HAe category.

5.5 Conclusion

- From the photometric and spectroscopic estimates we conclude that out of 157 surveyed e-stars 3 are probably HBe candidates while 2 are HAe candidates. The correlation between H_α EW and $(H-K_s)_0$ colour was used to classify HAeBe stars from CBe stars. The e-stars are found to show a linear correlation in H_α EW and $(H-K_s)_0$ colour with a clear offset between both classes. This striking correlation emphasises the role of dusty regions in the production of H_α radiation by recombination process. The correlation between OI 8446 Å line and near-IR colour $(H-K_s)_0$ is also found to distinguish CBe from HAeBe stars. Even though the colour excess $E(V-K_s)$ is found to correlate well with H_α EW, it cannot be effectively used as a criterion to

classify CBe stars from HAeBe stars.

- Bochum 6(1) is quite unusual among our surveyed stars due to the presence of intense spectral lines. The presence of HII region S309 might be contributing to the high value of H_{α} EW, which is -206 \AA . The e-star is found to be in HBe location in near-IR CCDm, which along with SED proves the presence of dusty circumstellar disk. Hence Bochum 6(1) is found to be a HBe star in a shell phase, which is inferred from the presence of forbidden FeII lines. Eventhough the turn-off age of the cluster is found to be 10 Myr, we found 20 PMS stars in age range 1 to 10 Myr in the cluster. The candidate PMS stars are located along the boundary of the cluster.
- We found that IC 1590(1) and IC 1590(2) belong to HBe and HAe respectively from optical & near-IR photometry, spectroscopy and SED. This is one of the rare young clusters (~ 4 Myr) in which HAeBe stars coexist with CBe candidate. The age of star 1 is found to be 2 Myr while that of star 2 is 3 Myr from PMS isochrone fitting. We identified 12 PMS candidates in the cluster, which are found to have an ages in the range 2–10 Myr. The e-stars are located close to the cluster center with few PMS candidates, suggesting active star formation. The active star formation is reflected by the presence of HII region, molecular clouds and the presence of trapezium system like the Orion.
- NGC 6823(1) is found to be a 6.3 Myr HBe star, reddened by 1 magnitude in near-IR CCDm and the spectra with helium lines either in emission or as shell feature. We have found 27 PMS stars in NGC 6823, in the age range 0.25–10 Myr, of which most are close to the cluster center, suggesting an ongoing star formation.
- NGC 7380(4) is a stand-alone candidate among the surveyed stars with NaI (5890, 5896 \AA), KI (7699 \AA) and NII (5530, 5535 \AA) lines in emission apart

from OI, CaII triplet, Balmer and Paschen lines. The star is found to be a HAe candidate with a near-IR excess of around 1 magnitude and excess flux in K_s band in SED. The star is associated with nebulosity and the location of the star in optical CMD indicates a very young age (≤ 0.25 Myr). We have identified 34 PMS stars, in NGC 7380, in the age range 0.25 – 10 Myr, which are distributed around 3 e-stars. This is indicative of the star formation occurring in the cluster, in a crescent like region located to the west of the cluster center.

- The duration of star formation was found to be about 10 Myr in all the 4 clusters, which host the identified HAeBe stars.

Chapter 6

Summary & Future Plans

6.1 Summary

In Chapter 1, we have given an introduction to the properties of CBe stars and briefly describe the studies done so far in optical, infra-red, ultraviolet, X-ray and γ -ray wavelength bands. A sneak preview of the mechanism of Be phenomenon is given and the developments in theoretical and observational fronts to tackle the problem is also addressed. The competing model in the theoretical front is magnetically torqued wind disk. Observers have detected magnetic field of considerable magnitude ($\sim 40\text{--}150$ G) in a few Be stars, which supports the formation of disk through the above mentioned model. Non-radial pulsations have been observed in a few stars like μ Cen, ω CMa etc. which can explain the short-term variability in CBe stars. But the open question is the reason for periodic outburst and whether polar wind can assist the production of circumstellar disk in CBe stars.

To address Be phenomenon we performed a survey to search for Be stars in young open clusters. Open clusters are ideal place to look for Be stars since they constitute a dynamically associated system of stars which are coeval, located at the same distance and have the same chemical composition. The e-stars are identified through slitless spectroscopy, which is a technique devised by us, using HFOSC at HCT. Using this method, the H_α emission above the continuum is identified from the dispersed image, which is cross-matched with the R band image to identify the

e-star. The details of the survey with the clusters which were found to harbour e-stars are given in Chapter 2. We have addressed each cluster individually to understand Be star parameters like age, distance and the role of MS evolution in the formation of Be stars. We have constructed optical CMD from the references mentioned, with the data taken from WEBDA. This has been combined with near-IR CCDm to understand the evolutionary nature of Be stars. The slit spectra of the identified candidate Be stars are obtained in the wavelength range 3700–9000 Å, which are presented for each cluster.

A comprehensive analysis of the surveyed stars is presented in Chapter 3. Emission-line stars in young open clusters are identified to study their properties, as a function of age, spectral type and evolutionary state. 207 open star clusters were observed using slitless spectroscopy and 157 e-stars were identified in 42 clusters. We have found 54 new e-stars in 24 open clusters, out of which 19 clusters are found to house e-stars for the first time. About 22% clusters harbour e-stars. The fraction of clusters housing e-stars is maximum in both the 0–10 and 20–30 Myr age bin ($\sim 40\%$ each). Most of the e-stars in our survey belong to CBe class ($\sim 92\%$) while a few are HBe ($\sim 6\%$) and HAe ($\sim 2\%$). The youngest clusters to have CBe stars are IC 1590, NGC 637 and NGC 1624 (all 4 Myr old) while NGC 6756 (125–150 Myr) is the oldest cluster to have CBe stars. The CBe stars are located all along the MS in the optical CMD of clusters of all ages, which indicates that the Be phenomenon is unlikely only due to core contraction near the turn-off. The distribution of CBe stars as a function of spectral type shows peaks at B1–B2 and B6–B7 spectral types. The Be star fraction ($N(\text{Be})/N(\text{B}+\text{Be})$) is found to be less than 10% for most of the clusters and NGC 2345 is found to have the largest fraction ($\sim 26\%$). Our results indicate there could be two mechanisms responsible for the Be phenomenon. Some are born CBe stars (fast rotators), as indicated by their presence in clusters younger than 10 Myr. Some stars evolve to CBe stars, within the MS lifetime, as indicated by the enhancement in the fraction

of clusters with CBe stars in the 20–30 Myr age bin.

The spectroscopic study of 157 candidate Be stars in 42 young open clusters was performed using medium resolution spectra in 3700–9000 Å range, which was described in Chapter 4. Apart from the Balmer lines in emission, spectra of most of the stars show FeII, Paschen and OI lines in emission while HeI is seen in absorption. About 86% of the surveyed emission stars show FeII lines in their spectra. We found Lyman β fluorescence as the mechanism for the production of OI 8446 Å line in 24% of the surveyed stars, while collisional excitation is the likely excitation mechanism for OI 8446 Å and 7772 Å lines found in 47% of the stars, suggesting a denser disk. The Balmer decrement is found to have a bimodal distribution which is correlated with the nature of H_β profile. Candidates with higher D_{34} (76%) were found to have more number of spectral lines, higher H_α equivalent width and $(H-K)_0$ values, suggesting an optically and geometrically thick disk. Massive Be stars of spectral type B0–B4 are found to have enhanced H_α emission at the end of their main sequence lifetime, as inferred from the enhancements observed at 12.5 and 25 Myr. The average emission region for H_α profile is found to be around 15 stellar radii, with a range of 7–30 stellar radii, assuming the circumstellar disk to be Keplerian. The rotation velocity of candidate stars is found to be in the range 150–300 km/s, which matches with that of field CBe stars. The rotation velocity of the disks were found to be in the range of 50–250 km/s. Thus the circumstellar disk is found to lag behind the star by 50–100 km/s. The angular momentum evolution of stars and their disk as a function of age and spectral type suggest a bimodal origin of Be stars. Stars in the B0–B2 spectral bin are found to be spun up towards the end of their MS life time, suggesting that early type stars evolve to become Be stars. Similar variation in properties were not found for stars in the later spectral types (B4–A0), suggesting that the Be phenomenon differs in early type and late type stars.

We have described the techniques used to identify most probable HAeBe candidates, among the surveyed Be stars, in Chapter 5. We found 5 HAeBe stars from a sample of 157 stars in 42 clusters. From optical/near-IR photometry and spectroscopy it is likely that Bochum 6(1), IC 1590(1) and NGC 6823(1) are HBe while IC 1590(2) and NGC 7380(4) are HAe candidates. Bochum 6(1) is an interesting HB[e] star with intense spectral lines and a high H_α EW of -206 \AA , which is the highest among surveyed stars. The HAeBe stars are found to show a linear correlation in H_α EW versus $(H-K_s)_0$ colour plot, with a clear offset from the distribution of CBe stars. The candidates are found to show near-IR excess which was revealed through near-IR CCDm and SED. An effort has been done to understand the star formation in the clusters which harbour HAeBe stars (Bochum 6, IC 1590, NGC 6823 and NGC 7380). We found ongoing star formation in all these clusters, with an appreciable number of PMS stars. The age of these candidates were estimated by PMS isochrone fitting in the optical CMD. Among the surveyed clusters, IC 1590 is a young cluster (~ 4 Myr) with 3 e-stars, each belonging to HAe, HBe and CBe types respectively.

6.2 Impact of this work

The survey and analysis presented here is first of its kind to understand Be phenomenon in CBe stars in open clusters. Our sample of 152 CBe stars was combined with the dataset of CBe stars in southern clusters (McSwain and Gies, 2005b) to get a complete picture of the formation and evolution of CBe stars in Galaxy (Martayan et al., 2009b). The method of slitless spectra to identify CBe stars was used by Martayan et al. (2009a), to study CBe stars in the SMC clusters.

6.3 Future Plans

- We plan to estimate accurate stellar parameters of Be stars by generating a grid of synthetic spectra and comparing them with the observed spectra.
- To address the role of companion in the formation of Be stars, we have launched a program to identify binary companions of some bright field Be stars using high spectral resolution facility in Vainu Bappu Telescope (VBT), Kavalur. The time-series analysis of the spectra provides an estimate about the period which in-turn can be phased to obtain the nature of the companion. Our cluster candidates are not bright enough to be included in this program. Hence we have used selected candidates from the catalogue of Jaschek and Egret (1982).
- To understand the role of cluster environment in Be phenomenon we have taken the spectra of 118 field CBe stars from the catalogue of Jaschek and Egret (1982). The spectra were taken using the similar setup used for cluster CBe star studies. This in-turn will be combined with high resolution spectra to understand rotation velocity distribution and angular momentum evolution in the system.
- To confirm the higher D_{34} values using near-IR spectra of field CBe stars.

Bibliography

- H. A. Abt. The occurrence of abnormal stars in open clusters. , 230:485–496, June 1979.
- H. A. Abt. The ages and dimensions of Trapezium systems. , 304:688–694, May 1986.
- F. Aharonian, A. G. Akhperjanian, K.-M. Aye, A. R. Bazer-Bachi, M. Beilicke, W. Benbow, D. Berge, P. Berghaus, K. Bernlöhr, C. Boisson, O. Bolz, I. Braun, F. Breitling, A. M. Brown, J. Bussons Gordo, P. M. Chadwick, L.-M. Chounet, R. Cornils, L. Costamante, B. Degrange, A. Djannati-Ataï, L. O’C. Drury, G. Dubus, D. Emmanoulopoulos, P. Espigat, F. Feinstein, P. Fleury, G. Fontaine, Y. Fuchs, S. Funk, Y. A. Gallant, B. Giebels, S. Gillessen, J. F. Glicenstein, P. Goret, C. Hadjichristidis, M. Hauser, G. Heinzlmann, G. Henri, G. Hermann, J. A. Hinton, W. Hofmann, M. Holleran, D. Horns, O. C. de Jager, S. Johnston, B. Khélifi, J. G. Kirk, N. Komin, A. Konopelko, I. J. Latham, R. Le Gallou, A. Lemièrre, M. Lemoine-Goumard, N. Leroy, O. Martineau-Huynh, T. Lohse, A. Marcowith, C. Masterson, T. J. L. McComb, M. de Naurois, S. J. Nolan, A. Noutsos, K. J. Orford, J. L. Osborne, M. Ouchrif, M. Panter, G. Pelletier, S. Pita, G. Pühlhofer, M. Punch, B. C. Raubenheimer, M. Raue, J. Raux, S. M. Rayner, I. Redondo, A. Reimer, O. Reimer, J. Ripken, L. Rob, L. Rolland, G. Rowell, V. Sahakian, L. Saugé, S. Schlenker, R. Schlickeiser, C. Schuster, U. Schwanke, M. Siewert, O. Skjæraasen, H. Sol, R. Steenkamp, C. Stegmann, J.-P. Tavernet, R. Terrier, C. G. Théoret,

- M. Tluczykont, G. Vasileiadis, C. Venter, P. Vincent, H. J. Völk, and S. J. Wagner. Discovery of the binary pulsar PSR B1259-63 in very-high-energy gamma rays around periastron with HESS. *A&A*, 442:1–10, October 2005.
- J. Albert, E. Aliu, H. Anderhub, P. Antoranz, M. Backes, C. Baixeras, J. A. Barrio, H. Bartko, D. Bastieri, J. K. Becker, W. Bednarek, K. Berger, C. Bigongiari, A. Biland, R. K. Bock, G. Bonnoli, P. Bordas, V. Bosch-Ramon, T. Bretz, I. Britvitch, M. Camara, E. Carmona, A. Chilingarian, S. Commichau, J. L. Contreras, J. Cortina, M. T. Costado, V. Curtef, F. Dazzi, A. De Angelis, R. de los Reyes, B. De Lotto, M. De Maria, F. De Sabata, C. Delgado Mendez, D. Dorner, M. Doro, M. Errando, M. Fagiolini, D. Ferenc, E. Fernández, R. Firpo, M. V. Fonseca, L. Font, N. Galante, R. J. García López, M. Garczarczyk, M. Gaug, F. Goebel, M. Hayashida, A. Herrero, D. Höhne, J. Hose, C. C. Hsu, S. Huber, T. Jogler, R. Kosyra, D. Kranich, A. Laille, E. Leonardo, E. Lindfors, S. Lombardi, F. Longo, M. López, E. Lorenz, P. Majumdar, G. Maneva, N. Mankuzhiyil, K. Mannheim, M. Mariotti, M. Martínez, D. Mazin, C. Merck, M. Meucci, M. Meyer, J. M. Miranda, R. Mirzoyan, S. Mizobuchi, M. Moles, A. Moralejo, D. Nieto, K. Nilsson, J. Ninkovic, E. Oña-Wilhelmi, N. Otte, I. Oya, M. Panniello, R. Paoletti, J. M. Paredes, M. Pasanen, D. Pascoli, F. Pauss, R. G. Pegna, M. A. Pérez-Torres, M. Persic, L. Peruzzo, A. Piccioli, F. Prada, E. Prandini, N. Puchades, A. Raymers, W. Rhode, M. Ribó, J. Rico, M. Rissi, A. Robert, S. Rügamer, A. Saggion, T. Y. Saito, A. Sánchez, M. A. Sánchez-Conde, P. Sartori, V. Scalzotto, V. Scapin, R. Schmitt, T. Schweizer, M. Shayduk, K. Shinozaki, S. N. Shore, N. Sidro, A. Sillanpää, D. Sobczynska, F. Spanier, A. Stamerra, L. S. Stark, L. Takalo, P. Temnikov, D. Tesaro, M. Teshima, D. F. Torres, N. Turini, H. Vankov, A. Venturini, V. Vitale, R. M. Wagner, W. Wittek, F. Zandanel, R. Zanin, J. Zapatero, M. A. Guerrero, A. Alberdi, Z. Paragi, T. W. B. Muxlow, and P. Diamond. Multiwavelength (Radio, X-Ray, and γ -Ray) Observations of the γ -Ray Binary LS I +61 303. , 684:

- 1351–1358, September 2008.
- G. Alter. A photographic survey of galactic clusters. V. NGC 189, I 1590, NGC 358, 366, 381, 433, 436, 457, 609, 637, I 166, NGC 743. *MNRAS*, 104:179–+, 1944.
- H. Ando. Active picture of rotation. *A&A*, 108:7–13, April 1982.
- H. Ando. Wave-rotation interaction and episodic mass-loss in Be stars. *A&A*, 163:97–104, July 1986.
- Y. Andrillat, M. Jaschek, and C. Jaschek. A survey of Be stars in the 7500-8800 Å region. *A&AS*, 72:129–149, January 1988.
- Y. Andrillat, M. Jaschek, and C. Jaschek. A study of Be stars in the wavelength region around Paschen 7. *A&AS*, 103:135–155, January 1994.
- K. M. V. Apparao. X-ray emission from Be star binaries. , 292:257–259, May 1985.
- N. M. Ashok and D. P. K. Banerjee. Near Infrared Spectroscopic Observations of Early-type Be Stars. In M. A. Smith, H. F. Henrichs, & J. Fabregat, editor, *IAU Colloq. 175: The Be Phenomenon in Early-Type Stars*, volume 214 of *Astronomical Society of the Pacific Conference Series*, pages 468–+, 2000.
- N. M. Ashok, H. C. Bhatt, P. V. Kulkarni, and S. C. Joshi. Infrared photometric studies of Be stars. *MNRAS*, 211:471–484, November 1984.
- D. Baade. An unusually short stable period of absorption line asymmetries and V/R variations in the spectrum of the Be star 28 CMa. *A&A*, 105:65–75, January 1982.
- D. Baade. Suggested new observational criteria and a new working hypothesis for the structural modeling of Be-star envelopes. *A&A*, 148:59–66, July 1985.

- D. Baade. A search for line profile variability in dwarfs and giants of spectral types B8-B9.5. II - Results and discussion. *A&A*, 222:200–204, September 1989.
- G. S. D. Babu. Membership of stars in faint galactic open clusters. *Journal of Astrophysics and Astronomy*, 4:235–252, December 1983.
- Z. Balog, A. J. Delgado, A. Moitinho, G. Fűrész, G. Kaszás, J. Vinkó, and E. J. Alfaro. Fundamental parameters and new variables of the galactic open cluster NGC 7128. *MNRAS*, 323:872–886, May 2001.
- L. A. Balona. Short-period variability in Be stars. *MNRAS*, 245:92–100, July 1990.
- L. A. Balona. Tests of the Pulsation and Starspot Models for the Periodic Be-Stars. *MNRAS*, 277:1547–+, December 1995.
- R. Barbon. The open cluster NGC 7128. *Memorie della Societa Astronomica Italiana*, 40:45–+, 1969.
- R. Barbon and S. M. Hassan. A new study of the young open cluster NGC 7510. *A&AS*, 115:325–+, February 1996.
- S. L. Barrell. The beat Cepheid V367 Scuti and NGC 6649. , 240:145–148, August 1980.
- A. Beauchamp, A. F. J. Moffat, and L. Drissen. The galactic open cluster NGC 7419 and its five red supergiants. *ApJS*, 93:187–209, July 1994.
- W. Becker. Die Entfernung des galaktischen Sternhaufens NGC 7235. *Memorie della Societa Astronomica Italiana*, 36:271–+, September 1965.
- W. Becker and J. Stock. Farben-Helligkeits-Diagramme und Entfernungen von 10 offenen Sternhaufen. Mit 10 Textabbildungen. *Zeitschrift fur Astrophysik*, 45: 282–+, 1958.

- G. Bertelli, A. Bressan, C. Chiosi, F. Fagotto, and E. Nasi. Theoretical isochrones from models with new radiative opacities. *A&AS*, 106:275–302, August 1994.
- M. S. Bessell and J. M. Brett. JHKLM photometry - Standard systems, passbands, and intrinsic colors. *A&AS*, 100:1134–1151, September 1988.
- B. C. Bhatt, A. K. Pandey, V. Mohan, H. S. Mahra, and D. C. Paliwal. CCD photometry of galactic open star clusters – 2: NGC 7419. *Bulletin of the Astronomical Society of India*, 21:33–45, March 1993.
- B. Bhavya, B. Mathew, and A. Subramaniam. Pre-main sequence stars, emission stars and recent star formation in the Cygnus region. *Bulletin of the Astronomical Society of India*, 35:383–411, 2007.
- W. P. Bidelman. A list of early-type shell stars. In A. Slettebak, editor, *Be and Shell Stars*, volume 70 of *IAU Symposium*, pages 457–465, 1976.
- W. P. Bidelman and D. J. MacConnell. The brighter stars of astrophysical interest in the southern sky. *AJ*, 78:687–733, October 1973.
- J. E. Bjorkman and J. P. Cassinelli. Equatorial disk formation around rotating stars due to ram pressure confinement by the stellar wind. *AJ*, 409:429–449, May 1993.
- V. Blanco, J. J. Nassau, J. Stock, and W. Wehlau. M-Type Stars in NGC 7419. *AJ*, 121:637–+, May 1955.
- E. Boden. Colours and magnitudes in the galactic cluster NGC 436. *Uppsala Astronomical Observatory Annals*, 2:1–+, 1950.
- I. S. Bowen. Excitation by Line Coincidence. *AJ*, 59:196–198, August 1947.
- D. Briot. Study of Be stars - The Balmer decrement. *A&A*, 11:57–64, March 1971.

- D. Briot. Paschen lines in Be stars - correlation between the presence of Paschen emission lines and the infrared excess. *A&A*, 54:599–606, January 1977.
- D. Briot. Infrared lines of O I and CA II in Be stars with Paschen emission lines. *A&A*, 103:1–4, November 1981.
- D. Briot and J. Zorec. Spectral Type Dependence of the Characteristics of Be-Stars. In C. Sterken and Groupe Etoiles Variables de L’Observatoire de Nice, editors, *Pulsating B-Stars*, pages 109–+, 1981.
- M. Brocklehurst. Calculations of level populations for the low levels of hydrogenic ions in gaseous nebulae. *MNRAS*, 153:471–490, 1971.
- G. R. Burbidge and E. M. Burbidge. The Balmer Decrement in Some be Stars. , 118:252–+, September 1953.
- G. Caron, A. F. J. Moffat, N. St-Louis, G. A. Wade, and J. B. Lester. The Lack of Blue Supergiants in NGC 7419, a Red Supergiant-rich Galactic Open Cluster with Rapidly Rotating Stars. *AJ*, 126:1415–1422, September 2003.
- J. M. Carpenter. Color Transformations for the 2MASS Second Incremental Data Release. *AJ*, 121:2851–2871, May 2001.
- J. P. Cassinelli, J. C. Brown, M. Maheswaran, N. A. Miller, and D. C. Telfer. A Magnetically Torqued Disk Model for Be Stars. , 578:951–966, October 2002.
- H.-Q. Chen and L. Huang. A statistical method of estimating the rotation of Be stars. *Chinese Astronomy and Astrophysics*, 11:10–14, March 1987.
- O. Chesneau, A. Meilland, T. Rivinius, P. Stee, S. Jankov, A. Domiciano de Souza, U. Graser, T. Herbst, E. Janot-Pacheco, R. Koehler, C. Leinert, S. Morel, F. Paresce, A. Richichi, and S. Robbe-Dubois. First VLTI/MIDI observations of a Be star: Alpha Arae. *A&A*, 435:275–287, May 2005.

- P. Collinder. On structured properties of open galactic clusters and their spatial distribution. *Annals of the Observatory of Lund*, 2:1–+, 1931.
- G. W. Collins, II. The use of terms and definitions in the study of Be stars. In A. Slettebak and T. P. Snow, editors, *IAU Colloq. 92: Physics of Be Stars*, pages 3–19, 1987.
- G. V. Coyne and I. S. McLean. Polarimetry and physics of Be star envelopes /Review paper/. In M. Jaschek and H.-G. Groth, editors, *Be Stars*, volume 98 of *IAU Symposium*, pages 77–92, April 1982.
- G. V. Coyne, W. Wisniewski, and C. Corbally. A survey for H α emission objects in the Milky Way. II. Cygnus. *Vatican Observatory Publications*, 1: 197–212, 1975.
- G. V. Coyne, W. Wisniewski, and L. B. Otten. A survey for H α emission objects in the Milky Way. *Vatican Observatory Publications*, 1:257–265, 1978.
- S. R. Cranmer. A Statistical Study of Threshold Rotation Rates for the Formation of Disks around Be Stars. , 634:585–601, November 2005.
- S. R. Cranmer. A Pulsational Mechanism for Producing Keplerian Disks Around Be Stars. , 701:396–413, August 2009.
- D. L. Crawford, J. V. Barnes, and G. Hill. Four-color and H-beta photometry of open clusters. XII - NGC 6910 and NGC 6913. *AJ*, 82:606–611, August 1977.
- J. Cuffey. NGC 1894, UBV photometry. *AJ*, 78:747–756, October 1973.
- J. Dachs, D. Rohe, and A. S. Loose. A study of Balmer decrements in Be star emission-line spectra. *A&A*, 238:227–241, November 1990.
- J. Dachs and W. Wamsteker. Infrared photometry of southern Be stars. *A&A*, 107:240–246, March 1982.

- H. J. Deeg and Z. Ninkov. Deep CCD photometry and the initial mass function of the core of the OB cluster Berkeley 86. *A&AS*, 119:221–230, October 1996.
- A. J. Delgado and E. J. Alfaro. Search for Pre-Main-Sequence Stars in the Young Galactic Cluster NGC 6910. *AJ*, 119:1848–1854, April 2000.
- A. J. Delgado, E. J. Alfaro, and J. Cabrera-Cano. CCD Stromgren Photometry of Young Reddened Clusters. *AJ*, 113:713–721, February 1997.
- A. J. Delgado, E. J. Alfaro, A. Moitinho, and J. Franco. Pre-Main-Sequence Stars in the Young Galactic Cluster IC 4996: A CCD Photometric Study. *AJ*, 116:1801–1809, October 1998.
- A. J. Delgado, L. F. Miranda, and E. J. Alfaro. Spectroscopy of Pre-Main-Sequence Candidates of Spectral Type AF in the Young Galactic Cluster IC 4996. *AJ*, 118:1759–1765, October 1999.
- A. J. Delgado, L. F. Miranda, M. Fernández, and E. J. Alfaro. Photometric and Spectroscopic Study of Stars in the Field of the Young Open Cluster Roslund 4. *AJ*, 128:330–342, July 2004.
- P. D. Diago, J. Gutierrez-Soto, M. Auvergne, J. Fabregat, A. . Hubert, M. Floquet, Y. Fremat, R. Garrido, L. Andrade, B. de Batz, M. Emilio, F. Espinosa-Lara, A. . Huat, E. Janot-Pacheco, B. Leroy, C. Martayan, C. Neiner, T. Semaan, J. Suso, C. Catala, E. Poretti, M. Rainer, K. Uytterhoeven, E. Michel, and R. Samadi. Pulsations in the late-type Be star HD 50209 detected by CoRoT. *ArXiv e-prints*, September 2009a.
- P. D. Diago, J. Gutiérrez-Soto, J. Fabregat, and C. Martayan. More on pulsating B-type stars in the Magellanic Clouds. *Communications in Asteroseismology*, 158:184–+, July 2009b.

-
- V. Doazan, G. Sedmak, M. Barylak, L. Rusconi, and B. Battrick, editors. *A Be star atlas of far UV and optical high-resolution spectra*, volume 1147 of *ESA Special Publication*, November 1991.
- V. Doazan and R. N. Thomas. Empirical atmospheric velocity patterns from combined IUE and visual observations: The Be stars. In E. Rolfe and A. Heck, editors, *Third European IUE Conference*, volume 176 of *ESA Special Publication*, pages 287–290, June 1982.
- M. V. Dolidze. Lists of S, C, and MS stars and emission-line objects revealed by red-light observations. *Abastumanskaia Astrofizicheskaia Observatoriia Biulleten*, 47:3–144, 1975.
- M. W. Dolidze. The stars with H alpha-emission around the cluster NGC 7380. *Abastumanskaia Astrofizicheskaia Observatoriia Biulleten*, 24:7–+, 1959.
- S. M. Dougherty, L. B. F. M. Waters, G. Burki, J. Cote, N. Cramer, M. H. van Kerkwijk, and A. R. Taylor. Near-IR excess of Be stars. *A&A*, 290:609–622, October 1994.
- B. G. Elmegreen and C. J. Lada. CO and H₂O observations of the H II region NGC 281. , 219:467–469, January 1978.
- J. Fabregat. The Be star content of young open clusters. In C. Sterken, editor, *Interplay of Periodic, Cyclic and Stochastic Variability in Selected Areas of the H-R Diagram*, volume 292 of *Astronomical Society of the Pacific Conference Series*, pages 65–+, March 2003.
- J. Fabregat and G. Capilla. CCD uvby β photometry of the young open cluster NGC 663. *MNRAS*, 358:66–70, March 2005.
- J. Fabregat and J. Gutierrez-Soto. The Evolutionary Status of Be Stars in Clusters and in the Galactic Field. *Publications of the Astronomical Institute of the Czechoslovak Academy of Sciences*, 93:9–13, December 2005.

- J. Fabregat and J. M. Torrejón. On the evolutionary status of Be stars. *A&A*, 357:451–459, May 2000.
- W. M. Fawley and M. Cohen. The open cluster NGC 7419 and its M7 supergiant IRC +60 375. , 193:367–372, October 1974.
- M. W. Feast. The cluster NGC 330 in the SMC (Paper II): H α emission in main sequence stars. *MNRAS*, 159:113–118, 1972.
- A. Feinstein. Infrared photometry of Be stars. In M. Jaschek and H.-G. Groth, editors, *Be Stars*, volume 98 of *IAU Symposium*, pages 235–238, April 1982.
- M. P. Fitzgerald and A. F. J. Moffat. Luminous Stars Beyond the Solar Circle - Investigation of a Galactic Field at L=231DEG. *MNRAS*, 193:761–+, December 1980.
- A. Fitzsimmons. CCD Stromgren UVBY photometry of the young clusters NGC 1893, NGC 457, Berkeley 94 and Bochum 1. *A&AS*, 99:15–29, May 1993.
- J. Fletcher. NGC869 and NGC884 - the Double Cluster in Perseus. *Journal of the British Astronomical Association*, 98:167–+, April 1988.
- D. Forbes. The young open clusters Berkeley 62 and Berkeley 86. , 93:441–446, August 1981.
- D. Forbes. Membership of the WR binary V444 Cygni in the open cluster Berkeley 86. , 85:213–+, August 1991.
- H. Fünfschilling. Der offene Sternhaufen NGC 6834. *Zeitschrift für Astrophysik*, 66:440–+, 1967.
- J. M. Garcia-Pelayo and E. J. Alfaro. UBV photoelectric photometry of faint stars in the clusters NGC 7235 and NGC 1778. , 96:444–446, June 1984.

- R. D. Gehrz, J. A. Hackwell, and T. W. Jones. Infrared observations of Be stars from 2.3 to 19.5 microns. , 191:675–684, August 1974.
- T. P. Gerasimenko. Open Star Cluster NGC957. *Soviet Astronomy*, 35:553–+, October 1991.
- D. R. Gies. Be stars: Single and Binary Components. In D. Vanbeveren, editor, *The Influence of Binaries on Stellar Population Studies*, volume 264 of *Astrophysics and Space Science Library*, pages 95–+, 2001.
- D. R. Gies, W. G. Bagnuolo, Jr., E. C. Ferrara, A. B. Kaye, M. L. Thaller, L. R. Penny, and G. J. Peters. Hubble Space Telescope Goddard High Resolution Spectrograph Observations of the Be + sdO Binary phi Persei. , 493:440–+, January 1998.
- A. Gimenez and J. Garcia-Pelayo. RGU photometry of the young open cluster NGC 957. *A&AS*, 41:9–12, July 1980.
- G. Gonzalez and G. Gonzalez. Estrellas con Half EM emission EN las longitudes galacticas de 59 a 90. *Boletin de los Observatorios Tonantzintla y Tacubaya*, 2:16–26, 1956.
- C. A. Grady, K. S. Bjorkman, and T. P. Snow. Highly ionized stellar winds in Be stars - The evidence for aspect dependence. , 320:376–397, September 1987.
- E. K. Grebel, T. Richtler, and K. S. de Boer. Be-Star Surveys with CCD Photometry - Part One - NGC330 and its High Be-Star Content. *A&A*, 254:L5+, February 1992.
- C. Grubissich. Three-colour photometry of the two galactic star clusters NGC 559 and NGC 637. *A&AS*, 21:99–107, July 1975.
- E. D. Grundstrom, S. M. Caballero-Nieves, D. R. Gies, W. Huang, M. V. McSwain, S. E. Rafter, R. L. Riddle, S. J. Williams, and D. W. Wingert. Joint H α and

- X-Ray Observations of Massive X-Ray Binaries. II. The Be X-Ray Binary and Microquasar LS I +61 303. , 656:437–443, February 2007.
- H. H. Guetter. Photometric studies of stars in the young open cluster NGC 6823. *AJ*, 103:197–203, January 1992.
- H. H. Guetter and D. G. Turner. IC 1590, A Young Cluster Embedded in the Nebulosity of NGC 281. *AJ*, 113:2116–+, June 1997.
- A. F. Gulliver. The spectrum variations of PLEIONE from 1938 to 1975. *ApJS*, 35:441–459, December 1977.
- F. Haberl and M. Sasaki. Doubling the number of Be/X-ray binaries in the SMC. *A&A*, 359:573–585, July 2000.
- G. Handschel. UBV-Photometrie der offenen Sternhaufen NGC 7419, K 10 und NGC 6192. *Thesis, 0 (1972)*, pages 0–+, 1972.
- R. W. Hanuschik. High-resolution emission-line spectroscopy of Be stars. I - Evidence for a two-component structure of the H-alpha emitting envelope. *A&A*, 166:185–194, September 1986.
- R. W. Hanuschik. On the structure of Be star disks. *A&A*, 308:170–179, April 1996.
- R. W. Hanuschik, W. Hummel, E. Sutorius, O. Dietle, and G. Thimm. Atlas of high-resolution emission and shell lines in Be stars. Line profiles and short-term variability. *A&AS*, 116:309–358, April 1996.
- J. Hardorp. Dreifarben-Photometrie einer Sternhaufengruppe in der Cassiopeia (NGC 103, NGC 129, NGC 136, NGC 146, K 14, und K 16). *Astronomische Abhandlungen der Hamburger Sternwarte*, 5:215–261, 1960.
- J. Hardorp and P. A. Strittmatter. Rotation and Evolution of be Stars. In *IAU Colloq. 4: Stellar Rotation*, pages 48–+, 1970.

- P. Harmanec. Non-Canonical Insights into the Evolution of Stars. 1. an Alternative Model of Massive X-Ray Binaries. *Bulletin of the Astronomical Institutes of Czechoslovakia*, 36:327–+, November 1985.
- L. Hartmann. Disk structure in early-type stellar envelopes. , 224:520–526, September 1978.
- S. M. Hassan. Three colour photometry of the five open clusters NGC 7039, NGC 7062, NGC 7067, NGC 7082, IC 1369. *A&AS*, 9:261–+, February 1973.
- U. Haug. UBV Observations of luminous stars in three Milky Way fields (Cassiopeia, Camelopardalis and Gemini). *A&AS*, 1:35–+, January 1970.
- A. Heger and N. Langer. Presupernova Evolution of Rotating Massive Stars. II. Evolution of the Surface Properties. , 544:1016–1035, December 2000.
- W. Hermsen, B. N. Swanenburg, G. F. Bignami, G. Boella, R. Buccheri, L. Scarsi, G. Kanbach, H. A. Mayer-Hasselwander, J. L. Masnou, and J. A. Paul. New high energy gamma-ray sources observed by COS B. , 269:494–+, October 1977.
- J. Hernández, N. Calvet, L. Hartmann, C. Briceño, A. Sicilia-Aguilar, and P. Berlind. Herbig Ae/Be Stars in nearby OB Associations. *AJ*, 129:856–871, February 2005.
- L. A. Hillenbrand, S. E. Strom, F. J. Vrba, and J. Keene. Herbig Ae/Be stars - Intermediate-mass stars surrounded by massive circumstellar accretion disks. , 397:613–643, October 1992.
- W. A. Hiltner. Infrared Spectra of Early-Type Stars. , 105:212–+, January 1947.
- W. A. Hiltner. Photometric, Polarization, and Spectrographic Observations of O and B Stars. *ApJS*, 2:389–+, October 1956.

- J. A. Hinton, J. L. Skilton, S. Funk, J. Brucker, F. A. Aharonian, G. Dubus, A. Fiasson, Y. Gallant, W. Hofmann, A. Marcowith, and O. Reimer. HESS J0632+057: A New Gamma-Ray Binary? *ApJL*, 690:L101–L104, January 2009.
- R. Hirata and T. Kogure. The Be star phenomena. II - Spectral formation and structure of envelopes. *Bulletin of the Astronomical Society of India*, 12:109–151, June 1984.
- A. A. Hoag, H. L. Johnson, B. Iriarte, R. I. Mitchell, K. L. Hallam, and S. Sharpless. Photometry of stars in galactic cluster fields. *Publications of the U.S. Naval Observatory Second Series*, 17:343–542, 1961.
- E. Høg, C. Fabricius, V. V. Makarov, S. Urban, T. Corbin, G. Wycoff, U. Bastian, P. Schwekendiek, and A. Wicenec. The Tycho-2 catalogue of the 2.5 million brightest stars. *A&A*, 355:L27–L30, March 2000.
- S.-S. Huang. Profiles of Emission Lines in Be Stars. , 171:549–+, February 1972.
- A. M. Hubert and M. Floquet. Investigation of the variability of bright Be stars using HIPPARCOS photometry. *A&A*, 335:565–572, July 1998.
- A.-M. Hubert-Delplace and H. Hubert. *An atlas of Be stars*. 1979.
- S. Hubrig, M. Schöller, I. Savanov, R. V. Yudin, M. A. Pogodin, S. Štefl, T. Rivinius, and M. Curé. Magnetic survey of emission line B-type stars with FORS 1 at the VLT. *Astronomische Nachrichten*, 330:708–+, 2009.
- G. Huestamendia, G. del Rio, and J.-C. Mermilliod. UBV photometry of open clusters in the Cassiopeia region. I - Photoelectric observations of NGC436 and 637. *A&AS*, 87:153–158, January 1991.
- W. Hummel and R. W. Hanuschik. Line formation in Be star envelopes. II. Disk oscillations. *A&A*, 320:852–864, April 1997.

-
- W. Hummel, T. Szeifert, W. Gässler, B. Muschielok, W. Seifert, I. Appenzeller, and G. Rupprecht. A spectroscopic study of Be stars in the SMC cluster NGC 330. *A&A*, 352:L31–L35, December 1999.
- W. Hummel and M. Vrancken. Line formation in Be star circumstellar disks. Shear broadening, shell absorption, stellar obscuration and rotational parameter. *A&A*, 359:1075–1084, July 2000.
- D. G. Hummer and P. J. Storey. Recombination-line intensities for hydrogenic ions. I - Case B calculations for H I and He II. *MNRAS*, 224:801–820, February 1987.
- G. H. Jacoby, D. A. Hunter, and C. A. Christian. A library of stellar spectra. *ApJS*, 56:257–281, October 1984.
- C. Jaschek and M. Jaschek. The frequency of Be stars. *A&A*, 117:357–+, January 1983.
- M. Jaschek and D. Egret. A Catalogue of Be-Stars. In M. Jaschek and H.-G. Groth, editors, *Be Stars*, volume 98 of *IAU Symposium*, pages 261–+, April 1982.
- M. Jaschek, C. Jaschek, and Y. Andrillat. The behavior of the O I line 7772 in Be and related stars. *A&AS*, 97:781–799, February 1993.
- M. Jaschek, A. Slettebak, and C. Jaschek. Be star terminology., 1981.
- V. Jasevicius. Three colour photometry and spectral classification of stars in the region of NGC133, NGC146, and K-14. *Vilnius Astronomijos Observatorijos Biuletenis*, 13:1–+, 1964.
- M. Jerzykiewicz, A. Pigulski, G. Kopacki, A. Mialkowska, and S. Niczyporuk. A CCD Search for Variable Stars of Spectral Type B in the Northern Hemisphere Open Clusters I. NGC 7128. *Acta Astronomica*, 46:253–277, April 1996.

- H. L. Johnson. Galactic clusters as indicators of stellar evolution and galactic structure. *Lowell Observatory Bulletin*, 5:133–147, 1961.
- S. Johnston, R. N. Manchester, A. G. Lyne, M. Bailes, V. M. Kaspi, G. Qiao, and N. D’Amico. PSR 1259-63 - A binary radio pulsar with a Be star companion. *ApJL*, 387:L37–L41, March 1992.
- U. C. Joshi and R. Sagar. Photometry of the open cluster NGC 654. *MNRAS*, 202:961–970, March 1983.
- S. C. Keller. Rotation of Early B-type Stars in the Large Magellanic Cloud: The Role of Evolution and Metallicity. *Publications of the Astronomical Society of Australia*, 21:310–317, 2004.
- S. C. Keller, M. S. Bessell, and G. S. Da Costa. Be Stars in the Magellanic Clouds. In M. A. Smith, H. F. Henrichs, and J. Fabregat, editors, *IAU Colloq. 175: The Be Phenomenon in Early-Type Stars*, volume 214 of *Astronomical Society of the Pacific Conference Series*, pages 75–+, 2000.
- S. C. Keller, E. K. Grebel, G. J. Miller, and K. M. Yoss. UBVI and H α Photometry of the η and χ Persei Cluster. *AJ*, 122:248–256, July 2001.
- S. C. Keller, P. R. Wood, and M. S. Bessell. Be stars in and around young clusters in the Magellanic Clouds. *A&AS*, 134:489–503, February 1999.
- P. N. Kholopov. The Unity in the Structure of Star Clusters. *Soviet Astronomy*, 12:625–+, February 1969.
- C. R. Kitchin and A. J. Meadows. The Behaviour of the Infrared Lines of Neutral Oxygen and the Balmer Lines of Hydrogen in the Spectra of Early-Type Stars with Emission Lines. , 8:463–470, September 1970.
- T. Kogure and R. Hirata. The Be-Star Phenomena - Part One - General Properties. *Bulletin of the Astronomical Society of India*, 10:281–+, December 1982.

-
- L. Kohoutek and R. Wehmeyer. Catalogue of H-alpha emission stars in the Northern Milky Way. *A&AS*, 134:255–256, January 1999.
- J. Koornneef. Near-infrared photometry. II - Intrinsic colours and the absolute calibration from one to five micron. *A&A*, 128:84–93, November 1983.
- P. Koubský. Be Stars in Binaries. , 296:165–168, April 2005.
- S. Kriz and P. Harmanec. A hypothesis of the binary origin of Be stars. *Bulletin of the Astronomical Institutes of Czechoslovakia*, 26:65–81, 1975.
- P. Kroll and R. W. Hanuschik. Dynamics of Self-Accreting Disks in Be Stars. In D. T. Wickramasinghe, G. V. Bicknell, and L. Ferrario, editors, *IAU Colloq. 163: Accretion Phenomena and Related Outflows*, volume 121 of *Astronomical Society of the Pacific Conference Series*, pages 494–+, 1997.
- J. Krzesinski and A. Pigulski. B-type pulsators in the open cluster NGC 884 (χ Persei). *A&A*, 325:987–993, September 1997.
- J. Krzesiński, A. Pigulski, and Z. Kołaczkowski. B-type pulsators in the central region of NGC 869 (h Persei). *A&A*, 345:505–513, May 1999.
- C. J. Lada and F. C. Adams. Interpreting infrared color-color diagrams - Circumstellar disks around low- and intermediate-mass young stellar objects. , 393:278–288, July 1992.
- J. D. Landstreet. Magnetic fields in hot stars (review). In U. Heber and C. S. Jeffery, editors, *The Atmospheres of Early-Type Stars*, volume 401 of *Lecture Notes in Physics*, Berlin Springer Verlag, pages 170–+, 1992.
- N. Langer and A. Heger. The Evolution of Surface Parameters of Rotating Massive Stars. In I. Howarth, editor, *Properties of Hot Luminous Stars*, volume 131 of *Astronomical Society of the Pacific Conference Series*, pages 76–+, 1998.

- D. Leisawitz. Physical Properties of the Molecular Clouds Found in a CO Survey of Regions Around 34 Open Clusters. In *Bulletin of the American Astronomical Society*, volume 21 of *Bulletin of the American Astronomical Society*, pages 1189–+, September 1989.
- U. Lindoff. The ages of open clusters. *Arkiv for Astronomi*, 5:1–21, 1968.
- T. Liu, K. A. Janes, T. M. Bania, and R. L. Phelps. Stellar and molecular radial velocities for six young open clusters. *AJ*, 95:1122–1131, April 1988.
- T. Lloyd Evans. Be stars in two open clusters. *MNRAS*, 192:47–51, July 1980.
- T. A. Lozinskaya and S. V. Repin. Infrared Shell in the Cygnus-X - CYGNUS-OB1 Region. *Soviet Astronomy*, 34:580–+, December 1990.
- G. Lynga. Distribution of OB associations and open star clusters. In J. Palous, editor, *European Regional Astronomy Meeting of the IAU, Volume 4*, volume 4, pages 121–127, 1987.
- B. F. Madore and S. van den Bergh. UBV photometry of the cepheid V367 Scuti in the open cluster NGC 6649. , 197:55–65, April 1975.
- A. Maeder. Stellar evolution with rotation IV: von Zeipel’s theorem and anisotropic losses of mass and angular momentum. *A&A*, 347:185–193, July 1999.
- A. Maeder, E. K. Grebel, and J.-C. Mermilliod. Differences in the fractions of Be stars in galaxies. *A&A*, 346:459–464, June 1999.
- A. Maeder and G. Meynet. Stellar evolution with rotation. VII. . Low metallicity models and the blue to red supergiant ratio in the SMC. *A&A*, 373:555–571, July 2001.
- M. Maheswaran. Magnetic Rotator Winds and Keplerian Disks of Hot Stars. , 592:1156–1172, August 2003.

- M. Maheswaran. A Magnetic Rotator Wind-Disk Model for Be Stars. In R. Ignace and K. G. Gayley, editors, *The Nature and Evolution of Disks Around Hot Stars*, volume 337 of *Astronomical Society of the Pacific Conference Series*, pages 259–+, November 2005.
- M. Maheswaran and J. P. Cassinelli. Protodisks around hot magnetic rotator stars. *MNRAS*, 394:415–426, March 2009.
- M. Maintz, T. Rivinius, O. Stahl, S. Stefl, and I. Appenzeller. 59 Cyg - A second Be binary with a hot, compact companion. *Publications of the Astronomical Institute of the Czechoslovak Academy of Sciences*, 93:21–28, December 2005.
- S. L. Malchenko and A. E. Tarasov. Population of Be Stars in Young Open Clusters. In V. Y. Choliy and G. Ivashchenko, editors, *Young Scientists 15th Proceedings*, pages 52–56, December 2008.
- A. Marco, G. Bernabeu, and I. Negueruela. Photometric and Spectroscopic Study of the Young Open Cluster NGC 1893. *AJ*, 121:2075–2088, April 2001.
- A. Marco and I. Negueruela. Pre-main-sequence stars in the young open cluster ;ASTROBJ;NGC 1893;/ASTROBJ;. I. A spectroscopic search for candidates in the area photometrically surveyed. *A&A*, 393:195–204, October 2002.
- A. Marco and I. Negueruela. Triggered massive star formation in the open cluster NGC 1893. In K. van der Hucht, A. Herrero, and C. Esteban, editors, *A Massive Star Odyssey: From Main Sequence to Supernova*, volume 212 of *IAU Symposium*, pages 562–+, 2003.
- J. M. Marlborough. Ultraviolet observations of Be stars. I - Macroscopic radial motions in the atmospheres of early Be stars. , 216:446–456, September 1977.
- C. Martayan, D. Baade, and J. Fabregat. The WFI H α spectroscopic survey of the Magellanic Clouds: Be stars in SMC open clusters. In J. T. van Loon and

- J. M. Oliveira, editors, *IAU Symposium*, volume 256 of *IAU Symposium*, pages 349–354, March 2009a.
- C. Martayan, D. Baade, Y. Fremat, and J. Zorec. Evolution and appearance of Be stars in SMC clusters. *ArXiv e-prints*, September 2009b.
- C. Martayan, M. Floquet, A. M. Hubert, J. Gutiérrez-Soto, J. Fabregat, C. Neiner, and M. Mekkas. Be stars and binaries in the field of the SMC open cluster NGC 330 with VLT-FLAMES. *A&A*, 472:577–586, September 2007a.
- C. Martayan, Y. Frémat, A.-M. Hubert, M. Floquet, J. Zorec, and C. Neiner. Effects of metallicity, star-formation conditions, and evolution in B and Be stars. I. Large Magellanic Cloud, field of NGC 2004. *A&A*, 452:273–284, June 2006.
- C. Martayan, Y. Frémat, A.-M. Hubert, M. Floquet, J. Zorec, and C. Neiner. Effects of metallicity, star-formation conditions, and evolution in B and Be stars. II. Small Magellanic Cloud, field of NGC330. *A&A*, 462:683–694, February 2007b.
- P. Massey, K. E. Johnson, and K. Degioia-Eastwood. The Initial Mass Function and Massive Star Evolution in the OB Associations of the Northern Milky Way. , 454:151–+, November 1995.
- B. Mathew, A. Subramaniam, and B. C. Bhatt. Be phenomenon in open clusters: results from a survey of emission-line stars in young open clusters. *MNRAS*, 388:1879–1888, August 2008.
- S. W. McCuskey and N. Houk. Galactic structure in Cassiopeia. *AJ*, 69:412–437, August 1964.
- M. V. McSwain and D. R. Gies. A Photometric Method to Search for Be Stars in Open Clusters. , 622:1052–1057, April 2005a.

- M. V. McSwain and D. R. Gies. The Evolutionary Status of Be Stars: Results from a Photometric Study of Southern Open Clusters. *ApJS*, 161:118–146, November 2005b.
- M. V. McSwain, W. Huang, and D. R. Gies. Variability of Be stars in southern open clusters. , 700:1216–1232, 2009.
- M. V. McSwain, W. Huang, D. R. Gies, E. D. Grundstrom, and R. H. D. Townsend. The B and Be Star Population of NGC 3766. , 672:590–603, January 2008.
- J. C. Mermilliod. Stellar Content of Young Open Clusters - Part Two - Be-Stars. *A&A*, 109:48–+, May 1982.
- J.-C. Mermilliod. UBV Photoelectric Cat: Data 1986-1992 (Mermilliod 1994). *VizieR Online Data Catalog*, 2193:0–+, November 1994.
- P. W. Merrill. Stars Having Shell Spectra. , 61:38–+, February 1949.
- G. Meynet and A. Maeder. Stellar evolution with rotation. V. Changes in all the outputs of massive star models. *A&A*, 361:101–120, September 2000.
- G. J. Miller, E. K. Grebel, and K. M. Yoss. Be Stars and Physical Properties of the Young Open Cluster NGC 6834. In *Bulletin of the American Astronomical Society*, volume 28 of *Bulletin of the American Astronomical Society*, pages 1367–+, December 1996.
- A. F. J. Moffat. Photometry and structure of the young open cluster NGC 7380. *A&A*, 13:30–39, June 1971.
- A. F. J. Moffat. Photometry of eleven young open star clusters. *A&AS*, 7:355–+, November 1972.
- A. F. J. Moffat. NGC 2345, a moderately young open cluster in Canis Major. *A&AS*, 16:33–+, 1974.

- A. F. J. Moffat, P. D. Jackson, and M. P. Fitzgerald. The rotation and structure of the galaxy beyond the solar circle. I - Photometry and spectroscopy of 276 stars in 45 H II regions and other young stellar groups toward the galactic anticentre. *A&AS*, 38:197–225, November 1979.
- A. F. J. Moffat and N. Vogt. An up-to-date picture of galactic spiral features based on young open star clusters. *A&A*, 23:317–320, March 1973.
- A. F. J. Moffat and N. Vogt. Southern open star clusters IV. UBV-Hbeta photometry of 26 clusters from Monoceros to Vela. *A&AS*, 20:85–124, April 1975.
- V. Mohan and A. K. Pandey. Photometry of open cluster King 21. *Bulletin of the Astronomical Society of India*, 12:217–222, September 1984.
- V. Mohan, A. K. Pandey, D. C. Paliwal, R. Sagar, and H. S. Mahra. CCD photometry of the galactic open star clusters. I - King 10. *Bulletin of the Astronomical Society of India*, 20:303–318, September 1992.
- D. Mourard, I. Bosc, A. Labeyrie, L. Koechlin, and S. Saha. The rotating envelope of the hot star Gamma Cassiopeiae resolved by optical interferometry. *A&A*, 342:520–522, November 1989.
- U. Munari and G. Carraro. UBV(RI)-C-H α photometry and GRISM spectroscopy of the young cluster Bochum 2 in the anticentre direction. *MNRAS*, 277:1269–1273, December 1995.
- U. Munari and L. Tomasella. Kinematics and binaries in young stellar aggregates. I. The trapezium system BD+00(deg) 1617 in Bochum 2. *A&A*, 343:806–812, March 1999.
- T. Neckel and G. Klare. The spatial distribution of the interstellar extinction. *A&AS*, 42:251–281, November 1980.

-
- A. D. Neto and J. A. de Freitas-Pacheco. Infrared Excess and Line Emission in Be-Stars. *MNRAS*, 198:659–+, February 1982.
- A. T. Okazaki. Long-term V/R variations of Be stars due to global one-armed oscillations of equatorial disks. , 43:75–94, February 1991.
- A. T. Okazaki and I. Negueruela. A natural explanation for periodic X-ray outbursts in Be/X-ray binaries. *A&A*, 377:161–174, October 2001.
- S. Ortolani, G. Carraro, S. Covino, E. Bica, and B. Barbuy. A photometric study of the young open cluster NGC 1220. *A&A*, 391:179–185, August 2002.
- Y. Osaki. Connection between nonradial pulsations and stellar winds in massive stars. I - Nonradial pulsation theory of massive stars. , 98:30–32, January 1986.
- A. Osman, A. Khalil, A. Aiad, and M. Marie. UBV Photometry of NGC581. In A. Maeder and A. Renzini, editors, *Observational Tests of the Stellar Evolution Theory*, volume 105 of *IAU Symposium*, pages 119–+, 1984.
- S. P. Owocki and S. R. Cranmer. The Link between Radiation-Driven Winds and Pulsation in Massive Stars (invited paper). In C. Aerts, T. R. Bedding, and J. Christensen-Dalsgaard, editors, *IAU Colloq. 185: Radial and Nonradial Pulsations as Probes of Stellar Physics*, volume 259 of *Astronomical Society of the Pacific Conference Series*, pages 512–+, 2002.
- S. P. Owocki, S. R. Cranmer, and J. M. Blondin. Two-dimensional hydrodynamical simulations of wind-compressed disks around rapidly rotating B stars. , 424:887–904, April 1994.
- A. A. Pamyatnykh. Pulsational Instability Domains in the Upper Main Sequence. *Acta Astronomica*, 49:119–148, June 1999.
- A. K. Pandey and H. S. Mahra. Interstellar extinction and Galactic structure. *MNRAS*, 226:635–643, June 1987.

-
- A. K. Pandey, K. Upadhyay, K. Ogura, R. Sagar, V. Mohan, H. Mito, H. C. Bhatt, and B. C. Bhatt. Stellar contents of two young open clusters: NGC 663 and 654. *MNRAS*, 358:1290–1308, April 2005.
- E. Paunzen, M. Netopil, I. K. Iliev, H. M. Maitzen, A. Claret, and O. I. Pintado. CCD photometric search for peculiar stars in open clusters. VI. NGC 1502, NGC 3105, Stock 16, NGC 6268, NGC 7235 and NGC 7510. *A&A*, 443:157–162, November 2005.
- E. Paunzen, M. Netopil, I. K. Iliev, H. M. Maitzen, A. Claret, and O. I. Pintado. CCD photometric search for peculiar stars in open clusters. VII. Berkeley 11, Berkeley 94, Haffner 15, Lyngå 1, NGC 6031, NGC 6405, NGC 6834 and Ruprecht 130. *A&A*, 454:171–178, July 2006.
- E. Paunzen, O. I. Pintado, and H. M. Maitzen. CCD photometric search for peculiar stars in open clusters. V. NGC 2099, NGC 3114, NGC 6204, NGC 6705 and NGC 6756. *A&A*, 412:721–725, December 2003.
- P. Pesch. The Galactic Cluster NGC 457. , 130:764–+, November 1959.
- P. Pesch. The Galactic Cluster NGC 654. , 132:696–+, November 1960.
- G. J. Peters. Orbital motion and mass flow in the interacting binary Be star HR 2142. , 95:311–318, May 1983.
- G. J. Peters and D. R. Gies. The Interacting Binary Be Star HR 2142. In C. A. Tout and W. van Hamme, editors, *Exotic Stars as Challenges to Evolution*, volume 279 of *Astronomical Society of the Pacific Conference Series*, pages 149–+, 2002.
- R. L. Phelps. A Photometric and [S II] Survey of the Young Cluster Roslund 4. *AJ*, 126:826–832, August 2003.
- R. L. Phelps and K. A. Janes. CCD photometry of the young open cluster NGC 663. *Memorie della Societa Astronomica Italiana*, 62:921–926, 1991.

- R. L. Phelps and K. A. Janes. Young open clusters as probes of the star formation process. 1: an atlas of open cluster photometry. *ApJS*, 90:31–82, January 1994.
- G. Pietrzynski. A CCD Search for Variable Stars in a Young Open Cluster IC 4996. *Acta Astronomica*, 46:349–355, July 1996.
- G. Pietrzynski. A CCD Search for Variable Stars in Young Open Cluster NGC 663. *Acta Astronomica*, 47:211–223, January 1997.
- G. Pietrzynski, L. Wyrzykowski, O. Szewczyk, and M. Bielewicz. Variable Stars in the Field of Young Open Cluster NGC 659. *Acta Astronomica*, 51:65–74, March 2001.
- A. Pigulski, M. Jerzykiewicz, and G. Kopacki. A CCD Search for Variable Stars of Spectral Type B in the Northern Hemisphere Open Clusters II. NGC 7235. *Acta Astronomica*, 47:365–380, July 1997.
- A. Pigulski and G. Kopacki. NGC 7419: An open cluster rich in Be stars. *A&AS*, 146:465–469, November 2000.
- A. Pigulski, G. Kopacki, and Z. Kołaczkowski. A CCD Search for Variable Stars of Spectral Type B in the Northern Hemisphere Open Clusters. IV. NGC663. *Acta Astronomica*, 51:159–174, June 2001a.
- A. Pigulski, G. Kopacki, and Z. Kołaczkowski. The young open cluster NGC 663 and its Be stars. *A&A*, 376:144–153, September 2001b.
- M. Plavec and R. S. Polidan. The ALGOLS, Red Spectra, BE Stars, and Even Neutrinos. In P. Eggleton, S. Mitton, and J. Whelan, editors, *Structure and Evolution of Close Binary Systems*, volume 73 of *IAU Symposium*, pages 289–+, 1976.
- C. H. Poe and D. B. Friend. A rotating, magnetic, radiation-driven wind model applied to Be stars. *A&AS*, 311:317–325, December 1986.

- R. Poeckert. Model atmospheres of Be stars. In M. Jасhek and H.-G. Groth, editors, *Be Stars*, volume 98 of *IAU Symposium*, pages 453–477, April 1982.
- V. F. Polcaro, F. Giovannelli, R. K. Manchanda, L. Norci, C. Rossi, and G. Tesicini. Berkeley 87. , 4845:2–+, September 1989.
- R. S. Polidan and G. J. Peters. Spectroscopic Observations of Be Stars in the Near Infrared. In A. Slettebak, editor, *Be and Shell Stars*, volume 70 of *IAU Symposium*, pages 59–+, 1976.
- D. M. Popper. Stellar masses. *ARAA*, 18:115–164, 1980.
- J. M. Porter. On the rotational velocities of Be and Be-shell stars. *MNRAS*, 280:L31–L35, June 1996.
- J. M. Porter and T. Rivinius. Classical Be Stars. , 115:1153–1170, October 2003.
- A. Quirrenbach, K. S. Bjorkman, J. E. Bjorkman, C. A. Hummel, D. F. Buscher, J. T. Armstrong, D. Mozurkewich, N. M. Elias, II, and B. L. Babler. Constraints on the Geometry of Circumstellar Envelopes: Optical Interferometric and Spectropolarimetric Observations of Seven Be Stars. , 479:477–+, April 1997.
- A. Quirrenbach, D. F. Buscher, D. Mozurkewich, C. A. Hummel, and J. T. Armstrong. Maximum-entropy maps of the Be shell star zeta Tauri from optical long-baseline interferometry. *A&A*, 283:L13–L16, March 1994.
- R. Racine. Ros 4, a distant open cluster associated with nebulosities. *AJ*, 74:816–817, August 1969.
- N. V. Raguzova. Population synthesis of Be/white dwarf binaries in the Galaxy. *A&A*, 367:848–858, March 2001.

- G. Ramsay and D. L. Pollaco. CCD observations in 7 open clusters - NGC2421, NGC2439, NGC2489, NGC2567, NGC2627, NGC2658 and NGC2910. *A&AS*, 94:73–102, July 1992.
- S. Rappaport and E. P. J. van den Heuvel. X-ray observations of Be stars. In M. Jасhek and H.-G. Groth, editors, *Be Stars*, volume 98 of *IAU Symposium*, pages 327–344, April 1982.
- G. H. Rieke and M. J. Lebofsky. The interstellar extinction law from 1 to 13 microns. , 288:618–621, January 1985.
- T. Rivinius. Links between Photospheric Activity and Formation of Circumstellar Structures of Be Stars. In A. T. Okazaki, S. P. Owocki, and S. Stefl, editors, *Active OB-Stars: Laboratories for Stellare and Circumstellar Physics*, volume 361 of *Astronomical Society of the Pacific Conference Series*, pages 219–+, March 2007.
- T. Rivinius, D. Baade, and S. Štefl. Non-radially pulsating Be stars. *A&A*, 411: 229–247, November 2003.
- T. Rivinius and S. Štefl. 59 Cygni: A Titled Persei like System. In M. A. Smith, H. F. Henrichs, and J. Fabregat, editors, *IAU Colloq. 175: The Be Phenomenon in Early-Type Stars*, volume 214 of *Astronomical Society of the Pacific Conference Series*, pages 581–+, 2000.
- J. Ruprecht. Classification of open star clusters. *Bulletin of the Astronomical Institutes of Czechoslovakia*, 17:33–+, 1966.
- R. Sagar and W. K. Griffiths. CCD photometry of the distant young open cluster NGC 7510. *MNRAS*, 250:683–691, June 1991.
- R. Sagar and U. C. Joshi. Study of the Galactic Cluster NGC 581. *Bulletin of the Astronomical Society of India*, 6:12–+, March 1978.

- H. Saio, C. Cameron, R. Kuschnig, G. A. H. Walker, J. M. Matthews, J. F. Rowe, U. Lee, D. Huber, W. W. Weiss, D. B. Guenther, A. F. J. Moffat, S. M. Rucinski, and D. Sasselov. MOST Detects g-Modes in the Late-Type Be Star β Canis Minoris (B8 Ve). , 654:544–550, January 2007.
- W. B. Samson. The Distribution of Interstellar Matter in NGC 654. , 34:363–376, May 1975.
- N. Sanduleak. The emission-line stars in NGC 663. *AJ*, 84:1319–1322, September 1979.
- N. Sanduleak. Further Observations of the Emission-Line Stars in the Open Cluster NGC 663. *AJ*, 100:1239–+, October 1990.
- J. Sanner, M. Geffert, J. Brunzendorf, and J. Schmoll. Photometric and kinematic studies of open star clusters. I. NGC 581 (M 103). *A&A*, 349:448–456, September 1999.
- M. Sasaki, W. Pietsch, and F. Haberl. XMM-Newton observations of High Mass X-ray Binaries in the SMC. *A&A*, 403:901–916, June 2003.
- G. Schaller, D. Schaerer, G. Meynet, and A. Maeder. New grids of stellar models from 0.8 to 120 solar masses at $Z = 0.020$ and $Z = 0.001$. *A&AS*, 96:269–331, December 1992.
- R. Schild and W. Romanishin. A study of Be stars in clusters. , 204:493–501, March 1976.
- R. E. Schild. B Stars in the Region of η and χ Persei. , 146:142–+, October 1966.
- Schimdt-Kaler. Schimdt-Kaler. *Springer Verlag*, 2:0–+, November 1982.
- T. Schmidt-Kaler. Emissions-B-Sterne und galaktische Struktur. Mit 6 Textabbildungen. *Zeitschrift für Astrophysik*, 58:217–+, 1964.

- H. Schneider. Stromgren and H-beta photometry of early type stars in northern open clusters. I - NGC 7039, NGC 7063. *A&AS*, 67:545–550, February 1987.
- W. Schöneich. The Reality of the Open Cluster NGC 7039 (Cr 431). *Soviet Astronomy*, 7:294–+, October 1963.
- S. Sharma, A. K. Pandey, D. K. Ojha, W. P. Chen, S. K. Ghosh, B. C. Bhatt, G. Maheswar, and R. Sagar. Star formation in young star cluster NGC1893. *MNRAS*, 380:1141–1160, September 2007.
- S. Sharpless. Multiple-Star Systems in Emission Nebulae. , 119:334–+, March 1954.
- V. S. Shevchenko, M. A. Ibragimov, and T. L. Chenysheva. SFR 2-CYGNI - a Star-Forming Region Associated with the Extremely Young Cluster NGC6910 and the Herbig Be-Stars BD+40DEG4124 and BD+41DEG3731. *Soviet Astronomy*, 35:229–+, June 1991.
- L. Siess, E. Dufour, and M. Forestini. An internet server for pre-main sequence tracks of low- and intermediate-mass stars. *A&A*, 358:593–599, June 2000.
- C. L. Slesnick, L. A. Hillenbrand, and P. Massey. The Star Formation History and Mass Function of the Double Cluster η and χ Persei. , 576:880–893, September 2002.
- A. Slettebak. Lines of Neutral Oxygen in the Infrared Spectra of Be Stars. , 113:436–+, March 1951.
- A. Slettebak. The Be stars. *Space Science Reviews*, 23:541–580, June 1979.
- A. Slettebak. Spectral types and rotational velocities of the brighter Be stars and A-F type shell stars. *ApJS*, 50:55–83, September 1982.
- A. Slettebak. Be stars in open clusters. *ApJS*, 59:769–784, December 1985.

- A. Slettebak, G. W. Collins, II, and R. Truax. Physical properties of Be star envelopes from Balmer and Fe II emission lines. *ApJS*, 81:335–376, July 1992.
- T. P. Snow. High-energy phenomena in Be stars. In A. Slettebak and T. P. Snow, editors, *IAU Colloq. 92: Physics of Be Stars*, pages 250–260, 1987.
- T. P. Snow and R. Stalio. Be star phenomena. In Y. Kondo, editor, *Exploring the Universe with the IUE Satellite*, volume 129 of *Astrophysics and Space Science Library*, pages 183–201, 1987.
- T. P. Snow, Jr. Stellar winds and mass-loss rates from Be stars. *ApJS*, 251:139–151, December 1981.
- T. P. Snow, Jr. and J. M. Marlborough. Evidence for mass loss at moderate to high velocity in Be stars. *ApJL*, 203:L87–L90, January 1976.
- J. R. Sowell. Yellow evolved stars in open clusters. *ApJS*, 64:241–267, May 1987.
- P. Stee and J. Bittar. Near-IR and visible interferometry of Be stars: Constraints from wind models. *A&A*, 367:532–548, February 2001.
- P. Stee, F. X. de Araujo, F. Vakili, D. Mourard, L. Arnold, D. Bonneau, F. Morand, and I. Tallon-Bosc. γ Cassiopeiae revisited by spectrally resolved interferometry. *A&A*, 300:219–+, August 1995.
- C. B. Stephenson and N. Sanduleak. New H-alpha emission stars in the Milky Way. *ApJS*, 33:459–469, April 1977.
- H. Steppe. RGU photometry of the open cluster NGC 581 (= M103), Tr 1 and NGC 659. *A&AS*, 15:91–105, 1974.
- R. C. Stone. Membership in the young open cluster NGC 654. *A&A*, 54:803–810, February 1977.

- R. C. Stone. The inner and outer membership regions of the young open cluster NGC 6823. *AJ*, 96:1389–1393, October 1988.
- R. Stothers. Fundamental Data for Massive Stars Compared with Theoretical Models. , 175:431–+, July 1972.
- O. Struve. On the Origin of Bright Lines in Spectra of Stars of Class B. , 73:94–+, March 1931.
- A. Subramaniam, B. Mathew, B. C. Bhatt, and S. Ramya. NGC 7419: a young open cluster with a number of very young intermediate mass pre-MS stars. *MNRAS*, 370:743–752, August 2006.
- A. Subramaniam, D. K. Sahu, R. Sagar, and P. Vijitha. NGC 146: a young open cluster with a Herbig Be star and intermediate mass pre-main sequence stars. *A&A*, 440:511–522, September 2005.
- S. Sujatha and G. S. D. Babu. NGC 1624 (OC1 403, Cr 53) A very young open cluster. , 305:399–410, December 2006.
- S. N. Svolopoulos. A Three Color Photometry of the Open Clusters NGC 6755 and NGC 6756. With 3 Figures in the Text. *Zeitschrift fur Astrophysik*, 61:105–+, 1965.
- F. D. Talbert. UBV photometry of NGC 6649. , 87:341–344, April 1975.
- M. Tapia, R. Costero, J. Echevarria, and M. Roth. Near-infrared and Stromgren photometry of the open clusters NGC 663, NGC 1502 and NGC 1893. *MNRAS*, 253:649–661, December 1991.
- L. Testi, F. Palla, and A. Natta. The onset of cluster formation around Herbig Ae/Be stars. *A&A*, 342:515–523, February 1999.

- P. S. The, D. de Winter, and M. R. Perez. A new catalogue of members and candidate members of the Herbig Ae/Be (HAEBE) stellar group. *A&AS*, 104:315–339, April 1994.
- P. S. The and C. Roslund. Photometry of the galactic cluster NGC 6649. *Contributions from the Bosscha Observatory*, 19:1–+, 1963.
- C. Thom, P. Granes, and F. Vakili. Optical interferometric measurements of Gamma Cassiopeiae’s envelope in the H-alpha line. *A&A*, 165:L13–L15, September 1986.
- J. M. Torrejon, J. Fabregat, G. Bernabeu, and S. Alba. Be stars in open clusters. II. Balmer line spectroscopy. *A&AS*, 124:329–347, August 1997.
- R. Townsend. The Coupling Between Pulsation and Mass Loss in Massive Stars. In R. J. Stancliffe, G. Houdek, R. G. Martin, and C. A. Tout, editors, *Unsolved Problems in Stellar Physics: A Conference in Honor of Douglas Gough*, volume 948 of *American Institute of Physics Conference Series*, pages 345–356, November 2007.
- R. H. D. Townsend, S. P. Owocki, and I. D. Howarth. Be-star rotation: how close to critical? *MNRAS*, 350:189–195, May 2004.
- R. J. Trumpler. Preliminary results on the distances, dimensions and space distribution of open star clusters. *Lick Observatory Bulletin*, 14:154–188, 1930.
- L. Turbide and A. F. J. Moffat. Precision photometry of young stellar groups towards the outer Galactic disk and the Galactic rotation curve. *AJ*, 105:1831–1854, May 1993.
- D. G. Turner and D. Forbes. Berkeley 87, a heavily-obscured young cluster associated with the ON2 star-formation complex and containing the WO star Stephenson 3. , 94:789–801, October 1982.

-
- C. Tycner, J. B. Lester, A. R. Hajian, J. T. Armstrong, J. A. Benson, G. C. Gilbreath, D. J. Hutter, T. A. Pauls, and N. M. White. Properties of the H α -emitting Circumstellar Regions of Be Stars. , 624:359–371, May 2005.
- A. Ud-Doula, S. P. Owocki, and R. H. D. Townsend. Dynamical simulations of magnetically channelled line-driven stellar winds - II. The effects of field-aligned rotation. *MNRAS*, 385:97–108, March 2008.
- S. Štefl, D. Baade, T. Rivinius, S. Otero, O. Stahl, A. Budovičová, A. Kaufer, and M. Maintz. Stellar and circumstellar activity of the Be star omega CMA. I. Line and continuum emission in 1996-2002. *A&A*, 402:253–265, April 2003.
- A. Vallenari, A. Richichi, G. Carraro, and L. Girardi. Near-infrared photometry of the young open clusters NGC 1893 and Berkeley 86. *A&A*, 349:825–833, September 1999.
- J. van Bever and D. Vanbeveren. The number of B-type binary mass gainers in general, binary Be stars in particular, predicted by close binary evolution. *A&A*, 322:116–126, June 1997.
- H. C. van de Hulst, C. A. Muller, and J. H. Oort. The spiral structure of the outer part of the Galactic System derived from the hydrogen emission at 21 cm wavelength. , 12:117–+, May 1954.
- S. Van den Bergh and J. de Roux. UBV Photometry of the Open Cluster NGC 663. *AJ*, 83:1075–+, September 1978.
- E. P. J. van den Heuvel and S. Rappaport. X-ray observations of B-emission stars. In A. Slettebak and T. P. Snow, editors, *IAU Colloq. 92: Physics of Be Stars*, pages 291–307, 1987.
- V. Vansevicius, A. Bridzius, A. Pucinskas, and T. S. Sasaki. BVRI CCD Photometry of the Open Cluster IC 4996. *Baltic Astronomy*, 5:539–548, 1996.

- N. Vogt and A. F. J. Moffat. Southern open clusters I. UBV and Hbeta photometry of 15 clusters between galactic longitudes 231d and 256d. *A&AS*, 7:133–+, October 1972.
- H. von Zeipel. The radiative equilibrium of a rotating system of gaseous masses. *MNRAS*, 84:665–683, June 1924.
- L. R. Wackerling. A catalogue of early-type stars whose spectra have shown emission lines. *MNRAS*, 149:405–+, 1970.
- A. R. Walker and C. D. Laney. CCD photometry of galactic clusters containing Cepheid variables. IV - NGC 6649. *MNRAS*, 224:61–74, January 1987.
- L. B. F. M. Waters. The density structure of discs around Be stars derived from IRAS observations. *A&A*, 162:121–139, July 1986.
- L. B. F. M. Waters, J. Cote, and H. J. G. L. M. Lamers. IRAS observations of Be stars. II - Far-IR characteristics and mass loss rates. *A&A*, 185:206–224, October 1987.
- L. B. F. M. Waters and J. M. Marlborough. The Structure of the Circumstellar Material in Be Stars. In L. A. Balona, H. F. Henrichs, & J. M. Le Contel, editor, *Pulsation; Rotation; and Mass Loss in Early-Type Stars*, volume 162 of *IAU Symposium*, pages 399–+, 1994.
- J. P. Wisniewski and K. S. Bjorkman. The Role of Evolutionary Age and Metallicity in the Formation of Classical Be Circumstellar Disks. I. New Candidate Be Stars in the LMC, SMC, and Milky Way. , 652:458–471, November 2006.
- J. P. Wisniewski, K. S. Bjorkman, A. M. Magalhães, J. E. Bjorkman, M. R. Meade, and A. Pereyra. The Role of Evolutionary Age and Metallicity in the Formation of Classical Be Circumstellar Disks. II. Assessing the Evolutionary Nature of Candidate Disk Systems. , 671:2040–2058, December 2007.

- K. Wood, K. S. Bjorkman, and J. E. Bjorkman. Deriving the Geometry of Be Star Circumstellar Envelopes from Continuum Spectropolarimetry. I. The Case of zeta Tauri. , 477:926–+, March 1997.
- R. K. S. Yadav, B. Kumar, A. Subramaniam, R. Sagar, and B. Mathew. Optical and near-infrared photometric study of the open cluster NGC 637 and 957. *MNRAS*, 390:985–996, November 2008.
- R. K. S. Yadav and R. Sagar. Non-uniform extinction in young open star clusters. *MNRAS*, 328:370–380, December 2001.
- R. K. S. Yadav and R. Sagar. UBVRI CCD photometry of the OB associations Bochum 1 and Bochum 6. *Bulletin of the Astronomical Society of India*, 31: 87–100, March 2003.
- R. K. S. Yadav and R. Sagar. A comprehensive CCD photometric study of the open cluster NGC 2421. *MNRAS*, 351:667–675, June 2004.
- R. Yudin, S. Hubrig, M. Pogodin, I. Savanov, M. Schöller, G. Peters, and M. Cure. Magnetic fields in classical Be stars. In *IAU Symposium*, volume 259 of *IAU Symposium*, pages 397–398, April 2009.
- N. Zacharias, D. G. Monet, S. E. Levine, S. E. Urban, R. Gaume, and G. L. Wycoff. NOMAD Catalog (Zacharias+ 2005). *VizieR Online Data Catalog*, 1297:0–+, November 2005.
- K. Zwintz and W. W. Weiss. Pulsating pre-main sequence stars in IC 4996 and NGC 6530. *A&A*, 457:237–248, October 2006.